

International Conference on Recent Advancements in Science and Engineering (RAiSE'24)



BOOK RIVERS
WE CREATE READERS

Published By: Book Rivers

Website: www.bookrivers.com

Email: publish@bookrivers.com

Mobile: +91-9695375469

1ST Edition: -2024

MRP: 799/-INR

ISBN: 978-93-5842-452-2

Copyright©: Authors

All Rights Reserved

No part of this publication may be reproduced, transmitted or stored in a retrieval system, in any form or by any means, electronic, mechanical, photocopying recording or otherwise, without the prior permission of the author.

[PRINTED IN INDIA]

Table of Content

S. No	Paper ID	Name	Topic	PG. NO
1.	CEPG001	Anju Suresh Priyanka Dilip P	Effect of Plate Thickness of Stainless Steel Core Plate Wall on Load Carrying Capacity under Pure Shear and Compression Shear Conditions	1 - 14
2.	CEPG002	Aarya Krishnan A.R Dr. Sabeena M V	Analysis Of Strength and Bond Behaviour Of Bacterial Concrete	15 - 26
3.	CEPG003	Arathi. A Dr. Sabeena	Behaviour of Reinforced Concrete Beams Strengthened for Shear with the CFRP Fabric Wrapping	27 - 39
4.	CEPG004	Aiswarya Jayaraj K Anila. S	Shape Optimisation of Grooves in Grooved Gusset Plate Damper used in X-braced Frame	40 - 48
5.	CEPG005	Arifa V Priyanka Dilip P	Numerical analysis of corrugated castellated beam with and without openings	49 - 60
6.	CEPG006	Shahaba Sherin P Jisha P Minu U	Analysis on the bending behaviour of t shaped glulam beam	61 - 69
7.	CEPG007	Hiba Parveen E Jisha P	Seismic Analysis Of Irregular Building Subjected To Pounding	70 - 78
8.	CEPG008	Ayisha Sana Abdul Salam Anila S	Response Of T Beam Bridge By Varying Skew Angle	79 - 84
9.	EXCEUG006	Shahla Thasni P Sandra E	Comparative Study of Reinforced Concrete Using Human Hair and Aluminium Fibers	85 - 97
10.	CEUG002	Heena Mariyam Rinsha Safa Sadique	Planning, Analysis and Design of Hotel Building at Karadi, Thamarassery	98 - 109
11.	CEUG001	Arya Ayisha Nasli Fathima Nida Hiba Department Ms Sindhu	Planning, Analysis and Design of Thermal Comfort Auditorium in KMCT Technical Campus	110 - 124
12.	EXCEUG007	NAFEESA MINHA P NIDHA SHERIN K	Utilization Of E-Waste in Strength Enhancement of Soil	125 - 135
13.	BMUG001	Arunima R Munseera P Nandana Anil Pavithra K	Object Detection Using Machine Learning For Blind People	136 - 145
14.	BMUG002	Adithya M Neha Vijay Aparna A K	Smart Headband For Rehabilitation	146 - 153
15.	BMUG003	Afeefa Askar Ahla Amal Abdulsalam Nandana Raj Ms Irfana Izzath	Heart Disease Detection Using ECG Waveforms	154 - 163
16.	BMUG004	Aparna Devaraj Ann Sunny Rana Abdul Shifa Thasneem Minilal M Mufliha T	IoT Based Prototype For Patient Monitoring And Medical Infusion Intravenously	164 - 173
17.	BMUG005	Naseeba Noori Nida Nishana Tisniya Vironi	Evaluating The Role of Dietary Factors in Predicting Blood	174 - 182

		Shibitha KP	Glucose Level for Type-1-Diabetes Using Machine Learning	
18.	BMUG006	Zahda Raheem Sreeja S Sharika E Dr. Sameera	Covid-19 Infected Lung Image Classification Using Inception-Res Net	183 - 191
19.	BMUG008	Fathima Fidha Fitha Firose Devika Sreekumar Fathimathu Riyada Ms Anusha	Mindmapper: Predicting Alzheimer's with Magnetic Resonance Imaging	192 - 199
20.	BMUG010	Yamuna S Asiya N Aleena K S Rukhya P Sivanath P I	Exoarm: Empowering Monoparesis Rehabilitation	200 - 209
21.	BMUG011	Kshaya T V Aziya Ashraf Nashwa T Navya Babu Anusha E P	Head Gesture Controlled and Obstacles Detected Automatic Wheelchair for Quadricplegic Patients	210 - 220
22.	EXCSUG001	Akshay Remesh P Akshay Dath Vinaya Br	Telecom Customer Churn Prediction Using Machine Learning	221 - 230
23.	EXCSUG002	Nandagopan P Sreehari Jayaraj	Foss folio: A Seamless Event Operations Platform	231 - 242
24.	EXCSUG003	Adarsh K E Gautham Unni T K Vishnu P Yaser Arafath	AR Menu Fusion: Seamless Dining With Augmented Reality	243 - 250
25.	EXEEUG005	Sona N M Nithya V G Alfin Mohammed Adarsh Kumar E Swetha Santhosh	Conversion of Conventional Energy Meter to Smart Energy Meter	251 - 258
26.	EXBMUG006	Jitha Bhaskar M Kailas Krishna	Eco trim auto-mower	259 - 266
27.	EMUGUG007	Namitha Krishnan Surya Gayathri U Ardra PV	Multi-Class Skin Disease Classification Using Convolutional Neural Network	267 - 280
28.	BMUG009	Shamna Backer Raihana Tk Sweety Pj Farhana Sherin Irfana Izzath Op	Brain Abnormality Classification By Combination Of Machine Learning And Deep Learning	281 - 291

Effect of Plate Thickness of Stainless Steel Core Plate Wall on Load Carrying Capacity under Pure Shear and Compression Shear Conditions

Anju Suresh

M tech Structural Engineering Student
Dept. of Civil Engineering,
AWH Engineering College, Kozhikode, Kerala,
India

Priyanka Dilip P

Asst. Professor
Dept. of Civil Engineering
AWH Engineering College, Kozhikode, Kerala,
India *Corresponding Author:
sureshanju10@gmail.com

ABSTRACT

The shear walls have been employed as a lateral force opposing systems in numerous multistorey buildings. The Stainless- Steel Core Plate Wall (SSCPW) is a recent and innovative addition to structural elements. The adoption of stainless steel over traditional steel has been driven by its advantageous properties, such as its lightweight nature, durability, and resistance to corrosion. The SSCPW comprises stainless-steel plates interconnected with orthogonally positioned stainless steel core tubes through welding. Depending on the specific orientations chosen, SSCPW can function as beams, columns, walls, floors and other essential structural components. Different cross-sectional shapes of SSCPWs are available, and this study focused on L- and T-shaped SSCPWs subjected to pure shear and compression shear conditions. The analysis and investigation of the impact of plate thickness on load-carrying capacities was conducted using ANSYS Workbench software. It was observed that the load carrying capacity of SSCPW increases as the plate thickness increases. Plate thicknesses of 8, 12,16 and 20 mm were chosen for modelling. Results shows that SSCPW of plate thickness 20 mm has the maximum load carrying capacity.

Keywords- ANSYS workbench, Compression shear, L and T-shaped SSCPW, Load carrying capacity, Pure shear.

INTRODUCTION

The Stainless-Steel Core Plate Wall (SSCPW) is a relatively latest addition to civil engineering, resembling the honeycomb sandwich structure in its construction. These versatile components function as specialized columns in prefabricated buildings, accommodating diverse layouts such as T-shapes, L-shapes, and cross-shapes. The positioning of flat-type SSCPW panels vertically in various configurations allows for the creation of these shapes. T-shaped walls find external and internal utility in buildings, while L-shaped walls are well-suited for building corners.

On the other hand, cross-shaped walls apply to irregularly shaped buildings, both internally and externally.

This study specifically focused on evaluating the performance of L and T-shaped SSCPWs under pure shear and compression shear conditions. Prior research has extensively explored various sandwich structural elements and has investigated this innovative system. Researchers conducted experiments and finite element analysis to assess the load-bearing capacity of T-shaped stainless-steel core plate wall panels under axial compression [1]. Additionally, they delved into the collapse mechanisms of L-shaped stainless-steel core plate wall panels when subjected to axial compression, employing a combination of experimental and computational methods [2]. A load-carrying capacity of cross-shaped stainless steel core plate wall under axial and eccentric compression was conducted, and a finite element analysis was performed [3].

Construction of the Stainless- Steel Core Plate Panels

Stainless-steel core plate panels consist of two stainless steel plates with multiple stainless steel tubes interconnected using copper brazing. This connection occurs at elevated temperatures, utilizing a copper-based brazing alloy as the filler material. This method is highly cost-effective and varies from traditional welding techniques.

Firstly, the copper-type filler is applied to the upper and lower ends of the stainless-steel core tubes. Subsequently, the plates and tubes are spot-welded to get the precise position of the core tubes. The collected components are then introduced into a high-temperature brazing furnace where an inert shielding gas, heated to approximately 1030 °C, is blown to facilitate brazing. Copper-type fillers have lower melting points than stainless steel fillers. The shielding gas temperature is carefully controlled to gain the melting point of the copper-type filler. This ensures the stainless steel tubes and plates remain unaffected while copper-type fillers melt. The molten filler material flows into gaps through capillary action, joining stainless steel plates and tubes. To maintain the process, the temperature of the shielding gas is kept for a specific duration. At last, by slowly reducing the shielding gas temperature to enable the fusion and cooling of fillers and weldments, the brazing joint is accomplished.

Merits

- The SSCPW resists sideward loads. Therefore, it helps to enhance the seismic performance of buildings.
- SSCPW helps reduce construction costs by increasing the net area of buildings.
- The compact design and adjustable configuration of the steel plate wall (SPW) system offer enhanced architectural attributes, conserving space, ensuring adaptability, and boosting interior space efficiency compared to standard reinforced concrete shear walls with a bigger footprint.
- Due to their significantly lighter weight compared to RC shear walls, SPWs exert less pressure on columns and footings. Due to that, they impose a reduced earthquake load that directly correlates with the structure's weight.

- SPWs can be assembled much faster than an RC structure, thus reducing the construction timeline and overall project costs.
- A well-designed SPW system offers a notably high capacity for energy dissipation and is suitable for deployment in high-risk seismic zones.
- Within these systems, the field experienced due to tension in the web portion operates similarly to a diagonal brace, offering a relatively higher initial rigidity that enhances its effectiveness in constraining wind drift.
- SPWs typically boast a notably simpler and faster installation process in seismic retrofit scenarios than reinforced concrete shear walls. This aspect is crucial when uninterrupted building occupancy is necessary during construction.

FINITE ELEMENT MODELLING

The finite element modelling of L and T-shaped stainless-steel core plate walls was carried out by incorporating the material properties of the specimen obtained from the experimental study accompanied by [1]. The boundary conditions of models were given as pinned at the topmost end and fixed at the bottom. Mesh size was selected as 25mm to model the element. The specimen's geometry is shown in Fig. 1. The loading was specified to be displacement-controlled at the upper end until failure ensued. Fig. 2 and 3 represent geometric models of L and T-shaped SSCPWs, respectively. The loading conditions of L and T-shaped SSCPWs under pure shear and compression shear conditions are shown in Fig. 4 and 5, respectively.

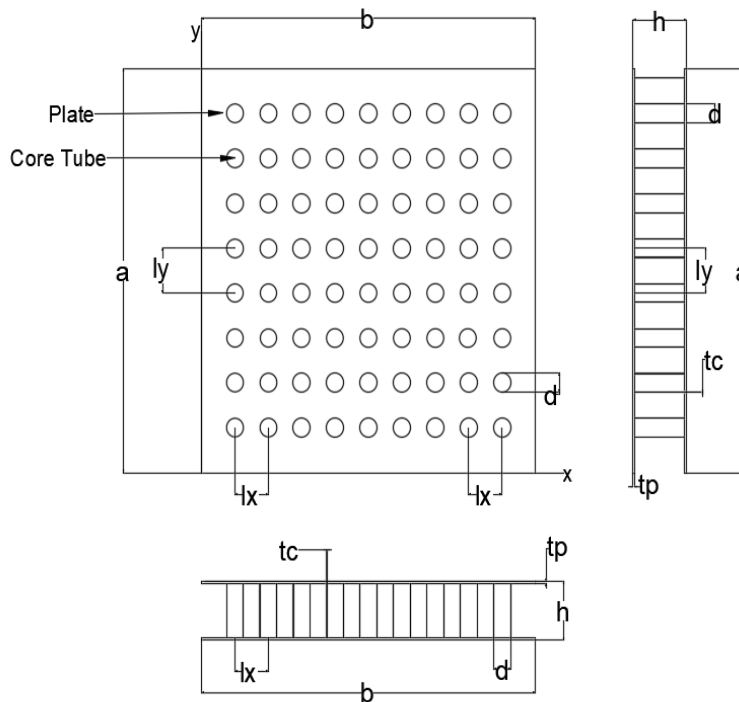


Figure 1: Geometry of specimen.

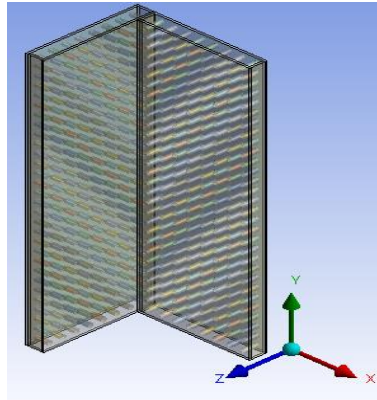


Figure 2: Geometry of L- shaped stainless-steel core plate wall.

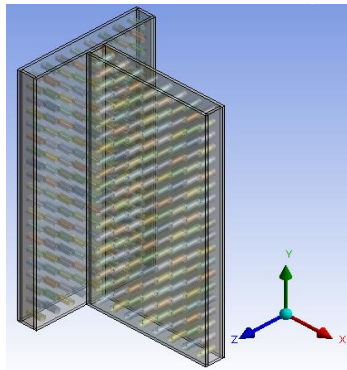
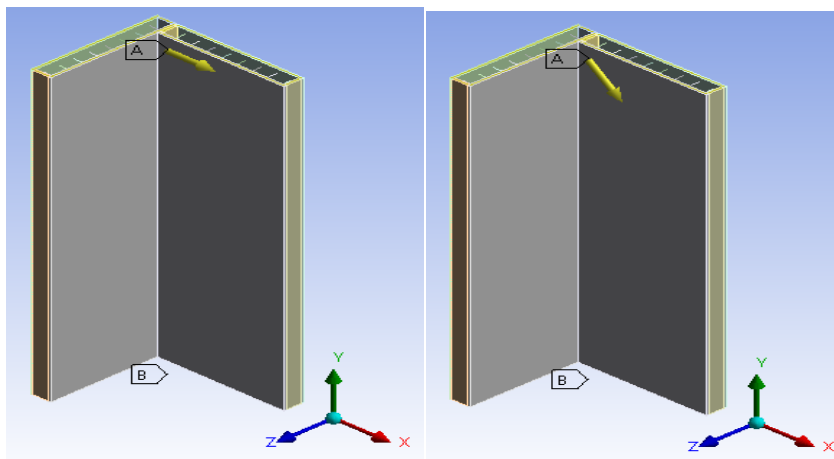


Figure 3: Geometry of T- shaped stainless- steel core plate wall.



(a)(b)

Figure 4: Loading conditions of L-shaped SSCPW a) Loading under pure shear b) Loading under *compression shear*.

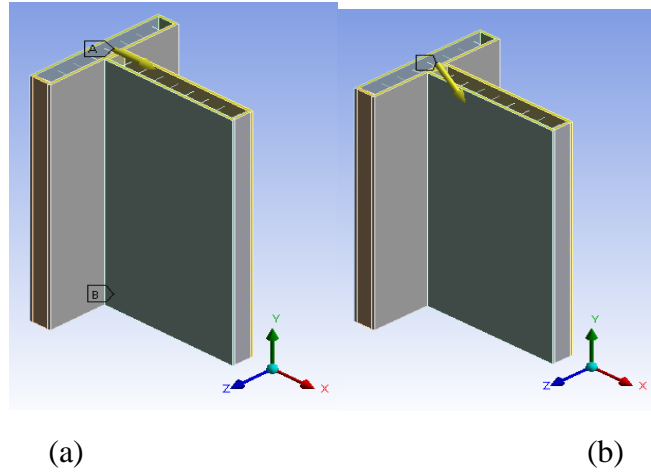


Figure 5: Loading conditions of T-shaped SSCPW a) Loading under pure shear b) Loading under compression shear.

EFFECT OF PLATE THICKNESS

The effect of the thickness of plates under pure-shear and compression-shear conditions was determined using L and T-shaped stainless steel core plate walls. Keeping all other parameters of models constant, the plate thickness (t_p) was varied. 8mm, 12mm, 16mm and 20 mm were the thickness chosen for L and T- shaped SSCPWs.

Table 1: Model description.

Geometric Parameters	Dimension (mm)
Length of plate, a	3000
Width of plate, b	1000
Length of core tube, h	159
The outer diameter of the core tube, d	51
Core tube thickness, t_c	0.5
Horizontal spacing, l_x	121
Vertical spacing, l_y	100

Table 2: Model name.

L8	L-shaped SSCPW of plate thickness 8 mm
L12	L-shaped SSCPW of plate thickness 12 mm
L16	L-shaped SSCPW of plate thickness 16 mm
L20	L-shaped SSCPW of plate thickness 20 mm
T8	T-shaped SSCPW of plate thickness 8 mm
T12	T-shaped SSCPW of plate thickness 12 mm
T16	T-shaped SSCPW of plate thickness 16 mm
T20	T-shaped SSCPW of plate thickness 20 mm

The behaviour of SSCPW Under Pure Shear in X Direction

It was observed that the load-carrying capacity of the models increased notably by 64.95% and 54.06% for L and T- shaped SSCPWs, respectively, as the thickness of the plate increased from 8mm to 20mm. The load-displacement graph for L and T- shaped SSCPWs under different plate thicknesses are shown in Fig. 6 and 7. Variations of peak load for different plate thicknesses for L and T- shaped SSCPWs are demonstrated in Fig. 8.

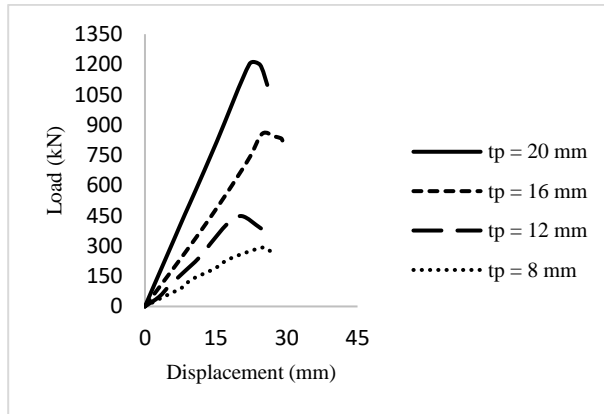


Figure 6: Load displacement graph of L-shaped SSCPW under pure shear in the x-direction for varying plate thickness.

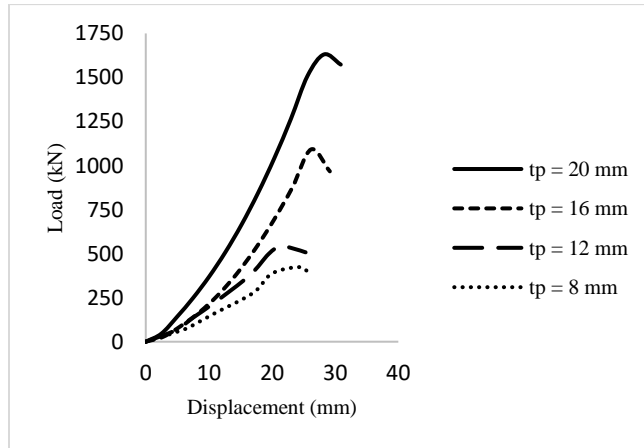


Figure 7: Load vs. displacement graph of T-shaped SSCPW under pure shear in the x-direction for varying plate thickness.

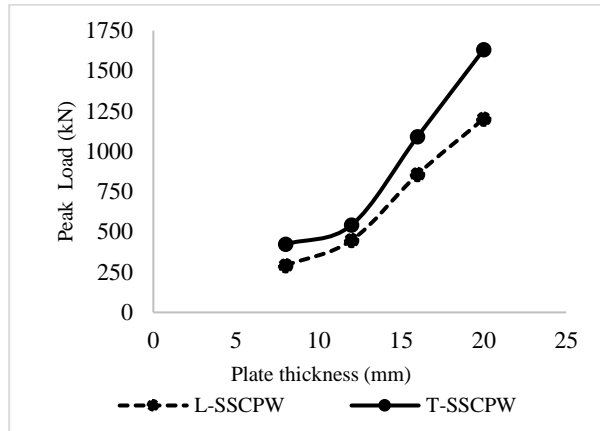


Figure 8: Peak load v/s plate thickness under pure shear in x-direction.

Table 3: Variation of peak load under pure shear in X direction.

Model Name	Peak Load (kN)
L8	291.37
L12	447.9
L16	856.8
L20	1201.6
T8	423.47
T12	542.32
T16	1091.74
T20	1631

The Behaviour of SSCPW Under Pure Shear in Z Direction

It was observed that the load-carrying capacity of the models increased notably by 59.34% and 60.17% for L and T- shaped SSCPWs, respectively, as the thickness of the plate increased from 8mm to 20mm. The load-displacement graph for L and T- shaped SSCPWs under different plate thicknesses are shown in Fig. 9 and 10, respectively. Variations in peak load for different plate thicknesses for L and T- shaped SSCPWs are demonstrated in Fig. 11.

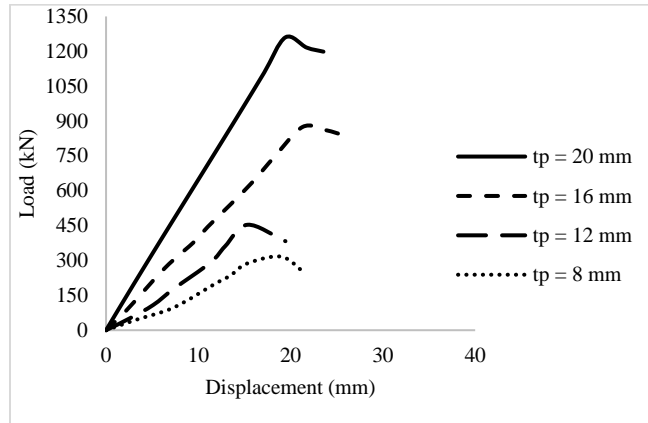


Figure 9: Load vs. displacement graph of L- L-shaped SSCPW under pure shear in z-direction for varying plate thickness.

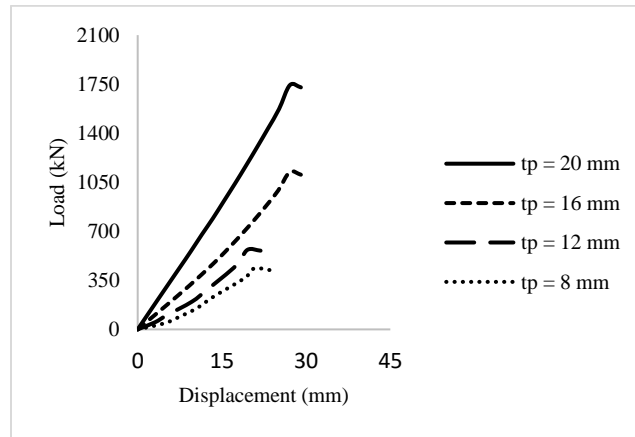


Figure 10: Load vs. displacement graph of T-shaped SSCPW under pure shear in the z-direction for varying plate thickness.

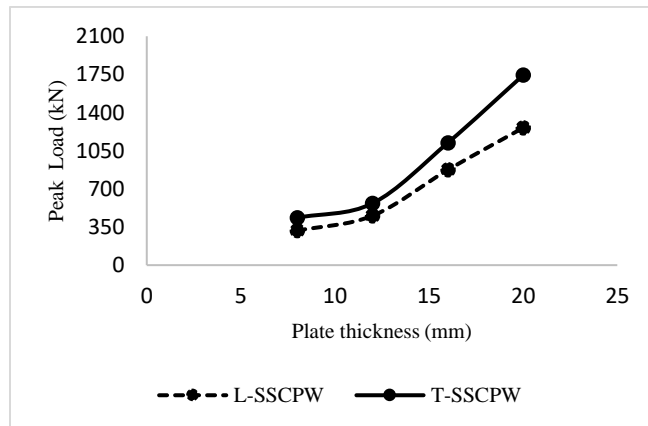


Figure 11: Peak load v/s plate thickness under pure shear in z-direction.

Table 4: Variation of peak load under pure shear in z direction.

Model Name	Peak Load (kN)
L8	316.3
L12	453.6
L16	874.34
L20	1260
T8	435.3
T12	567.43
T16	1123
T20	1743.2

The Behaviour of SSCPW Under Compression Shear in X Direction

It was observed that the load-carrying capacity of the models increased notably by 94.46% and 92.8% for L and T- shaped SSCPWs, respectively, as the thickness of the plate increased from 8mm to 20mm. The load-displacement graph for L and T- shaped SSCPWs under different plate thicknesses are shown in Fig. 12 and 13, respectively. The variation in peak load for different plate thicknesses for L and T- shaped SSCPWs are demonstrated in Fig. 14.

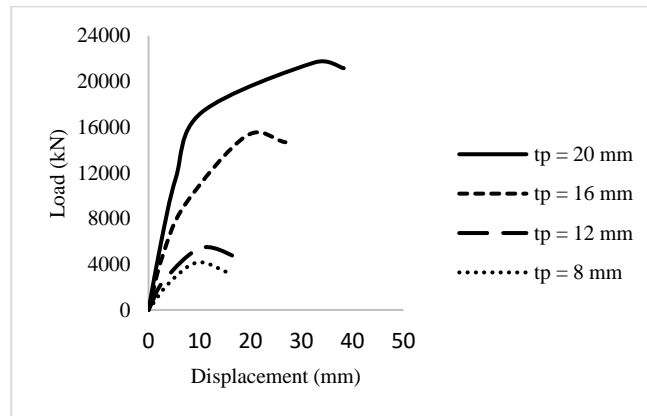


Figure 12: Load vs. displacement graph of L-shaped SSCPW under compression shear in the x-direction for varying plate thickness.

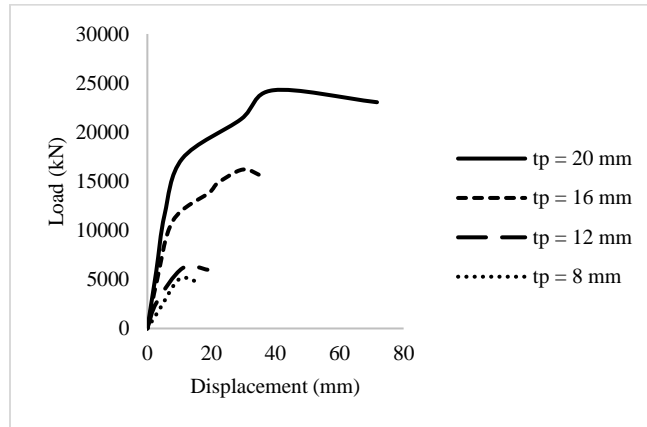


Figure 13: Load vs. displacement graph of T-shaped SSCPW under compression shear in the x-direction for varying plate thickness.

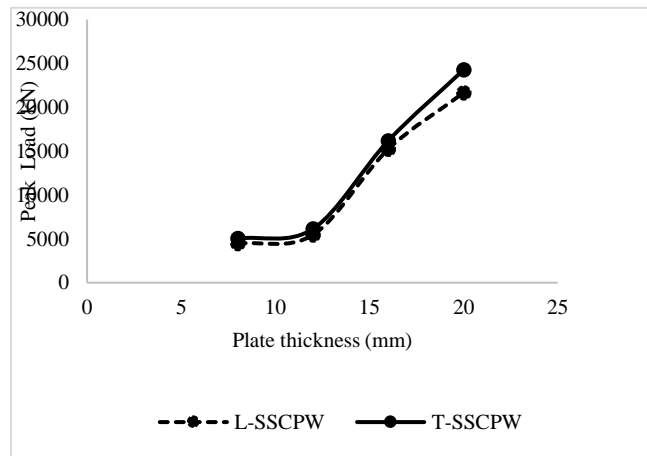


Figure 14: Peak load v/s plate thickness under compression shear in the x-direction.

Table 5: Variation of peak load under compression shear in x direction.

Model Name	Peak Load (kN)
L8	4454
L12	5467.2
L16	15226
L20	21653
T8	5034.7
T12	6143.4
T16	16187
T20	24267

The Behaviour of SSCPW Under Compression Shear in Z Direction

It was observed that the load-carrying capacity of the models increased notably by 89.96% and 78.74% for L and T- shaped SSCPWs, respectively, as the thickness of the plate increased from 8mm to 20mm. The load-displacement graph for L and T- shaped SSCPWs under different plate thicknesses are shown in Fig. 15 and Fig. 16, respectively. The variation in peak load for different plate thicknesses for L and T- shaped SSCPWs are demonstrated in Fig. 17.

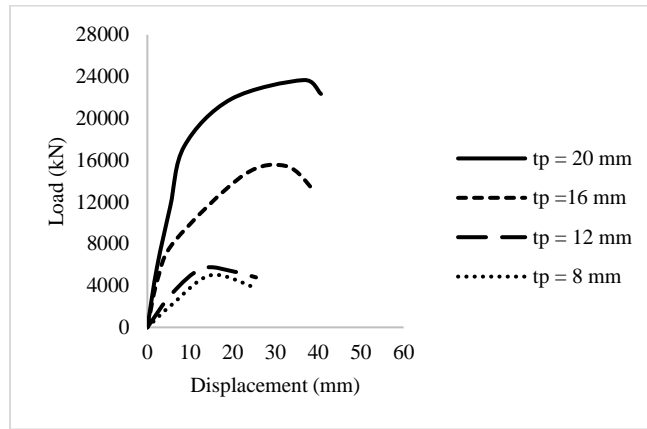


Figure 15: Load vs. displacement graph of L-shaped SSCPW under compression-shear in the z-direction for varying plate thickness.

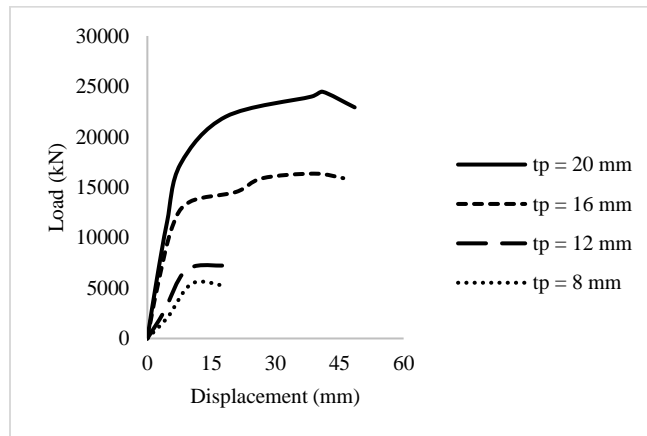


Figure 16: Load vs. displacement graph of T-shaped SSCPW under compression shear in the z-direction for varying plate thickness.

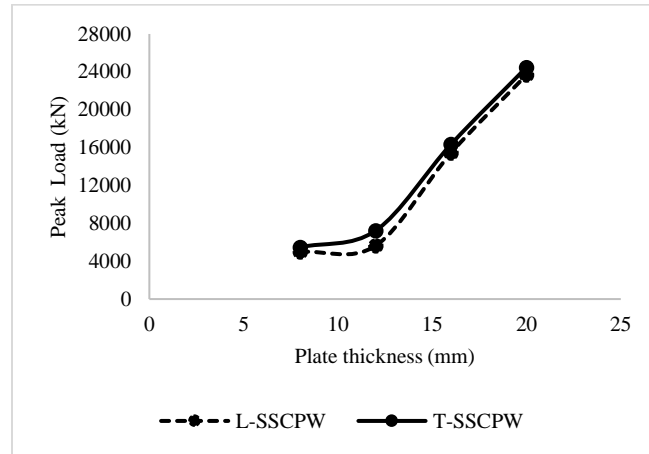


Figure 17: Peak load v/s plate thickness under compression shear in z-direction.

Table 6: Variation of peak load under compression shear in z direction.

Model Name	Peak Load (kN)
L8	4984.3
L12	5643
L16	15436
L20	23671
T8	5476
T12	7231.7
T16	16348
T20	24471

CONCLUSION

The impact of plate thickness on the load-carrying capacity of SSCPW under pure shear and compression shear conditions was studied. After the analysis, the following conclusions were made.

- The thickness of the plate was a critical parameter for the carrying capacity of the stainless-steel core plate wall.
- An increment in plate thickness improves the load-carrying capacity under pure shear and compression-shear conditions.
- An increase in plate thickness leads to an increase in its weight so it can withstand higher loads.
- T-shaped SSCPWs had greater load-carrying capacity than L-shaped SSCPWs due to their geometry.

- Load carrying capacity was more experienced in the z-direction under pure shear and compression shear conditions than in the x-direction.
- Load carrying capacity increased by 59.34% and 60.17% as the thickness of the plate increased from 8 mm to 20 mm for L and T-shaped SSCPWs, respectively, under pure shear in the z-direction.
- Load bearing capacity increased by 89.96% and 78.74% as the thickness of the plate increased from 8 mm to 20 mm for L and T-shaped SSCPWs, respectively, under compression-shear in the z-direction.

ACKNOWLEDGMENT

I am sincerely thankful for all the guidance I received from the professors and staff at the institution.

REFERENCES

1. [1] Shu, X. P., Yan, S., Li, Y., & Lu, B. R. (2021). Strength design of T-shaped stainless steel core plate wall under axial compression. *Journal of Constructional Steel Research*, 186, 106891. <https://doi.org/10.1016/j.jcsr.2021.106891>
2. [2] Shu, X. P., Wang, H. B., Li, Y., Yuan, Z. S., & Li, K. (2021). Study on the bearing resistance of axially compressed L-shaped stainless steel core plate wall based on the stability loss. *Engineering Structures*, 249, 113264. <https://doi.org/10.1016/j.engstruct.2021.113264>
3. [3] Chaithanya, & Nijesh, C. (2023). Numerical study on cross-shaped stainless steel core plate wall. *International Journal of Engineering Research & Technology*, 11(2), 42-46. <https://www.ijert.org/research/numerical-study-on-cross-shaped-stainless-steel-core-platewall-IJERTCONV11IS02009.pdf>
4. [4] Wang, M. Z., Guo, Y. L., Zhu, J. S., Yang, X., & Tong, J. Z. (2019). Sectional strength design of concrete-infilled double steel corrugated-plate walls with T-section. *Journal of Constructional Steel Research*, 160, 23-44. <https://doi.org/10.1016/j.jcsr.2019.05.017>
5. [5] Wang, K., Zhang, W., Chen, Y., & Ding, Y. (2021). Seismic analysis and design of composite shear wall with stiffened steel plate and infilled concrete. *Materials*, 15(1), 182. <https://doi.org/10.3390/ma15010182>
6. [6] Zhu, J. S., Guo, Y. L., Wang, M. Z., Yang, X., & Pi, Y. L. (2020). Seismic performance of concrete-infilled double steel corrugated-plate walls: Experimental research. *Engineering Structures*, 215, 110601. <https://doi.org/10.1016/j.engstruct.2020.110601>
7. [7] Liu, X., Xu, C., Liu, J., & Yang, Y. (2018). Research on special-shaped concrete-filled steel tubular columns under axial compression. *Journal of Constructional Steel Research*, 147, 203-223. <https://doi.org/10.1016/j.jcsr.2018.04.014>
8. [8] Chen, L., Wang, S., Lou, Y., & Xia, D. (2019). Seismic behavior of double-skin composite wall with L-shaped and C-shaped connectors. *Journal of Constructional Steel Research*, 160, 255-270. <https://doi.org/10.1016/j.jcsr.2019.05.033>

9. [9] Chen, L., Yin, C., Wang, C., & Liu, Y. (2020). Experimental study on seismic behavior of double-skin composite wall with L-shaped connectors. *Journal of Constructional Steel Research*, 174, 106312. <https://doi.org/10.1016/j.jcsr.2020.106312>
10. [10] Xu, D., Wang, J., Xiang, B. Q., Yan, J. B., & Wang, T. (2023). Behavior of double skin composite core wall subject to biaxial cyclic loads. *Engineering Structures*, 279, 115591. <https://doi.org/10.1016/j.engstruct.2023.115591>

Analysis Of Strength and Bond Behaviour of Bacterial Concrete

Aarya Krishnan A.R
Dept. of Civil Engineering
AWH Engineering College
Kozhikode, Kerala, India

Dr. Sabeena M V
Dept. of Civil Engineering
AWH Engineering College
Kozhikode, Kerala, India

Abstract- The incorporation of bacterial activity within concrete holds promise for enhancing its mechanical and durability characteristics. This research delves into the assessment of the strength and adhesion behavior of bacterial concrete, investigating the synergistic effects arising from bacterial activity. Scientific inquiry has confirmed the effectiveness of *Bacillus* species as microbial agents in augmenting concrete's self-repair capabilities. *Bacillus Subtilis* is employed for sample preparation, with a concentration of 10^5 cells per milliliter chosen as the parameter. The mechanical properties of bacterial concrete are analyzed, taking into account the impact of bacterial strains on these properties. The study also focuses on evaluating the bonding behavior of bacterial concrete through pull-out tests, aiming to assess the efficacy of bacterial activity in enhancing the bond strength of the concrete matrix. This investigation yields a comprehensive understanding of the intricate interplay of bacterial activity within concrete. The findings contribute to optimizing bacterial concentration and mix proportions for the development of sustainable and high-performance construction materials.

Keywords. — *Bateria, Bacillus Subtilis, pull out test, Bond strength.*

I. INTRODUCTION

In the realm of concrete structures, fissuring emerges as a prevalent occurrence attributed to the comparatively diminished tensile strength inherent to the material. Elevated tensile stresses can arise from external loads, induced deformations stemming from factors such as temperature differentials, confined shrinkage, and uneven settling, as well as phenomena like plastic shrinkage, plastic settlement, and expansive reactions triggered by elements such as reinforcement corrosion, alkali silica reaction, and sulphate attack. Absent timely and appropriate intervention, these fissures tend to propagate, necessitating eventually costly remedial measures. Moreover, the integrity of concrete durability suffers from these fissures, given their propensity to provide conduits for the ingress of fluids and gases containing potentially deleterious substances. Should micro-cracks propagate to the reinforcement, the ramifications extend beyond the concrete matrix itself, leading to corrosion of the reinforcement when exposed to environmental elements such as water, oxygen, and potentially carbon dioxide and chlorides. Thus, micro-cracks serve as precursors to structural debilitation[1]. The formation of carbonate precipitate through bacterially

induced mineralization emerges as a sustainable and cost-effective material. Presently, this carbonate precipitate finds utility across various engineering domains. Predominantly, in engineering applications, bacterially induced mineralization yields calcium precipitate, a process commonly denoted as microbially induced calcite precipitation (MICP) technique. Notably, researchers domestically and internationally have recently harnessed this technique for the remediation of concrete cracks and enhancement of concrete longevity[3]. The bond strength assumes a critical structural attribute within reinforced concrete structures, facilitating efficient transmission of forces between the concrete matrix and the encased reinforcing steel. This mechanism ensures compatibility of strains and engenders composite behavior within the material. Insufficient bond strength can precipitate a notable decline in both the structural load-bearing capacity and stiffness, particularly under diverse loading scenarios.

A. MICP – Microbially Induced Calcite Precipitation

Microbial Induced Calcite Precipitation (MICP) is a process by which biomineralization occurs, facilitated by microbial activity. This process involves the hydrolysis of urea by microbial urease, resulting in the generation of ammonia and carbon dioxide. Subsequently, the released ammonia leads to the deposition of insoluble calcium carbonate in the surrounding environment [6]. MICP presents a viable and sustainable approach to crack repair. This phenomenon is observed in various geological settings such as soils and limestone caves. Calcium carbonate (CaCO_3) crystals are produced biologically through autotrophic and heterotrophic pathways. Biotechnological advancements have proposed the development of bio-concrete utilizing microorganisms' innate ability to induce calcium carbonate precipitation [7],[8]. Upon crack formation, activated bacteria within the crack initiate the production of calcium carbonate minerals, effectively sealing the crack. In comparison to conventional self-healing concrete methods, MICP-based techniques offer a durable and environmentally friendly solution to cracking issues. The quantity and quality of induced minerals significantly influence the efficiency of the MICP process [10].

OBJECTIVES

The prime research objectives of this present work are as follows:

- To determine the mechanical properties of concrete specimens.
- To determine the mechanical properties of self healing concrete and compare with traditional concrete.
- To determine the bond strength corresponding to the pull-out force in rebar embedded in bacterial concrete specimen experimentally.

II. EXPERIMENTAL PROGRAMME

A research study was undertaken to evaluate the mechanical properties, bond stress-slip relationship, and extraction resistance of steel reinforcement bars incorporated within bacterially augmented concrete. Two distinct sizes of reinforcing steel bars (referred to as ϕ), namely 8mm

and 12mm, were examined. Three samples were subjected to each parameter, and the average of the outcomes was computed for subsequent analysis.

A. Materials

Pozzolanic cement of 53rd grade, adhering to IS: 1489 part 1:1991(reaffirmed 2005), was employed. Cement tests were executed following IS 4031-1988 standards. Fine aggregate sieved through a 4.75 mm IS sieve, conforming to grading zone III of IS: 383- 1970, was utilized. Crushed stone, with a maximum dimension of 20 mm, was employed. The reinforcement bars utilized were of Fe500 TMT grade. Bacillus subtilis bacteria were utilized for sample preparation. The bacterial concentration adopted for sample preparation was 10⁵ cells per milliliter. The particulars of the bacterial strain are furnished in Table I, whereas Table II presents the properties of reinforcement bars ascertained through tension tests.

II. TABLE I : BACTERIAL STRAIN DETAILS

Fields	Detailed information
Taxonomic designation	Bacillus Subtilis
Medium name	Nutrient agar
pH	11.8
Temperature of growth	30°C
Incubation period	24 to 48 hours
Subculturing period	2 months
Additional information	An adept manufacturer of alkali-tolerant protease and amylase, displaying alkaliphilic and thermotolerance characteristics, employed in the enhancement of composting processes.

TABLE II Reinforcement Bar Details

Properties	12mm	8mm
Yield point stress(MPa)	501.4	520.14
Ultimate stress(MPa)	642.1	535.2

B. MIX PROPORTIONS

In this experimental investigation, M25 grade concrete was employed, and the mixture formulation was formulated in accordance with the guidelines outlined in IS 10262:2019. The

specifics of the mixture ratios are delineated in Table III. The formulation of mixtures for both conventional concrete and bacterially augmented concrete was undertaken.

TABLE III MIX PROPORTION

Item	Quantity
Cement	478.5 kg/m ³
Fine aggregate	578.93 kg/m ³
Coarse aggregate	1028.75 kg/m ³
Water	220.3 kg/m ³
Water cement ratio	0.46

Specimen preparation

Concrete cubes with dimensions of 150mm were fabricated for the determination of compressive strength, while prismatic specimens measuring 100x100x500mm were fabricated to assess flexural strength. Moreover, cylindrical specimens with a diameter of 150mm and a height of 300mm were prepared to evaluate split tensile strength. Workability examinations were also conducted on the concrete blend. Cast iron moulds were employed for specimen fabrication, with the concrete being poured into the moulds in layers and each layer compacted using a tamping rod, as illustrated in Figure 1. In the instance of bacterially augmented concrete, around 10% of the total water content was extracted and utilized for mixing with the bacterial solution. The remaining 90% of water was subsequently combined with dry aggregates and cement, mixed for a duration of 1 minute, after which the diluted bacterial solution was introduced and mixed with the concrete for an additional 3 minutes.



Fig. 1. Specimen For Finding Mechanical Properties

D. CASTING OF PULL OUT SPECIMENS



Pull-out specimens were fabricated in accordance with the standards outlined in IS 516-1959 (reaffirmed 2004). Each specimen consisted of concrete cubes measuring 150mm, with a singular vertical reinforcing bar (either 8mm or 12mm in diameter) embedded along the central axis. The protrusion of the bar was set to approximately 10mm below the bottom surface of the cube to gauge bar slip, while extending approximately 85cm above the top face to ensure adequate grip in the testing apparatus. The terminations of the reinforcing bars, where the tip of the LVDT was attached during testing, were smoothed to create a perpendicular surface to the bar axes, as depicted in Figure 3. Additionally, specimens were enhanced with a helical arrangement of 6mm diameter mild steel bars spaced at intervals of 25mm to mitigate the risk of splitting failure, as illustrated in Figure 2. Following a 24-hour demolding period, specimens were promptly immersed in a curing tank for a curing duration of 28 days.



A. Fig 2. A) Helix

B) Mould

C) Specimen for test

E. Testing Of Pullout Specimens

The experimentation adhered to IS 2770 Part 1:1967 – (reaffirmed 2002) specifications, employing a universal testing machine with a 600kN capacity. Throughout the testing procedure, the pullout specimen was situated on the testing apparatus to facilitate axial extraction of the embedded bar. In accordance with IS 2770 directives, the end of the bar subjected to the pulling force was the one extending from the top surface of the cast cube. The experimental arrangement is depicted in Figure 3. A linear variable differential transformer (LVDT) was utilized to quantify bar displacement. Two LVDTs were installed, one at the loaded termination and the other at the unconfined end of the bar, to gauge bar slip in relation to the concrete. The LVDT positioned at the unconfined end was situated to make contact with the exposed extremity of the rebar on the rearward section of the specimen, facilitating the measurement of bar slip. Loading of the

reinforcing bars ensued monotonically at a maximum velocity of 22.5 kN/min. Loading persisted until specimen failure transpired. Continuous recording of loads and deformations was executed throughout the testing regimen. Subsequently, the recorded loads were converted into bond stress. Assuming an even distribution of bond stress across the embedment length within the concrete, the mean bond stress (τ_b) linking the reinforcing bar to the adjacent concrete was computed.

$$\tau_b = \frac{P}{\pi dl}$$

where, τ_b is the bond stress in (MPa), P is the applied load (N), d is the diameter of bar (mm) and l is the embedded length of bar (mm).



Fig 3. Pullout test setup

Table IV Specimen description

Specimen designation	Description
NC	Normal Concrete
BC	Bacterial Concrete

III. RESULTS AND DISCUSSION

A. Compressive strength: On 28th day three cubes of each normal concrete and bacterial concrete were tested and average of the compressive strength were obtained as 33.7 MPa and 38.9 Mpa. Table V shows that bacterial concrete cubes have 15.43% higher compressive strength than the normal concrete .

III. TABLE V COMPRESSIVE STRENGTH

IV. 28 TH DAY COMPRESSIVE STRENGTH IN MPA	
V. NORMAL CONCRETE	VI. 33.7
VII. BACTERIAL CONCRETE	VIII. 38.9

IX.

B.Flexural strength : : On 28th day three cubes of each normal concrete and bacterial concrete were tested for flexural strength. From Table VI, the Flexural strength of bacterial concrete was obtained as 5.26 Mpa and 6.06 MPa. The flexural strength of bacterial concrete showed an increase of 15.21% than normal concrete.

X. TABLE VI FLEXURAL STRENGTH

XI. 28 TH DAY FLEXURAL STRENGTH IN MPA	
XII. NORMAL CONCRETE	XIII. 5.26
XIV. BACTERIAL CONCRETE	XV. 6.06

C.Split tensile strength: : On 28th day three cubes of each normal concrete and bacterial concrete were tested for split tensile strength. The average of the result of split tensile strength were obtained as Mpa and 3.43 MPa. The results in table VII shows that the bacterial concrete has 33.98% greater tensile strength than normal concrete.

XVI. TABLE VII SPLIT TENSILE STRENGTH

XVII. 28 TH DAY SPLIT TENSILE STRENGTH IN MPA	
XVIII. NORMAL CONCRETE	XIX. 2.56
XX. BACTERIAL CONCRETE	XXI. 3.43

A. Bond Stress

The bond stress values at displacements of 0.025mm and 0.25mm, as stipulated by IS 2770 Part (1):1967 (reaffirmed 2002), are outlined in Table VIII alongside the ultimate load and ultimate

bond stress of all specimens subjected to pullout of reinforcement bars. A comparative examination of bond stress in accordance with IS 2770 specifications at displacements of 0.025mm and 0.25mm was executed. As depicted in Figure 4, the outcomes indicated that, for both 8mm and 12mm bars, the bond stress in bacterial specimens surpassed that of the control specimens. It was noted from Table VIII that, within a given embedment length and concrete composition, the bond stress for smaller diameter bars exceeded that of larger diameter bars. This variation could be ascribed to the increased ratio of concrete cover to bar diameter available in the case of smaller diameter bars, potentially augmenting the bond resistance of the bar. An augmentation in the thickness of the cover surrounding the reinforcement might necessitate a higher load for crack initiation, thereby enhancing bond strength.



a)NCΦ8

b) BCΦ8



a)NCΦ12

b) BCΦ12

Fig 4.Pullout failure

A NOTABLE ENHANCEMENT IN BOND STRESS WAS OBSERVED CONCERNING BOTH 8MM AND 12MM BARS WITH THE INCLUSION OF BACTERIA IN THE CONCRETE MIXTURE. FOR THE 8MM BAR, THERE WAS A RISE OF 4.9% IN COMPARISON TO THE CONTROL SPECIMEN WITH BACTERIAL CONCRETE. LIKewise, FOR THE 12MM BARS, UPON THE ADDITION OF BACTERIA TO THE CONCRETE MIX, THERE WAS A 3.2% INCREASE RELATIVE TO THE CONTROL SPECIMEN.

TABLE VIII PULLOUT TEST RESULTS

Sl no	Specimen designation	Bond stress at 0.025mm slip	% Increase or decrease in bond stress compared to NC	Bond stress at 0.25mm slip	% Increase or decrease in bond stress compared to NC	Ultimate load (kN)	Ultimate bond stress (MPa)	Failure mode
1	NCØ8	8.6	-	8.9	-	37.28	9.9	Pullout
2	BCØ8	8.8	5.88	9.1	2.24	40.21	10.7	Pullout
4	NCØ12	8.2	-	8.5	-	49.63	8.8	Pullout
5	BCØ12	8.1	10	8.7	2.35	55.6	14.7	Pullout

B. Bond Stress-Slip Behaviour

Broadly, the relationship between bond stress and slip characterizes the bonding behavior in reinforced concrete elements. The adhesion between bars and concrete serves as the primary determinant of the bonding performance of the bar during initial loading phases. Once the adhesion between the bar and concrete is compromised, the bar initiates slipping, and the friction between the outer surface of the bar and the concrete governs the bonding mechanism. During testing, the load-slip values were documented for all specimen types, and these values were graphically plotted. All curves exhibited a nearly identical trend. Figure 5 illustrates the graph depicting the bond stress versus slip behavior of specimens with 8mm bars, while Figure 6 displays the corresponding behavior for specimens with 12mm bars. Each curve displayed an initial ascending segment leading to the maximum stress, τ_{max} , followed by a descending or softening segment subsequent to achieving the maximum bond stress. This segment of the curve was distinguished by a notable decline in bond stress concurrent with an increase in bar slip.

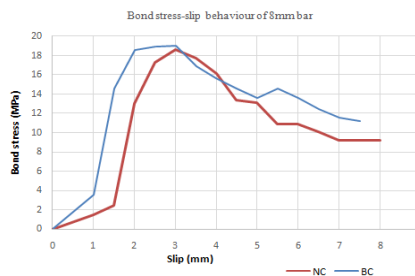


Fig 5. Bond stress – slip behavior of specimens with 8mm bar

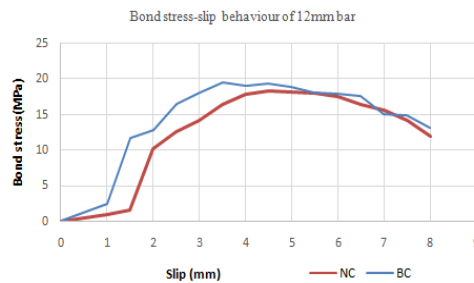


Fig 6..Bond stress vs slip behavior of specimens 12 mm bar

CONCLUSIONS

Based on the experimental results of the study presented in this paper the following conclusions are made.

1. Bacillus subtilis is a soil bacterium with a safer bio safety value of 1 and it can be prepared in a laboratory.
2. The result of compressive strength indicates that the introduction of bacteria in concrete cubes increases the strength compared to conventional cubes. The 28th day compressive strength after curing shows that the strength increased by 15.43%.
3. Flexural strength results of bacterial concrete is increased by 15.21%. Likewise split tensile strength of bacterial concrete is 33.98% more than that of conventional concrete.
4. Contribution of bacteria in concrete increased the bond strength by 4.9% for 8mm bars and 3.2% for 12mm bars.
5. Concrete embedded with smaller diameter bars demonstrates greater strength compared to that of larger bars also all specimens exhibited pullout failure.

REFERENCES

1. Kim Van Tittelboom, Nele De Belie, Willem De Muynck, and Willy Verstraete. (2010) "Use of bacteria to repair cracks in concrete" *cem.conc.res*; 40(1) 157-156
2. Mingyue Wu, Xiangming Hu, Qian Zhang , Weimin Cheng , Di Xue , Yanyun Zhao (2015) "Application of bacterial spores coated by a green inorganic cementitious material for the self-healing of concrete cracks", *cement and concrete composites* 113(2020) 103718
3. Chandni Kumari; Bhaskar Das; R. Jayabalan; Robin Davis; and Pradip Sarkar (2016) "Effect of Nonureolytic Bacteria on Engineering Properties of Cement Mortar toughness" *journal of material in civil engineering* 2016
4. N. Ganesan, P.V. Indira, M.V. Sabeena (2014) "Bond stress slip response of bars embedded in hybrid fibre reinforced high-performance concrete" *Construction and Building Materials* 50

(2014) 108–115

5. Sandip Mondal, Aparna Ghosh (2019) “Review on microbial induced calcite precipitation mechanisms leading to bacterial selection for microbial concrete” *Construction and Building Materials* 225(2019) 77-75.
6. Henk M. Jonkers, Arjan Thijssen, Gerard Muyzer, Oguzhan Copuroglu, and Erik Schlangen. (2010). “Application of bacteria as self-healing agent for the development of sustainable concrete.” *Ecol. Eng.*, 36(2), 230–235
7. Tanvir Manzura, Rafid Shams Huq, Ikram Hasan Efaz, Sumaiya Afrozd , Farzana Rahmane , Khandaker Hossain (2019) “Performance enhancement of brick aggregate concrete using microbiologically induced calcite precipitation” *case studies in construction material* 11(2019) e00248
8. Nguyen Ngoc Tri Huynh, Ngi Mai Phuong, Nguyen Phung Anh Toan (2017) “Bacillus subtilis HU58 immobilised in microbes of diatomite for using in self-healing concrete”, *Procedia engineering* 178(2017) 598-605
9. Manas Sarkar, Dibyendu Adak, Abiral Tamang, Brajadulal Chattopadhyay and Saroj Mandal (2015) “Genetically-enriched microbe-facilitated self-healing concrete a sustainable material for a new generation of construction technology” *Royal society of chemistry* December 2015
10. Hazha Mohammed, Montserrat Ortoneda-Pedrola, Ismini Nakouti, Ana Bras (2020) “Experimental characterisation of non-encapsulated bio-based concrete with self-healing capacity” *Construction and building materials* 256(2020) 119411.
11. Hui Rong, Guanqi Wei, Guowei Ma, Ying Zhang, Xinguo Zheng, Lei Zhang, Rui Xu (2020) “Influence of bacterial concentration on crack self-healing of cementbased material” *Construction and building materials*, 244(2020) 118372.
12. Partheeban Pachaiyannan, C. Hariharasudhan, M Mohanasundram , M. Anitha Bhavani (2020) “Experimental analysis of self-healing properties of bacterial concrete” *Materials today;processings* 33 (2020) 3148-3154
13. Pitcha Jongvivatsakul, Karn Janprasit, Peem Nuaklong, Wiboonluk Pungrasmi, Suched Likitlersuang (2019) “Investigation of the crack healing performance in mortar using microbially induced calcium carbonate precipitation (MICP) method.” *Construction and building materials* 212, 737–744.
14. Mostafa Seifan, Ali Khaje Samani, Aydin Berenjian, (2016) “Bio concrete; next generation construction material.” *Construction and building materials* 100:2591– 2602
15. Ismaeel H.Musa Albarwary, James H.Haido, (2013)“Bond strength of concrete with the reinforcement bars polluted with oil”, *European Scientific Journal*, vol.9, No.6, pp. 255-272, February 2013.
16. Juan Murcia-Delso, Andreas Stavridis,(2011) “Modelling the bond-slip behaviour of confined

large-diameter reinforcing bars”, III ECCOMAS Thematic Conference on Computational Methods in Structural Dynamics and Earthquake Engineering, pp. 1-14, May 2011.

17. P Eswanth, G Dhinakaran,(2017) “Experimental and Theoretical Investigations on Bond Strength of GFRP Rebars in Normal and High Strength Concrete”, IOP Conference Series: Earth and Environmental Science, vol. 80, pp. 1-6, 2017.
18. M Manca1, D Ciancio1and P Dight1(2017)” Fibre reinforced concrete in flexure and single fibre pull-out test: a correlation”, IOP Conf. Series: Materials Science and Engineering 246 (2017) 012017

Behaviour of Reinforced Concrete Beams Strengthened for Shear with the CFRP Fabric Wrapping

Arathi. A
Dept. of Civil Engineering
AWH Engineering College
Kozhikode, Kerala, India
arathia1999@gmail.com

Dr. Sabeena. M V
Dept. of Civil Engineering
AWH Engineering College Kozhikode, Kerala,
India
sabeena@awhengg.org

Abstract— Strengthening of reinforced concrete (RC) beams using carbon fiber reinforced polymer (CFRP) fabric wrapping is a proactive approach aimed at enhancing the structural capacity and resilience of beams before they undergo excessive loading or encounter other stressors. Experimental and numerical studies in this area showed that using fiber-reinforced polymer (FRP) materials to strengthen RC members in shear, flexure and confinement for columns is an effective method to strengthening. This method has numerous advantages over conventional methods, such as increased load carrying capacity, improved durability, rapid installation, minimal additional weight. This experimental paper focus on the CFRP strengthening of RC beams which are shear deficient. Different configurations of fabric wrapping were performed such as 90° U-wrapping (WU1) and strip wrapping (WS1), 45° U-wrapping (WU2) and strip wrapping (WS2). The test results are studied in terms of load-deflection behaviour, ultimate load carrying capacity, energy absorption and crack pattern. The results shows that the beam strengthened by 45° strip wrapping (WS2) increased the ultimate load carrying capacity by 75% with respect to the control beam, while the others WU1, WS1, WU2 the load carrying capacity increased by 40%, 45% and 60% respectively.

Keywords— *Shear strengthening, The reinforced concrete beam, CFRP fabric wrapping, Ultimate load-carrying capacity.*

INTRODUCTION

In recent years, the field of concrete structure strengthening has emerged as a significant area of interest. Consequently, the development of effective strengthening techniques has become a crucial research area in structural engineering. There are several effective methods to enhance the structural performance, the extension of service life, and ensuring safety under increased loading conditions. Some of the primary techniques used in RC beam strengthening are external bonding of FRP composites, steel plate bonding, section enlargement, near surface mounted reinforcement (NSM), prestressed FRP systems.[1] In this study, shear strengthening with CFRP fabric wrapping involves the application of CFRP strips in RC beam with different configurations to enhance their

resistance to shear forces. This approach has gained prominence due to its effectiveness, ease of implementation, and capacity to address shear deficiencies in existing reinforced concrete (RC) structures. Utilizing CFRP fabric wrapping alters the performance of RC beams in several ways. Initially, it boosts the shear capacity of the beams by imparting extra tensile strength to the concrete in the shear-critical zone. Additionally, CFRP wrapping enhances the ductility and deformation capability of beams under load. Moreover, it can delay or thwart the emergence of shear cracks in RC beams, thereby reducing the risk of sudden failure and enhancing overall safety. By confining the concrete and providing supplementary reinforcement, CFRP wrapping effectively manages crack width and halts crack propagation.

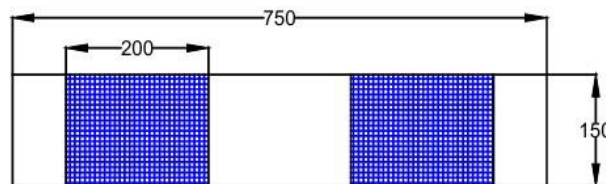
OBJECTIVES

The prime research objectives of this present work are as follows:

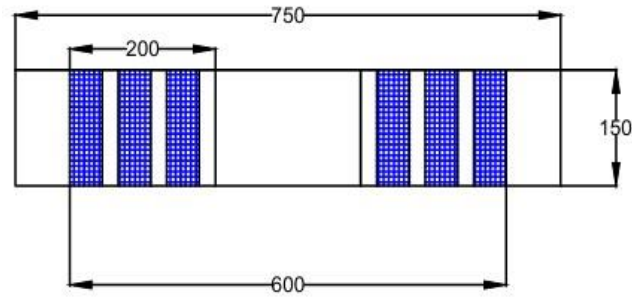
- To determine the mechanical properties of concrete specimens.
- To study the shear behaviour of unstrengthen RC beam.
- To analyze the shear behaviour of strengthened beam for the shear zone wrapping using CFRP fabrics with different alignment.

EXPERIMENTAL PROGRAMME

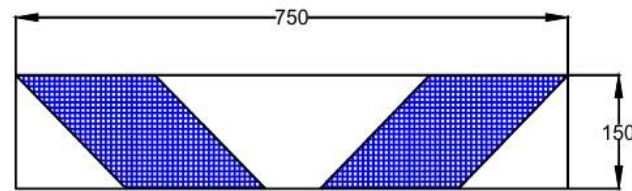
This experimental programme was carried out to evaluate the load-deflection behaviour of reinforced concrete beams in shear with and without carbon fiber reinforced polymer (CFRP) fabric wrapping. This experimental work consisted of casting and testing eight reinforced concrete beams made of M25 grade concrete having cross-sectional dimensions 100x150 mm and a length of 750mm. The reinforcing bar of 8mm diameter were used for both main bar and stirrup. Of the eight beams for studying shear behaviour two beams were control beams, with no wrapping named as SCB1 and SCB2. While other remaining beams were wrapped with CFRP in four patterns shown in Fig.1. First pattern is 90° U-wrapping (WU1), second pattern 90° strip wrapping (WS1), the third pattern 45° U-wrapping (WU2), fourth pattern 45° strip wrapping (WS2). Epoxy resin Vittspol-2007 were applied to the concrete surface, then the CFRP fabric is placed on top of epoxy resin coating and the resin is squeezed through the roving of the fabric with the roller.



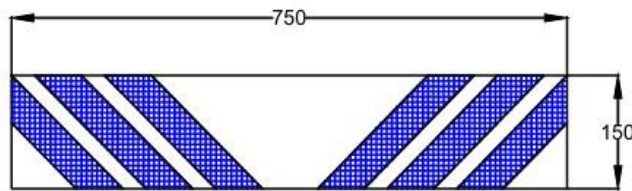
(a)



(b)



(c)



(d)

Fig.1: Different patterns, (a) 90° U-wrap, (b) 90° Strip Wrap, (c) 45° U-wrap, (d) 45° Strip wrap

A. Materials

Portland Pozzolana Cement of 53-grade, complying with IS 1489 (part 1) : 1991 (fly ash-based) standards [11], was employed. Cement tests were carried out in accordance with IS 4031-1988 [12]. Manufactured sand (M-sand), meeting the criteria of passing through a 4.75mm IS sieve and conforming to grading zone II of IS 383-1970 [13], was utilized as fine aggregate. Crushed stones with a maximum size of 20mm were utilized. Epoxy resin Vittspol-2007, with a specific gravity of 1.12, was utilized as adhesive, conforming to IS 6746-1994 [14]. The epoxy resin's properties are outlined in Table 1. Carbon fiber reinforced polymer (CFRP) fabric, with a thickness of 0.3mm, was employed. Details of the CFRP fabric are provided in Table II. Fe500 TMT reinforcement bars, 8mm in diameter, were utilized. Properties of the reinforcement bars obtained through tension tests are presented in Table III.

B. Epoxy Resin

Epoxy resin is a liquid material which is made from many synthetic polymers. Epoxy has been widely used with fiber reinforced polymer composites. For good adhesion hardener and catalyst was added to the epoxy. Catalyst plays a major role during the setting.



Fig.2 : Epoxy resin and hardener.



Fig.3 : CFRP fabric

TABLE I: The properties of Epoxy resin Vittspol-2007

Description	Value
Appearance	Pale yellow, clear liquid
Specific gravity	1.12
Poisson's ratio	0.23
Density	2160 kg/m ³
Viscosity at 25° C	454 cps
Gel time	12 Min

TABLE II: Properties of CFRP fabrics

Properties	Specifications
Thickness	0.3mm

Weight	350gsm
Tensile strength	3530 MPa
Elastic modulus	230 GPa
Poisson's ratio	0.3

B. Detailing of reinforcement

The RC beam measures 750mm in length. Regarding reinforcement detailing for shear behavior, stirrups are solely placed at load and support points. The reinforcement layout is illustrated in Fig 4. The beams had dimensions of 100mm width and 150mm depth, respectively. Fe500 grade TMT bars were employed for reinforcement. At the bottom, two 8mm diameter bars served as the main reinforcement. Additionally, two 8mm diameter bars were positioned at the top as stirrup holders. Vertical stirrups, consisting of four 8mm bars spaced at 200mm intervals, were incorporated.

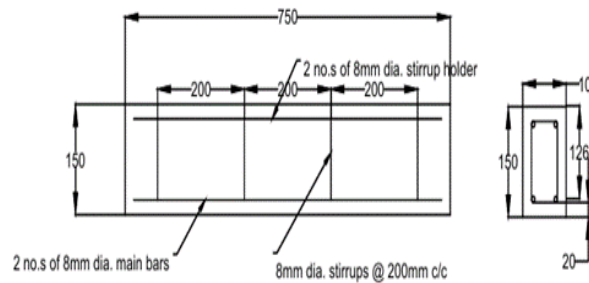


Fig 4: Reinforcement Detailing

TABLE III : Properties of the reinforcement bar

Description	Values
Nominal diameter of the bar	8mm
Actual diameter of bar	8.17mm
Ultimate strength	568 N/mm ²
Yield strength	485 N/mm ²
Modulus of elasticity	242 N/mm ²

C. Mix Proportions

In this experimental investigation, concrete of M25 grade was utilized, and the mix design was formulated according to IS 10262:2019 [15]. The specific mix proportions are outlined in Table IV. Initially, the necessary quantities of cement, M-sand, and coarse aggregate were combined thoroughly in a standard concrete mixer for a duration of 2 minutes. During the mixing process, 80% of the water was added initially and mixed uniformly, followed by the addition of the remaining 20% of water later on.

TABLE IV: Mix Proportion for M25 Grade Concrete

Designation	Ultimate load (kN)	Percentage increase (%)
SCB 1	30	-
WU1	42.0	40
WS1	43.5	45
WU2	48.2	60
WS2	52.5	75

D. Specimen Preparation

Concrete cube of size 150mm, Prism of size 100 x 100 x 500 mm and cylinders with a size 150 mm x 300 mm was prepared for testing compressive strength, flexural strength and tensile strength respectively.[16] To evaluate workability of concrete standard test with actions described with Indian standards BIS 1199-1959 [17] are conducted. Cast iron mould was used to cast specimens and all specimens were filled in concrete with three layers and tamping rod was used to compact the specimens in each layer. After 24 hours of air curing, specimens are demoulded and transferred to the curing tank. After 28 days of curing, the specimens were tested.



Fig.5: Prepared cubes, beams and cylinders

E. Casting of reinforced concrete beams

Cement	478.5 kg/m ³
Fine aggregate	578.93 kg/m ³
Coarse aggregate	1038.75 kg/m ³
Water	220.31 kg/m ³

Wooden molds with inner dimensions of 750x150x100 mm were employed. Oil was applied to the inner surface of the formwork to facilitate easy demolding. The required quantities of aggregate, cement, and water were measured according to the mix design. Concrete was mixed using a standard concrete mixer machine to ensure uniform quality. Mixing was carried out for two minutes after all ingredients were introduced into the mixer, as per IS 456:2000 standards. Following the pouring of the first layer of concrete into the mold and leveling it to a height of 25mm (clear cover), the shear reinforcement cage was carefully positioned. Subsequent layers of concrete were poured, compacted, and leveled. After 24 hours of air curing, the specimens were demolded and transferred to a curing tank. After 28 days of curing, the specimens were removed from the water bath.



Fig. 6: Reinforcement cage

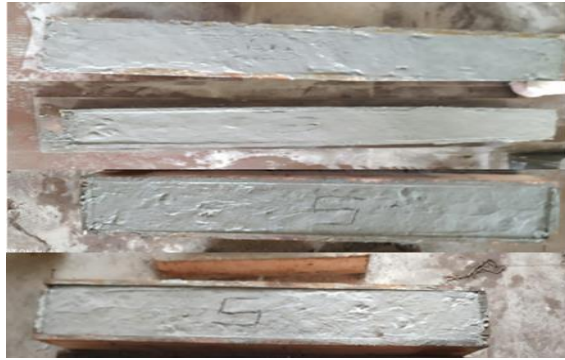


Fig 7: Prepared RC beams

F. CFRP wrapping on RC Beams

After 28 days of curing, the specimens were labeled according to their designated wrapping patterns. Any loose particles on the concrete surface in the required area were removed using coarse sandpaper and cleaned with dry cloths to eliminate dirt and debris, ensuring preparation to the necessary standard. The fabric was then cut to size. Epoxy resin was mixed according to the manufacturer's instructions, using a plastic container (100 parts by weight of Vittspol-2007 to 10 parts by weight of Hardener), and continued until the mixture achieved uniformity. The epoxy resin was then applied to the concrete surface, followed by placing the CFRP sheet on top of the epoxy resin coating, with the resin being squeezed through the fabric's roving using a roller. Air bubbles trapped at the epoxy/concrete or epoxy/fabric interface were removed. Throughout the epoxy hardening process, constant pressure was applied to the fabric surface to extrude excess epoxy resin and ensure good contact between the epoxy, concrete, and fabric. This procedure was conducted at room temperature. Concrete beams reinforced with carbon fiber fabric were air cured for 24 hours before testing.





Fig.7: Wrapped specimen

G. Test Setup and Instrumentation

All the eight beams were tested under two-point loading. UTM of capacity 600kN is used for testing. LVDT was kept at the mid span of the beam to measure central deflections. A dial gauge was kept on the tension side of the beam to measure the lateral deflections at $1/3^{\text{rd}}$ distances. The control beam and strengthened beams were tested up to failure load and deflection values were noted for each load increment of 2.5 kN.



Fig.8: Test Setup

RESULTS AND DISCUSSIONS

H. Testing of R.C Beams

Beams cast were wrapped with CFRP for four different cases as given in Table V. The behaviour of each beam was analyzed by considering its load deflection behaviour, the first crack load and ultimate load.

Table V: Types of beams

Sl. No	Type of beam	Type of wrapping
1	SCB	Control beam
2	WU1	90° U-wrapped beam
3	WS1	90° Strip wrapped beam
4	WU2	45° U-wrapped beams
5	WS2	45° Strip wrapped beam

1. Load Deflection Behaviour

The load-deflection history of all beams was documented, with deflections noted at one-third span and mid-span. It was observed that the deflection at mid-span exhibited a higher value compared to the one-third deflection. Therefore, for comparing load-deflection behavior, the deflection at mid-span was considered. Fig.9 illustrates the load-deflection behavior of all beams. The control beam failed in a brittle manner. Strengthened beams exhibited a higher load-carrying capacity and displayed significant deflection before failure.

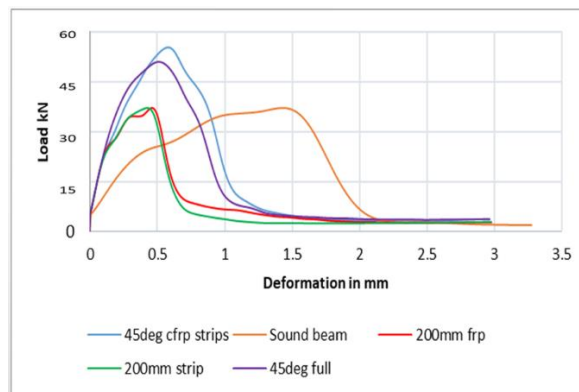


Fig.9: Load – deflection behaviour of beams

J. First Crack Load and Ultimate Load

The crack load and ultimate load of the strengthened beam with their increases with respect to control beam were noted and tabulated.

Table VI: First crack load

Designation	First crack load (kN)	Percentage increase (%)
SCB 1	6.25	-
WU1	7.5	20
WS1	7.5	20
WU2	12	92
WS2	14.2	127

Table VII: Ultimate load

Designation	Ultimate load (kN)	Percentage increase (%)
SCB 1	30	-
WU1	42.0	40
WS1	43.5	45
WU2	48.2	60
WS2	52.5	75

According to Table VI, there is a 20% increase in the first crack load for beams reinforced with shear zone wrapping, both in 90-degree U-wrapping and 90-degree strip wrapping configurations. Beams reinforced with 45-degree U-wrapping exhibit a 92% increase, while those strengthened with 45-degree CFRP strip wrapping show a substantial increase of 127%. The results for load carrying capacity are presented in Table VII. Beams reinforced with 90-degree U-wrap and strip wrap in the shear zone demonstrate load carrying capacities 40% and 45% higher than control beams, respectively. In contrast, the load carrying capacities of the other two beams, reinforced with 45-degree U-wrap and strip wrap, are increased by 60% and 75%, respectively.

K. Deformation at Ultimate load

Deformation at the ultimate load of each specimen were noted. Beams with 90-degree U-wrap and strip wrap shows a percentage increase of 47.3% and 56.05% with that of control beams. The percentage increase in the deflection for 45-degree U-wrap and strip wrap is 118.42% and 143.42% respectively. Beams with 45-degree U-wrap and strip wrapping shows more ductile due to its confinement.

Table VII: Deformation at Ultimate Load

Beam designation	Ultimate deflection (mm)	Percentage increase (%)
SCB 1	7.6	-
WU1	11.2	47.3
WS1	11.86	56.05
WU2	16.6	118.42
WS2	18.5	143.42

IV CONCLUSIONS

- Strengthening of structures using CFRP is an easy technique to be adopted. It helps in reducing the deformation demand and increase the strength and ductility of the structure.
- These materials are of low density, so they can be handled easily and also cost-effective.
- In this experimental study, load-deflection behaviour of reinforced concrete beams wrapped using CFRP is studied.
- Compared to 90-degree U-wrap and strip wrapping, beams strengthened with 45-degree U-wrap and strip wrapped beams shows 60%, 75% increase in the ultimate load carrying capacity.
- From the results, it was found that CFRP wrapping strengthens the beams by delaying the initiation or appearance of cracks.

REFERENCES

- [1] Mehmet Mustafa Onal (2015) “ Strengthening Reinforced Concrete Beams With CFRP and GFRP” *Advances in Materials science and engineering*, Vol.10
- [2] Mohammed Suneer, Er. Rajeev V.S and Er. Sajan jos (2022) “Strengthening of rc beams using glassfibre reinforced polymer sheets and comparison of u wrap and 90 degree strip wrap” *International Research Journal of Engineering and Technology (IRJET)*. Vol.9, Issue 08.
- [3] Haya H. Mhanna and Rami A. Hawileh (2019) “Shear Strengthening of Reinforced Concrete Beams Using CFRP Wraps” *ICSI The 3rd International Conference on Structural Integrity*.
- [4] Mehdi Ebadi-Jamkhaneh, Amir Homaioon-Ebrahimi and Denise-Penelope N. Kontoni (2021) “Numerical finite element study of strengthening of damaged reinforced concrete members with carbon and glass FRP wraps” *Computers and Concrete*, Vol. 28
- [5] M. Chellapandian and S. Suriya Prakash (2019) “Experimental and finite element studies on the flexural behavior of reinforced concrete elements strengthened with hybrid FRP technique” *Composite Structures* Vol.208.

- [6] M. Z. Naser and Rami Antoun Hawileh (2021) “Modeling Strategies of Finite Element Simulation of Reinforced Concrete Beams Strengthened with FRP: A Review” *journal of composite sciences*.
- [7] Muhammad Habib, Chen Zhijun and Zhou Zipei (2018) “Non-Linear Finite Element Analysis Of Reinforced Concrete (Rc) Beams Strengthened With Carbon Fiber Reinforced Polymer (Cfrp) Sheets For Flexure And Shear Using Ansys” *Asian Journal of Mathematics and Computer Research*, Vol.24.
- [8] Dinesh Kumar J and Sattainathan Sharma A (2021) “Study On Flexural Behaviour Of Rc Beam Strengthened With FRP” *International Conference on Physics and Energy*.
- [9] Tulajannanavar and Ranjith P (2018) “Experimental and Analytical Investigation of PCC and RCC Beams Strengthened with CFRP and GFRP Laminates by ANSYS” *IUP Journal of Structural Engineering*, Vol 11, Issue 1.
- [10] Ricardo José Carvalho Silva and David Ermerson Farias Eugênio (2020) “Analysis of reinforced concrete beams strengthened with different CFRP lengths” *Acta Scientiarum. Technology*, Vol.42.
- [11] IS 1489 part 1 : 1991(reaffirmed 2005), Portland Pozzolana Cement Specification.
- [12] IS 4031 Part 4, Methods of physical tests for hydraulic cement Determination of consistency of standard cement paste, Bureau of Indian Standards.
- [13] IS 383, Specification for Coarse and Fine aggregate from natural sources for concrete, 1970.
- [14] IS 6746:1994 Specifications for Unsaturated Polyester Resin Systems.
- [15] IS 10262:2019, Concrete Mix Design Proportioning- Guidelines, Bureau of Indian Standards, New Delhi.
- [16] IS 516-1959 (reaffirmed 2004). Method of test for strength of concrete, Bureau of Indian Standards. New Delhi.
- [17] BIS 1199- 1959, —Methods of Sampling and Analysis of Concrete,2001.

Shape Optimisation of Grooves in Grooved Gusset Plate Damper used in X-braced Frame

Aiswarya Jayaraj K
Dept.of Civil Engineering
AWH Engineering College
Kozhikode, India
aiswaryajr220@gmail.com

Anila. S
Dept.of Civil Engineering
AWH Engineering College
Kozhikode, India
anila@awhengg.org

Abstract— The X-braced frame represents a specialized variation of concentric braced frames. It can be used as a resistance towards the lateral load acting on the structural system. X-braced frames generally exhibit lower ductility when compared to eccentrically braced as well as moment frames, which is often perceived as a drawback of this structural system. To address this limitation, energy dissipation devices can be integrated into the system with X-bracings so that the plastic action will be absorbed and safeguard other structural elements such as columns, beams and connections from earthquake forces. Specifically, X-concentrically braced frames are tailored through variations in groove shapes. Furthermore, the investigation encompasses determining the load bearing capacity and energy dissipation capacities of the dampers. The assessment commences with cyclic load testing conducted using the ANSYS software. The grooves present in GGPD helps in dissipating the seismic energy. The energy dissipation capacity and load bearing capacity of the x-concentrically braced frame equipped with grooved gusset plate damper were compared based different groove shapes. The different shapes used for the analysis were L shape, oval, rectangular and stadium shape. It was observed that among 4 different groove shapes, oval shaped grooves has more energy dissipation capacity with an increase of 10.74%.

Keywords— X-CBFs, GGPD, Energy dissipation capacity, Load bearing capacity, bracings

INTRODUCTION

X braced frame, one of the type of concentric braced frame, can be used for resisting lateral loads. Since X-braced frame has desirable stiffness as well as strength, they are used for resisting seismic loads in structures. Despite this fact, X- braced frames have low ductility compared to eccentrically braced frames as well as moment frames, which can be considered as one of its disadvantage. Lately, investigations have predominantly centered on enhancing braces by integrating energy dissipation devices. These devices aim to absorb plastic action and avert structural failure.

As previously noted in numerous studies, the gusset plate linking the two X braces at the center can fracture as a result of excessive post-buckling deformations of the braces, leading to inadequate energy dissipation behaviour in concentrically braced frames. Over the past two

decades, the utilization of grooved gusset plate dampers for dissipating seismic energy in steel structures has been developed and investigated by various researchers. In this study the material used was structural steel. Characterized as a unique form of steel, structural steel is predominantly utilized in construction for its remarkable stiffness and impressive strength-to-weight ratio. A suggested layout for the X-centrally braced frame includes dividing each of the two cross braces into two segments. These four segments are linked at the bay's center using a grooved gusset plate damper (GGPD), designed with a square aperture at its core. As a result, when a brace experiences tension or compression, it leads to the even distribution of forces across the corresponding sections of the gusset plate, causing in-plane shear. The presence of grooves in the damper helps in energy dissipation by yielding. To study the effect of groove shapes on energy dissipation capacity of the damper, the frame was equipped with different groove shapes within the damper. The different shapes analysed were L shape, rectangular shape, oval and stadium shape. Optimized groove shape with higher energy dissipation capacity as well as load bearing capacity was determined.

METHODOLOGY

L. Description of damper

The braced frame system entails dividing each of the two cross braces into two segments. These four segments are then interconnected at the center of the bay of the frame with the help of GGPD.

Table No.1 Dimension details of GGPD

Description	Value
Dimension of the middle opening	247.1 mm
Length of grooves	70 mm
Width of grooves	20 mm
Width of bracings	40 mm

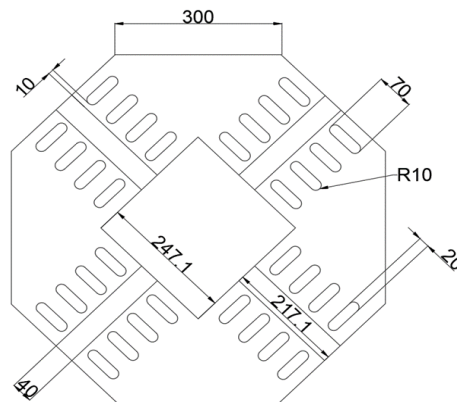


Fig.1. Dimensions of damper

M. Description of groove shapes

Grooves were provided for the gusset plate connecting the bracing at the centre of the bay, this was done to make the gusset plate weaker by keeping the other structural members strong. Different groove shapes were compared for higher load bearing and energy dissipation capacity. Grooved gusset plate damper with L shape, oval, rectangular and stadium shaped grooves were analysed using ANSYS software to study the energy dissipation capacity and the load bearing capacity of the damper. Corresponding hysteresis loops were drawn for each case. The area of the groove shapes were maintained same.

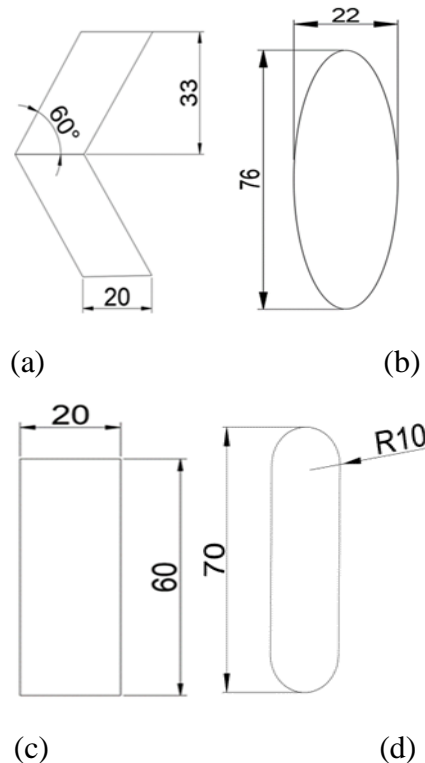


Fig.2. The proposed groove shapes (a) L shape, (b) Oval, (c) Rectangle, (d) Stadium shape

Description of frame

In the steel X-braced frame, the main structural elements, columns, braces, beams, and connections are same. Hinged configurations were provided for all connections. The one and only one difference between the frames are the groove shapes within the damper. It is designed in such a way that all components undergoes inelastic actions and the GGPDs remains in elastic range under the cyclic loading. For columns, braces and beams, channel, tube section and I sections have been chosen respectively.

Table no.2 Dimension details of frame

Description	Value
Span of frame	2897.5 mm
Height of frame	2857.5 mm
Column section	UNP 80
Beam section	IPE 120
Braces	Tube section (40x40x6mm)

RESULT AND DISCUSSIONS

N. Influence of groove shape on the strain energy

Results of analysis of the systems with different groove shapes under cyclic loading are given below in this section.

The structural elements of frames studied in this section are same. The only difference between the frames are the groove shapes in the damper. Distribution of strain energy are shown in Fig.1, Fig.2, Fig.3, Fig.4 for L shaped, oval, rectangular and stadium shaped grooves respectively.

As observed, the cyclic behaviour of GGPD has improved when the damper was equipped with oval shaped grooves compared to other shapes.

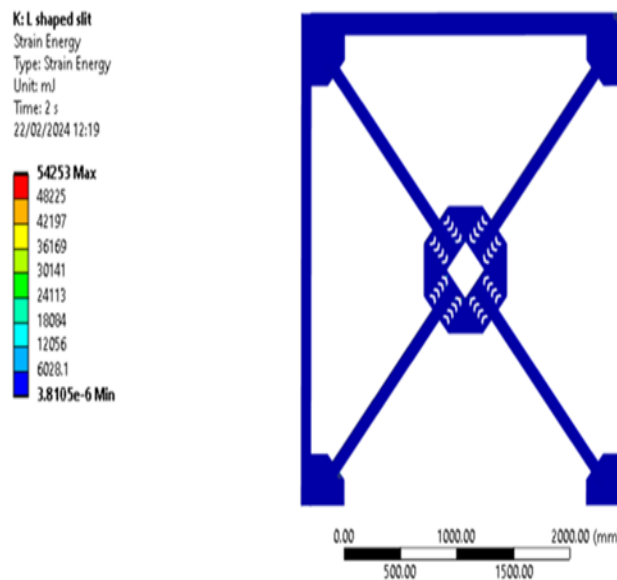


Fig.3. Strain energy of frame with L shaped grooves

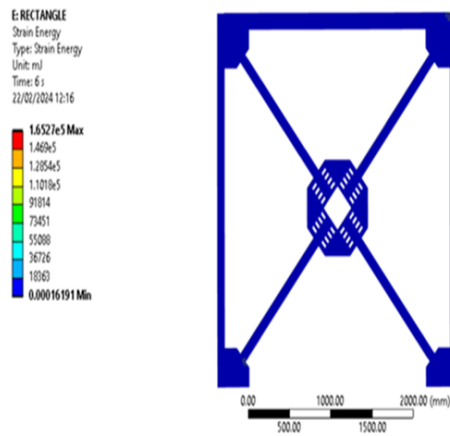


Fig.4. Strain energy of frame with rectangular shaped grooves

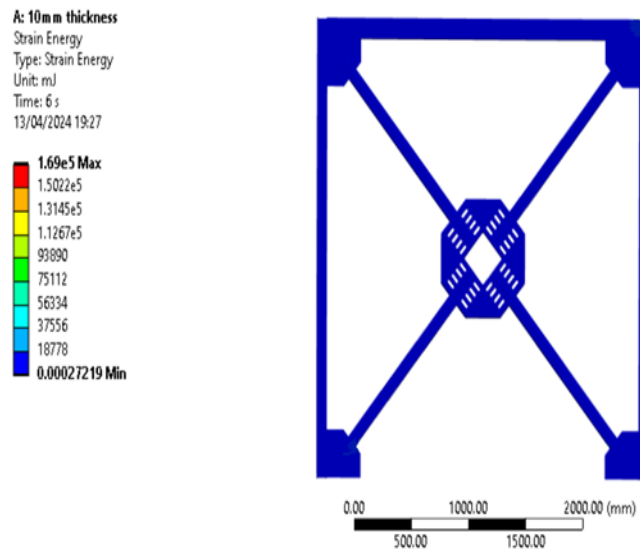


Fig.5. Strain energy of frame with stadium shaped grooves

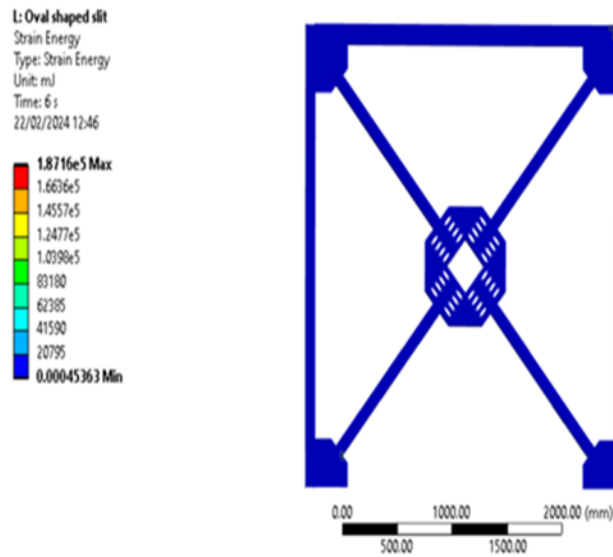


Fig.6. Strain energy of frame with oval shaped grooves.

The following are the results (refer table no. 3) of the frames equipped with GGPDs having L shape, rectangular, stadium and oval shaped grooves.

Table no.3 Effect of groove shape on strain energy

Groove Shape	Strain Energy (mJ)
L Shape	54253
Rectangular shape	165270
Stadium shape	169000
Oval	187160

From the analysis result it was found that oval shaped grooves were having higher energy dissipation capacity with an increase of 10.74%.

O. Effect of groove shape on loading bearing capacity

For studying the effect of different groove shapes under load bearing capacity, load-displacement curves were drawn for each frames. The X-braced frame with the oval shaped grooves in GGPD enjoys well shaped hysteresis curves. It is apparent in Fig.10 that oval shaped grooves were showing greater load bearing capacity.

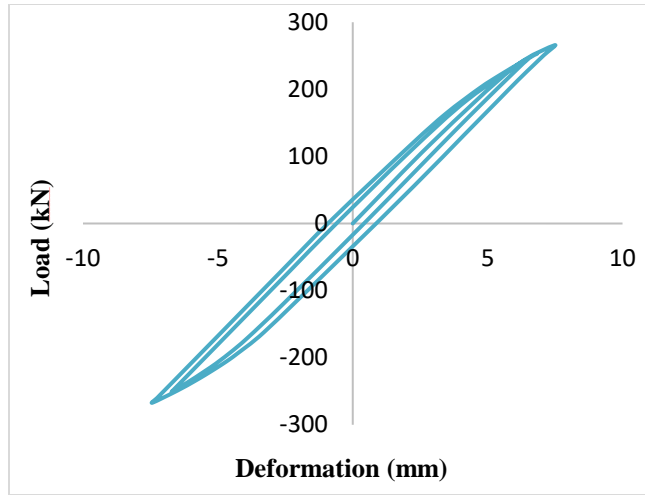


Fig.7. Hysteresis loop of frame with L shaped grooves

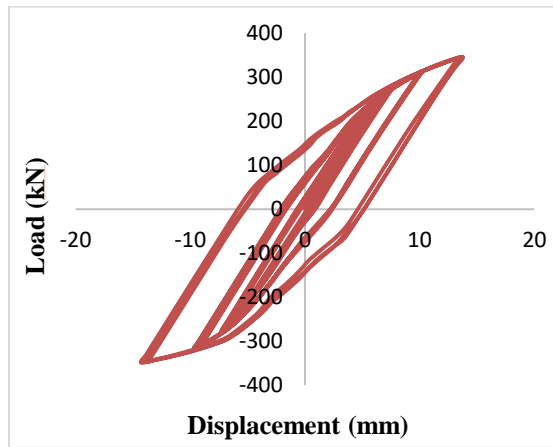


Fig.8. Hysteresis loop of frame with rectangular shaped grooves

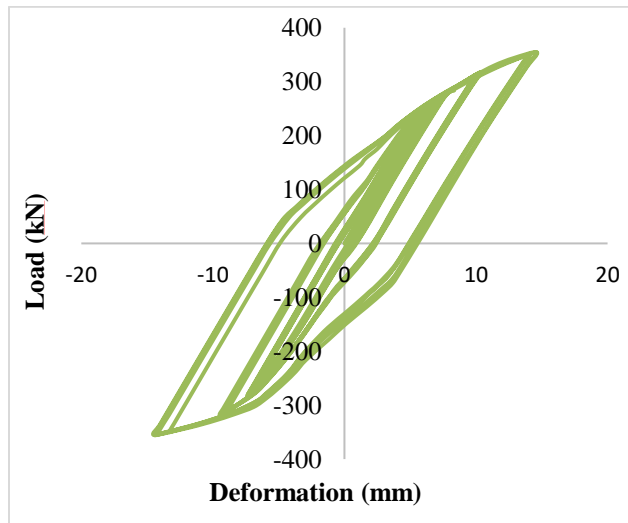
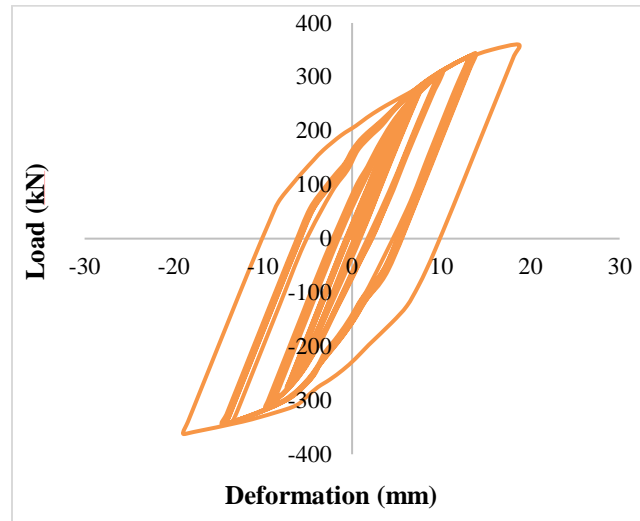


Fig.9. Hysteresis loop of frame with stadium shaped grooves*Fig.10. Hysteresis loop of frame with oval shaped grooves*

CONCLUSIONS

In this study, the X-braced frame equipped with grooved gusset plate damper was analysed for determining the best groove shape with higher energy dissipation capacity. The different groove shapes adopted for analysis were L shape, oval, rectangular and stadium shape. The energy dissipation capacity of GGPD with L shaped, rectangular and oval shaped grooves were compared with stadium shaped grooves. It was concluded that:

- GGPD with L shape, rectangular, stadium and oval shaped grooves dissipates an amount of strain energy of 54253mJ, 165270mJ, 169000mJ and 187160Mj respectively.
- The maximum energy dissipation capacity was attained for oval shaped grooves with an increase of 10.74% when compared with stadium shaped grooves.
- The L shaped grooves were having the least energy dissipation capacity.
- The X-braced frame with the oval shaped grooves in GGPD enjoys well shaped hysteresis curves without any sorts of pinching.
- Among L shaped, oval, rectangular and stadium shaped grooves, the load bearing capacity was higher for GGPD with oval shaped grooves.

Hence from the research it was inferred that frame equipped with grooved gusset plate damper shows higher energy dissipation capacity and load bearing capacity, when the gusset plate has oval shaped grooves.

REFERENCES

- [18] H.A. Amiri, E.P. Najafabadi, H.E. Estekanchi (2018), Experimental and analytical study of block slit damper, Journal of Construction Steel Research, vol. 141, pp. 167–178.
- [19] S.S. Askariani, S. Garivani, A.A. Aghakouchak (2020), Application of slit link beam in eccentrically braced frames, Journal of Construction Steel Research, vol. 170 106717.

- [20] B. Zhao, B. Lu, X. Zeng, Q. Gu (2021), Experimental and numerical study of hysteretic performance of new brace type damper, *Journal of Construction Steel Research*, vol. 183, pp. 106–717.
- [21] Babak Keykhosro Kiania, Behrokh Hosseini Hashemia, Shahabeddin Torabianb (2020), Optimization of slit dampers to improve energy dissipation capacity and low-cycle-fatigue performance, *Engineering Structures*, vol. 214, pp. 110–609.
- [22] Masoud Aminzadeh, Haleh Sadat Kazemi, Seyed Mehdi Tavakkoli (2020), A numerical study on optimum shape of steel slit dampers, *Advances in structural engineering*, Volume 23.
- [23] Seyed Saeed Askariani, Sadegh Garivani (2020), Introducing and numerical study of a new brace-type slit damper, *Structures*; Volume 71, 702-717.
- [24] Jinkoo Kim, Minjung Kim, Mohamed Nour Eldin (2017), Optimal distribution of steel plate slit dampers for seismic retrofit of structures, *Steel and Composite Structures*, vol. 25, pp. 473–484.
- [25] Lee CH, Lho SH, Kim DH, Oh J, Ju YK (2016), Hourglass-shaped strip damper subjected to monotonic and cyclic loadings, *Engineering Structures*, vol. 119, 122–32.
- [26] Lee J, Kim J (2017), Development of box-shaped steel slit dampers for seismic retrofit of building structures, *Engineering Structures*, vol. 150, 934–46.
- [27] Chang-Hwan Lee a, Young K. Ju b, Jeong-Ki Min c, Seung-Hee Lho d, Sang-Dae Kim b (2015), Non-uniform steel strip dampers subjected to cyclic loadings, subjected to cyclic loadings, *Engineering Structures*, vol. 99, 192–204.

Numerical Analysis Of Corrugated Castellated Beam With And Without Openings

Arifa V
Post Graduate student,
Dept. of Civil Engineering
AWH Engineering College
Kozhikode, India
arifav13@gmail.com

Priyanka Dilip P
Assistant Professor,
Dept. of Civil Engineering
AWH Engineering College
Kozhikode, India

Abstract — The construction industry is constantly seeking innovative solutions to optimize the performance and efficiency of structural elements. In this pursuit, castellated beams with corrugated webs have emerged as a promising option. Their unique geometry, including web holes, makes estimating shear load capacity different from traditional beams with solid webs. These beams are becoming increasingly popular in engineering and economics due to their advantages. The openings in the web can take various shapes, as detailed in the research paper, which compares the load versus deflection for castellated beams with rectangular and hexagonal openings, analyzed using software ABAQUS® CAE. The trapezoidal corrugated web configuration notably augments the beam's resistance to buckling failure and furnishes superior resistance to buckling in contrast to a plain web beam. Predominant factors impacting the efficacy of castellated-corrugated web beams encompass the overall beam height and the size of the web opening. The study conducts a comparative analysis of the ultimate load-bearing capability of these beams in relation to both plain and corrugated web beams. Moreover, the manuscript advances an original technological proposal entailing the integration of a trapezoidal-shaped web into a castellated beam. The load-bearing capacity of castellated beams with various web opening shapes, such as rectangles and hexagons, was contrasted with that of the I beam. Among these shapes, hexagon web opening TWHC has higher Material savings with an increase of 13 % compared to the I beam. The results detail that the corrugated web rectangular castellated beams have less weight and more strength than the corrugated web hexagon castellated beam.

Keywords: *Castellated beam, trapezoidal corrugated web, rectangular web opening, ABAQUS® CAE.*

I. INTRODUCTION

Castellated beams are increasingly favoured for their structural benefits, including lightweight construction, cost-effectiveness, high resistance, and quick assembly on-site. Their versatility in applications leverages their enhanced strength and cost efficiency. These beams commonly feature hexagonal, square, or circular openings, with circular-hole beams often referred to as cellular beams. The main reasons for fabricating castellated beams are (a) Increased Strength: By making the beam taller, it becomes stronger against bending and flexing; (b) Reduced Weight: Cutting holes in the beam reduces its weight, making the overall structure lighter and saving on construction

materials; (c) Optimal Use of Materials: They're efficient because they make the most out of existing beam profiles; (d) No Need for Extra Plates: They don't require additional plating, which simplifies construction; and (e) Space for Services: They allow for the passage of utilities and other services. The corrugated design of the web serves as a safeguard, preventing the web from failing prematurely before the beam section reaches its yield capacity. This design ensures that the beam maintains stability and deforms transversely only after reaching its full load-bearing potential. The corrugation geometries of rectangular, trapezoidal, triangular, and sinusoidal are possible. In recent years, trapezoidal and sinusoidal corrugations have increasingly become the preferred choices among structural designers. The incorporation of corrugated steel webs in bridges results in reduced seismic stresses and lighter substructures, facilitating cost-effective and straightforward construction. Despite requiring fewer stiffeners, the corrugated steel web exhibits superior out-of-plane stiffness and shear buckling resistance compared to the flat steel web, thereby significantly reducing material and labor costs for fabrication.

Castellated beams achieve an impressive strength-to-weight ratio and offer significant material cost savings. By cutting and rejoining the web for pattern members, they effectively increase the depth of the beam compared to its original section, enhancing its overall performance.

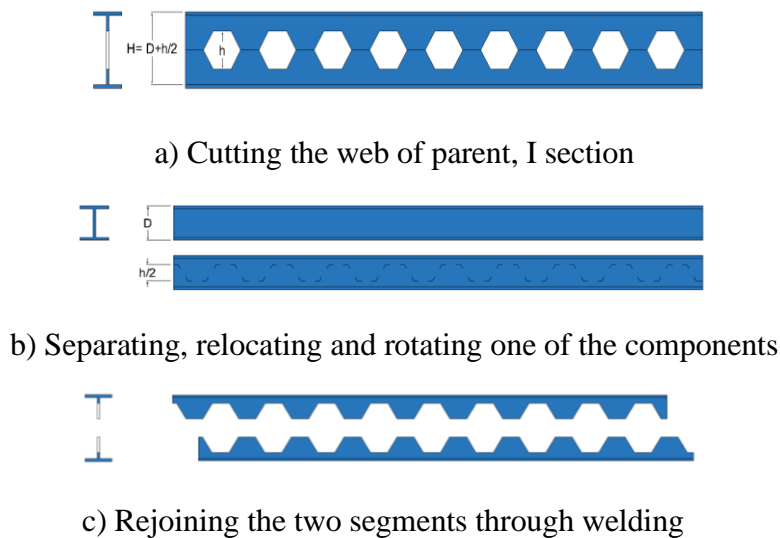


Fig 1. Castellated Beam- Hexagonal Opening,

Castellated beams are constructed from wide-flange I-beams. The web of the section is severed by flame along the horizontal x-x axis in a "Zigzag" configuration as depicted in Figure 1. Subsequently, the two segments are fused together to yield a beam of increased depth featuring a hexagonal aperture in the web. This outcome enhances the beam's sectional modulus and bending stiffness without a corresponding weight increment. Nonetheless, the introduction of apertures in the web will alter the structural performance of the beam compared to that of plain-webbed beams.

II. INVESTIGATION OF CASTELLATED BEAM

Advantages and Applications of Castellated Beams

1. Castellated beams find widespread acceptance in industrial structures, power facilities, and high-rise buildings due to their advantageous affordability in labor expenses.

2. Regarding structural efficacy, the process of dividing and enlarging rolled sections aids in augmenting the section modulus of the beams.
3. Increased load-carrying capacity of the beam and stiffness, leading to improved strength without additional weight.
4. Web holes increasingly serve functional purposes for accommodating piping, conduits, and ductwork in modern construction.
5. Castellated beams are efficient for moderately loaded longer spans, offering increased vertical bending stiffness.
6. Due to their elevated strength-to-weight ratios and reduced maintenance expenses, they have the capability to substitute built-up girders.
7. Widely used in light to medium constructions for medium to long spans, both as secondary or main units.

NUMERICAL PARAMETRIC STUDY

A. Basic Terminology of Castellated Beam

For the parametric study, the corrugated castellated beam model was prepared from the parent I beam section. Figure 2 provides the terminology utilized in the analysis and design of castellated beams, while Table 1 presents their dimensions

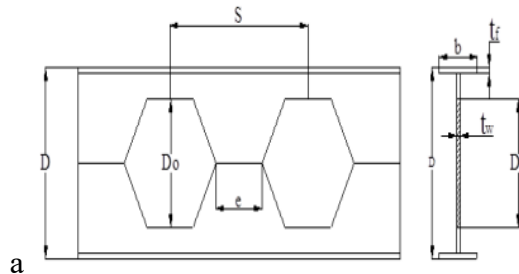


Fig 2. Typical cross-section of the beam

Table 1: Parameter of hexagonal castellated beam

Parameter (mm)	
The total depth of castellated beam D	135
Depth of the opening D_o	50
Width of the flange of castellated beam b	50
Distance between the two perforations measured from centre to centre S	99
Clear distance between two perforations e	30

The thickness of the flange of castellated beam t_f	5
Web thickness of the flange of castellated beam t_w	5

In this study, an I-section (914mm x 95mm x 50mm) beam has been used. Given its castellated nature, two types of apertures are implemented within the web of the beam: hexagonal and rectangular opening shapes. Following the specifications outlined in Euro Code 3 [7], a castellated beam measuring 914mm x 135mm x 50mm was fabricated, featuring an overall thickness of 5mm. Further details regarding the geometry can be found in Table 2, as illustrated in Figure 3.

Table 2: Geometrical specifications of I-beam

Item	Value (mm)
Beam Height	95
Beam Length	914
Web & Flange Thickness	5
Flange Width	50

The beam is constructed using the ABAQUS[®] CAE software. Figure 3 shows the 3D view of the I-section beam

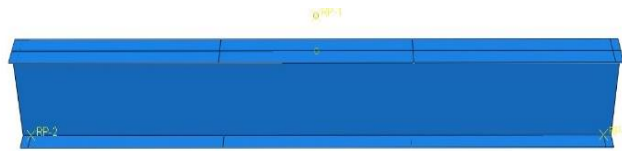


Fig 3. 3D view of I-section beam

B. Basic Terminology of Trapezoidal Corrugated Beam

The Corrugated web beams consist of the trapezoidal corrugated web having 45⁰ corrugations. The side view and top view of a typical trapezoidal web profile are shown in Figure 4.

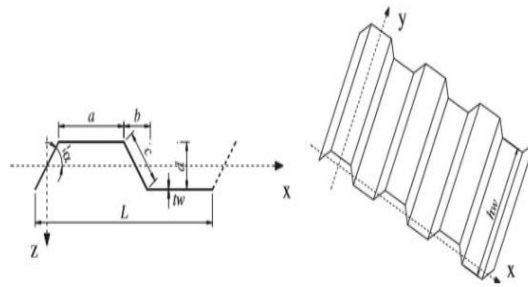


Fig 4. The configuration of trapezoidal corrugated web

Table 3: Corrugation details

Corrugation details	
α	45^0
a	32 mm
b	17
c	26.25
d	20
tw	5

IV.MATERIAL PROPERTIES AND MODELLING

In this study, the finite-element method (FEM) using ABAQUS® CAE software was done on a corrugated castellated beam. The span length of the beam was considered to be 914 mm. Figure 5 illustrates the two distinct types of web openings employed in this research, which are rectangular and hexagonal. The material characteristics of the utilized substances are detailed in the subsequent table 4.

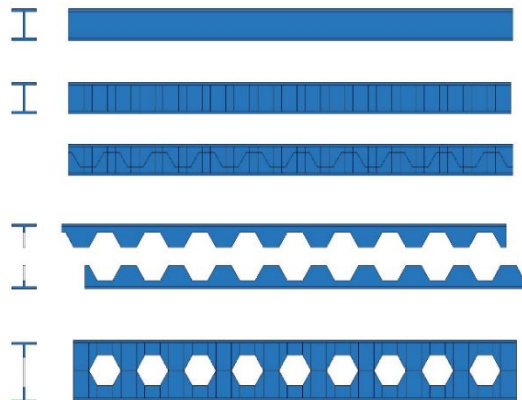


Table 4: Material specifications for the beam model

Material Properties	Specification
Material Used	Structural Steel
Density	7850 kg/m ³
Young's Modulus	200 GPa
Tensile Yield Strength	250 MPa
Compressive yield strength	250 MPa
Poisons Ratio	0.3

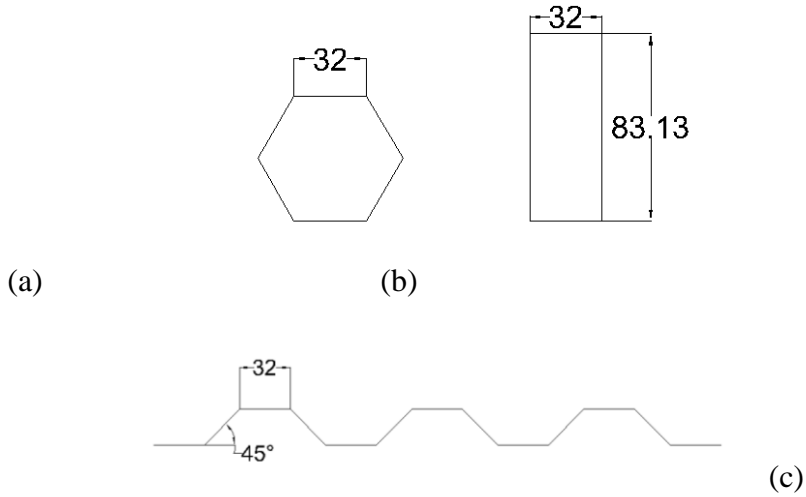


Fig.5 The proposed web opening (a) Hexagon (b) Rectangle (c) without opening

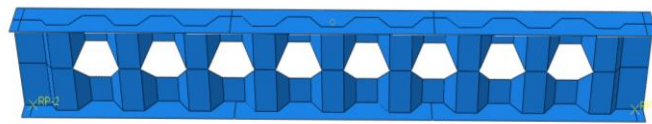
Table 5: Geometric properties of web opening

	1	2
Model	TWHC	TWRC
Web opening type	hexagon	Rectangle
Width of opening (mm)	32	32
Area opening (mm ²)	2660.43	2660.43
Center to center distance (mm)	99	99
No of opening	8	8

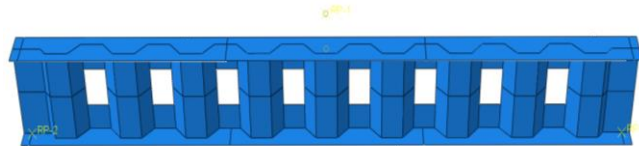
Cutting area per opening is considered the common parameter among the two types of openings. In this study, it is considered that the geometrical shape would be the parameter to select the opening type's name, not the size. To understand the effect of a particular shape of the opening, it is necessary to try the shape with different sizes. Figure 7. shows the rectangular and hexagonal open openings in the web of a castellated beam. The configuration of these specimens has been indicated in Figure 6

Fig.6. (a) To make trapezoidal corrugation in the web. (b) Cutting the web of the Parent I section, (c) Separating, shifting & rotating one of the parts and (d) Rejoining the two parts by welding.

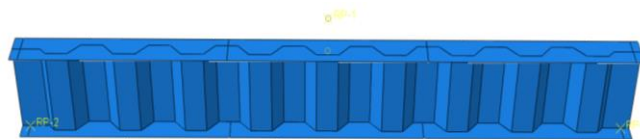
The built-up I-section, with dimensions identical to 85 mm, served as the parent section and is detailed in Figure 3. Additionally, two built-up sections represented castellated beams with a corrugated web. Furthermore, there was a trapezoidal corrugated steel web beam, with specifications provided in Table 5. The configuration of these specimens is illustrated in Figure 7.



a) Trapezoidal web Hexagonal castellated - TWHC



b) Trapezoidal web rectangular castellated TWRC



c) without opening TW

Fig 7. Models of a) TWHC b) TWRC c) TW

V. MESHING

Meshing is an essential property of the model that defines the entire geometry, which is divided into smaller elements to obtain an accurate result. The finer the mesh, the more accurately the 3D model will be defined. In this study, the meshing was done using the mesh module of the

ABAQUS® CAE. Customized meshing was used for the analysis to obtain accurate results and to avoid numerical errors. The generated mesh for different openings is shown in Figure 8.

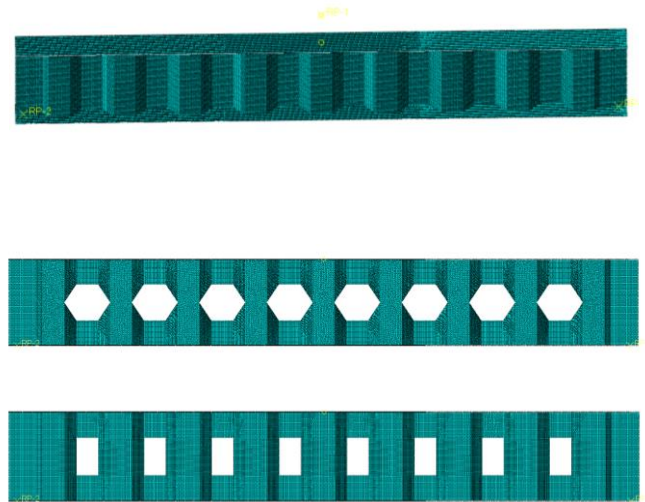


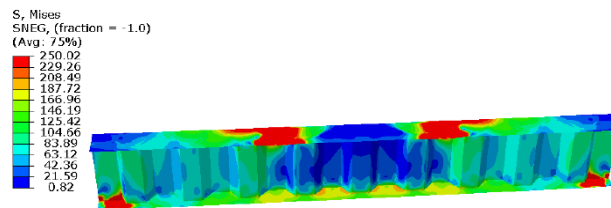
Fig 8. Meshing of the model beam with various openings and without opening

VL. RESULTS AND DISCUSSION

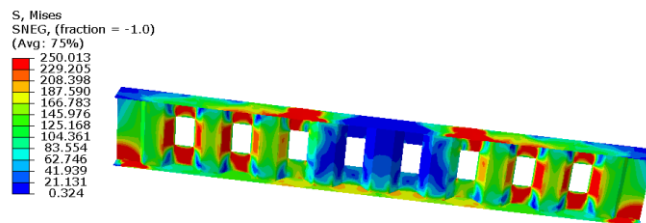
A. Stress analysis

The behavior of corrugated castellated beams was studied. A four-point bending configuration is adopted for analysis of the behavior of the corrugated castellated beam. The numerical model constructed in ABAQUS® CAE software

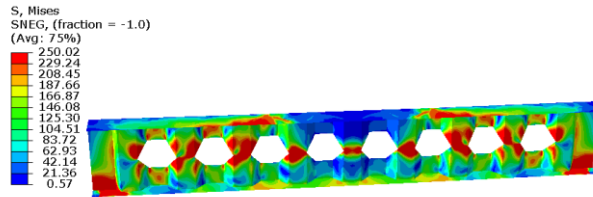
Initially, the I-beam was analyzed without any openings to compare the results with the other models that have openings on the web. The result is shown in Figure 9.



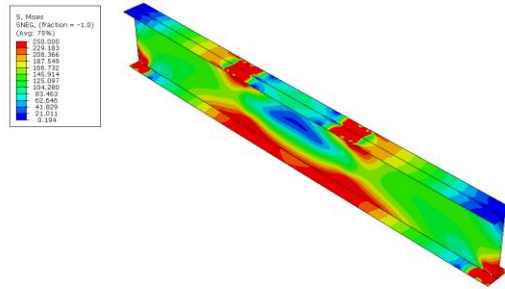
a) Without opening (Trapezoidal corrugated web – TW)



b) TWRC



c) TWHC



d) I beam

Fig 9. Equivalent stress of a) Trapezoidal corrugated web – TW, b) TWRC, c) TWHC & d) I beam

B. Deformation analysis

The deformation analysis of corrugated castellated beams involves evaluating the structural response of beams with corrugated webs and various web openings under loading conditions. This type of analysis helps in understanding how the beam deforms, including aspects such as total deformation, flexural behavior, and the efficiency of different web configurations. The flexural behaviour of the castellated beam was examined under loading in the preceding section for TWHC, TWRC 1, and TWRC 2. In this section, total deformation was obtained. The result is shown in Figure 10.

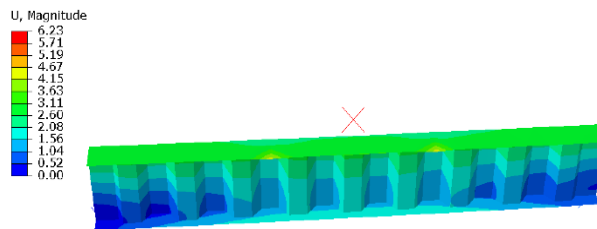
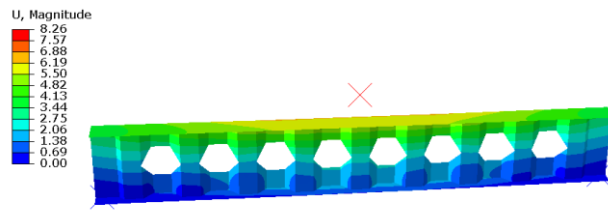
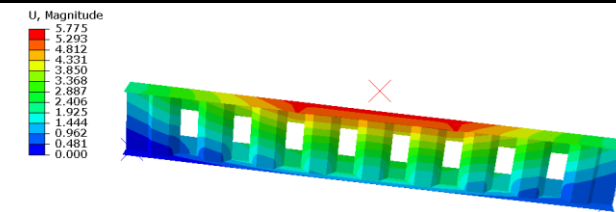


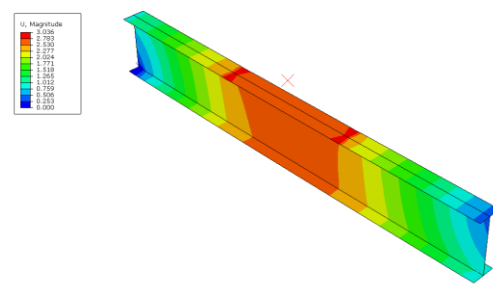
Table 6: comparative behavior of corrugated castellated beam with and without opening

a)

Sl. no	Specimen	Critical load (kN)	Weight (kg)	Strength / weight
1	I B	34.83	8	4.35
2	TW	44.44	9	4.94
3	TWHC	39	7.95	4.91
4	TWRC	41.6	7.95	5.23



c)



d)

Fig.10. Total deformation of a) Trapezoidal corrugated web – TW, b) TWRC, c) TWHC & d) I beam

Table 6 presents the load-bearing capacity and weight of various corrugated web castellated steel beams. Among these, the TW configuration exhibits the highest load-bearing capacity. However, its strength-to-weight ratio is considerably lower than that of the standard I-section beam. In contrast, the TWRC configuration demonstrates the highest strength-to-weight ratio, indicating a more efficient structural performance relative to its weight.

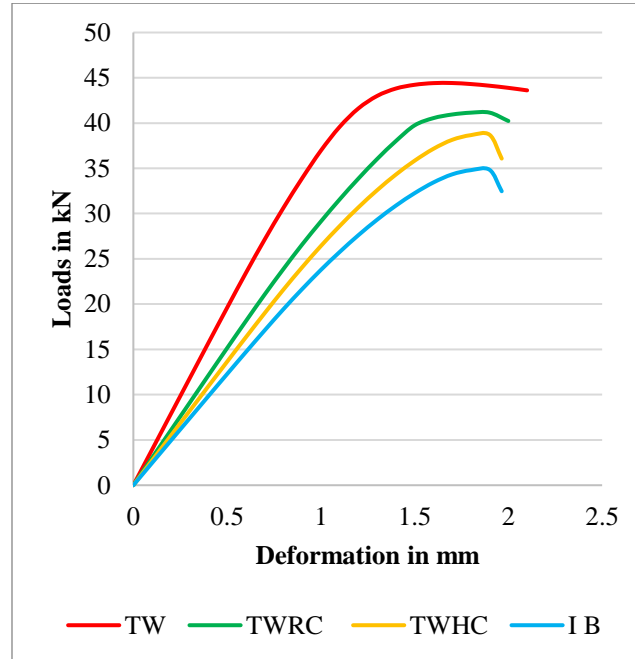


Fig.11 Load deformation graph

VII. CONCLUSIONS

In this study, the finite element method is employed to analyze an I-beam of specified length, incorporating various web openings on the beam's web to evaluate the effectiveness of castellated beams with corrugated webs. The findings derived from the analysis presented in this paper lead to the following conclusions.

- The load-bearing capacity of the castellated beam with and without openings (rectangle and hexagon) was compared with the I beam.
- Hexagon web opening TWHC had higher Material savings with an increase of 13 % compared to I beam.
- The strength-to-weight ratio ranges from 4.35 to 5.23 across the specimens, among these shapes, TWHC showed higher strength-to-weight ratio of 5.23.
- It was observed that TWRC had greater load-bearing capacity compared to the I beam. The Trapezoid web design excels in critical load, and also TWHC showcases higher material savings, (13%).
- The TWRC strikes a balance with a competitive weight-strength ratio of 11.67%.

ACKNOWLEDGMENT

I am sincerely grateful for all the guidance I received from the professors and staff at the institution.

References

- [28] [3] Hadeed, S. M., & Alshimmeri, A. J. H. “*Comparative Study of Structural Behavior for Rolled and Castellated Steel Beams with Different Strengthening Techniques*” Civil Engineering Journal, 5(6), 1384- 1394.
- [29] K. Sriman Narayanan¹, N. Arun Prakash and B. Anupriya “*Comparative Study on Castellated Beam for Circular and Hexagonal Opening Using ANSYS,*” The Asian Review of Civil Engineering Journal of Construction Steel Research, vol. 170 106717, 2020. 3 Vol.7 No.2, 2018, pp. 20-23
- [30] MR, W., AV, S., & Auti, V. A. “*Parametric study of castellated beam with varying depth of web opening*” International Journal of scientific and Research publications, 287
- [31] Larice Gomes Justino, José Carlos Lopes Ribeiro, Gustavo de Souza Veríssimo, José Luiz Rangel Paes, Leonardo Gonçalves Pedroti “*Shear buckling strength of web-posts in castellated steel beams in fire*”. Engineering Structures, 209, 109960.
- [32] Samadhan G. Morkhade, Mrunmayi U. Chavan., “*Structural behaviour of castellated steel beams with reinforced web openings.*” Asian Journal of Civil Engineering, vol. 21, 1067-1078, 2020
- [33] Wakchaure M.R., Sagade A.V and Auti V. A., “*Parametric study of castellated beam with varying depth of web opening.*” International Journal of Scientific and Research Publications, vol. 2, no. 8, pp. 1-5, 2012
- [34] EC3. Euro code 3: Design of steel structures part1-1, General rules for buildings. London (UK), British standard institution BS EN 1993-1-1,2005.
- [35] H W Al-Thabthawee and A Mohammed., “*Experimental study for strengthening octagonal castellated steel beams using circular and octagonal ring stiffeners.*” International Conference on Civil and Environmental Engineering Technologies, 012063. 2019
- [36] amadar A. M. and Kumbhar P. D., “*Parametric Study Of Castellated Beam With Circular And Diamond Shaped Openings.*” International Research Journal of Engineering and Technology, p-ISSN: 2395-0072. 2015
- [37] Frans, R., Parung, H., Sandy, D., & Tonapa, S. “*Numerical modelling of hexagonal castellated beam under monotonic loading*” Procedia engineering, 171, 781-788.

Analysis On The Bending Behaviour Of T Shaped Glulam Beam

Shahaba Sherin P
AWH Engineering college
Kozhikode, India

Jisha P
AWH Engineering college
Kozhikode, India

Minu U
AWH Engineering college
Kozhikode, India

Abstract— Glulam, a sustainable manufactured wood product, is gaining prominence for its numerous advantages. The current study employed an analytical approach using a finite element model developed in ANSYS Workbench 2023 R2 to investigate the flexural properties of glued laminated timber beams (glulam) compared to solid T beams. The research focused on assessing the impact of different lamina thicknesses on glulam beams, using Larix wood. Glulam beams were categorized into three groups based on lamina thickness: 30 mm, 15 mm, and 10 mm. Additionally, solid T beams were modelled for comparison. Both solid wood and laminated wood of Larix species were analysed in ANSYS 23.2.

Keywords— *Glulam Beam, Bending*

INTRODUCTION

Wood is a very old material that people have been using for construction for a long time. It's one of the oldest materials still used in construction. This material has been used for thousands of years before concrete and steel used in construction. Nowadays, timber still used in construction because of its eco-friendly nature, recyclability, light weight and also it is easier to transport, produce, and handle. Today, timber continues to be utilized in construction because of its eco-friendly nature, recyclability, and lightweight yet strong properties, which make it easier to transport, produce, and handle. Timber also can give more variation in architectural design due to its aesthetic qualities and its flexibility can benefits more for the building during earthquake rather than conventional materials such as steel and concrete.

Glued-laminated timber is made by gluing graded sawn timber pieces to create a strong engineered product. The wood products used in construction can be grouped into structural timber, which are boards sawed from logs harvested from the forest, and engineered wood products (EWP), which are usually made from wood in the form of swan lamellas, veneers, particles, or fibres, usually glued together with some kind of adhesive. Typical EWP products are: glued laminated timber (GLT), laminated veneer lumber (LVL), fibreboards, oriented strand boards (OSB), plywood, and cross-laminated timber (CLT). The thickness of individual laminations may not exceed 50 mm. The advantage of glulam is shorter lengths of commercially available sawn timber can be structurally end jointed with adhesives to produce the required full-length laminations. Glulam offers the additional advantage of virtually unlimited flexibility in shape and size.

Glued laminated timber or glulam is a construction material crafted through a precise manufacturing process that capitalizes on the strength and durability of wood. It commences with the selection of superior softwood lumber, which is then processed into uniform laminations of specific thickness. These laminations undergo careful grading to ensure consistent quality with any defects like knots or splits being meticulously removed. It ensures structural integrity, uniform stress distribution, optimal adhesive bonding, dimensional stability, aesthetic appeal, and compliance with industry standard and also to prevent issues such as warping, the moisture content of the laminations is controlled. High-strength adhesives are then applied to the surfaces of the laminations and they are stacked in a parallel arrangement to ensure uniform strength properties. Each type of glue requires a certain temperature and compression to cure. Besides the quality of the glue, this curing process defines the quality of the end product. If the glue is not cured well, the glue laminated timber can delaminate after a certain period of time. Hydraulic presses exert pressure during the curing process, creating a robust bond. After curing, the glulam beams are shaped, sized, and undergo quality control inspections. All glue laminated timber products are checked one last time during packaging to ensure a flawless high-quality product. Depending on the application and aesthetic requirements, glulam beams may receive surface finishes or treatments such as sanding or coating for enhanced performance. This process yields structurally sound, aesthetically pleasing, and environmentally sustainable construction elements, often used as beams, columns, or trusses in a wide range of architectural and structural projects.

FINITE ELEMENT MODELLING

P. Description of Experiment

In this experiment, T-shaped glulam beams with various lamina thickness (30 mm, 15mm and 10 mm) and solid T-beams is considered. The objective of this study is to assess the flexural properties of T-shaped glulam timber beams and its comparison with solid T-beams. Its focus lies in analytically determining whether laminated wood could effectively replace solid wood. A two-point bending test was performed to determine the bending behaviour of glulam beams.

Q. Material and modelling

In this analytical investigation, finite element analysis was carried out employing the ANSYS version 23.2 software for the study. Table I provides the dimensions of the model, while the different dimensions of the specimens are indicated in Figure 1. All the models in this study are of same dimension.

TABLE I. DIMENSIONS OF MODEL

l (mm)	b (mm)	h (mm)	t ₁ (mm)	t ₂ (mm)
2300	225	330	25	30

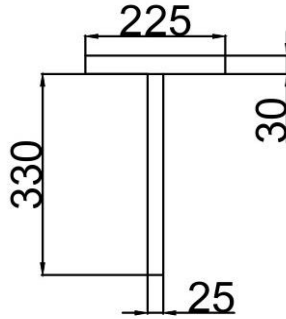


Fig. 1. Dimension of T beam

The glulam beam constructed from laminated engineered wood products, exhibits anisotropic plastic deformations. Table II details the mechanical properties of glulam, while Table III presents the properties of glue. Wood demonstrates orthotropic behavior with considerations for three primary directions: longitudinal, tangential, and radial. This orthotropy is characterized by three moduli of elasticity (E_1 , E_2 , and E_3), three moduli of rigidity (G_1 , G_2 , and G_3), and three Poisson's ratios.

TABLE II. MECHANICAL PROPERTY OF GLULAM

Elastic modulus (MPa)	E_1	12690
	E_2	954.1
	E_3	528.8
Shear modulus (MPa)	G_1	954.1
	G_2	791.2
	G_3	46.5
Poisson's ratio	ν_1	0.3
	ν_2	0.3
	ν_3	0.4
Density (kg/m^3)		670
Yield strength (MPa)		71.75

TABLE III. PROPERTIES OF GLUE

Description	Value
Elastic modulus (MPa)	471
Poisson's ratio	0.3



Fig. 2. Solid T beam

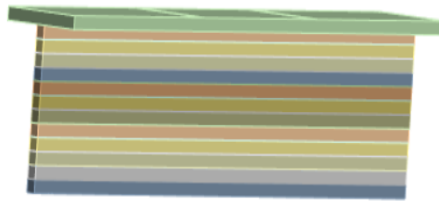


Fig. 3. T-shaped beam with lamina thickness of 30mm

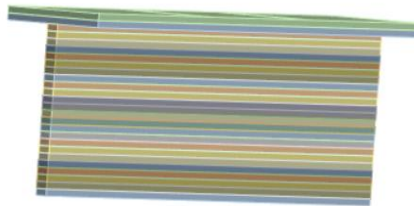


Fig. 4. T-shaped beam with lamina thickness of 15mm

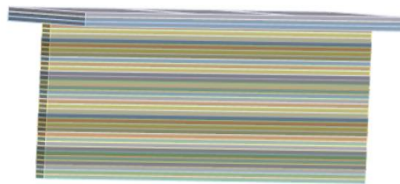


Fig. 5. T-shaped beam with lamina thickness of 10mm

In this study, the initial finite element model focuses on solid wood simulated using ANSYS 23.2. To enhance the accuracy of the numerical simulation in static structural analysis, various mesh sizes were evaluated. The model incorporates engineering data such as density, orthotropic elastic properties and strength properties. Geometry construction was achieved using ANSYS sketching and extruding tools. Loading and support conditions were applied to the top and bottom faces of the wood respectively using the projection tool on a new plane.

Mesh refinement was iteratively performed to improve accuracy, utilizing the sweep method with 250 divisions. Each loading point experienced a force of $0.5F$ kN, where F represents the total force applied. For both the wood laminations and the adhesive layers in the glulam beam, a non-

linear material law from ANSYS was implemented. The interface between laminas utilized poly urethane glue, with a thickness of 0.5mm. Given the minimal thickness of the glue compared to the lamina thickness, a bonded contact connection, an ANSYS feature, was applied to effectively simulate the glue's effect.

RESULTS AND DISCUSSIONS

R. Computational results

The computational results are presented in the following figures. These diagrams illustrate the total deformation and equivalent von Mises stress for the T-shaped solid beam and T beam with varying lamina thicknesses under load as analyzed in the finite element models included in the study.

Fig. 6. Total deformation diagram of solid T beam

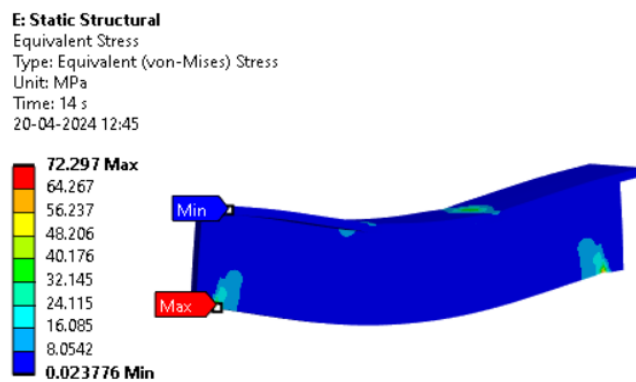


Fig. 7. Von-mises stress diagram of solid T beam

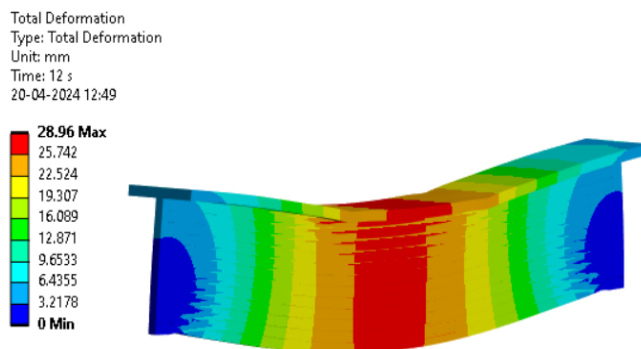


Fig. 8. Total deformation diagram of 30mm thick laminated wood

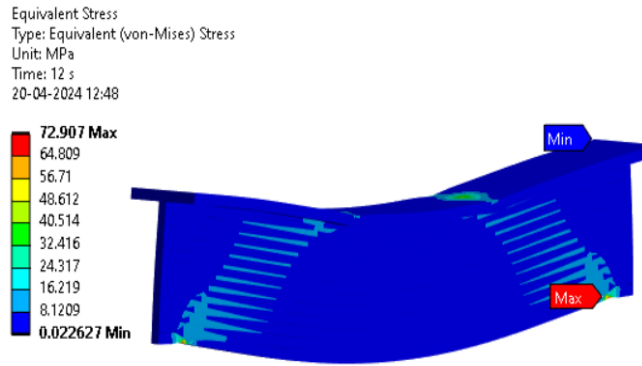


Fig. 9. Von-mises stress diagram of 30mm thick laminated wood

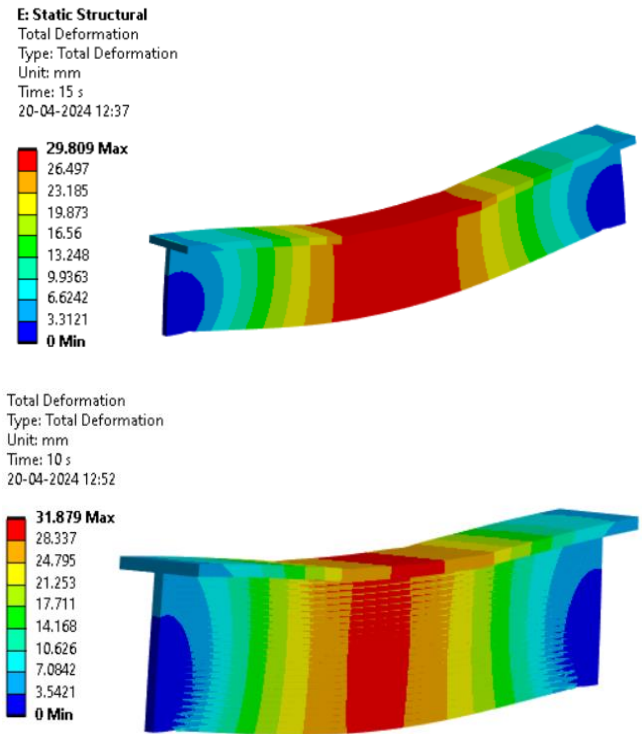


Fig. 10. Total deformation diagram of 15mm thick laminated wood

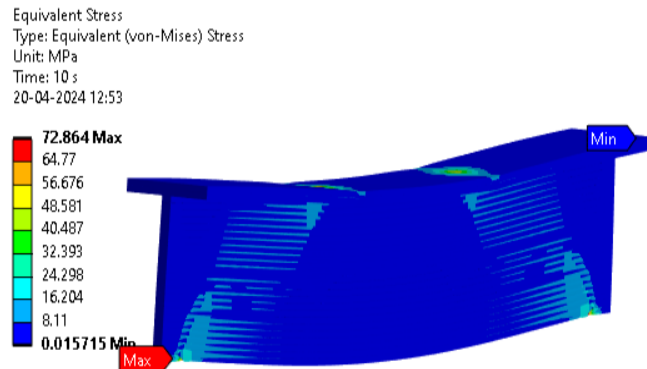


Fig. 11. *Von-mises stress diagram of 15mm thick laminated wood*

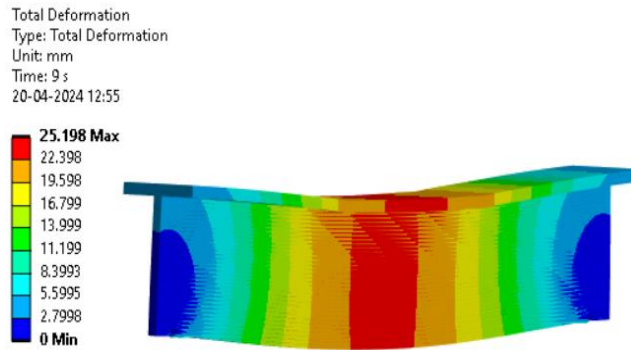


Fig. 12. *Total deformation diagram of 10mm thick laminated wood*

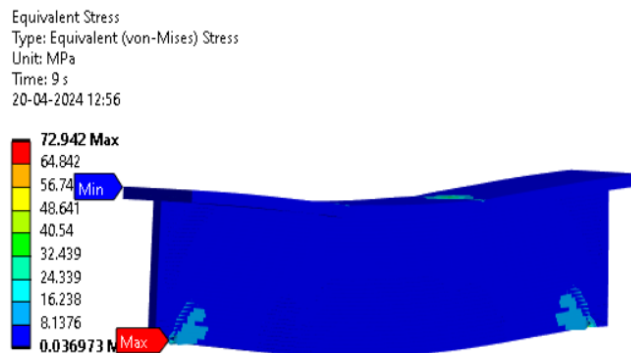
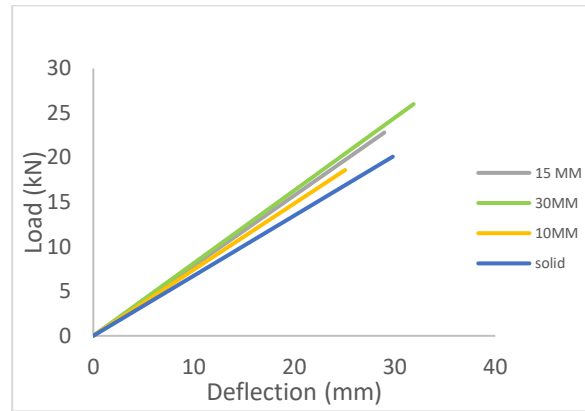


Fig. 13. *Von-mises stress diagram of 10mm thick laminated wood*

Following the modeling of solid wood and laminated wood in ANSYS, they undergo static structural analysis. Subsequently, diagrams depicting the equivalent von Mises stress and corresponding deformation are generated (Fig. 6 - Fig. 13). In these diagrams, the maximum value is represented by red, while the minimum value is depicted in blue.

S. Load deflection curve

A load-deflection graph was generated using the obtained values. Following the analysis of all models, load-deflection graphs were plotted. These graphs for each laminated model were compared with the load-deflection graph of the solid wood model.



Analysis of the load-deflection graph reveals that the ultimate load increased by 29.35% for the 30mm thick laminated beam and by 13.43% for the 15mm thick laminated beam, compared to the solid T beam. Conversely, the ultimate load decreased by 7.46% for the 10mm thick laminated beam when compared to the solid T beam.

CONCLUSIONS

A finite element analysis of glulam T beams and solid T beam was done. Based on the parametric study, the following conclusions have been drawn:

- The ultimate load increased by 29.35% for 30mm thick laminated beam when compared to solid T beam.
- The 15mm thick laminated beam experienced a 13.43% increase in ultimate load compared to the solid T beam.
- The ultimate load for the 10mm thick laminated beam decreased by 7.46% compared to the solid T beam.
- 30mm thick laminated beam has greater load bearing capacity compared to solid T beam.
- With an increase in the number of layers, there is a corresponding increase in deflection, whereas the ultimate load tends to decrease.

REFERENCES

- [38] Zhang, X., Luo, J., Luo, L., Sun, Y., & Li, Z., "Experimental and numerical investigation into the bending behaviour of stiffened hollow glulam beams" *Journal of Building Engineering*, Vol.45, 103488,2022.
- [39] C. Arumb, O.O. Ekundayo, J. M. Owoyemic, "Bending Strength Evaluation of Glulam Beams Made from Selected Nigerian Wood Species" *International Journal of Engineering*, Vol. 35, No. 11, 2022.
- [40] Cristian Timbolmas, Rafael Bravo, Francisco J. Rescalvo, Antolino Gallego, "Development of an analytical model to predict the bending behavior of composite glulam beams in tension and compression" *Journal of Building Engineering*, Volume 45, 10347,2022.

- [41] Zhenyu Rao, Fan Ning, Junzhu Li, and Jiejun Wang, "Experimental Study on Bending Behavior and Finite Element Simulation Analysis of Glued Wood Inverted T-beam" *Journal of Engineering Science and Technology*,147-159,2020.
- [42] Alireza Bahrami, Dawod Azizian, "Assessment of Glulam and Reinforced Concrete Beams in Multi-Storey Building" *Civil and Environmental Engineering*, Vol. 18, Issue 1, 66-75,2022.
- [43] Xiaofeng Zhang and Zheng Li, "Shear behaviour of stiffened hollow glulam beams: Experiments, analytical model, and finite element analysis". *Construction and building Materials*,2023.
- [44] M. Khadafi, B. Anshari and J. Fajrin, "Experimental investigation on flexural properties of glulam timber beam reinforced by bamboo strips". *International Journal of Civil Engineering and Technology (IJCET)*Volume 9, Issue 5.69-76, 2018.

Seismic Analysis Of Irregular Building Subjected To Pounding

Hiba Parveen E
AWH Engineering college
Kozhikode, India
hibaparvine@gmail.com

Jisha P
AWH Engineering college
Kozhikode, India City, Country

Abstract— Earthquakes have always been a source of great devastation for mankind. Nowadays with the fast growth of metropolitan cities, land limitation has become a critical issue, thereby resulting in construction of high-rise buildings very close to each other. Such buildings are prone to seismic pounding. Different combination of 12 storey and 8 storey building having different plan irregularities was considered for the analytical study using ETABS software. The pounding effect depends on building characteristics, ground motion characteristics and soil structure interaction. The parameters like displacement, impact force, storey shear was determined.

Keywords— *Seismic pounding, plan irregularity, soil structure interaction.*

INTRODUCTION

Areas with dense populations often feature buildings with insufficient gap distances due to commercial and architectural considerations. Insufficient gap distances can lead to adjacent structures colliding with each other under seismic loads. The increase of demand in structures and decrease in space availability has led to the phenomenon of ‘building at proximity’ [1]. If two structures have same dynamic property or have sufficient separation gap among each other, the ground motion leads to in phase vibration among them and there will not be any sign of pounding between them. But, if the ground motion results in out of phase vibration the chance of collision is high, if there is insufficient separation gap among the same. The representation of above-mentioned phenomenon is shown in Figure 1. The effects of pounding may range from non-structural to structural failures and can even led to total collapse of the buildings.

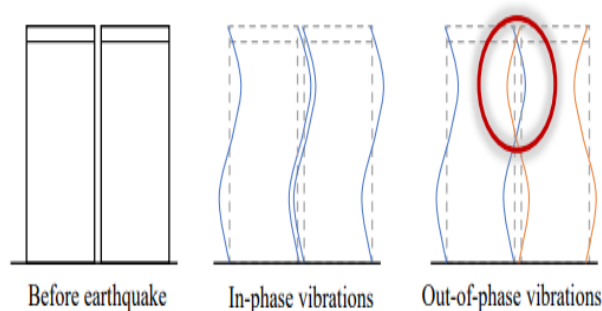


Fig. 1. In-phase and out-of-phase vibrations

T. Causes and effects of pounding

The type and severity of damage to structures during pounding vary depending on the intensity of the collision. Damage can range from local failures to global collapses. Local failures occur when the point of impact between two structures differs in height, number of stories, or phase, especially when the shorter structure is less flexible than the taller one. Additionally, local pounding can be caused by thermal expansion at construction joints. Insufficient lateral separation between neighboring structures or insufficient lateral resistance can also lead to local pounding damage. To mitigate the risk of pounding, neighboring structures should have similar dynamic characteristics and equal heights.

Global failures can result from the collapse of damaged floors or the total collapse of an entire structure. For example, when the roof of one structure collides with the columns of another, the columns may sustain localized damage. To prevent structural pounding, it is necessary to either provide sufficient separation between structures or design the structures to withstand the additional forces resulting from pounding.



Fig .2. Effect of pounding high rise buildings

OBJECTIVES

- To analyze the pounding effect by considering plan irregularity of RC structure.
- To study the soil structure interaction effect on pounding in irregular structure.

METHODOLOGY

Developing modal using Commercial finite element analysis Software ETABS. Then load cases and time history function were defined to perform time history analysis. Time history analysis of a 12 storey and 8 storey building to find the pounding effect between the building by time history analysis for Kobe earthquake is done. The buildings were connected using a compression only gap element to simulate pounding. Extracting result like displacement, storey drift, storey shear and impact force.

BUILDING MODELLING

For this study, a 12-story building and 8 storey building with 3.75m storey height, regular in plan was modelled. These buildings were designed in compliance to the Indian Code of Practice for Seismic Resistant Design of Buildings IS1893 part 1 2016 .The buildings were provided with fixed base. The buildings were modelled using software ETABS.

TABLE I. BUILDING PARAMETERS.

No of bays in x direction	4
No of bays in y direction	4
Spacing of each bay	5m
Grade of concrete	M25
Grade of steel	Fe415
Slab thickness	150mm
Soil type	II
Live load	$4kN/m^2$
Zone	IV

TABLE II. SECTION PROPERTIES.

	Storeys	Column (mm)	Beam (mm)
12 storey	1-4	650X650	500X600
	5-8	300X600	550X550
	9-12	300X550	450X450
8 storey	1-4	600X600	300X600
	5-8	500X500	300X550

U. Gap Element

Gap element is used to model the pounding force between buildings. Gap element should be approximately 10 times stiffer than the lateral storey stiffness of stiffer building. 40 mm gap was provided for all models. For no pounding cases the gap provided was 1m.

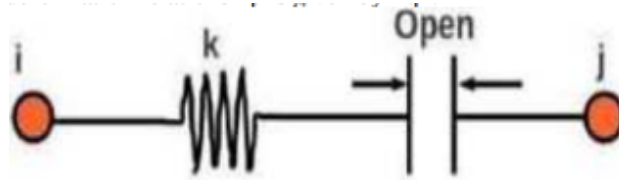


Fig .3. Gap element

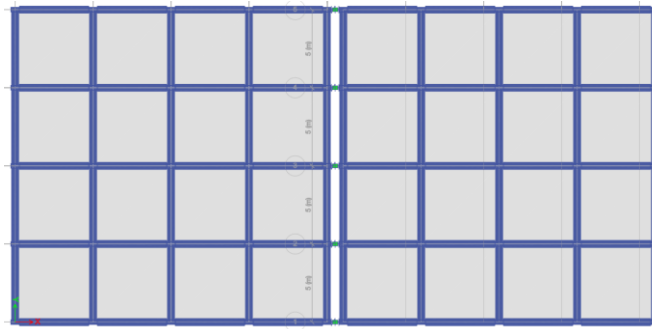


Fig .4. Plan view (R12-R8)

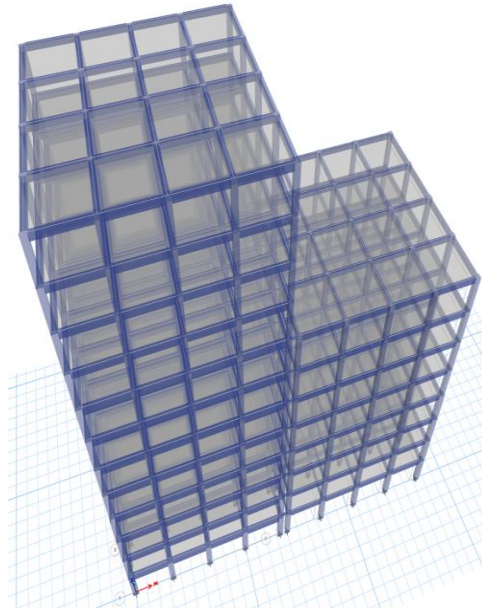
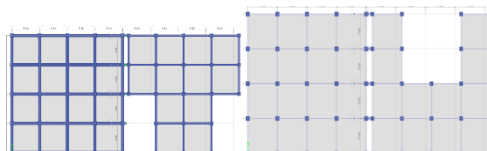


Fig .5. 3-D View (R12-R8)

V. Irregularities

For the combination with the irregular structures the modals with plan irregularity (T, U, H) are used.



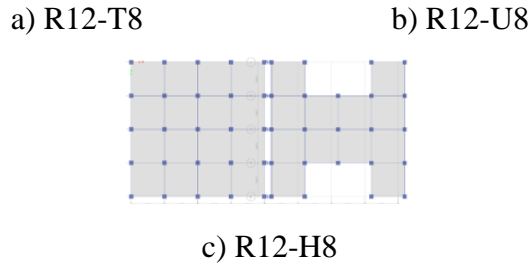


Fig 6. Plane view of a) R12-T8, b) R12-U8, c) R12-H8

W. Ground motion charecteristics

The earthquake Kobe was considered for the time history analysis.

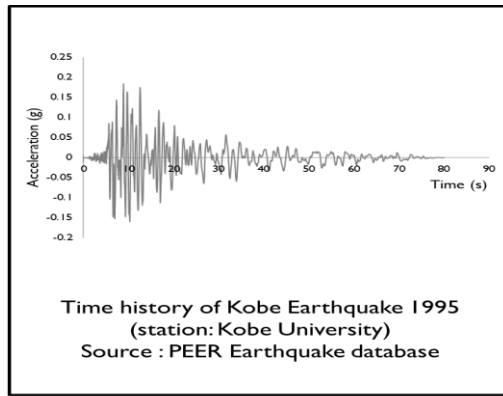


Fig 6. Ground motion charecteristics

X. Soil structure interaction

Soil stiffness calculated based on formulas by Richart and Lysmer [10].Effect of soil structure interaction is considered by equivalent springs with six degrees of freedom (DOF)

TABLE III. PROPERTIEAS OF SOIL[10]

Property / Soil type	Hard (S1)	Medium (S2)	Soft (S3)
γ (Unit weight) (kN/m ³)	21	18.5	17
G (Shear modulus) (kN/m ²)	30000	20000	10000
ν (Poisson's ratio)	0.2	0.25	0.3
ϕ (Friction angle) (degrees)	42	37	30
V_s (Shear wave velocity)	500	275	150
E (Modulus of elasticity)	72000	50000	26000

K_x, K_y, K_z be the stiffness of equivalent soil springs along the translation degree of freedom along X, Y and Z-axes.

$K_{\phi x}$, $K_{\phi y}$, $K_{\phi z}$ be the stiffness of equivalent rotational soil springs along the rotational degree of freedom along X, Y and Z-axes

TABLE IV. RICHART AND LYSMER FORMULAS [10]

Direction	Spring value	Equivalent radius
Vertical	$K_z = \frac{4Gr_z}{1 - \nu}$	$r_z = \sqrt{\frac{LB}{\pi}}$
Horizontal	$K_x = \frac{32(1 - \nu)Gr_x}{7 - 8\nu}$	$r_x = \sqrt{\frac{LB}{\pi}}$
	$K_{zy} = \frac{32(1 - \nu)Gr_y}{7 - 8\nu}$	$r_y = \sqrt{\frac{LB}{\pi}}$
Rocking	$K_{\phi x} = \frac{8Gr_{\phi x}^3}{3(1 - \nu)}$	$r_{\phi x} = \sqrt[4]{\frac{LB^3}{3\pi}}$
	$K_{\phi y} = \frac{8Gr_{\phi y}^3}{3(1 - \nu)}$	$r_{\phi y} = \sqrt[4]{\frac{LB^3}{3\pi}}$
Twisting	$K_{\phi z} = \frac{16Gr_{\phi z}^3}{3}$	$r_{\phi z} = \sqrt[4]{\frac{LB^3 + BL^3}{6\pi}}$

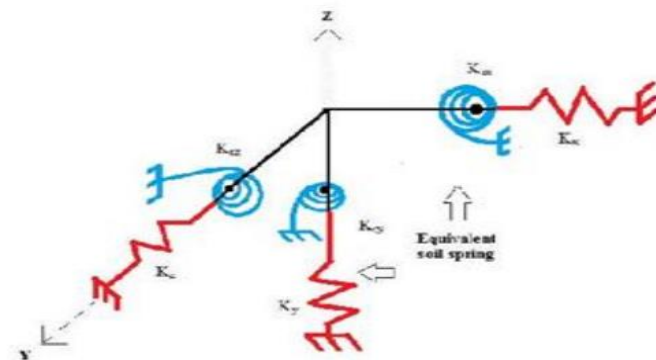


Fig 7 Equivalent Spring Stiffness [7]

XXII. RESU LT AND DISCUSSION

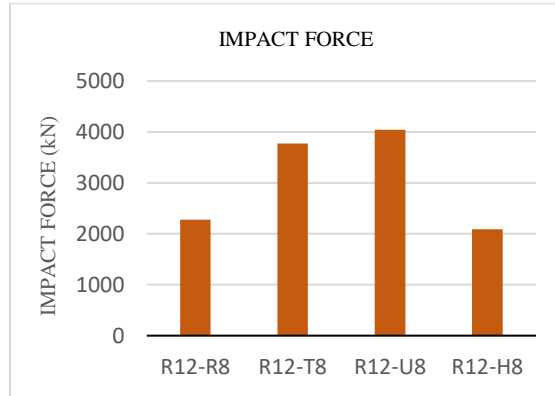


Fig .8. Impact Force

The modal R12-U8 shows large pounding force at the 8th storey when compared to others modals. And this modal has 43% increased value of pounding force when compared to the regular building R12-R8. The mass of the colliding buildings increases the effect of seismic pounding.

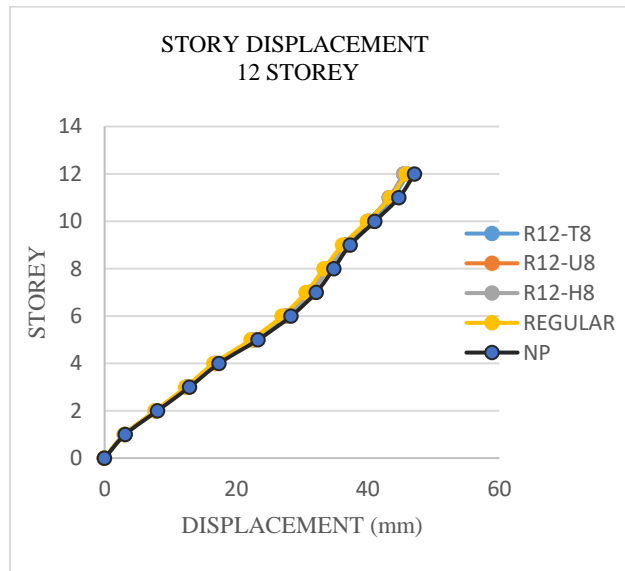


Fig .9. Story Displacement 12 Storey

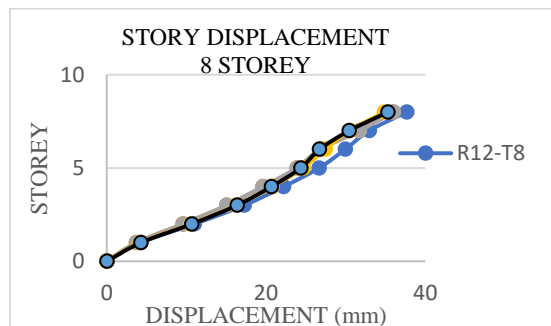


Fig .10. Story Displacement 8 Storey

The maximum displacement of the 12-storey structure subjected to pounding shows less than the building subjected to no pounding case. As a result of pounding the 8-storey building in the modal R12-T8 (T shape building) shows maximum displacement when compared to other models.

The storey shear forces is decreased by around 3.7 times when different irregular structure compared in 12 storey and 8 storey building shown in fig 11. However, the decrease in the shear force leads to increase in the pounding force 1.5 to 4 times in different structures.

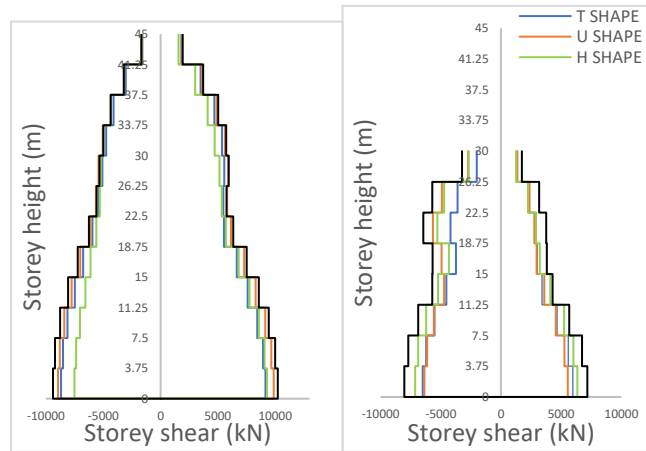


Fig .11. Story shear

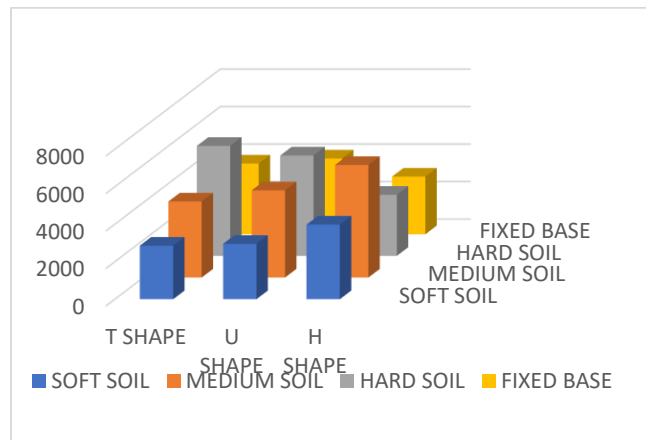


Fig .12. Impact force

From soft to hard soil, maximum pounding force is increased by around 30% to 40% and very large value of pounding force is shown in T shape building in hard soil.

CONCLUSIONS

The structural response of buildings varies significantly when considering the effects of pounding compared to no pounding cases. This study examines the seismic behaviour of mid-rise reinforced concrete (RC) frame buildings, taking into account irregularities and the impact of pounding between adjacent structures.

- Pounding forces are highest near the top of the adjacent buildings.
- In U-shape building (R12-R8) the impact force was increased 43% than the regular model R12-R8.
- Low rise buildings experience greater displacement during pounding and are more susceptible to damage than adjacent high-rise buildings The displacement at the top floor of the T shape and H shape building shows very large displacement.
- The pounding forces increases as the soil stiffness changes from soft to hard.
- In contrast, the adjacent buildings with H-shaped plan irregularity show relatively less pounding effect.

REFERENCES

- [45] T. Brown and A. Elshaer, "Pounding of structures at proximity: A state-of-the-art review," *Journal of Building Engineering*, vol. 48. Elsevier Ltd, May 01, 2022. doi: 10.1016/j.jobe.2022.103991.
- [46] Mahmoud Miari, Robert Jankowski "Analysis Of Pounding Between Adjacent Buildings Founded On Different Soil Types" 2022
- [47] Mahmoud Miari and Robert Jankowsk "Seismic gap between buildings founded on different soil types experiencing pounding during earthquakes" Volume 38, Issue 3, 2022
- [48] Fig .11. Story shear
- [49] seismic pounding between adjacent RC buildings" *IJCRT Volume 10, Issue 6, 2022*
- [50] Muhammad Noman , Bashir Alam "Effects of pounding on adjacent buildings of varying heights during earthquake in pakistan" 2016
- [51] Aditi V. Khurd¹, Jui S. Dixit, Manjiri V. Paraskar, Nitin R. More⁴ & Prof. Suhasini N "Seismic pounding effect on adjacent RC framed multistorey buildings using time history analysis", 2023.
- [52] Akim Bolshakova ,Zufar Beloviey "Study on Geometrically Irregular Reinforced Concrete Frame Structures Considering the Effect of Seismic Soil Structure Interaction and Building Collision" Volume 4 Issue 10, 2022
- [53] Asharani B. Karamadi¹, Rajani Togarsi , "Analysis of Seismic Pounding between Adjacent Buildings IRJET", Volume: 04 Issue: 05, 2017.
- [54] Mehmet Eren, Anna Jakubczyk-Galczy and Robert Jankowski , "Numerical Analysis of Seismic Pounding between Adjacent Buildings Accounting for SSI", <https://www.mdpi.com/journal/applsci>, 2023.
- [55] V. S. Bangde, M. P. Kawade, and G. H. Sawai, "Response Of High-Rise Building Subjected To Seismic Forces And Its Effect Considering Soil Structure Interaction," *International Research Journal of Modernization in Engineering Technology and Science*, vol. 02, no. 09, pp. 1123–1139, Sep. 2

Response Of T Beam Bridge By Varying Skew Angle

Ayisha Sana Abdul Salam
Dept. of civil engineering
AWH Engineering college
Kuttikkattoor, Calicut
sanabdussalam@gmail.com

Anila S
Dept. of civil engineering
AWH Engineering college
Kuttikkattoor, Calicut
anila@awhengg.org

Abstract— Bridges are ensuring the smooth flow of goods and people. The seismic performance of bridges, especially those with unique geometries such as T-beam bridges with zero skew angles, is of paramount importance in earthquake-prone regions. This project presents a comprehensive analysis of a T-beam bridge with a 10° to 50° skew angle.

The study encompasses several key aspects: Detailed documentation of the bridge's geometry, materials used, and construction techniques employed in the T-beam bridge under consideration. Development of a finite element model to represent the T-beam bridge accurately, comparison by varying the skew angles

Application of various seismic ground motion records to simulate the bridge's response under earthquake-induced loading.

Assessment of the bridge's performance using performance metrics such as moment, shear and torsion levels.

Keywords— Skew angle, T beam bridge, Skew bridge, torsion, shear, moment

INTRODUCTION

Concrete is used for construction of most of the buildings and bridges in India it can be called as back-bone to the infrastructural development of the nation. A concrete T-beam bridge is a fundamental and widely used structural engineering marvel that plays a pivotal role in modern transportation infrastructure. It represents a robust and efficient solution for spanning rivers, roads, railways, and other obstacles, facilitating the smooth flow of traffic and commerce. Characterized by its distinctive T-shaped cross-section, this type of bridge combines the advantages of both reinforced concrete and steel to create a durable and economical structure. From their origins to their contemporary significance, these bridges have left an indelible mark on civil

If a road alignment crosses a river or any other obstruction at an inclination different from 90° , a skew crossing may be necessary. Skewed bridges are one of the most economical and satisfying construction.

METHODOLOGY

A. Description of T beam bridge

A 4 lane concrete bridge of 72m long was modelled and designed in CSI bridge software. Lane width was 3.65 m each. Grade of concrete used here is M30

Table No.1 Sectional details

PROPERTY	VALUES
TOTAL DEPTH	1.5m
TOTAL WIDTH	14.6m
ABUTMENT DIMENSIONS	2m x 4m
PILE DIAMETRE	1.5m
NUMBER OF CAPBENT	2
CAPBENT DIMENSIONS	1.5m x 2m
NUMBER OF COLUMNS	4
DECK SECTION	TEE BEAM
COLUMN HEIGHT	10m
CAPBEAM LENGTH	14.6m

B. Description of girder

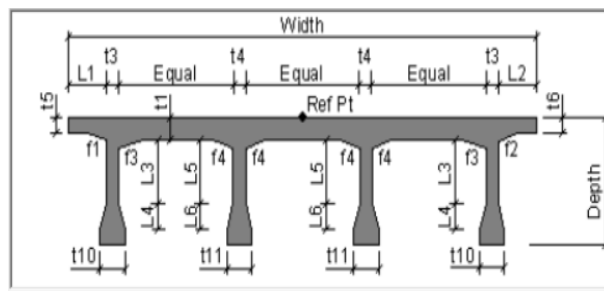


Table No. 2 girder detail

Number of interior girder	4
Depth above flare (L3)	0.7m
Flare depth (L4)	0.3m
Thickness of flare (t)	0.35m
Overhanging length	0.25m
Overhanging thickness	0.5m

*C. Loading description***Table No 3 loading**

LINE AND AREA LOAD	
TYPE	VALUE
Borders	1600 N
Pedestrians	1840 N
Sidewalk	720 N
Railings	2000 N
Asphalt	880 N

D. Skew Angle

Skew angle typically refers to the deviation or tilt of an object, often measured in degrees, from its usual or expected orientation. This term is commonly used in various fields such as engineering, mathematics, and physics.

In engineering and construction, skew angle commonly refers to the angle at which a structural element, such as a beam or column, is positioned relative to a reference axis. For example, in bridge construction, the skew angle is the angle at which the axis of the bridge deck deviates from a perpendicular alignment with the supporting piers or abutments. It's essential to consider skew angle in design and construction to ensure structural stability and load-bearing capacity.

In mathematics, skew angles can also be encountered in geometry, where they describe the angular relationship between two lines or planes that are not parallel or perpendicular to each other. For instance, in the context of 3D geometry, the skew angle between two non-intersecting lines or planes determines the degree of deviation from parallelism.

Understanding skew angle is crucial in various practical applications, including structural design, geometric calculations, and spatial analysis, as it provides insights into the orientation and alignment of objects in relation to their surroundings.

E. Variation in skew angles

A skew bridge is a type of bridge that spans an obstacle such as a river, road, railway, or other terrain feature at an angle other than 90 degrees. Fig 1 shows plan of skew bridges in 5 different skew angles.

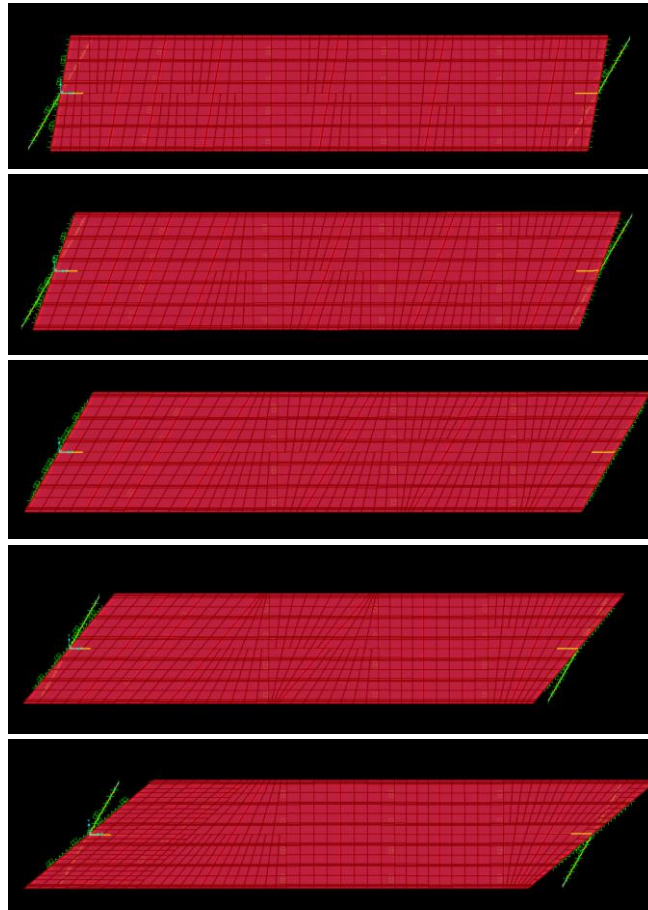


Fig.1. Skewed model 10°, 20°, 30°, 40°, 50°

RESULT AND DISCUSSIONS

F. Response in T beam bridge due to dead load

As the skew angle increases, the load distribution across the bridge changes. With a higher skew angle, the load tends to distribute more evenly across the structure, reducing localized stress concentrations that could lead to torsion.

In many cases, increasing the skew angle may result in a more symmetric load distribution. This symmetry can help balance out forces acting on the structure, reducing the overall torsional effects.

Higher skew angles may introduce additional support mechanisms or structural elements that help stabilize the bridge against torsional forces. This could include diagonal bracing or modifications to the bridge design that mitigate torsion.

From fig 4, the graph shows variation of moment shear and torsion when skew angle is increased from 10 to 50 degree.

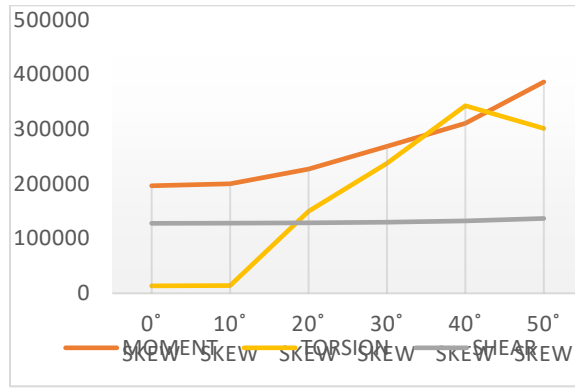


Fig.2. Graph showing Response due to dead load

G. Response in T beam bridge due to service load

- ❖ Torsion and shear forces in a skew bridge are primarily affected by load distribution and bridge geometry.
- ❖ Fig 3 shows, A lower skew angle, like 10 degrees, leads to a more even distribution of these forces along the bridge's length, reducing their magnitudes, This minimizes torsional and shear effects.
- ❖ On the other hand, bending moments are influenced by load distribution and the moment arm between the load and bridge supports. However, excessively high skew angles can reduce the effective width of the bridge deck, which contributes to resisting bending moments.
- ❖ Hence, an optimal skew angle for minimizing bending moments might be around 50 degrees, where the benefits of reducing the moment arm outweigh the reduction in effective width.

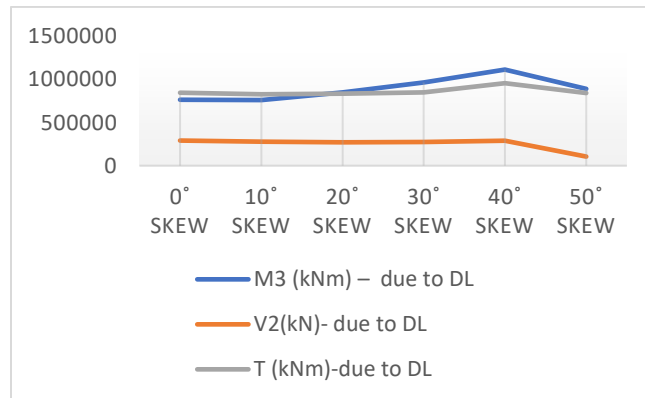


Fig 2: Graph showing Response due to service load

IV CONCLUSIONS

- T Beam bridge experience increase in moment and shear with increasing skew angles, although torsion initially increases up to 40 degrees but then decreases as the skew angle approaches 50 degrees.
- This trend is followed under both dead load and service load.

- Additionally, while both exterior and interior girders experience an increase in torsion with increasing skew angles, the interior girder exhibits a higher torsion due to the net effect.
- At very high skew angles, the alignment of the forces may change in a way that is more favorable for the piers.

REFERENCES

- [56] YATI AGGARWAL (2014) “Analysis of concrete box girder bridges using csi bridge 2014” *Bulletin of Earthquake Engineering* 21 (1), 319-34
- [57] S Maleki et.al (2002) “Deck modeling for seismic analysis of skewed slab-girder bridges”. *Journal of Bridge Engineering* Volume 24, Issue 10, October 2002, Pages 1315-1326.
- [58] S. Maleki (2006) “Orthogonal effects in seismic analysis of skewed bridges” *Journal of Bridge Engineering* Volume3, Issue 5, October 2006, Pages 1315-1326.
- [59] JY Meng et.al (2000) “Seismic analysis and assessment a skew highway bridge” Volume 22, Issue 11, November 2000, Pages 1433-1452.
- [60] M Mallick et.al (2015) “Seismic analysis of highway skew bridges with nonlinear soil–pile interaction” volume 23,issue 23.
- [61] Nikhil v. deshmuKh1, Dr U.P waghe (2016) “Analysis and design of skew bridges” *International journal of science and research* Volume 2, Issue 12 (August 2012), PP. 13

Comparative Study of Reinforced Concrete Using Human Hair and Aluminium Fibers

<p>Shahla Thasni P</p> <p>Student</p> <p>Dept. of Civil Engineering, AWH Engineering College, Kuttikkattoor, Kozhikode, Kerala, India</p>	<p>Sandra E</p> <p>Student</p> <p>Dept. of Civil Engineering, AWH Engineering College, Kuttikkattoor, Kozhikode, Kerala, India</p>	<p>Najil N</p> <p>Student</p> <p>Dept. of Civil Engineering, AWH Engineering College, Kuttikkattoor, Kozhikode, Kerala, India</p>	<p>Muhammed Saneed PP</p> <p>Student</p> <p>Dept. of Civil Engineering, AWH Engineering College, Kuttikkattoor, Kozhikode, Kerala, India</p>
<p>Jithma T</p> <p>Assistant Professor</p> <p>Dept. of Civil Engineering, AWH Engineering College, Kuttikkattoor, Kozhikode, Kerala, India</p>			

Abstract— This study investigates the efficacy of human hair and aluminum fibers as reinforcements in concrete, analyzing their impact on compressive, flexural, and tensile strengths. Different fiber percentages (0%, 0.5%, 1%, and 1.5% by weight of cement) are systematically incorporated into concrete mixtures. Compressive strength tests on cubes, flexural strength assessments on beams, and tensile strength evaluations on cylinders reveal insights into the material's load-bearing, bending, and stretching capacities. Results indicate a gradual strength increase in human hair fiber reinforced concrete (HHFRC) up to an optimal percentage, while aluminum fiber reinforced concrete (AFRC) shows significant enhancement at higher fiber content. AFRC's superior mechanical properties stem from aluminum fibers high tensile strength and stiffness, enhancing bond formation and resulting in denser, stronger concrete. These findings inform the selection of fiber reinforcement for concrete structures, tailored to specific project needs

Keywords: Fiber Reinforced Concrete, Human Hair Fiber, Aluminium Fiber Reinforced Concrete, Compressive Strength, Flexural Strength, Split Tensile Strength

1. INTRODUCTION

Concrete has been a cornerstone of construction for centuries, renowned for its compressive strength and durability. However, its inherent weaknesses, particularly in tension, have spurred continuous innovation in the field of structural engineering. One such innovation is Fiber Reinforced Concrete (FRC), which enhances the mechanical properties of traditional concrete by incorporating various types of fibers into the cement matrix. These fibers, ranging from steel and

glass to natural materials like human hair, impart increased tensile strength, ductility, and crack resistance to the concrete composite.

The advent of Fiber Reinforced Concrete (FRC) marks a significant advancement in construction materials and techniques. Traditional concrete, while excellent in compression, is susceptible to cracking and failure under tensile stresses. FRC addresses this vulnerability by dispersing fibers throughout the concrete matrix, providing additional reinforcement and mitigating the propagation of cracks. This composite material exhibits enhanced mechanical properties, making it well-suited for a wide range of structural applications.

Among the diverse array of fibers used in FRC, human hair emerges as a unique and promising reinforcement material. Composed primarily of keratin, a proteinaceous substance, human hair exhibits remarkable tensile strength and flexibility. This natural fiber, often considered a waste product, offers an environmentally friendly and cost-effective alternative for reinforcing concrete. By harnessing the inherent properties of human hair, researchers aim to not only improve the performance of concrete structures but also address concerns related to waste management and sustainability.

In parallel, aluminum fiber reinforced concrete (AFRC) represents another innovative approach to enhancing the mechanical properties of concrete. Aluminum fibers, characterized by their lightweight nature and corrosion resistance, offer unique advantages in concrete reinforcement. When incorporated into the concrete mix, these fibers augment tensile strength, durability, and resistance to cracking. The utilization of aluminum fibers opens up new avenues for structural design and construction, particularly in applications where weight reduction and corrosion resistance are paramount considerations. In this study, we embark on a comprehensive exploration of Fiber Reinforced Concrete (FRC), with a specific focus on the utilization of human hair and aluminum fibers as reinforcement materials. By examining the interplay between fiber type, content, and concrete mix design, we aim to contribute valuable insights to the ongoing discourse on sustainable construction practices and materials innovation.

METHODOLOGY

In our experimental setup, we adhered to Indian Standard (IS) codes to ensure the suitability of human hair and aluminum fibers for concrete reinforcement. Following material assessment, concrete mixtures were meticulously designed to achieve M25 grade concrete. The casting process involved careful preparation of moulds and precise hand compaction to minimize air voids. Subsequent curing for 28 days facilitated optimal strength development. Tests for compressive, flexural, and tensile strengths were then conducted on specimens with varying percentages (0%, 0.5%, 1%, and 1.5% by weight of cement) of human hair and aluminum fibers, along with plain concrete specimens for comparison. The findings from these experiments contribute valuable insights into the effectiveness of different fiber percentages in enhancing concrete's mechanical properties.

MATERIALS AND PROPERTIES

Materials used are OPC, river sand, 20mm sized coarse aggregate, human hair, aluminium fiber and water

A. Cement (OPC)

We opted for Ordinary Portland Cement (OPC) Grade 53 due to its exceptional strength characteristics. Extensive testing revealed a fineness of 3%, consistency of 31%, specific gravity of 3.15, and an initial setting time of 55 minutes. These parameters ensure the cement meets stringent quality standards and provides the necessary foundation for our concrete mixtures.

B. Fine Aggregate (River Sand)

River sand serves as our fine aggregate, boasting a specific gravity of 2.56, fineness modulus of 2.704, and bulk density of 1.62 g/cm³. With a porosity of 0.37 and void ratio of 0.587, it offers excellent properties for enhancing the workability and durability of our concrete structures.

C. Coarse Aggregate (20mm)

Our coarse aggregate, with a size of 20mm, underwent comprehensive testing, revealing a specific gravity of 2.65, fineness modulus of 7.42 and bulk density of 1.61 g/cm³. Its porosity of 0.645 and void ratio of 0.392 ensure optimal interlocking within the concrete matrix, contributing to structural integrity.

D. Aluminum Fiber and Human Hair Fiber:

Aluminum fibers, with a silvery appearance and size ranging from 40mm to 50mm, along with human hair fibers of similar dimensions (40mm to 50mm) and diameter (100-120 μ m), are incorporated into our concrete mixtures. These fibers, added in proportions of 0.5%, 1%, and 1.5% by weight of cement, work synergistically to reinforce the concrete and enhance its mechanical properties, ensuring resilience and longevity.

MIX DESIGN

Our mix design, tailored for Grade M25 concrete, utilizes OPC 53 grade cement, with a maximum nominal aggregate size of 20mm. With a minimum cement content of 300 kg/m³ and a maximum water-cement ratio of 0.50 our concrete achieves optimal strength and workability. Good quality control and moderate exposure conditions further guarantee the durability of our structures.

Table 1: Mix preparation

Cement (kg)	Fine aggregate (kg)	Coarse aggregate (kg)	Water (liter)
394	662.135	1113.95	197
1	1.68	2.83	0.5

EXPERIMENTS CONDUCTED

A. Compressive strength

Compression testing involves subjecting small cubes, typically 150 mm x 150 mm x 150 mm, to axial pushing forces to measure their compressive strength.

B. Flexural strength

The flexural strength test assesses the ability of concrete beams, typically sized at 100 mm x 100 mm x 500 mm, to withstand bending without breaking.

C. Split tensile strength

Split tensile strength evaluates its ability to withstand tensile forces perpendicular to the direction of compression. Cylindrical specimens, usually measuring 150 mm x 300 mm, are tested under a split tensile testing machine

These tests, conducted after 28 days of curing.

VI. RESULT AND DISCUSSION

A. Compressive strength

Human hair-reinforced concrete showed significant improvements in compressive strength. Compared to conventional concrete at 0.5 % hair content, strength increased by 6.6% and at 1% content, it increased by 14.48%. At 1.5%, strength slightly decreased, suggesting excess fiber may compromise strength due to clustering or uneven dispersion.

Table 2: Compressive strength result of human hair fiber reinforced concrete

1) Sl No.	2) Hair % (by weight of cement) added in concrete.	3) Compressive strength N/mm ²
4) 1	5) 0	6) 33.77
7) 2	8) 0.5	9) 36.05
10) 3	11) 1	12) 38.66
13) 4	14) 1.5	15) 34

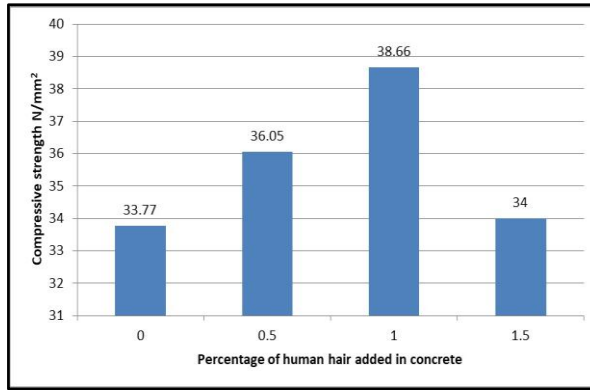


Fig 1: Compressive strength test result of human hair reinforced concrete

The addition of aluminum fibers to concrete significantly boosts compressive strength, peaking at 1.5% content. With 0.5% aluminum fibers, strength increased by 12.57% compared to conventional concrete. At 1%, there was a 27.74% increase, while at 1.5%, it increased 31.6%. This underscores aluminum fibers' effectiveness in reinforcing concrete, with the greatest enhancement seen at 1.5% content.

Table 3: Compressive strength test result of aluminium fiber reinforced concrete

16) Sl No.	17) Aluminium % (by weight of cement) added in concrete.	18) Compressive strength N/mm ²
19) 1	20) 0	21) 33.77
22) 2	23) 0.5	24) 38
25) 3	26) 1	27) 41.11
28) 4	29) 1.5	30) 44.44

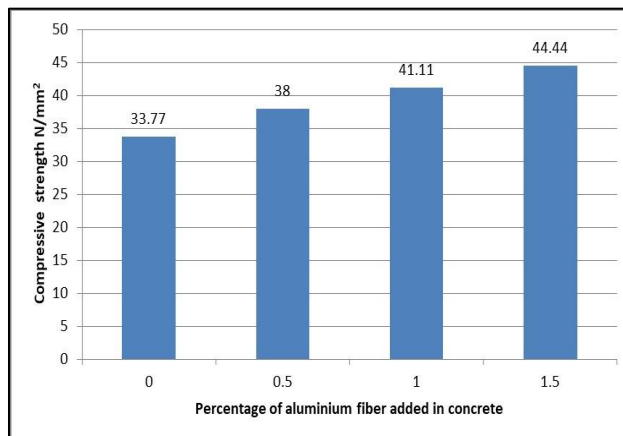


Fig 2: Compressive strength test result of aluminium fiber reinforced concrete

B. Flexural strength

The flexural strength of human hair-reinforced concrete increases consistently with the addition of hair fibers, peaking at 1.5% content. With 0.5% hair fibers, strength increased by 13.31% compared to conventional concrete. At 1%, the increase was 9.72%. The optimum enhancement occurred at 1.5% hair content 16.28% increase over conventional concrete. This consistent improvement underscores the reinforcing effect of human hair fibers in the concrete matrix, with the highest enhancement at 1.5% content. Figure 3 provides a graphical representation of the flexural strength test results.

Table 4: Flexural strength test result of human hair fiber reinforced concrete

31) Sl No.	32) Hair % (by weight of cement) added in concrete.	33) Flexural strength 34) N/mm^2
35) 1	36) 0	37) 7.41
38) 2	39) 0.5	40) 8.48
41) 3	42) 1	43) 8.13
44) 4	45) 1.5	46) 8.617

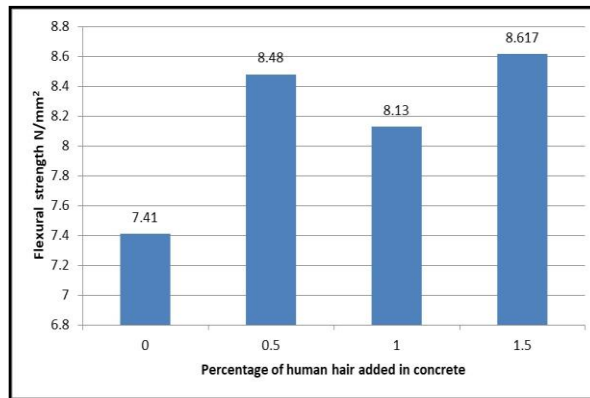


Fig 3: Flexural strength test result of HHFRC

Table 5: Flexural strength test result of human hair fiber reinforced concrete

47) Sl No.	48) Aluminium % (by weight of cement) added in concrete.	49) Flexural strength N/mm ²
50) 1	51) 0	52) 7.416
53) 2	54) 0.5	55) 9
56) 3	57) 1	58) 9.55
59) 4	60) 1.5	61) 9.639

The flexural strength of aluminum fiber-reinforced concrete consistently increases with the addition of aluminum fibers, peaking at 1.5% content. Incorporating 0.5% aluminum fibers results in a notable 21.36% increase compared to conventional concrete. At 1% aluminum fiber content, the flexural strength rises by 28.77% indicating a significant enhancement. The highest improvement is observed at 1.5% aluminum fiber content, 29.97% increase over conventional concrete. This consistent rise underscores the reinforcing effect of aluminum fibers within the concrete matrix, with the most significant enhancement at 1.5% content.

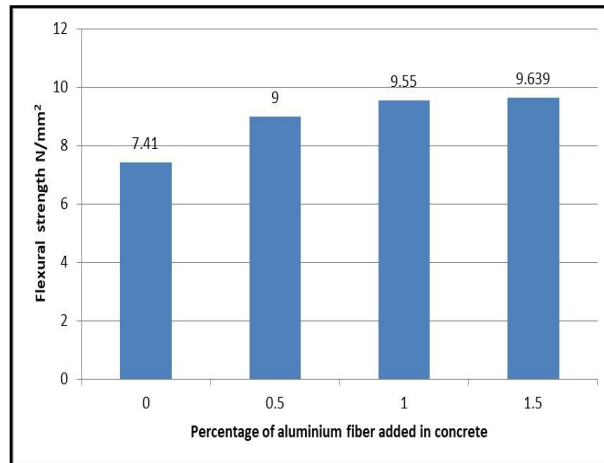


Fig 4: Flexural strength test result of AFRC

C. Split tensile strength

The table 6 and figure 5 shows the split tensile strength of human hair fiber reinforced concrete.

Table 6: Split tensile strength test result of human hair fiber reinforced concrete

62) Sl No.	63) Hair % (by weight of cement) added in concrete.	64) Split tensile strength N/mm^2
1	0	1.87
2	0.5	1.98
3	1	2.122
4	1.5	2.4

The split tensile strength of human hair-reinforced concrete improves with the addition of human hair fibers, gradually increasing up to 1.5% content. Incorporating 0.5% human hair fibers results in a modest 5.88% increase compared to conventional concrete. At 1% human hair content, the split tensile strength rises by 13.48% demonstrating further enhancement. The optimum improvement occurs at 1.5% human hair content, 28.34% increase over conventional concrete. This gradual increase underscores the beneficial effect of human hair fibers in enhancing the tensile properties of concrete, with the highest enhancement achieved at 1.5% content.

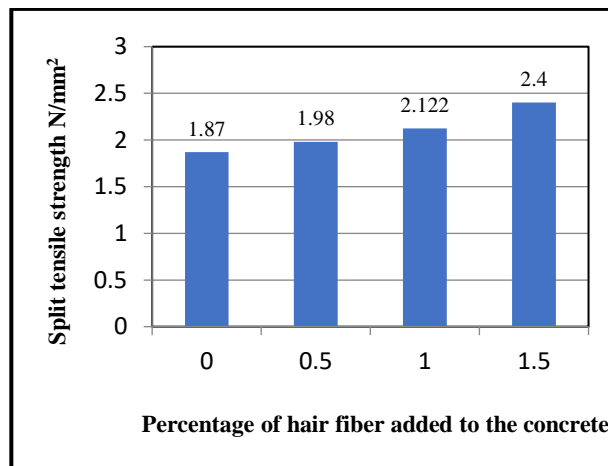


Fig 5: Split tensile strength test result of HHFRC

Table 7: Split tensile strength test result of aluminium fiber reinforced concrete

65) Sl No.	66) Aluminium % (by weight of cement) added in concrete.	67) Split tensile strength N/mm ²
68) 1	69) 0	70) 1.87
71) 2	72) 0.5	73) 2.36
74) 3	75) 1	76) 2.5
77) 4	78) 1.5	79) 2.67

The table 7 and figure 6 shows the split tensile strength aluminium fiber reinforced concrete. The split tensile strength of aluminum fiber-reinforced concrete also improves with the addition of aluminum fibers, gradually increasing up to 1.5% content. Incorporating 0.5% aluminum fibers results in a significant 26.2% increase compared to conventional concrete. At 1% aluminum fiber content, the split tensile strength rises by 33.68% demonstrating further enhancement. The optimum improvement occurs at 1.5% aluminum fiber content, reaching a split tensile strength 42.78% increase over conventional concrete. This gradual increase underscores the beneficial effect of aluminum fibers in enhancing the tensile properties of the concrete, with the highest enhancement achieved at 1.5% content.

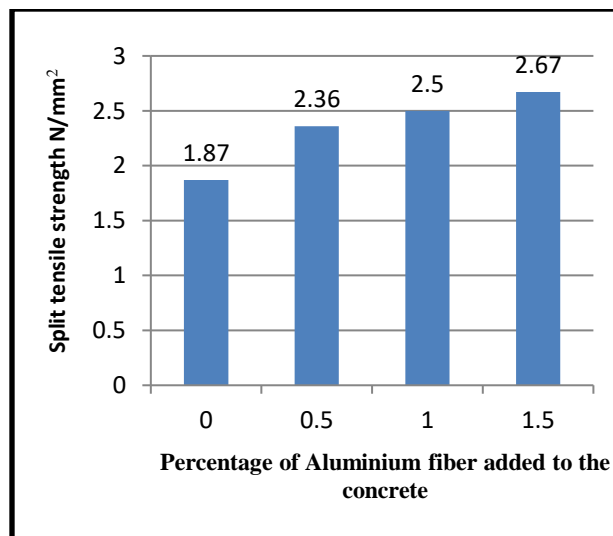


Fig 6: Split tensile strength test result of AFRC

D. Comparative discussion

When comparing the compressive strength of aluminum fiber-reinforced concrete to human hair fiber-reinforced concrete, the percentage increase for a 0.5% addition of fibers is 5.4%. At 1% addition, aluminum fiber exceeds human hair fiber by 6.3% and at 1.5%, the difference is 30.7%. The significant increase can be attributed to the optimal percentage of human hair fiber added to concrete being 1%, while for aluminum fibers, it extends to 1.5%. Figure 7 shows the comparison of compressive strength of HHFRC and AFRC.

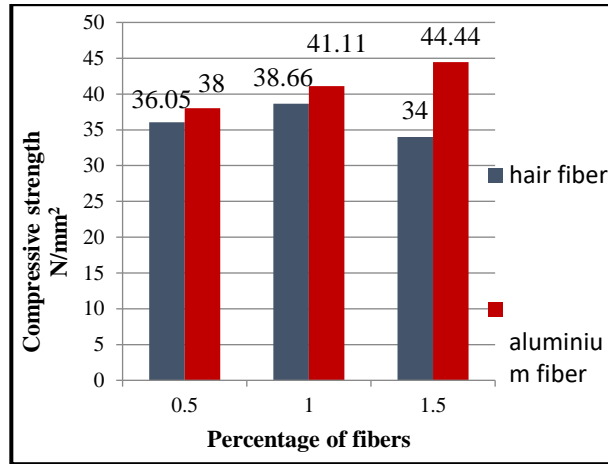


Fig 7: Comparison of compressive strength of HHFRC and AFRC.

When comparing the flexural strength of aluminum fiber-reinforced concrete to human hair fiber-reinforced concrete, the increase with a 0.5% addition of aluminum fiber compared to human fiber is 6.13%. At 1% addition, aluminum fiber exceeds human fiber by 17.46%, and at 1.5%, it's 11.82% higher than human fiber. The reason for the 17.46% difference at 1% addition is that human hair fiber shows an optimal value, while for aluminum, it's at 1.5%. Figure 8 shows the comparison of flexural strength of HHFRC and AFRC.

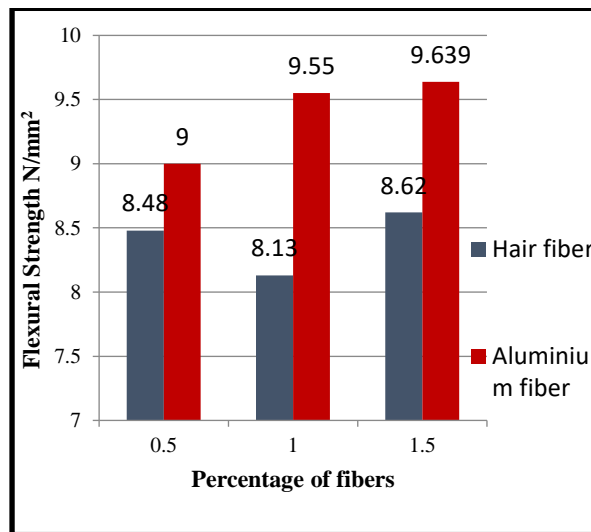


Fig 8: Comparison of flexural strength of HHFRC and AFRC.

When comparing the split tensile strength of aluminum fiber-reinforced concrete to human hair fiber-reinforced concrete, the increase with a 0.5% addition of aluminum fiber compared to human fiber is 19.19%. At 1% addition, aluminum fiber exceeds human fiber by 17.81%, and at 1.5%, it's 11.25% higher than human fiber. In materials like concrete reinforced with fibers, even slight differences in the percentage of added fiber can significantly impact the overall strength. This is because fibers play a crucial role in reinforcing the concrete matrix, altering its composition and structure. Each increment in fiber percentage can lead to notable variations in mechanical properties, such as tensile strength. Hence, careful consideration and optimization of fiber content are vital for achieving desired concrete performance. Figure 9 shows the comparison of split tensile strength of HHFRC and AFRC.

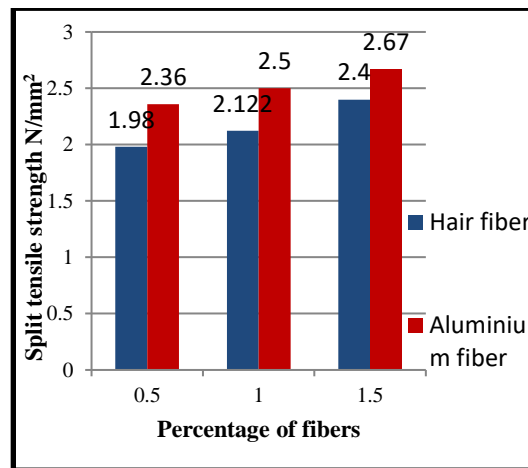


Fig 9: Comparison of split tensile strength of HHFRC and AFRC

CONCLUSION

Findings reveal that aluminum fiber-reinforced concrete consistently exhibited higher compressive strength, flexural strength, and split tensile strength compared to human hair-reinforced concrete.

In human hair fiber-reinforced concrete, the optimal percentage is 1%, resulting in significant increases in compressive strength by 14.48%, flexural strength by 16.28%, and split tensile strength by 28.34% compared to conventional concrete. Conversely, for aluminum fiber-reinforced concrete, the optimal percentage for compressive strength, flexural strength, and split tensile strength is 1.5%, leading to remarkable increases of 31.6%, 29.97%, and 42.78% respectively compared to conventional concrete.

The superior mechanical properties observed in aluminum fiber-reinforced concrete can be attributed to the high tensile strength and stiffness of aluminum fibers, which effectively enhance the bond between cement paste and aggregates. Additionally, aluminum fiber-reinforced concrete results in a denser and more cohesive concrete structure, contributing to its enhanced performance compared to hair fiber-reinforced concrete.

Aluminum fiber reinforced concrete is widely employed in critical infrastructure projects like bridges, tunnels, and highways due to its exceptional strength and durability. It ensures structural integrity and longevity, making it suitable for demanding applications. High-rise buildings benefit from its superior stability and resistance to seismic activity and wind loads, enhancing overall safety. In marine structures, aluminum fiber reinforced concrete's corrosion resistance ensures reliability in harsh environments. Industrial facilities utilize it for durable flooring, while airports rely on its strength for runways and taxiways. Conversely, human hair fiber reinforced concrete offers an eco-conscious option for low-impact projects, with applications in artistic installations, DIY projects, and decorative structures. Ongoing research explores its mechanical properties and expands its usage in sustainable construction practices.

ACKNOWLEDGEMENT

First and the foremost, we shall thank God Almighty who gave us the inner strength, resource and ability to complete the work successfully, without which all our efforts would have been in vain. We are deeply indebted to our guide Ms. Jithma T, Assistant Professor, Department of Civil Engineering for her excellent guidance, positive criticism and valuable comments. We are greatly thankful to Dr. Sabeena M.V, Principal of our institution AWH Engineering College for her support and cooperation. We are thankful to Ms. Jisha P, Head of the Department, for her valuable advice and motivation. Finally, we thank our parents, friends, near and dear ones who directly and indirectly contributed to the successful completion of our project.

REFERENCES

- [1] Narain Das Bheel (2017)"Effect of Human hair as Fibers in Cement Concrete". International Conference on Sustainable Development in Civil Engineering (ICSDC 2017)
- [2] Ajna Manaf and George M Varghese (2017)"Human Hair Fibre Reinforced Concrete" International journal of engineering research & technology
- [3] Alfya Basheer, Anitta Paul and Anjana Krishnan K.R, Aswin Nath G (2023) "Human hair fibre reinforced concrete" International journal of engineering research & technology (ijert)
- [4] Jain D. and Kothari A (2012)"Hair Fibre Reinforced Concrete"Sanghvi Institute of Management and Science, Indore, MP, INDIA Research Journal of Recent Sciences ISSN 2277 - 2502Vol.
- [5] Geeta Batham (2023)"Flexural and Split tensile Strength of Concrete Reinforced with Human Hair" International Journal of Engineering Research and Applications
- [6] Manjunath Maddikeari, Balaji Kvgd,Lr Manjunatha(2021)"Experimental study on the use of human hair as fiber to enhance the performance of concrete"
- [7] Dr.a.s.kanagalakhmi, b.indhuj, u.rithisri, r.p.kowsalya "Study on human hair in concrete asa fiber reinforcement" International Journal of Advanced Research in Science, Communication and Technology (IJARSCT)"
- [8] Jain D. and Kothari A (2012) "Hair Fibre Reinforced Concrete" Research Journal of Recent Sciences ISSN 2277 – 250 Vol. 1(ISC-2011), 128-133 (2012)

- [9] Y.K. Sabapathy (January 2021)"Experimental study on strength properties of aluminium fibre of reinforced concrete"Journal of King Saud University - Engineering SciencesVolume 33, Issue1
- [10] J Rajaraman (2017)"Study on structural behaviour of Aluminium fiber in concrete" Journal of Engineering and Application science 12(Special Issue11):9182-9183
- [11] J Rajaraman (2017)"Study on structural behaviour of Aluminium fiber in concrete" Journal of Engineering and Application science 12(Special Issue11):9182-9183
- [12] Imran Ali Channa and Abdullah Saand"Mechanical Behavior of Concrete Reinforced with Waste Aluminium Strips"Civil Engineering Journal 7(7):1169-1182
- [13] A. Oan (2019) "The aluminum can fiber in concrete"International Research Journal of Engineering and Technology (IRJET)

Planning, Analysis and Design of Hotel Building at Karadi, Thamarassery

Heena

Dept. of Civil Engineering
KMCT CEW Kozhikode, India
heenamusthafa007@gmail.com

Mariyam Rinsha M

Dept. of Civil Engineering
KMCT CEW Kozhikode, India
mariyamrinsha4321@gmail.com

Safa Sadique P P.

Dept. of Civil Engineering
KMCT CEW Kozhikode, India
safasadique421@gmail.com

Swetha N

Dept. of Civil Engineering
KMCT CEW Kozhikode, India
swethaamms@gmail.com

Aswathi K V

Dept. of Civil Engineering
KMCT CEW Kozhikode, India
aswathikv@kmctcew.ac.in

U C Ahammed Kutty

Dept. of Civil Engineering
KMCT CEW Kozhikode, India
ucakutty@gmail.com

Abstract—The project deals with the planning, analysis and design of a hotel building. The site of the proposed building is at Karadi, Thamarassery. The building is aimed at providing multi-dimensional and comprehensive usage of space nearby a crowded city highway. The building is basically a reinforced concrete framed structure consisting of (G+4) floors, with adequate facilities and amenities. The functional planning is done using KMBR and IS codes. The structure shall be designed to resist and bear all loads liable to act on it at some point of its lifestyle. It also satisfies serviceability requirements including limitations on deflections and cracking. Drawing is done by using AUTOCAD software and building analysed by STAAD Pro software.

Index Terms—Analysis, Design, Hotel, Planning, StaadPro

I. INTRODUCTION

A hotel is a type of institution that offers short-term, paid accommodation. A hotel room's amenities might vary from a little room with a low-quality mattress to a spacious suite with superior mattresses, a wardrobe, and private bathrooms. A hotel may have amenities like a play area, restaurants, lounge areas, conference or assembly halls, and swimming pools. The aim of the project is to plan, analyse and design a (G+4) hotel building. The planning is carried out as per Kerala Municipal Building Rule (KMBR). The building is design as framed structure. the plan is drafted using Auto Cad Software and analyse and designed using STAAD Pro Software. All the structures and structural elements are designed according to the limit state. The aim of this design is to establish a structure that full fills all the requirements and performs satisfactorily during its intended life, with an appropriate degree of freedom, also have an adequate resistance against seismic loads.

II. LITERATURE REVIEW

Vikash Agrawal et.al (2022): The study utilizes STAAD Pro to analyze and design residential buildings (G+4). The examination of different loads, including seismic, dead, live, and combinations of loads, is the conclusion of these articles. Shear force, bending moment, and support responses are assessed as a consequence of the study. The structure is manually developed and cross-referenced with the program findings based on the analysis results.

Sowrav saha et.al (2021): The design and analysis of a multistory (G+14) residential building using STAAD Pro and AutoCAD is the main topic of this article. The design and analysis of a multi-story residential building with two flats on each floor, located in G+14, are reviewed in this paper. STAAD Pro is used to derive the design for the beams, columns, and footings once the dead and live loads have been applied.

Kunal wailker et.al (2021): The design and structural study of a multistory residential building are the topics of this research. Three phases of the project were finished. The building was first modeled and analyzed, then the structural components were designed, and finally the structural elements were detailed. STAAD Pro is the program utilized in this study to analyze the building.

Banavanru Vinod kumar ready et.al (2021): The research project examines how STAAD Pro and AutoCAD are used to efficiently model. High rise building manual calculations are laborious and time-consuming. We have a fast, accurate, and efficient platform for evaluating and creating structures with STAAD Pro.

K. Harshitha et.al (2021): This article focuses on using E-Tabs for the Analysis and Design of Five Star Hotel Buildings. The goal of this project is to use ETABS software to assess and design a commercial building. This analysis takes into account a structure with ten stories (G+10). The static technique is used for analysis, and IS principles are followed when designing.

Jiixin Cheng et.al (2021): The study focuses on the examination of sharing strategies and demand forecasting for hotel parking. It creates a trustworthy model to forecast a hotel parking lot's parking demand in real time and then assesses if offering shared parking spots is feasible.

Dev Dutt Chaubey et.al (2021): Reviewing the literature on seismic analysis of irregularly planned RC frame buildings built in accordance with capacity-based design principles is the main goal of the work. The review looks at the standards and variables applied to the design of weak beams and strong columns in irregularly built reinforced concrete frame buildings subject to seismic action. In addition to structural height and seismic zone, it takes into account analytical techniques, capacity ratio of beam columns, collapse mechanism, and chance of collapse.

M. Durga rao et.al (2021): The planned and assessed (G+6) multistory structure using STAAD Pro in limit state approach is the main subject of this research. The user-friendly interface of STAAD Pro enables users to create mounts and enter dimensions and load values. Details for reinforcement are included in the design of the members for RCC frames. After the analysis for two-dimensional frames is finished, it is completed for multistord2-D and three-dimensional frames under different load combinations.

Athul Kurzekar, et.al (2021): Structural design is an investigation method of the stiffness, strength, and stability of the building, according to the journal "Analysis and design of a residential building by using STAAD Pro." The primary goal of structural design is to build a structure that can withstand all applied loads without failing for the course of its planned life. A structural frame plan is created, a model is obtained, the structure is analyzed, and the structure is designed, among other steps in the structural design process.

Adhiraj wadekar et.al (2020): An analysis and design review using STAAD Pro is conducted for a multi-story structure. Planning is done using AutoCAD, load calculations are done by hand, and STAAD Pro is used for structural analysis. Calculations are made and applied to the structure for the dead load, imposed load, and wind load with load combination. Additionally, each structural element's precise shear force, bending moment, and torsion values that fall within IS code bounds are provided by the STAAD Pro program.

Dunnala Lakshmi Anuja et.al (2019): The planning, research, and design of a four-story residential structure with eight apartments on each floor are attempted in this project. STAAD PRO is the program used for frame analysis and design while analyzing structural analyses. Plans, stair cases, beam and column framing, and other details are drawn using AUTOCAD as well. Slabs, columns, footings, staircases, sunshades, lintel, septic tanks, and raised tanks were all designed for this project utilizing the IS: 456-2000 code book and the "Limit State Method."

T. Sahithi Gupta et.al (2017): The effect of floating columns in RC frames in various seismic zones in India is the main topic of this article. In addition to examining the impact of floating columns' placement at various points within the proposed design, the study takes into account the floating columns of an RC frame structure for (G+14) storeys in various seismic zones in India.

S.K. Abdul Rehaman et.al (2017): The principal subject of the study is the seismic analysis of frame constructions with and without floating columns. As a result of space constraints, population density, and aesthetic and functional requirements, multistory structures in metropolitan areas are needed to feature column-free space. An earthquake-resistant multistory framed structure's ability to accommodate more parking spaces and other amenities depends on its ability to support floating columns.

Deevi Krishna Chaitanya et.al (2017): The study utilizes Staad pro to analyze and design a multistory (G+6) structure. For the stability of the building structure's members, the moment at each consecutive joint in the frame and continuous beam was distributed using the Kanis technique.

B. Gireesh Babu (2017): Design and Seismic Analysis of the G+7 Residential Structure The seismic response of the structures under earthquake excitation is examined in this study using STAADPRO. The results are given as member forces, joint displacement, support reaction, and story drift. The STAAD PRO designing program is utilized to study the reaction for g+7 building constructions.

Susanne Bodach (2016): The paper focuses on Nepali hotels' energy-efficient design principles. By adjusting design elements such the window-to-wall ratio, glass type, shading

devices, and insulation levels, these reference designs were made more aesthetically pleasing. Energy demand and cost- effectiveness were assessed during the design optimization process.

III. CATEGORY

Based on the classification as per KMBR the hotel building comes under group A2. It includes lodging or rooming houses, seminaries/convents, orphanage, dormitories, tourist homes, tourist resorts (or by whatever name called), hostels, hotels with or without conference halls, dining halls or assembly rooms. Creches, daycare centres, children's nurseries reading rooms, libraries and educational buildings not exceeding 150 sq. metres of floor area are also included in this rule

IV. METHODOLOGY

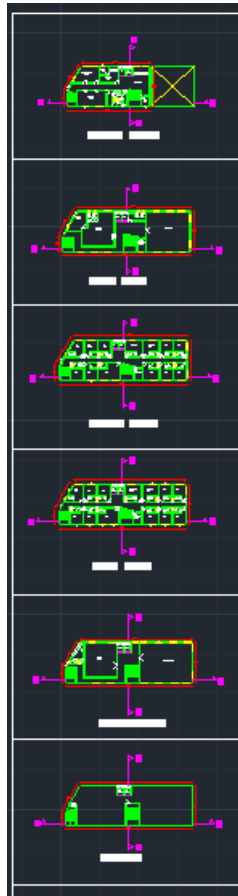
- Field Survey
- Planning
- Structural Analysis
- Structural Design
- Detailing

A. *Field Survey*

The practice of measuring an object's relative position on Earth's surface and drawing it to a manageable scale is known as surveying. A thorough survey and reconnaissance were conducted to ascertain the border and other pertinent information.

B. *Planning*

An architectural design, a landscape architecture document, and a thorough technical drawing of a suggested improvement on a specific lot are all included in a site plan. A site plan often displays the location of parking, traffic routes, and buildings. It demonstrates how a place or property is laid up.



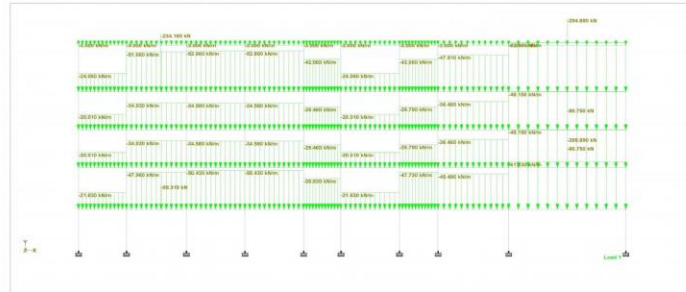
C. *Structural Analysis*

The analysis of a multistory building's frame is the primary component of its structural study. Determining the internal forces in component members, such as axial compression, bending moment, shear force, twisting moment, etc., for which the members are to be constructed under the action of external loads, is the study of a framed structure.

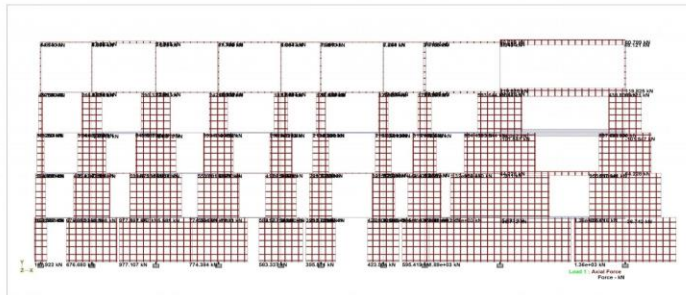
Analysis of the structure is done by STAAD. Analytical tasks can be completed in a single run and are integrated.

Using the editor or a CAAD-based input generator, one may construct the robust STAAD pro graphics input. STAAD utilizes the command language BA format. STAAD produces crisp, printed plots with excellent presentation quality for the run document in addition to comprehensive numerical findings for analysis.

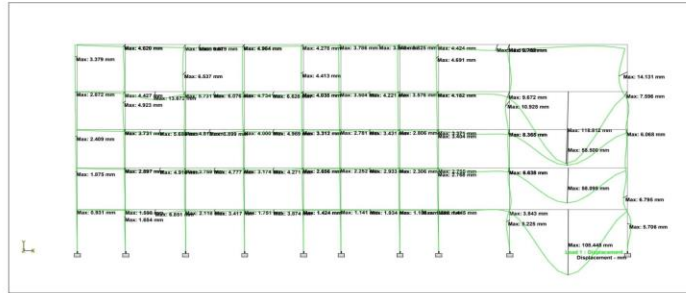
1) Long Frame



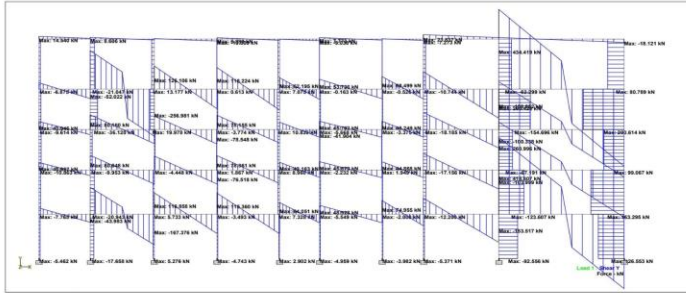
LOADING DIAGRAM



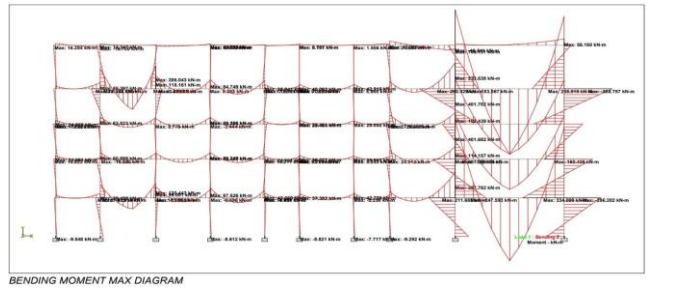
AXIAL FORCE DIAGRAM



DISPLACEMENT DIAGRAM

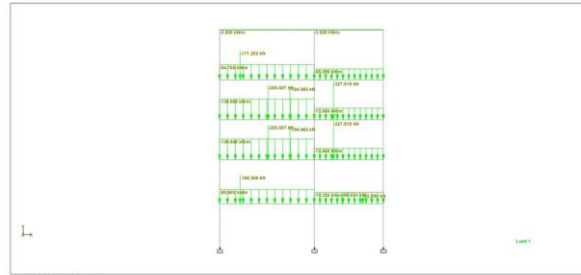


SHEAR FORCE MAX DIAGRAM

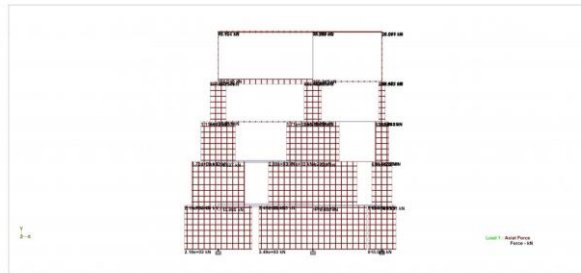


BENDING MOMENT MAX DIAGRAM

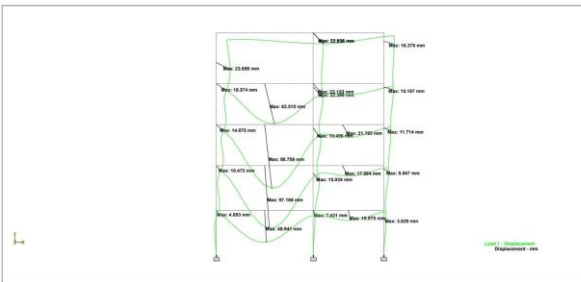
2) Short Frame



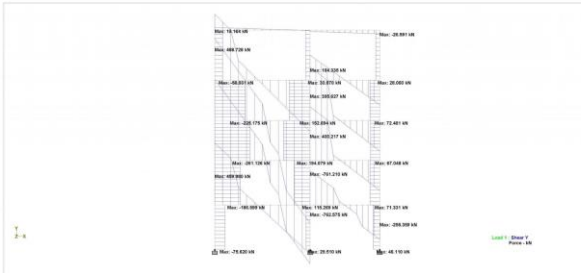
LOADING DIAGRAM



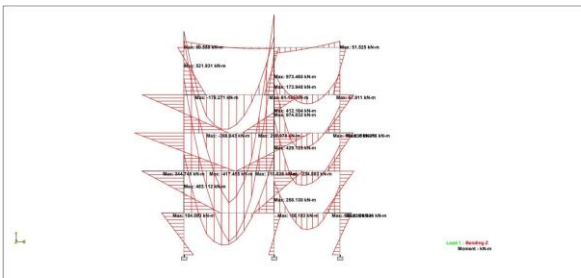
AXIAL FORCE DIAGRAM



DISPLACEMENT DIAGRAM



SHEAR FORCE MAX DIAGRAM



BENDING MOMENT MAX DIAGRAM

D. Structural Design

Working stress and limit state approaches are the most widely used methods of design for reinforced concrete members, as advised by IS 456 2000. The goal of design is to arrive at reasonable odds that the buildings will remain suitable for their intended use. The partial safety factors—one for material strength and another for load—are used to generate the design values from the characteristic value.

One-way Slab Design:

Table 16: Design of One-Way Slab(Second& Third Floor)

Slab No.	slab size (mm)	Dia of bar (mm)	Bending moment (Nmm)	A_{st} (mm ²)	Spacing (mm)
S15	440 × 200	8	3×10^6	1675.35	350
S16	740 × 280	8	11.76×10^6	3353.3	150
S18	440 × 160	8	2.4×10^6	1437.1	350
S20	440 × 140	8	2.94×10^6	1437.1	350
S21	580 × 187	8	2.805×10^6	1437.1	300
S23	640 × 161	8	3.88×10^6	1676.6	300
S25	503 × 100	8	1.5×10^6	1676.6	400
S27	290 × 120	8	1.8×10^6	1676.6	400
S29	440 × 160	8	3.84×10^6	1676.6	300
S30	440 × 150	8	3.37×10^6	1676.6	300

Table 17: Design of One-Way Slab(Fourth Floor)

Slab No.	slab size (mm)	Dia of bar (mm)	Bending moment (Nmm)	A_{st} (mm ²)	Spacing (mm)
S9	540 × 240	8	8.64×10^6	2515	200
S14	750 × 290	8	12.61×10^6	3809.2	130
S15	440 × 190	8	5.415×10^6	1676.7	300
S16	440 × 140	8	2.94×10^6	1437.1	350
S19	580 × 187	8	2.805×10^6	1437.1	300
S20	390 × 160	8	3.84×10^6	1676.6	300
S21	580 × 240	8	8.64×10^6	1676.6	300
S23	600 × 260	8	10.14×10^6	3143.75	160
S24	520 × 140	8	2.94×10^6	1437.6	350
S25	340 × 140	8	2.94×10^6	1437.6	350

1) Two-way Slab Design:

Table 18: Design of Two-Way Slab

Slab No.	slab size (mm)	Condition	Dia of bar (mm)	Bending moment (Nmm)	A_{st} (mm ²)	Spacing (mm)
S1	590 × 430	One short edge	8	$X' = 14.52$	4569.9	110
S2		discontinues		$X'' = 10.91$	3141.25	160
S3				$Y' = 10.91$	3141.25	160
S7				$Y'' = 8.312$	2393.3	210
S4, S5, S13, S27, S30	290 × 250	Interior Panels	8	$X' = 2.865$	1675.33	300
				$X'' = 2.58$	1675.33	300
				$Y' = 2.4$	1675.33	300
				$Y'' = 1.8$	1675.33	300
S26, S27	530 × 430	One short edge discontinues	8	$X' = 11.17$	3350.66	150
				$X'' = 8.20$	2393.33	210
				$Y' = 8.20$	2513	200
				$Y'' = 6.594$	1861.49	270
S8, S10	750 × 430	Two adjacent edges discontinues	8	$X' = 18.78$	7180	70
				$X'' = 14.05$	4569.9	130
				$Y' = 10.91$	5584.2	160
				$Y'' = 8.13$	3866.15	130

2) Beam Design:

Table 20: Design of Beam - Mid Span

Beam	W _u (kN)	Max Span (m)	W _d (kN)	W _t (kN)	Deflection (mm)		Stress (N/mm ²)	Strain
					1/4th span	Mid span		
B7	46.077	0.538	1.501	0	10	276.95	8	8
B8	28.421	38.74	0.93	0	6	103.18	8	5
B9	10.391	15.86	0.68	0	6	103.18	8	45
B11	103.04	30.53	1.20	0	10	203.32	8	5
B12	182.25	70.00	1.20	0	10	203.32	8	5
B14	20.20	28.07	0.93	0	6	103.18	8	36
B16	10.98	19.02	0.68	0	6	103.18	8	45
B17	79.23	40.92	1.20	0	10	203.32	8	8
B18	31.26	30.06	1.20	0	10	203.32	8	10
B19	20.06	27.29	0.68	0	6	103.18	8	36
B21	70.26	48.26	1.20	0	10	203.32	8	8
B24	58.08	30.16	1.20	0	10	203.32	8	11
B25	30.03	20.03	1.06	0	6	102.6	8	10
B26	10.20	10.07	0.68	0	6	103.18	8	25
B27	10.20	10.06	0.68	0	6	103.18	8	45
B28	40.08	17.50	0.68	0	6	103.18	8	45
B29	118.28	64.80	0.68	0	6	103.18	8	5
B30	150.06	62.18	0.68	0	6	103.18	8	5

3) Column Design:

Table 24: Design of Column

column No.	column size (mm)	P_u (kN)	A_c (mm ²)	P_u (%)	A_{st} (mm ²)	Dia. of bar	No. of bar
C1	350 × 350	1786.214	2000	0.1	5000×10^3	20	8
C2	400 × 600	3667.119	4000	0.4	10000×10^3	25	10
C3	350 × 550	2523.818	2500	0.4	625×10^3	20	8
C4	350 × 550	2496.196	2500	0.4	625×10^3	20	8
C5	500 × 800	7930.063	8000	0.8	1000×10^3	32	10
C6	400 × 600	3618.711	4000	0.6	666.67×10^3	25	10
C7	400 × 600	3156.193	4000	0.6	666.67×10^3	25	10
C8	500 × 800	5390.382	8000	0.6	5000×10^3	32	10
C9	350 × 550	1687.929	1500	0.1	150×10^3	20	6
C11	300 × 450	814.079	1000	0.4	250×10^3	16	4
C12	300 × 450	540.995	500	0.8	62.5×10^3	16	4
C15	300 × 450	567.774	500	0.8	62.5×10^3	16	4
C16	350 × 550	1191.871	1000	1.2	83.3×10^3	20	4
C17	300 × 450	933.632	1000	0.6	160×10^3	16	6
C18	300 × 450	966.983	1000	0.6	160×10^3	16	6
C19	400 × 600	3108.822	3000	0.6	5000×10^3	25	8
C21	300 × 450	676.68	500	0.6	83.3×10^3	16	4
C22	300 × 450	774.384	500	1.4	31.25×10^3	16	4
C23	300 × 450	583.337	500	0.8	62.5×10^3	16	4
C26	300 × 450	595.419	500	0.8	62.5×10^3	16	4

4) **Lintel Design:**

Clear span	1.6 m
Effective span	1.75 m
Width	0.2 m
Depth	0.15 m
Dia of main bars	10 mm
Dia of holding bars	8 mm
Dia of stirrup	6 mm

5) **Footing Design:**

Dimension	1.6 × 1.3m
Depth of Foundation	4 m
Net Safe Ultimate Bearing Capacity	647.036KN/m ²

6) **Stair Design:**

Area of stair case	5.6 × 4.6 m
Area of landing	4.6 × 1 m
Width of stair	2 m
Tread	30 cm
Rise	15 cm
Thickness of waist slab	290 mm

7) **Septic Tank Design:**

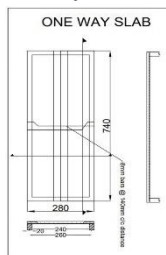
Population	150 persons
Sewage/Capita/Day	120 L
Quantity of sewage produced	18000 litre/day
Total required capacity of tank	18.9 m ³

8) **Water Tank Design:**

Size of tank	5 × 3 × 2 m
Capacity of Tank	30000 L
Free board	30 cm
Thickness of base slab	200 mm
Thickness of wall	300 mm
Dia of bars	12 mm

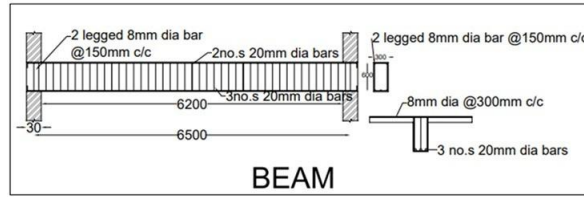
E. Detailing

1) **One-way Slab:**

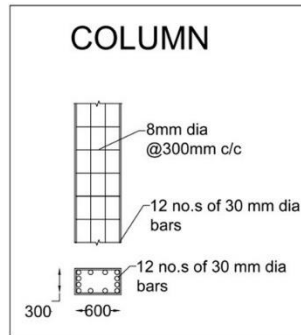


2) **Two-way Slab:**

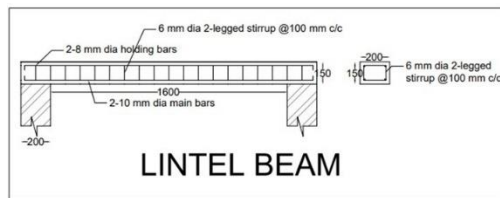
3) **Beam:**



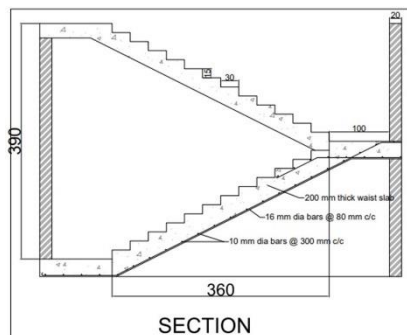
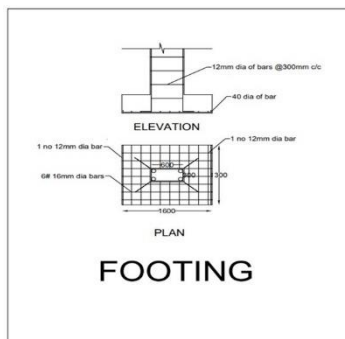
4) **Column:**



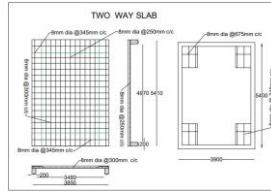
5) **Lintel:**



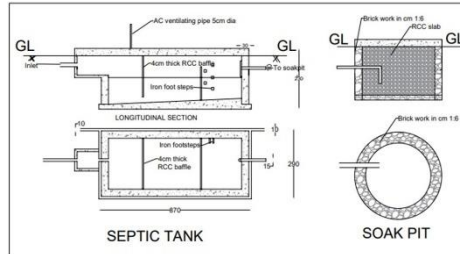
6) **Footing:**



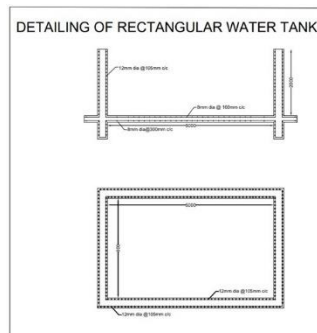
7) **Staircase:**



8) **Septic Tank:**



9) **Tank:**



V. **METHODOLOGY**

The planning, analysis and design of the (G + 4) Hotel building. The planning of the building was according to Kerala Municipal Building Rules. Analysis using STAAD Pro was done. The building was designed according to IS 456-2000, IS 875(Part 1,2,3) . Limit state method was adopted for the design of various building elements such that it full fills all the requirements and performs satisfactorily during its intended life, with an appropriate degree of freedom.

REFERENCES

- [1] Vikash Agrawal et al. “Analysis and Design of Residential Building (G+4) by STAAD Pro”, *International Journal of Research Publication and Reviews*, VOL. 3,NO. 6, JUNE 2022
- [2] Saha Sowravet al. “Design and Analysis of Multistorey (G+14) Resi- dential Building Using Staad.Pro & Autocad,” *International Journal of Scientific Research in Civil Engineering*, VOL. 5,JUNE 2021.
- [3] Banavanuru Vinod Kumar Reddy et al. “Analysis and Design of Residen- tial Building (G+4) by STAAD Pro”, *International Journal of Research*, VOL. 8, NO. 3, MARCH 2021

- [4] K. Harshitha et al. "Analysis & Designing of Five Star Hotel building by using E-Tabs", *International Journal for Scientific Research & Development*, VOL. 9,NO. 4, JUNE 2021
- [5] Mr. M Durga Rao et al."Analysis and Design of G+6 Residential Building Using Staadpro", *International Journal of Research Science and Advanced Engineering Technology*, VOL. 8,NO. 9, SEPTEMBER 2020
- [6] Wadekar Adhiraj et al."Analysis and Design of a Multistorey Building by Using STAAD Pro", *International Journal of Advanced Research*, VOL. 8, 2020
- [7] Dunnala Lakshmi Anuja et al."Analysis and Design of G+5 Residential Building Using Staadpro", *International Journal of Engineering Development and Research*, VOL. 7,NO. 3, 2019
- [8] Neelam Sharma, R. C. C. Design and Drawing, S.K. Kataria & Sons, 3, 2013.
- [9] Kerala Muncipal Building Rules, 2019.
- [10] IS 456-2000, Design Code of Practise for Plain and Reinforced Concrete, Bureau of Indian Standards, New Delhi
- [11] IS 875 1987 (PART 1, PART2)
- [12] IS 875 1987 (PART3)

Planning, Analysis and Design of Thermal Comfort Auditorium in KMCT Technical Campus

Arya KV

Dept. of Civil Engineering

KMCT CEW Kozhikode, India
aryakv2003@gmail.com

Ayisha Nasli PC

Dept. of Civil Engineering

KMCT CEW Kozhikode, India
ayshaneslipc@gmail.com

Fathima Nida TP

Dept. of Civil Engineering

KMCT CEW Kozhikode, India
fathimanida668@gmail.com

Hiba

Dept. of Civil Engineering

KMCT CEW Kozhikode, India
hibakprkdd1@gamil.com

Ms Sindhu V

Dept. of Civil Engineering

KMCT CEW Kozhikode, India
sindhuv@kmctcew.ac.in

Prof. UC Ahammed Kutty

Dept. of Civil Engineering

KMCT CEW Kozhikode, India
ucakutty@gmail.com

Abstract—The project deals with Planning, Analysis and Design of a proposed auditorium for KMCT Technical Campus. The proposed site is located at Kalanthode, Calicut district. The building is three storeyed (G+2) and is designed as framed structure. Concrete mix used for the RCC structure is M20 and steel used is high yield strength deformed bars of grade Fe415. The functional planning is done using KERALA PANCHAYATH BUILDING RULE and INDIAN STANDARD CODES. The structure shall be designed to resist and bear all loads liable to act on it. The plan is drafted using AUTOCAD software and analysis is done using STAAD.Pro software. Project is based on limit state method.

16-1980. Kerala panchayath building rules were also referred for fixing setback, F.A.R, parking etc.

II. LITERATURE SURVEY

Hong Chang, et.al (2023): This journal presents a comprehensive introduction to an experimental study focused on unravelling the intricate thermodynamic properties of high thermal conductivity Energy piles. As a pivotal component of modern geothermal systems, energy piles have the potential to influence the efficiency and environmental impact of building operations significantly.

INTRODUCTION

The aim of this project is to plan, Analyse and design a three storied auditorium building. The planning is carried out as per Kerala Panchayath Building Rules (KPBR). The building is designed as a framed structure. The plan is drafted using Auto Cad software and analysed and designed using STAAD Pro software. All the structures and structural elements are designed according to the Limit State Method. The proposed site for the establishment of the project is located at Kalanthode. The area of the plot is about 1591.3105 sq m. In this project,

thermal comfort is provided to the auditorium by constructing energy piles. Energy piles are a sustainable and innovative foundation technology to enhance energy efficiency and thermal comfort. Constructing an auditorium with energy piles offers structural support, thermal comfort and sustainability to the auditorium. The aim of this design is to establish a structure that fully fills all the requirements and performs satisfactorily during its intended life, with an appropriate degree of freedom. The IS codes used in this project are IS 456-2000, IS 875 (part 3)-1987, SP 16-1980, SP 34 (s & t)-187, IS 3370(part 2)-1967. The wind loads are calculated as per IS 875 (part 3)-1987 and seismic loads are calculated by adopting IS 1893(part 1)-2002. Design of concrete element is carried out as per IS 456-2000 and SP

Mahesh B. Chougule (2023): The study of sound, or wave motion in gases, liquids, and solids, as well as the consequences of that wave motion, is known as acoustics. Acoustic absorption is the primary acoustic phenomenon taken into account while planning an amphitheater.

It has been explained physically, and a comparative analysis of two auditoriums has summarized the key ideas for their practical implementation.

Shafi Ahmad, et.al (2023): The project's goal was to forecast the thermal comfort of people using various UFAD ventilation configurations in an indoor auditorium. This paper analyzes the temperature distribution and thermal comfort of human occupants under four distinct ventilation scenarios using a simulated auditorium model.

Neha Sharma, et.al (2022): The project's goal was to design the auditorium's steel framework. In STAAD, a prototype is created. Pipe and tube parts are inspected for both the steel curving roof and the pro. Section selection is first done using the hit-and-trial approach, and then STAAD optimization is carried out. Pro: The optimal portion is recommended when cost analysis is completed.

Zahraa Mohamad, et.al (2021): The present article functions as a preface to an extensive review that delves into the various facets of Energy pile design, evaluation, and optimization. The objective of this paper is to present a thorough summary of the most recent methods for designing energy piles, taking into account factors including environmental impact, thermal performance, and structural issues.

Rupesh S, et.al (2021): The project's goal was to analyze the seismic and structural design of an auditorium in Puducherry state that could accommodate 700 people and had diverse soil conditions. The software STAAD.Pro was used to analyze and design the auditorium in detail for this work.

Akshay K Ghuge, et.al (2021): The project's study and design focused on an auditorium building in the Maharashtra state's Aurangabad city. The building of the auditorium offers a solution to the numerous cultural events that are conducted. STAAD.Pro analysis with generic loading turned out to be a high-end program with a lot of potential for the construction industry's analysis and design divisions.

Ashwini Mareena Sam, et.al (2020): This technical paper presents the project work on the extended 3D analysis of building system, or ETABS, computer program for the structural analysis and design of a multipurpose theater. The National Building Code was used for the planning of the acoustic and visual points of view, and the corresponding IS codes were used to limit state mode of collapse.

Maria Cairolì (2020): The project's focus was on the multipurpose auditorium's architectural and acoustic design. The case study was conducted in the "Le Serre" hall, which can accommodate up to 1000 people, at the Villa Erba Convention Centre in Cernobbio, Italy. The study focused on the development of various configurations of movable architectural pieces to create a multipurpose space.

Kishan Dewangan, et.al (2020): The seismic study and design of an auditorium with 964 seats are the subjects of this project. Planning, load analysis, and structural element design depending on the loads acting on them are all included in this. The main goal of this project is to further design and plan acoustics in Safead Pro v8i using standard provisions and appropriate analysis of the various types of loads in the various seismic zones (II, III, and IV).

Richard J. Zhang (2020): This work investigates the properties of a 1D harmonic plane wave and applies it to a quarter-ellipsoid model of an amphitheater. The primary topics of this essay include frequency variations, reverberation, interruption of the performance, and transmission loss. This work attempts to review a large portion of the theoretical foundation of acoustics and investigate the acoustical characteristics of a theoretical auditorium shaped like a quarter of an ellipse.

Andreea-Roxana Vasilescu (2019): The primary goal of this thesis is to determine and measure the key variables that affect the geotechnical design of pile foundations when temperature fluctuations are linked to geothermal activation. The experimental findings are utilized to calculate how a pile foundation's geothermal activation will affect both its long-term exploitation and bearing capacity.

K Anand Babu, et.al (2019): The project's goals are to optimize and estimate the cost of designing a steel roof truss over an auditorium. STAAD.Pro is used to create a prototype model, with the I and channel sections being used as sections that are available according to the IS code. The entire truss section is examined for self-weight and has a substantial amount of roofing material covering it.

Shankar Saj T K, Sachin Saj T K (2019): A dining hall and an auditorium with seats for 1000 people are included in the design. Artificial lighting and ventilation are implemented in consideration of current market trends. It is suggested to use a trussed roof with a fall ceiling. We have incorporated load calculations, slab, stair, beam, and column designs, as well as footings, in this project work.

C R Vigneshwar (2018): The project's objectives were auditorium planning, analysis, design, and estimation. Every plan is created using AutoCAD. The auditorium is laid out in accordance with the NBC criteria. It is intended to be a framed building.

III. METHODOLOGY

- Field Survey
- Planning
- Structural Analysis
- Structural Design
- Detailing

A. *Field Survey*

Surveying is the art of determining the relative positions of objects on the surface of the earth's measurements and drawing them to a convenient scale. Reconnaissance and detailed survey are carried out to determine the boundary and various other details.

B. *Planning*

An architectural plan, a landscape architecture document, and a thorough engineering drawing of the suggested improvements on a specific lot are all included in a site plan. A site plan typically displays the location of parking, travelways, and buildings. It displays a property or site's plan.



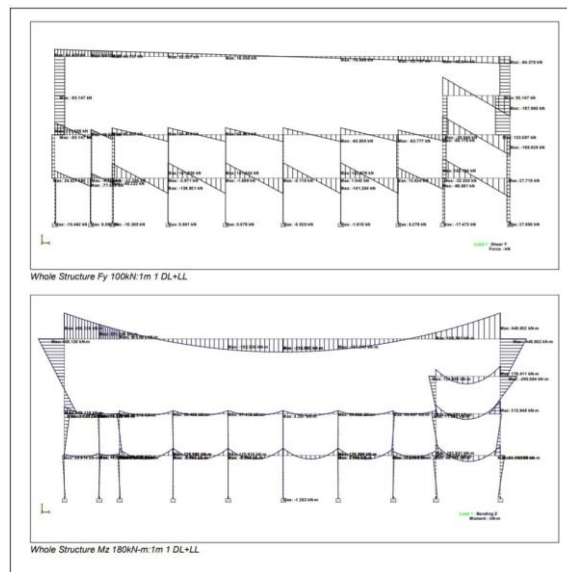
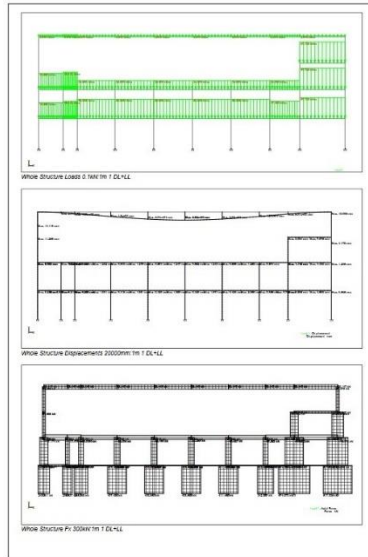
C. Structural Analysis

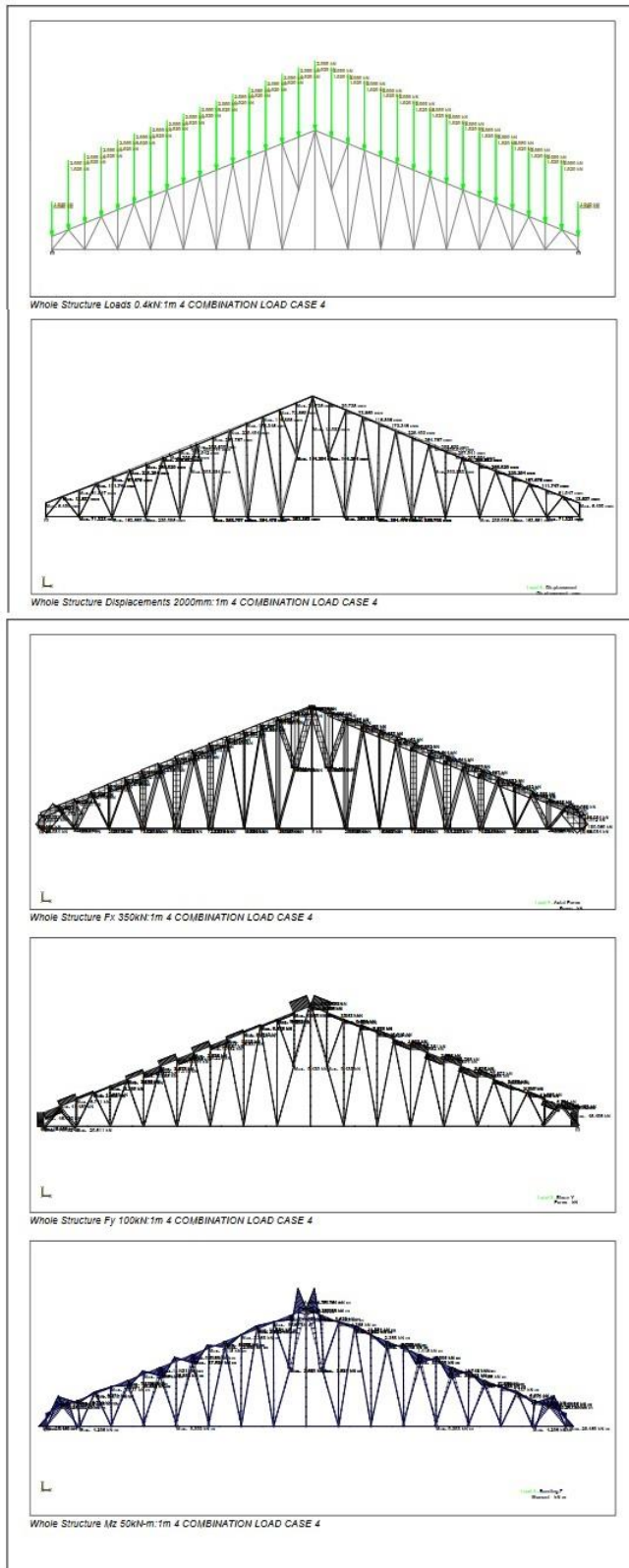
Determining the internal forces in component members, such as axial compression, bending moment, shear force, twisting moment, etc., for which the members are to be constructed under the action of external loads, is the study of a framed structure.

STAAD performs the analysis of the structure. The process of analysis is integrated and can be performed in the samerun. STAAD uses command language ba format which can be created through the editor; the powerful STAAD pro graphics input is generated or through CAAD-based input generator.

The output generated by STAAD consists of detailed numerical results for analysis and sharp presentation quality printed plots as part of the run document.

1) Long Frame

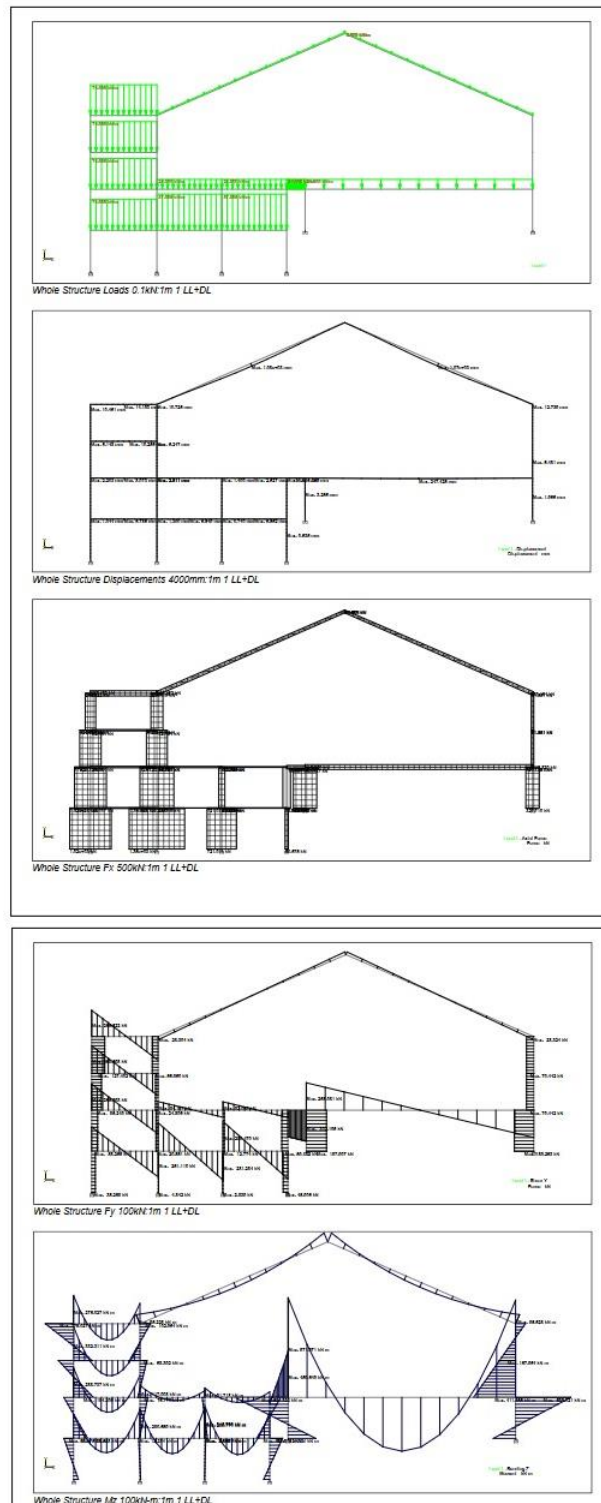




2) Main Frame

H. 2) Truss

D. Structural Design



According to IS 456 2000, the working stress technique and the limit state method are the most often applied methods of design for reinforced concrete members. The design seeks to

attain reasonable odds that the buildings won't degrade beyond their intended use. Using a partial safety factor—one for material strength and another for load—the design values are obtained from the characteristic value.

1) One-way Slab Design:

Table 11: DESIGN OF ONE WAY SLAB

Slab No.	slab size (mm)	Dia of bar (mm)	Bending moment (Nmm)	A_{st} (mm ²)	Spacing (mm)
S2	635 × 195	10	3.49×10^6	174.532	450

2) Two-way Slab Design:

Table 10: DESIGN OF TWO WAY SLAB

Slab No.	slab size (mm)	Condition	Dia of bar (mm)	Bending moment (Nmm)	A_{st} (mm ²)	Spacing (mm)
S1	335 × 479	2 adjacent edges discontinues	10	$X^- = 10.575$	224.399	350
				$X^+ = 7.895$	196.349	400
				$Y^- = 6.922$	196.349	400
				$Y^+ = 5.155$	196.349	400
S4, S5, S6, S7, S8	530 × 635	One short edge discontinues	10	$X^- = 17.328$	392.699	200
				$X^+ = 12.903$	280.499	280
				$Y^- = 13.641$	302.076	260
				$Y^+ = 10.323$	224.399	350
S9	410 × 635	One short edges discontinues	10	$X^- = 12.796$	280.499	280
				$X^+ = 9.707$	224.399	350
				$Y^- = 8.163$	196.349	400
				$Y^+ = 6.177$	196.349	400
S10	620 × 635	2 adjacent edges discontinues	10	$X^- = 24.217$	560.998	140
				$X^+ = 18.162$	413.367	190
				$Y^- = 23.719$	560.998	140
				$Y^+ = 17.658$	392.699	200
S14, S15	530 × 635	Interior panel	10	$X^- = 15.484$	356.999	230
				$X^+ = 11.429$	261.799	300
				$Y^- = 11.797$	261.799	300
				$Y^+ = 8.848$	196.349	400

Slab No.	slab size (mm)	Condition	Dia of bar (mm)	Bending moment (Nmm)	A_{st} (mm ²)	Spacing (mm)
S22	450 × 667	One short edge discontinues	10	$X^- = 14.883$	341.477	230
				$X^+ = 11.428$	261.799	300
				$Y^- = 9.833$	224.399	350
				$Y^+ = 7.441$	196.349	400
S23	630 × 496	One short edge discontinues	10	$X^- = 16.144$	373.999	230
				$X^+ = 12.270$	270.826	300
				$Y^- = 11.947$	261.799	350
				$Y^+ = 9.041$	196.349	400

3) Beam Design:

Table 12: DESIGN OF BEAM

Beam	M_u (KNm)	Max Shear force(KN)	Reinforcement Details			Stirrup Provided	
			Dia of Bar(mm)	No of Bar	Ast req (mm ²)	Dia of bar(mm)	Spacing (mm)
B1(SF)	232.503	236.293	20	6	1853.73	8	20
B2(SF)	287.508	277.421	20	6	1853.73	8	20
B3(SF)	316.795	289.47	20	6	1853.73	8	20
B6(SF)	288.737	255.093	20	6	1853.73	8	20
B7(SF)	47.008	84.197	20	6	1853.73	8	20
B8(SF)	91.718	82.053	20	6	1853.73	8	20
B10(SF)	971.971	268.081	20	14	4435.02	8	20
B11(SF)	332.311	268.598	20	6	1853.73	8	20
B16(SF)	275.027	255.522	20	6	1853.73	8	20
B1(LF)	24.218	68.398	20	6	1853.73	8	20
B2(LF)	28.437	45.256	20	6	1853.73	8	20
B3(LF)	107.654	134.719	20	6	1853.73	8	20
B4(LF)	126.692	141.936	20	6	1853.73	8	20
B5(LF)	125.918	141.634	20	6	1853.73	8	20
B6(LF)	124.820	141.162	20	6	1853.73	8	20
B7(LF)	126.866	142.878	20	6	1853.73	8	20
B8(LF)	72.444	95.76	20	6	1853.73	8	20
B9(LF)	182.931	182.194	20	6	1853.73	8	20
B10(LF)	129.119	111.005	20	6	1853.73	8	20
B11(LF)	18.766	48.329	20	6	1853.73	8	20

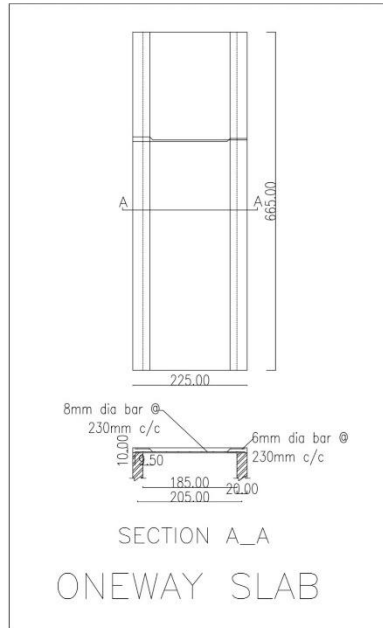
4) Column Design:

Table 13: DESIGN OF COLUMN

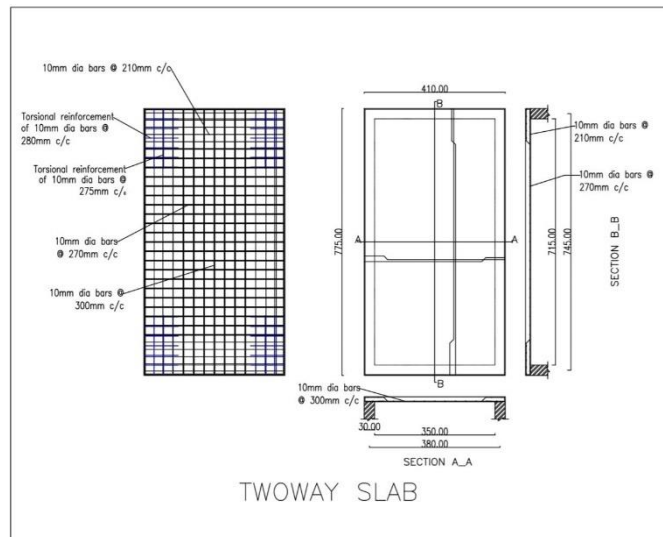
Column No	Size of Column (mm)	Axial load (KN)	A_s (mm^2)	P_t (%)	A_g (mm^2)	Diameter of bar(mm)	No of bars
C26(SF)	600 × 400	1015.506	1000	0.8	125×10^3	20	4
C7(SF)	600 × 400	721.011	1000	0.6	166.67×10^3	20	4
C1(LF)	600 × 400	617.035	1000	0.6	166.67×10^3	20	4

E. Detailing

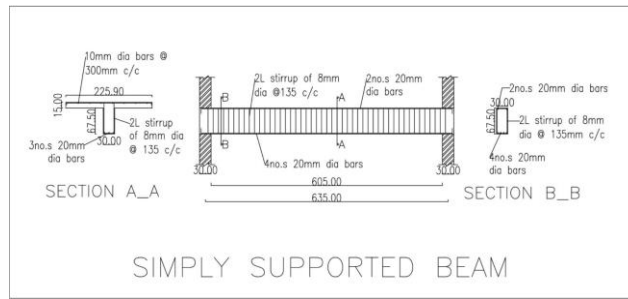
1) One-way Slab:



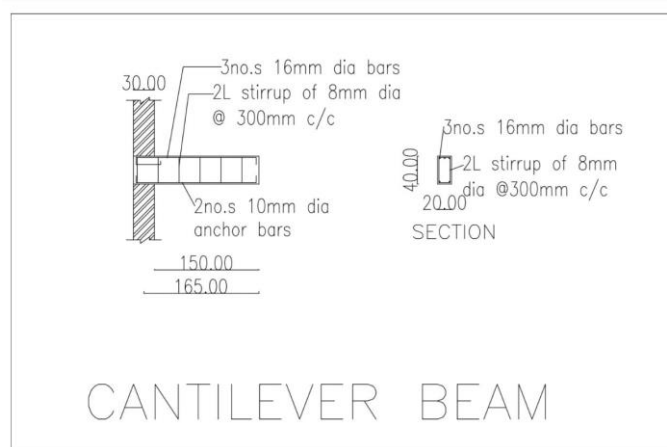
2) Two-way Slab:



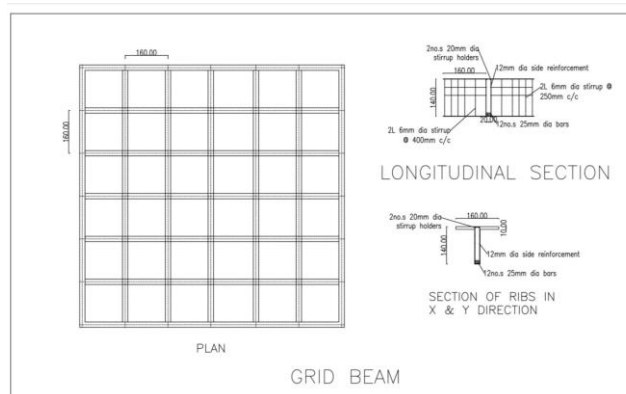
Beam:



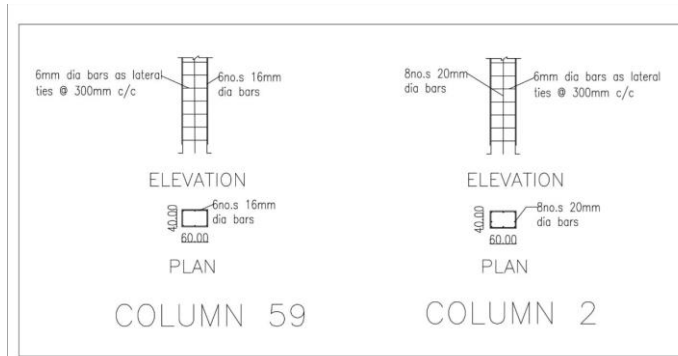
3) Cantilever Beam:



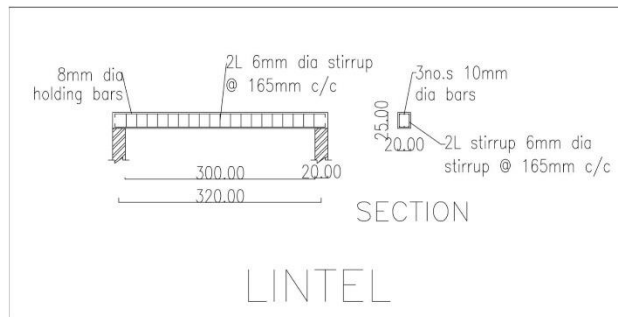
4) Grid Beam:



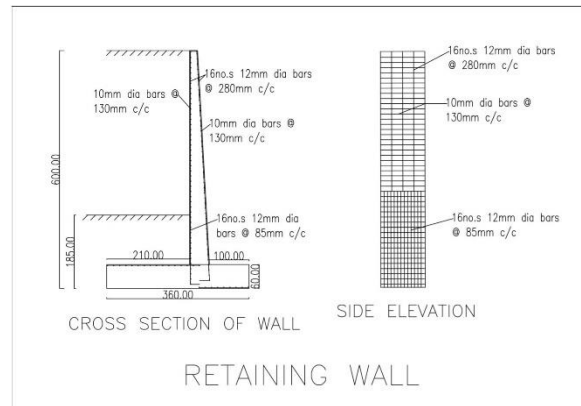
5) Column:



6) Lintel:



7) Retaining Wall:



support and renewable energy generation. Their primary purpose is to:

- 1) Provide Structural Support
- 2) Harness Renewable Energy

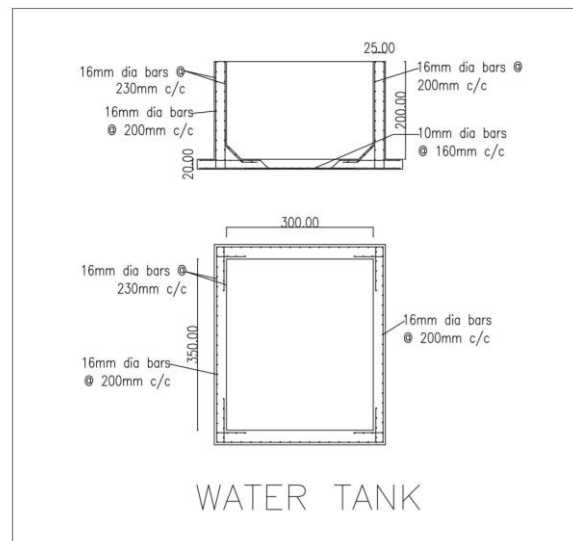
B. Working Principle OF Energy Piles

The working principle of Energy piles involves using the foundation piles of a building or structure as a means to exchange heat with the surrounding environment, typically the ground, to provide heating or cooling. Energy piles are embedded with a network of pipes containing a heat transfer fluid, often a mixture of water and antifreeze. A heat pump or heat exchanger circulates the heat transfer fluid through the pipes within the energy pile. As the fluid moves through the pipes, it absorbs heat from the relatively warm ground during winter and the process is reversed during summer.

V. CONCLUSION

Enhancing audience happiness, decreasing weariness, and improving attention may all be attributed to a well-designed auditorium that places a high priority on thermal comfort. Energy piles improve thermal comfort and give an auditorium structural stability when they are incorporated into the design. Overall, STAAD pro is used to analyze and the limit state approach is used to build an auditorium that can accommodate 1200 people.

12) Tank:



IV. THERMAL COMFORT

A. Energy piles

Energy piles are a sustainable and innovative geotechnical engineering solution that combines the functions of structural

REFERENCES

- [1] Shafi Ahmad, et.al (2023), "Predicting Thermal Comfort Of Occupance In An Indoor Auditorium Space With Different UFAD Ventilation Arrangement".
- [2] Hong Chang, et.al, (2023), "Experimental Study of the Thermodynamic Properties of High Thermal Conductivity Energy Pile".
- [3] Neha Sharma, et.al, (2022), "Design Of Steel Structure Of An Auditorium".
- [4] Zahraa Mohamad, et.al, (2021), "A Review on Energy Piles Design, Evaluation, and Optimization".
- [5] Akshay K Ghuge, et.al, (2021) "Design And Analysis Of Auditorium Using STAAD.Pro Software".
- [6] Rupesh S, et.al (2021), "Analysis Of A Structural And Seismic Design Of An Auditorium".
- [7] K. Anand Babu, et.al (2019), "Steel Roof Truss And Optimisation Design And Cost Estimation Over Auditorium Hall".
- [8] Badhira E.A , et.al (2019), "Planning, Analysis And Design Of An Auditorium Building".
- [9] C.R Vigneshwar (2018), "Planning, Analysis, Design And Estimation Of An Auditorium".
- [10] Sachin Saj T K , et.al (2018), "Planning , Analysis And Design Of An Auditorium".

Utilization Of E-Waste in Strength Enhancement of Soil

NAFEESA MINHA P

Student

Dept. of civil engineering,
AWH engineering college kuttikattoor, kerala, india

NIDHA SHERIN K

Student

Dept. of civil engineering,
AWH engineering college kuttikattoor, kerala, india

SAHLA SHERIN M

Student

Dept. of civil engineering,
AWH engineering college kuttikattoor, kerala, india

SACHINLAL C

Assistant Professor

Dept. of civil engineering,
AWH engineering college kuttikattoor, kerala, india

RAMEEZA JAHAN M

Ug Student

Dept. of civil engineering,
AWH engineering college kuttikattoor, kerala, india

Abstract—Soil stabilization involves the modification of soil properties, both index and engineering, with the aim of enhancing its performance. The primary objective in construction is to bolster soil strength and stability, thereby reducing costs. A contemporary focus lies on integrating waste materials with soil, offering potential solutions to the escalating challenge of waste management. Looking ahead, the looming issue of E-waste presents a significant concern, necessitating proactive solutions. The study emphasizes the potential of E-waste as a sustainable solution for enhancing soil quality, offering benefits in waste management and infrastructure development. Through an experimental program, the research investigated the impact of different doses of E-waste on soil. Various amounts of E-waste, ranging from 2% to 8%, were introduced into the soil. To evaluate the efficacy of E-waste treatment, the soil underwent several physical and strength tests, including Atterberg's limits, specific gravity, compaction, unconfined compressive strength, and California bearing ratio (CBR). These assessments aimed to measure improvements in soil strength characteristics. The findings revealed a decrease in optimum moisture content (OMC), an increase in unconfined compressive strength, and enhanced soil bearing capacity as a result of E-waste incorporation.

keywords— Electronic waste, soil Stabilization, Unconfined Compressive Strength, dry density, Optimum Moisture Content, California Bearing Ratio.

INTRODUCTION

Soil stabilization means making soil better for building construction by using mechanical or chemical methods. The goal is to make soil stronger and more durable. It includes squash the soil down, make sure water drains out, change the size of the soil particles, or add many artificial or natural stabilizers as E-waste used in this study. Engineers care about how strong the soil is, how much it can squash down, how tightly packed it is, and how long it will last. This achieved by

performing tests in labs and out in the field to figure out which method and material will work best. Extensive soil testing ensures the effectiveness of methods such as compaction, strength, drainage.

Electronic waste, commonly known as E-waste refers to discarded electronic devices such as computers, smartphones, and televisions. E-waste represents a swiftly expanding waste category, surging nearly three times faster than municipal waste. A considerable fraction of municipal solid waste comprises plastic waste, with an estimated generation of about 10 thousand tons per day. The global yearly consumption of plastic materials has surged from roughly 5 million tons in the 1950s to nearly 100 million tons presently. After dismantling it is then grinded. This grinded waste were add in different distributions into soil and enhance the strength of weak soil.

Principles of Soil Stabilization:

Assessing the soil characteristics of the designated area, determining the specific soil property requiring modification to achieve the desired design value, and selecting the most efficient and cost-effective stabilization method. Subsequently, creating a stabilized soil mix sample, conducting laboratory tests to ensure the desired stability and durability values are met.

OBJECTIVES

- To evaluate the strength properties by Unconfined Compression Strength (UCS) test on various mixes and to find optimal mix.
- To find the dry density and Optimum Moisture Content (OMC) of the soil by proctor compaction test.
- To find the California Bearing Ratio (CBR) values of the soil and optimal mix.
- To assess the usefulness of E-waste-soil mix for the strength enhancement of soil.

METHODOLOGY

1. The soil sampling process involves collecting soil.
2. Physical properties of soil identified, including texture and consistency.
3. Basic tests conducted on soil samples: Sieve analysis, Atterberg limits, Specific gravity, and Hydrometer analysis.
4. Soil mixed with various proportions of E-waste (2%, 4%, 6%, and 8%).
5. Tests performed on soil-E-waste mixtures: Proctor compaction test, Unconfined Compression Test (UCC), and California Bearing Ratio (CBR) test.
6. Test result were analyzed, tabulated and graphs were plotted.

MATERIALS AND PROPERTIES

Soil:

The soil was collected from the site of river bank at kadalundi near Feroke, located at Kozhikode district at a depth of 1.5m and is shown in Figure 1. Organic wastes are removed after drying the

soil and is then surface dried for 1 week. soils are sieved according to each test. Different properties of soil were determine by various tests. The properties of soil are shown in Table 1.



Figure 1 : Soil collected

Table 1 : Properties of Soil

Properties	Values
Specific Gravity	2.68
Liquid Limit (%)	45
Plastic Limit (%)	30.4
Plasticity Index	14.6
OMC (%)	23
MDD g/cc	1.56
Classification	OL (Organic silt with low liquid limit)
CBR value (%)	12.49

A. E-waste:

E-waste is collected from the scrap stores. The E-waste consists of Printed Circuit Board (PCB), electric wires and electric fuses. The composition of E-waste shown in figure 2. These items are collected, sorted and often disassembled or salvageable components like metals, plastics and circuitry. After dismantling it is then grinded, the grinded E-waste were add in different percentages into soil. E-waste after grinding is shown in Figure 3.

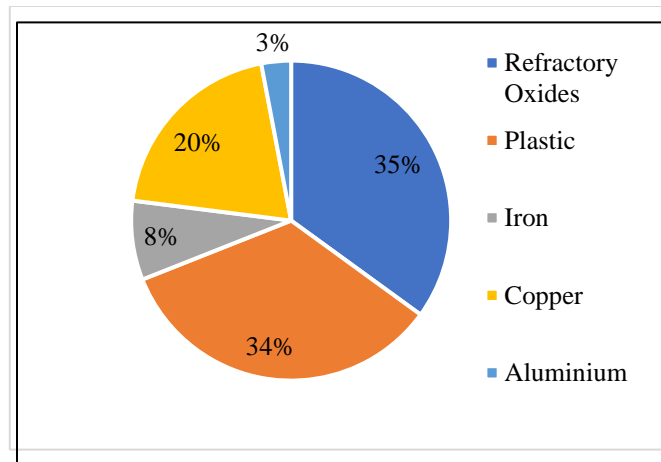


Figure 2 : Composition of E-waste



Figure 3 : E-waste after grinding

I. SPECIMEN PREPARATION

The grinded E-waste particle were mixed with soil thoroughly using a mechanical mixer or manually, ensuring that the mixture is homogenous. The quality of E-waste added depends on the specific surface area of soil particles. Therefore, here mixed e-waste with soil in varying percentages (0%,2%,4%,6%, 8% by weight).

II. EXPERIMENTS CONDUCTED

A. *Unconfined Compressive strength*

Unconfined compressive test is an important test used for determination of compressive strength of soil. Place the soil in a constant volume mould, having an internal height of 7.2 cm and internal diameter of 3.9 cm.

B. **Proctor compaction test**

Proctor compaction test is performed for determination of Optimum Moisture Content and Maximum Dry Density. Light compaction is done using 4.89 kg hammer with 25 blows in each layer is filled in proctor mould.

C. California Bearing Ratio test

This test is used for determination of bearing capacity of soil. The soil is filled in a mould of 2250 cc volume in 5 layers, 56 blows are given in each layer by 4.89 kg hammer with addition of water at OMC.

III. RESULT AND DISCUSSION

After analyzing the basic properties of soil and soil treated with E-waste, Various strength parameters such as Maximum Dry Density (MDD), Optimum Moisture Content (OMC), California Bearing Ratio (CBR), and Unconfined Compressive Strength (UCS), were determined through compaction, CBR and UCS tests.

A. *Effect of E-Waste on Dry Density* The variation of dry density and E-waste are as respectively. The 6% E waste stabilized soil shows maximum dry density and the improvement in dry density is about 8% as compared to unstabilized soil. and is shown in Figure 4. The dry density of E-waste stabilized soil is more than the soil mass alone. The maximum dry density is 1.56 g/cc, 1.57 g/cc, 1.65 g/cc, 1.66 g/cc and 1.54 g/cc respectively for 0, 2%, 4%, 6% and 8% of E-waste.

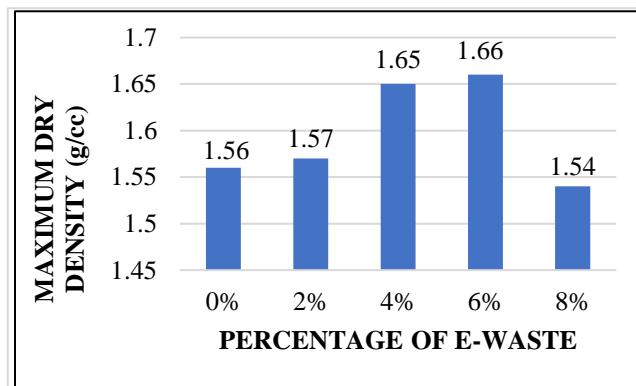


Figure 4 : Effect of E-waste on Dry Density

B. Effect of E-waste on Optimum Moisture Content

The variation of water content and E-waste are as shown in Figure 5. As the addition of E-waste increases, dry density increases and at the same time optimum moisture content decreases up to 6%. The optimum moisture content is 23%, 21.9%, 21.42%, 20.6% and 26.66% at 0, 2, 4, 6 and 8% E-waste respectively. The 6% E waste stabilized soil shows the minimum optimum moisture content and the decrease in the optimum moisture content is about 26.98% as compared to the unstabilized soil.

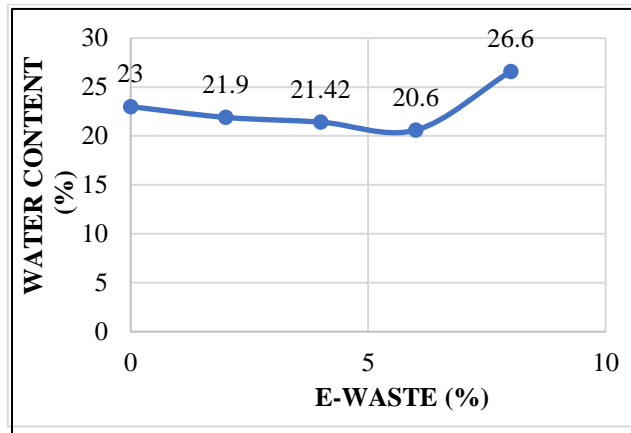


Figure 5 : Effect of E-waste on water content

C. Effect of E-waste on Compaction

Figure 6 shows the dry density v/s water content graph for 0, 2, 4, 6 and 8% E waste stabilized soil. The 6% E waste stabilized soil shows maximum dry density and 6% E-waste stabilized soil shows minimum optimum moisture content.

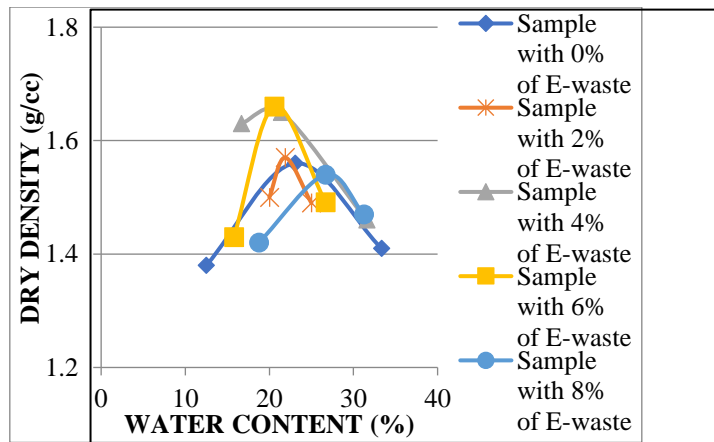


Figure 6 : Effect of E-waste on Compaction

D. Effect of E-waste on Stress Strain Behaviors

Figure 7 shows the stress strain behavior of soil and E waste stabilized soil. The maximum stress in E waste stabilized soil is greater than the un-stabilized soil. The 6% E waste stabilized soil shows the maximum unconfined compression strength and the increase in the unconfined compression strength is about 70.5% as compared to un-stabilized soil.

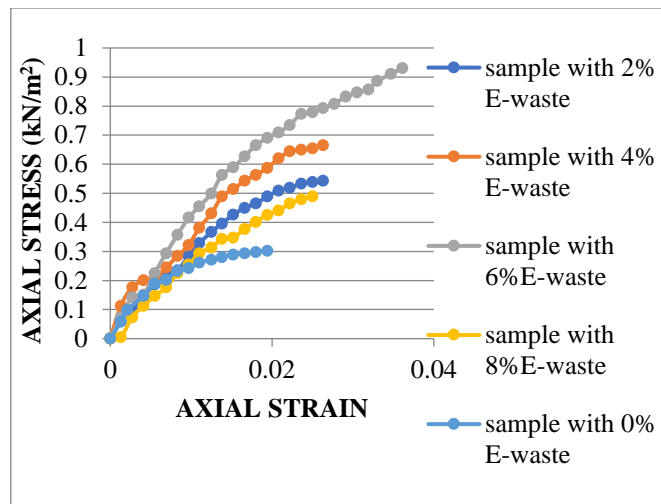


Figure 7 : Effect of E-waste on UCC Characteristics

Unconfined compression test values of soil with different percentages (0%, 2%, 4%, 6%, 8%) are shown in the Table 2. The 6% E-waste stabilized shows maximum value of strength of 9.11 kN/m²

Table 2 : UCC Values

SAMPLE	UCC (kN/m ²)
Soil+0% E-WASTE	2.96
Soil+2% E-WASTE	5.32
Soil+4% E-WASTE	6.51
Soil+6% E-WASTE	9.11
Soil+8% E-WASTE	4.79

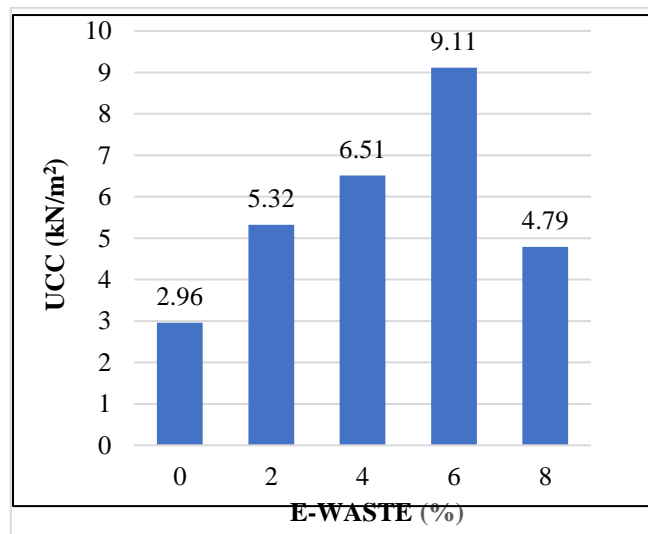


Figure 8 : Effect of E-waste on Unconfined strength

E. Effect of E-waste on Undrained strength

The variation of undrained strength and E-waste are as shown in Figure 9. The undrained strength of E-waste stabilized soil is more than the soil mass alone. The maximum undrained strength is 1.48 kN/m², 2.66 kN/m², 3.25 kN/m², 4.55 kN/m² and 2.39 kN/m² respectively for 0, 2%, 4%, 6% and 8% of E waste respectively. The 6% E waste stabilized soil shows maximum un-drained strength and the improvement in undrained strength is about 8% as compared to unstabilized soil.

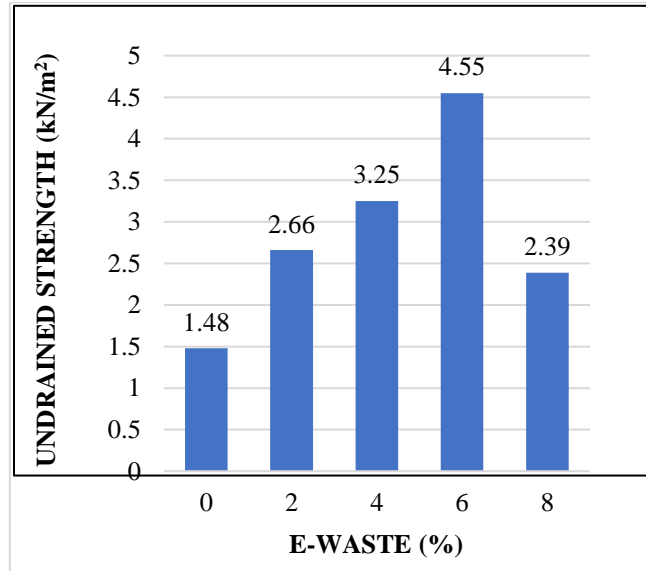


Figure 9 : Effect of E-waste on Undrained strength

F. Effect of E-waste California Bearing Ratio test

The variation of CBR value and E-waste are as shown in Figure 9. As the addition of E-waste increases, CBR value also increases. The CBR value is 12.49%, 14.8%, 16.5%, 17.41% and 20.02% at 0, 2, 4, 6 and 8% E waste respectively. The 8% E waste stabilized soil shows the maximum CBR value and increase in the optimum CBR value is about 26.98% as compared to the un-stabilized soil.

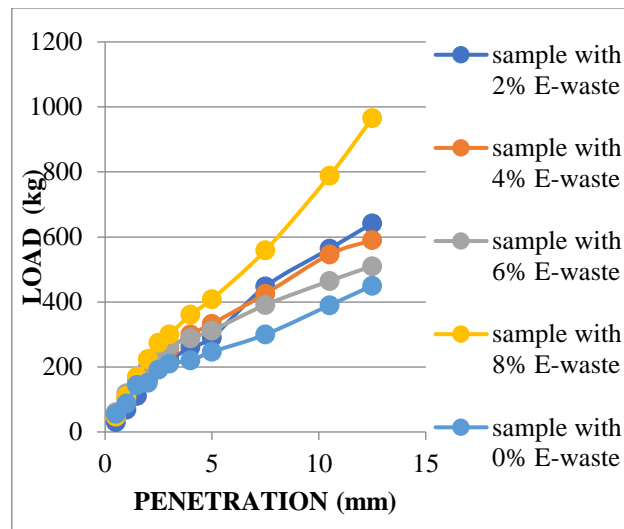


Figure 10 : Effect of E-waste on CBR value

The addition of E-waste enhances the California Bearing Ratio (CBR) values of soil, fulfilling the objective of increasing the CBR value. The Figure 11 illustrates the progression of CBR values of E-waste is introduced, showcasing the variation in CBR value.

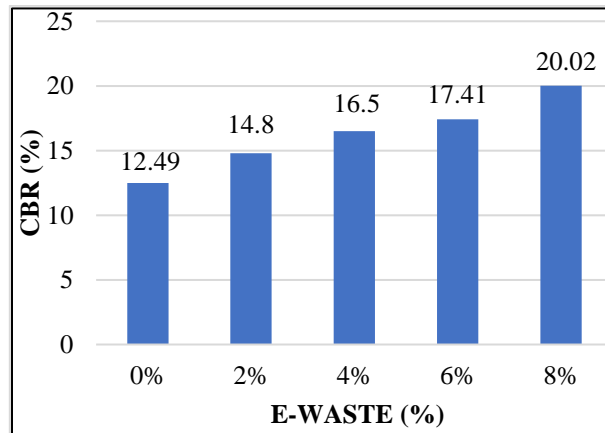


Figure 11 : CBR value with addition of E-waste

CONCLUSION

Following are the conclusions drawn based on the results obtained from the testing of soil stabilized with E-waste

1. Treatment with e-waste resulted in a reduction in the optimum moisture content (OMC) as e-waste content increased up to 6%, while the maximum dry density increased from 1.56 g/cc for untreated soil to 1.66 g/cc after the addition of 6% e-waste.
2. The CBR value of e-waste treated soil exhibited a progressive increase with higher percentages of e-waste, peaking at 20.02% when 8% of e-waste was incorporated, compared to the initial value of 12.49% for untreated soil.

3. The unconfined compressive strength (UCC) demonstrated a peak value at 6% e-waste addition, attributed to the strengthening properties of e-waste, with UCC increasing from 2.96 kN/m² for untreated soil to 9.11 kN/m².
4. Additionally, the undrained strength (Cu) increased from 1.48 kN/m² to 4.56 kN/m² with the addition of e-waste up to 6%, suggesting that a small addition of e-waste could enhance the strength of unstabilized soil.
5. Incorporating a small amount of e-waste enhances the strength of unstabilized soil, as evidenced by UCC and CBR tests.
6. This addition boosts the soil's load-bearing capacity while simultaneously reducing pavement thickness and overall maintenance costs.
7. Utilizing e-waste, sourced from scrap, proves cost-effective and beneficial for enhancing construction strength properties.

It has been observed that there is an maximum improvement in strength properties for the combination of E-waste with soil.

SCOPE FOR FUTURE WORK

- The conducted work occurred under controlled laboratory conditions, but its practical feasibility on-site needs examination.
- Beyond the mentioned admixture, can explore additional types from various industries to assess their impact on soil stabilization.

ACKNOWLEDGEMENT

Above all, we express gratitude to the divine for granting us the resilience, resources, and capability to accomplish the task successfully; without this, our endeavors would have been futile.

We express our deep gratitude to Mr. Sachinlal C, Assistant Professor of Civil Engineering, for his outstanding guidance and constructive feedback. We appreciate Ms. Jisha P, the Head of the Department, for her valuable advice and encouragement. Lastly, we extend our heartfelt thanks to our parents, friends, and all those who supported us throughout our project.

REFERENCES

- [14] Bindiya K ,Chaya D (2022) “Stabiliation of soil using E-waste” Journal of engineering& Management ,volume 6,No.2
- [15] Dr. K Prabhin , Anil kumar (2022) “Study on soil and stabilization using E-waaste” Journal of positive school psychology ,Volume 6,No.3
- [16] M.Dinesh,S.Mathri Raghisha (2021) “Improving soil stabilization by using fly ash and E-waste” ,Volume 25,Issue 3
- [17] Estabrah, AR. Javadi (2020) “Assessment of different agents for stabilization of clay soil” Journal of pavement engineering
- [18] Hani Baloochi (2020) “Soil stabilization using waste paper fly ash: precuations for its correct use” Journal of soil engineering and management ,Volume 10 , No 6

- [19] Chijioke Christopher Ikeagwani (2019) “Emerging trends in expansive soil stabilization: A review” Journal of rock mechanics and geotechnical engineering 1
- [20] Rohit Pal, Dr. Rajeev jain (2018) “Soil stabilization using E-wires”, Volume 5, Issue 12
- [21] Mr. Shirsanth H.A (2018) “Soil stabilizers for soil stabilization: a review” Journal of research in engineering and application Volume 3, Issue 4
- [22] S M V S Prsasanna Kumar (2018) “A study on expansive soil by using agricultural by-products” Journal of civil engineering, Volume 5, Issue 8
- [23] Ankiet Ravindra Ingole,Rasheed Ullah Khan (2018) “ Improvement of black cotton soil using E-waste and lime”.Volume 6,Issue 1
- [24] Aref al-Swaidani,Ibrahim Hammoud “Effect of natural pozzolona on geotechnical properties of lime-stabilized clay soil” (2016) Journal of Rock mechanics and engineering 8
- [25] Achmad Fauzi, Zuraida Djaubari (2016) ”Soil engineering properties improvement by utilization of cut waste plastic and crushed waste glass as additive” Journal of engineering and technology, Volume 8,No 1
- [26] Vikash Kumar Gautam , Devesh Jayaswal (2017) “A research paper on stabilization of soil by using bituminous material” Journal of engineering and technology , Volume 3, Issue 4
- [27] J. Olumfowbi ,A. Ogumndoju (2014) “Clay soil stabilization using powdered glass” Journal of engineering science and technology, Volume 9,No 5
- [28] Aly Ahmed, Usama H. Issa (2014) “ Stability of soft clay soil stabilised with recycled gypsum in a wet environment” Journal of soils and foundation 54(3)
- [29] Z. Sharifah Zaliha, H. Kamarudin (2013) “Review on soil stabilization techinques” Journal of Basic and applied science” Volume 8, Issue 5
- [30] Tamadhert T.Abood ,Anur Bin Kasa (2007) “Stabilisation of silty clay soil using Chloride compouns” Journal of engineering science and technology, Volume 2, No 1

Object Detection Using Machine Learning For Blind People

Arunima R

Dept. of Biomedical Engineering
KMCT CEW Kozhikode, India
arunimar3033@gmail.com

Munseera P

Dept. of Biomedical Engineering
KMCT CEW Kozhikode, India
munseerap27@gmail.com

Nandana Anil

Dept. of Biomedical Engineering
KMCT CEW Kozhikode, India
nandanaanil2000@gmail.com

Pavithra K T

Dept. of Biomedical Engineering
KMCT CEW Kozhikode, India
pavithrapavizz5878@gamil.com

Sandra S Rajeevan

Dept. of Biomedical Engineering
KMCT CEW Kozhikode, India
sandraraajeevan794@gmail.com

Dr. Sameera V Mohd Sagheer

Dept. of Biomedical Engineering
KMCT CEW Kozhikode, India
hodbm@kmctcew

Abstract—The “Object detection using machine learning for blind people” solution uses wearable ESP cams, microcontrollers, and a computing device to provide real-time environmental information, enhancing mobility and independence for visually impaired individuals. This technology reduces dependence on external assistance and improves spatial awareness, fostering self-reliance and reducing dependence on visual information.

I. INTRODUCTION

Visual impairment is a global issue, impacting over 43 million people and 285 million visually impaired individuals. Independent mobility is a major challenge, leading to social isolation and reduced quality of life. Traditional assistive technologies like white canes and guide dogs have limitations, such as limited information and high costs. Smart glasses, using object detection technology, offer a promising solution by providing real-time environmental information. These glasses use a wearable camera to capture live video of the user's environment, processed by a computer to identify objects and obstacles, and sent through audio feedback. Benefits include enhanced spatial awareness, increased independence, reduced reliance on external assistance, and greater participation in society. These smart glasses are becoming more affordable and accessible.

II. LITERATURE SURVEY

In 2022, researchers V.P.Gowtham Raj, E.Esakki Vigneswaran, M.Deshnaa, and K. Raj Prasanth proposed a system to help visually impaired individuals walk independently. The virtual smart glass, installed on a glass frame, uses object detection technology to detect obstacles and alert the user with an audio form if necessary. This innovative solution aims to help visually impaired individuals overcome their disability.

Dr.Karim Q. Hussein proposed the Glasses project in 2021, which uses mobile technology to assist blind people in detecting and recognizing objects through a tiny camera on their glasses.

The system uses a Raspberry Pi and deep learning algorithms like Convolution Neural Network to recognize objects and transmit their sounds. The project achieved a 100 Per precision on the COCO dataset.

The study proposes a deep learning-based smart glasses application system for visually impaired individuals. The system uses voice response to help visually impaired individuals understand objects in their surroundings. The system takes 3.788 seconds to create voice results and has a 96.3 percent success rate in object detection. The goal is to improve the quality of life for visually impaired individuals.

In 2020, G. Kumar, N. Harshith, and P. Vadivu developed the Smart Glasses project, a computer-aided tool that helps visually impaired individuals detect and recognize office tools. The project uses a camera fixed on glasses to send voice messages to an earphone, allowing the blind to find items independently and save time. The Raspberry Pi, a device similar to the human brain, analyzes images and scenes.

Feng yang and Alan Bovik developed a multi-axis MLP-based architecture called MAXIM in 2022. MAXIM is an efficient and flexible general-purpose vision backbone for image processing tasks. It uses a UNet-shaped hierarchical structure and supports long-range interactions enabled by spatially-gated MLPs. The architecture includes a multi-axis gated MLP for efficient spatial mixing of local and global visual cues and a cross-gating block for cross-feature conditioning.

In 2012, Debey, Nandita, and Tiwari proposed a pattern recognition system for automatic classification of digitally modulated communication signals. The system consists of a feature extraction sub-system (FESS) and a classifier sub-system (CSS). Comparatively, PNN outperforms MLPFN in terms of classification accuracy and training time. The approach is robust to phase offset and additive Gaussian noise. In 2021, Xin Sun and Shengua Gao proposed an Axial Shifted MLP architecture (AS-MLP) for a system that focuses on local feature interaction. This architecture captures local dependencies and allows for the same local receptive field as CNN-like architecture. The model achieved 83.3 percentage Top-1 accuracy with 88M parameters and 15.2 GFLOPs on the ImageNet-1K dataset, outperforming all MLP-based architectures and achieving competitive performance.

Neha Jogi proposed AI-enabled smart eyewear in 2023, which incorporates computer and smartphone features for improved user experience. These glasses allow users with visual impairments to read and write without scribes, using AI to organize visual information and communicate it verbally.

In 2022, Prathima Samuda proposed a system for visually challenged people, focusing on vision as a primary requirement for survival in fast-changing environments. The paper proposes a method to support visually challenged people, using existing smart aid techniques for obstacle detection, fire detection, and background detection. The low-cost solution uses input and output sensors connected through an Arduino board, alerting the user with buzzer or beep sounds.

Y D Sravani proposed a system for obstacle detection for blind people using the latest ARDUINO technology. The project aims to provide safety for blind people by detecting near-by

obstacles and notifying them of their direction. The device uses an ultrasonic sensor and an embedded microcontroller to monitor the components. The device is designed to be carried by blind people, providing a warning signal when an obstacle is detected, allowing them to move accordingly.

In 2019, Yanchiew Wong and Feeza Radsai proposed a smart object detection system using Convolutional Neural Network (CNN) to provide a safer living for visually impaired people. The system uses edge box algorithms to produce region proposals from image edges, passes through a fine-tuned CaffeNet model, captures real-time object scenes, extracts features, and generates an audio-based detector to notify visually impaired individuals.

In 2019, G Jagadheeshwaran proposed a system for blind people to run their daily lives. This device, using an Arduino UNO board, detects obstacles and is more efficient than existing systems. The buzzer sound allows users to judge objects, and the system has a higher detection range. Surveys were conducted to assess the project's effectiveness.

D Sireesha proposed a system using ultrasonic sensors to design glasses for blind people. The glasses detect obstacles and send their distance to an Arduino, which then sends the information to a speaker. The goal is to improve vision for low-vision individuals, who are officially blind. The glasses enhance mobility, communication, and participation in society. The project aims to improve the independence of users and make them feel more normal, thereby enhancing their social and academic life. The goal is to make the glasses accessible to all.

Kalaivani and Yaswin Vikhaash proposed an intelligent stick using Raspberry Pi to assist visually challenged people in their daily activities. The stick offers artificial vision, object identification, and real-time GPS guidance. It senses objects nearby, delivers voice information, alerts via earphones, and provides GPS navigation. The goal is to provide a subtle, effective direction finding and obstruction detecting assist, allowing the blind to walk autonomously and perceive the ecological situation of nearby objects.

Robin Christopherson introduced three smart glass systems in 2022: NuEyes, AIRA, and QD laser. NuEyes is an electronic visual prosthesis for people with low or no vision, offering features like up to 12x magnification, color and contrast adjustments, bar/QR code scanning, and OCR recognition. AIRA uses a camera and connectivity to provide assistance, with trained assistants providing spoken feedback. QD laser, a technology that projects images directly onto the retina using lasers, is still a year away.

AMR Sarawy proposed a wearable device in 2020 to assist visually impaired individuals in social interactions. The device uses Amazon Rekognition to identify classmates, friends, and relatives, and provides notifications for new users. It also allows users to tag images with identity or complete information. The device captures images of books or newspapers, processes them, and converts them into speech, making users independent and able to read.

In 2020, a team proposed a system for object detection using computer vision across indoor and outdoor classes. They proposed a multi-label approach using machine learning and vision technologies, focusing on accuracy and effectiveness. The system uses classification/clustering techniques to reduce recognition time.

Ali Salem Bin Sama proposed an EDSGS to improve mobility and safety for visually impaired people. The system uses an intelligent system to recognize objects in unfamiliar environments, using a combination of Support Vector Machine(SVM) and Gray Wolfe Optimizer. The system uses auditory cues to guide users, and images are used to evaluate its performance and accuracy.

Jayaseeli G, Durga K, Ayesha bi.B, Athira VM, Kumarase-nan.A T proposed a system which helps the blind to detect obstacles. We, propose a smart glass for visually impaired people to overcome traveling difficulties. This device is used to assist the blind to detect obstacles. This is sheltered and hearty direction support which helps many visually impaired people with no stress over any barrier on their moving way.

Sayanthan M, This proposed system of glass has the Ar- duino Nano as the brains of the system.The person will wear the glasses and switch it on.Now he starts walking. As the ultrasonic sensor detects that if the distance between the personand an obstacle is below 20 cm..he will get an alert over the 32Ohm headphone Speaker attached in his ear.And he will immediately be aware of that obstacle. So the collision willbe prevented.

Researchers in 2020 proposed a guidance system for visu- ally challenged individuals who struggle with traveling and managing challenges. The system uses smart glasses paired with sensors to capture images from the environment, allowingthe user to navigate safely. The glasses can detect obstacles andprovide a speech-based interface, alerting the user in advance about their destination. This system allows the blind person to hear the recorded location, providing a more comprehensive view of the navigation process.

This paper proposes a low-cost solution for visually chal- lenged people to improve their vision in fast-changing envi- ronments. The system uses input and output sensors connectedthrough an Arduino board to detect the environment in frontof the subject. The processor responds to the input and sendsa signal to the output transducer, which triggers a buzzer or beep sound to alert the user.

Rohit Mohit Nikhil proposed a device in 2020 that includes glasses, an obstacle detection module, a processing unit, an output device (beeping component), and a power supply. The device uses an ultrasonic sensor, a control module, anda buzzer to detect obstacles. The Ultrasonic Smart Glassesfor Blind People are portable, user-friendly, lightweight, and affordable, guiding and avoiding obstacles.

Jinquiang Bai and Shiguo Lian developed a novel ETA (Electronic Travel Aids) smart guiding device in the formof eyeglasses to help visually impaired individuals travel efficiently and safely. The device uses a multi-sensor fusion- based obstacle avoiding algorithm, auditory cues for blindpeople, and visual enhancement using Augment Reality for weak-sighted people. The prototype, consisting of display glasses and low-cost sensors, was tested and found to improve users' travel experience.

In 2021, M V S Arvitha and Ambresh B Biradar proposeda wearable prototype using Echolocation Technology for visu-ally challenged individuals. The prototype uses Ultrasonic and IR sensors for obstacle and water detection, and is interfaced with Arduino UNO for processing.

The prototype allows visually challenged individuals to navigate without a stick, functioning accurately with only some training.

III. METHODOLOGY

The methodology includes feature detection, feature extraction, classification and speech conversion. Feature detection is the process of identifying and locating distinctive features in an image, such as edges, corners, and blobs. In the context of a smart glass project for blind people, feature detection can be used to identify objects and text in the users environment. Feature extraction is the process of converting detected features into a numerical representation that can be used by a machine learning algorithm. Feature extraction can be used to create a unique representation of each object. Classification is the process of assigning a class label to a feature vector. , classification can be used to identify the type of object or text in the users environment.

Multilayer Perceptron (MLP) is a type of artificial neural network (ANN) with multiple layers of interconnected nodes or neurons. MLPs are feedforward neural networks, where information flows from the input layer through hidden layers to the output layer. They employ a supervised learning approach and can be applied to various tasks, such as classification, regression, and pattern recognition. MLPs have advantages such as nonlinear modeling, universal approximation, and adaptability. However, they have limitations such as their black-box nature, overfitting, and computational complexity, especially for large networks and datasets. Despite these limitations, MLPs remain versatile and can be applied to various tasks.

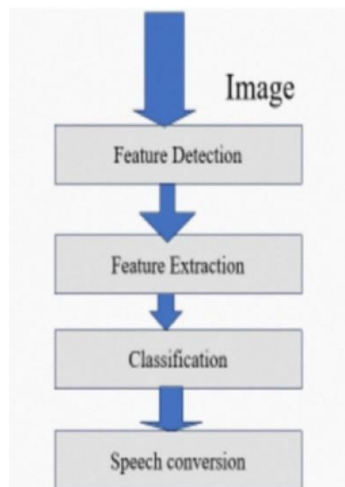


Fig. 1. Methodology.

A. Block Diagram

The ESP-CAM is a camera module designed for the ESP8266 MCU, which captures and transmits images for processing. The ESP8266 is the central processing unit, receiving and processing image data. The ESP Programmer is a hardware tool that flashes firmware onto the ESP8266 MCU via GPIO pins and allows programming using software like Arduino IDE. A power source, such as a USB power supply or battery, is required for the system. The ESP Programmer is only needed for flashing firmware onto the ESP8266, and the computing device connects to the ESP8266 via Wi-Fi for object detection and speech generation.

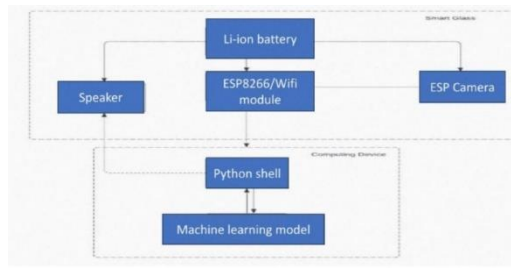


Fig. 2. block diagram

B. Circuit diagram

The ESP8266 is a low-cost Wi-Fi microcontroller unit (MCU) that serves as the central processing unit for an object detection system. It handles image acquisition, initial processing, and Wi-Fi communication. The ESP-CAM is a camera module designed for the ESP8266 MCU, responsible for image capture, preprocessing, and frame transmission. A Li-ion battery powers the ESP8266 and ESP-CAM, ensuring continuous operation even in remote or off-grid locations. The computing device receives the processed image data via Wi-Fi and performs object detection using machine learning algorithms. The device then converts the detected object label into speech using a text-to-speech engine. A Bluetooth speaker receives the generated speech audio from the computing device, providing audible feedback on the detected object. The system's components and interactions are illustrated in a block diagram.

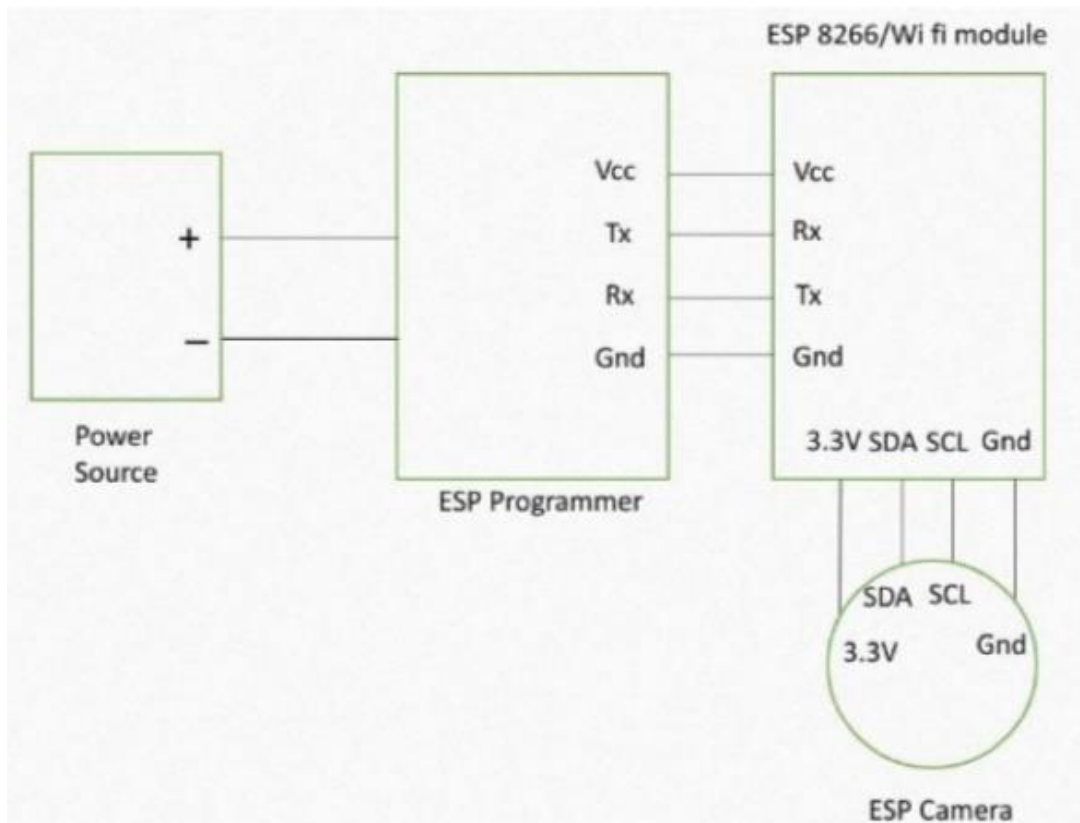


Fig. 3. Circuit diagram

C. Flowchart

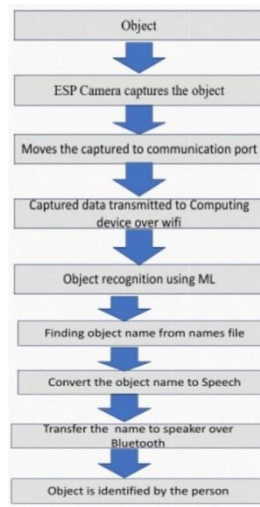


Fig. 4. Flowchart

The ESP32-CAM is a camera that uses image processing techniques to detect and locate objects within captured frames. It compresses or encodes the captured frames for transmission, then transmits them to a communication port for further processing. The encoded data is then transmitted to a computing device over a Wi-Fi network for wireless data transfer. The encoded frames are decoded and fed into a machine learning model for object recognition. The model classifies objects based on their features and patterns. The model outputs a unique object label, which is then matched against a corresponding names file. The object name is converted into speech using a text-to-speech (TTS) engine, and the speech is transmitted to a Bluetooth speaker for wireless feedback.

IV. RESULT

This section discusses the implementation of a machine learning-based object detection device for blind people. The device captures live video footage and sends it over Wi-Fi to a server or computer. The server must have sufficient computational power to handle deep learning model processing. The video stream is decoded into individual frames, which are pre-processed before being fed into the YOLOv4 model. The pre-processed frames are then used in the model.

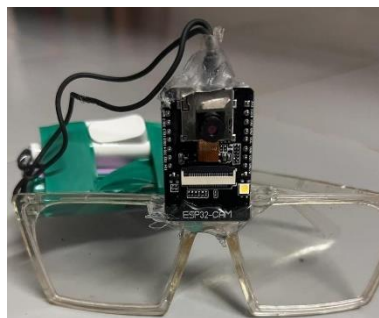


Fig. 5. Hardware setup

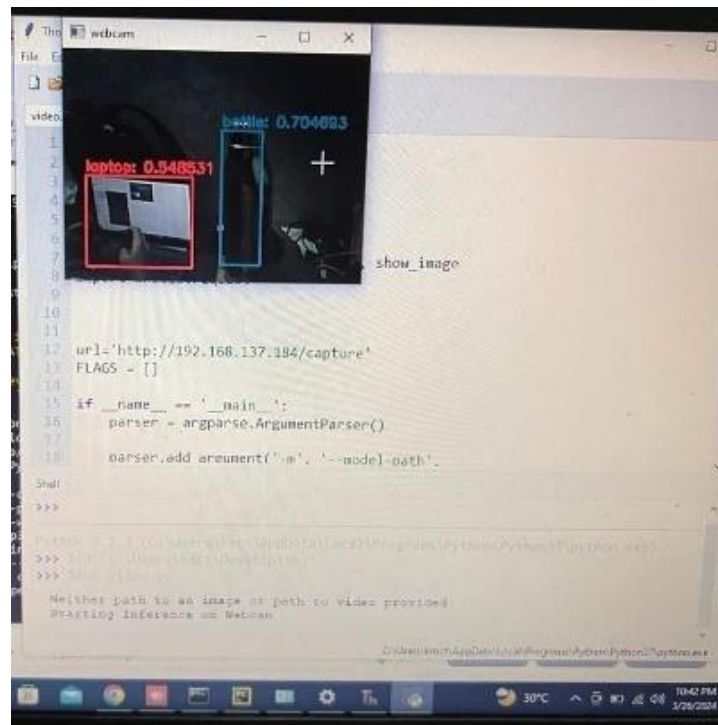


Fig. 6. video output

V. CONCLUSION

This paper highlights the need for a voice assistant system for blind people worldwide. It proposes a practical, wearable device that uses machine learning to detect objects and convert them into audio, thereby guiding the blind community.

REFERENCES

- [1] Journal 2022 4th International Conference on Smart Systems and Inventive Technology (ICSSIT) Authors V.P.Gowtham Raj; E.Esakki Vigneswaran; M. Deshnaa; K. RajPrasanth Published date 2022-1-20 DOI 10.1109/icssit53264.2022.9716412
- [2] Rana Jawad Ghali, Dr. Karim Q. Hussein a Computer Science Dept. College of Science Mustansiriyah University, Baghdad, Iraq.
- [3] Y. Lin, C. -L. Chiang, M. -J. Wu, C. -C. Yao and M. -C. Chen, "Smart Glasses Application System for Visually Impaired People Based on Deep Learning," 2020 Indo.
- [4] Naveen Tiwari, Sadhna Kumari, Shivansh Sharmar, Rajat Awasthi Department of Electronics and Communication Axis Institute of Technology and Management, India
- [5] Zhengzhong Tu, Hossein Talebi, Han Zhang, Feng Yang, Peyman Milanfar, Alan Bovik, Yinxiao Li Submitted on 9 Jan 2022 (v1), last revised 1 Apr 2022
- [6] H. C. Dubey, Nandita and A. K. Tiwari, "Blind modulation classification based on MLP and PNN," 2012 Students Conference on Engineering and Systems, Allahabad, India, 2012, pp. 1-6, doi: 10.1109/SCES.2012.6199042.
- [7] Comments Accepted by ICLR2022 Subjects Computer Vision and Pattern Recognition (cs.CV) Cite as: arXiv: 2107.08391 [cs.CV] (or arXiv:2107.08391v2 [cs.CV] for

<https://doi.org/10.48550/arXiv.2107.08391>

- [8] Retrieval Number: B3565079220/2020BEIESP
DOI:10.35940/ijrte.B3565.079220 Journal Website: www.ijrte.org
- [9] Surendra Kumar, Ram veer Singh,” 2012 Students Conference on Engineering as SystemsAllahabad, India, 2012, pp. 1-6, doi: 10.1109/SCES.2012.6199042.
- [10] Adegoke A. O, Oluseun D Oyeleke, Mahmud B , Ajoje J. O , Sadiq Thomase Milanfar, Alan Bovik, Yinxiao Li Submitted on 9 Jan 2019 (vi), last revised 1 Apr 2019 (this version, v2)
- [11] Y.C. Wong, J.A. Lai, S.S.S. Ranjit, A.R. Syafeeza, N. A. Hamid Micro and Nano Electronic (MINE) Research Group, Centre for Telecommu- nication Research Information Fakulti Kejuruteraan Elektronik dan Ke- juruteraan Komputer, Hang Tuah Jaya, 76100 Durian Tunggal, Melaka, Malaysia yewong@utem.edu.
- [12] Maragatharajan, G. Jegadeeshwaran, R. Askash, K. Aniruth, Sarath Retrieval Number: A10901291S419/2019@BEIESP
DOI:10.35940/jeat.A1090.1291S419 Journal Website: www.ijeat.org
- [13] Satya Institute Of Technology And Management , Vizianagaram JE- TIR1904F07 Journal of Emerging Technologies and Innovative Research(JETIR) www.jetir.org
- [14] Dobbelle WH, Quest DO, Antunes JL, Roberts TS, Girvin JP. Artificial vision for the blind by electrical stimulation of the visual cortex. *Neurosurgery*. 1979 Oct;5(4):521-7. doi: 10.1227/00006123-197910000-00022. MID: 534058
- [15] Robin Christopherson AbilityNet 2023. Ability Net is a company limited by guarantee in England and Wales No: 3469653. Ability Net is a Charity, registered in England and Wales, registration number 1067673, and in Scotland registration number SC039866. Amir Sarawy July 2020 DOI:10.1007/978-3-319-4126782 Department of Electrical and Electronic Engineering, Universiti Teknologi PETRONAS
- [17] Object Detection Using Machine Learning for Visually Impaired People , Venkata Naresh Mandala N Thripouthi Rao January 2020 DOI: 10.31782/IJCRR.2020.122032
- [18] Ali Salem Bin Sama1, 1Department University, Country1Computer and Information Science Department, Al-Imam Mohammad In Saud Islamic University, AlHofuf, Kingdom of Saudi Arabia Geology Engineering Department, Faculty of Oil Minerals Aden University,
- [19] Jayaseeli.G, Durga.K, Ayesha bi.B, Athira. VM, Kumaresan.A UG students, 5As-sistant Professor Department of Biomedical Engineering Rajiv Gandhi College of Engineering and Technology, Puducherry, India.
- [20] SayantanM4, ” Anti Collision Glasses for the Blind” in 2014 5th IEEE Conf. Cognitive Infocommunications (CogInfoCom), Vietri sul Mare, 2014, pp. 343-347.
- [21] S. Rajendran, P. Krishnan and D. J. Aravindhar, ” Design and Im- plementation of Voice Assisted Smart Glasses for Visually Impaired People Using Google Vision API,” 2020 4th International Conference on Electronics, Communication and Aerospace Technology (ICECA), Combatore
- [22] Prathima Samuda N G Praveena C Nithiva B J KomathiArduino based Customized Smart Glasses for the Blind People February 202 DOI:10.1109/ICAIS53314.2022.9742799 Conference: 2022 Second In- ternational Conference on Artificial Intelligence and Smart Energy (ICAIS).

- [23] Prathima Samuda N G Praveena C Nithiva B J Komathi Arduino based Customized Smart Glasses for the Blind People February 202 DOI:10.1109/ICAIS53314.2022.9742799 Conference: 2022 Second International Conference on Artificial Intelligence and Smart Energy (ICAIS).
- [24] Jinqiang Bai, Shiguo Lian, Member, IEEE, Zhaoxiang Liu, Kai Wang, Dijun Liu- "Smart Guiding Glasses for Visually Impaired People in Indoor Environment" Published IN THE transactions on consumer. 27 September 2017 Computer Science, Engineering.
- [25] Published in 2021 International Conference on Emerging Smart Computing and Informatics (ESCI) Date of Conference 5-07 March 2021 Date Added to IEEE Xplore 09 April 2021 ISBN Information DOI 10.1109/ESCI50559.2021.9397015 Publisher: IEEE Conference Location Pune, India

SMART HEADBAND FOR REHABILITATION

Adithya M
Dept. of Biomedical
Engineering
KMCT CEW Kozhikode,
India
adithyam806@gmail.com

Neha Vijay
Dept. of Biomedical
Engineering
KMCT CEW Kozhikode,
India
nehavijay722@gmail.com

Aparna A K
Dept. of Biomedical Engineering
KMCT CEW Kozhikode, India
aparnaprabha20@gmail.com

Sivanath P I
Dept. of Biomedical Engineering
Assistant Professor
KMCT CEW Kozhikode, India sivanathpi@gmail.com

Nandana O
Dept. of Biomedical Engineering
KMCT CEW Kozhikode, India
nandanaoniyam@gmail.com

Abstract—The “Smart Headband for Rehabilitation” project is a wearable headband with advanced sensors and a micro- controller that provides real-time data and insights to aid in rehabilitation programs. The headband includes sweat sensors for hydration, accelerometers for head movements, heart rate sensors for cardiovascular assessment, and SPO2 sensors for blood oxygen levels. The system allows healthcare providers to tailor programs to individual needs and offers real-time feedback. The social impact is significant, promoting self-awareness and active participation in recovery. The solution could reduce healthcare system burden, improve patient outcomes, and improve quality of life.

Index Terms—microcontroller, accelerometer, spo2 sensor, sweat sensor

I. INTRODUCTION

Rehabilitation is a complex and individualized process that helps individuals recover from injuries, illnesses, and disabilities. Traditional rehabilitation programs rely on subjective feedback from patients and therapists, which can be time-consuming and expensive. Technological advancements have revolutionized the healthcare landscape, leading to innovative rehabilitation solutions like the Smart Headband for Rehabilitation. This wearable device uses advanced sensors and a microcontroller to collect, process, and transmit real-time data on patients' health status and progress. The Smart Headband addresses key needs in rehabilitation, such as personalized programs, real-time feedback, and remote monitoring.

The headband provides comprehensive data on patients' physical and physiological parameters, enabling healthcare professionals to tailor programs to individual needs. This helps patients achieve their recovery goals more quickly and effectively. Real-time feedback helps patients stay motivated, identify areas for improvement, and make necessary adjustments to exercises and activities. Remote monitoring allows healthcare professionals to track patients' progress and intervene early, especially for patients in rural areas or those with difficulty

traveling. The Smart Headband for Rehabilitation has the potential to revolutionize the rehabilitation landscape and improve the quality of life for millions of people worldwide.

II. LITERATURE REVIEW

Bhuvan Kumar introduced Smart gloves in 2023 to enhance stroke patients' living standards by facilitating muscle memory re-enhancement, facilitating exercise, and providing immediate feedback for physicians.

Roberto De Fazio's 2023 paper explores wearable sensors and smart devices for monitoring rehabilitation and sports performance, discussing their efficacy in healthcare, physiological parameter classification, and electromechanical transduction mechanisms.

Jiachengwan's 2022 proposal for intelligent poststroke rehabilitation uses biological signal-based closed-loop signals, promising motor function rehabilitation. New theories and technological approaches can further exploit their potential.

Caren Da Silva Dias' 2021 study found no significant association between tactile sensibility and cutaneous temperature in stroke patients, suggesting that sensory-motor recovery is correlated with body temperature differences.

Dandan Cao introduced a 2021 design model for human motion rehabilitation using object-oriented technology, incorporating a visual dynamic tracking model and fuzzy PID superheterodyne control method for bone training.

Ricardo Alexandre introduced Virtual Reality and Augmented Reality technologies in 2021 for smart physical rehabilitation, improving user engagement, training outcomes, and data storage. These solutions, part of the IoT Physical Rehabilitation ecosystem, use Unity game development software.

Manuel Reis Carneiro introduced a comfortable textile-based EEG headband system in 2020 for long-term forehead EEG signal acquisition, reducing noise and facilitating vertical interconnect access.

A 2020 study proposes a wearable brain oxygenation monitoring system using neural network techniques to accurately classify different Chronic Pain Factors (CPF) groups, potentially aiding in CVD severity evaluation and rehabilitation.

Paplo Maceora Elvira's 2019 stroke rehabilitation system uses wearable technology to assess and monitor patients, enabling detailed therapy evaluation and individualization. Challenges and opportunities discussed.

In 2019, Traian Popa introduced a wearable system for stroke rehabilitation, enabling detailed assessment and personalized therapy evaluation. This review explores wearable sensors, challenges, opportunities, and data acquisition for future studies.

Mary M Rodgers' 2019 paper discusses wearable technologies for active living and rehabilitation, highlighting recent developments, challenges, and future opportunities. It provides examples and suggests future directions for wider deployment. 2018 study proposes rehabilitation

support system using EMG, acceleration, and gyro sensors, with Brain Engagement Index (BEI) linked to exercise difficulty and temporary functional change.

Shih Kai Lin developed a smart headband for epileptic seizure detection in 2018, featuring analog circuitry, ESDT, Bluetooth Low Power chip, and customized electrodes for 92.68

Aleksandar Vakanski introduced the University of Idaho's Physical Rehabilitation Movement Data in 2018, a publicly available dataset of common exercises performed by patients in rehabilitation programs.

Andrew Brueck developed a real-time hydration monitor using sweat data, achieving an 18 Geng Yang's 2018 study developed an IoT-enabled stroke rehabilitation system using a smart wearable armband, machine learning algorithms, and a 3-D printed robot hand, achieving 96.20

A 2017 study evaluated the MAX30100 SpO₂ /Heartbeat sensor's performance in various body regions, revealing similar results to a reference device. Researchers plan to create a wearable device for daily activities.

Sara Plege Shani's 2017 study found a correlation between exercise difficulty and Brain Engagement Index (BEI) and temporary functional change during motor rehabilitation sessions, regardless of feedback use.

Cuong Pham introduced the MobiRAR system in 2015, a real-time human activity recognition system using accelerometer data, achieving over 93

Willy Chou's 2012 smart headband system uses near-infrared spectroscopy to evaluate stroke rehabilitation effectiveness, revealing improved cardiopulmonary function through wearable technology and wireless transmission.

A 2012 study found that effective treatment on bicuspid artery hypertension (BHI) is associated with normal BHI values and neurological severity, with ipsilateral BHI, age, and depression being key predictors.

The 2010 paper reviews wearable accelerometer-based motion detectors' principles, properties, and applications, including posture classification, energy expenditure estimation, fall detection, and balance control evaluation.

Sanghyun Kim introduced a wearable healthcare system in 2008 that monitors physiological signals using a smart headband, counting steps and alerting for emergencies.

The 2001 study tested pulse oximetry recordings in 15 stroke patients, revealing a consistent mean SpO₂ of 96 percentages and a mean HR of 81 bpm on both affected and nonaffected sides.

III. METHODOLOGY

To create specific measurements based on blood flow changes, specific indexes are defined. Heart rate can be measured from the forehead, which is a good spot for integration into helmets, headbands, and other head-worn apparel. SpO₂ measurements are less common compared to fingertip measurements, but advancements in wearable technology have introduced forehead-based SpO₂ measurement using specialized sensors.

Headbands can also monitor sweat rate by placing electrodes along the forehead where sweat is likely to accumulate, ensuring good skin contact for accurate measurements. The headband should be designed to suit the patient's comfort preferences and activity level.

Movement tracking can be done by placing an accelerometer on the head of stroke patients, allowing for better detection of head movements during rehabilitation exercises. The Cardiovascular Fitness Index (CFI) is a crucial parameter that provides insights into an individual's overall cardiovascular health and fitness level. It can help detect early signs of cardiovascular issues or oxygenation problems, making it a valuable indicator for the effectiveness of rehabilitation.

A. Block Diagram

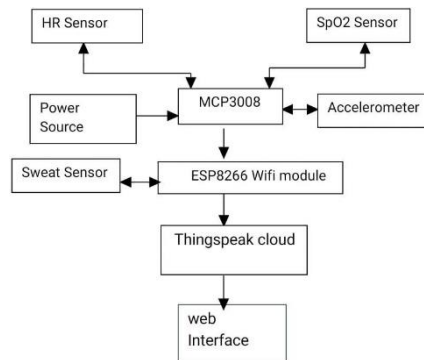


Fig. 1. block diagram.

The headband uses sensors to measure various health and fitness metrics. The heart rate sensor measures the user's heart rate, while the SPO2 sensor measures blood oxygen saturation. The accelerometer measures the user's head movement, providing data on steps and distance traveled. The sweat rate sensor measures the user's sweat production, providing insights into hydration levels and exercise intensity. The headband uses a Wi-Fi microcontroller unit (MCU) called ESP 8266 for processing sensor data, controlling power consumption, and communicating with the Android app. The Thingspeak cloud is an IoT platform that allows users to collect, analyze, and act on data from sensors or devices. The headband operates on a rechargeable lithium battery and has a web interface that displays collected data for healthcare professionals or patients.

B. Circuit Diagram

The ESP8266 microcontroller is a smart headband that uses sensors to track health and fitness metrics. The Li-ion battery powers the analog to digital converter and other components, while the 3.3V pin supplies the heart rate sensor, SPO2 sensor, accelerometer, and esp8266 microcontroller. The sweat sensor is directly connected to the microcontroller. The GND pin ensures a common ground reference. The heart rate sensor's VCC and GND pins are connected to the ESP8266 microcontroller's 3.3V and GND pins, allowing the ESP8266 to read heart rate data. The SPO2 sensor's VCC and GND pins are connected to the ESP8266 microcontroller's SDA and SCL pins, allowing the ESP8266 to communicate with the SPO2 sensor and read blood oxygen saturation data. The accelerometer's VCC and GND pins are connected to the ESP8266 microcontroller's 3.3V and GND pins, allowing the ESP8266 to read acceleration data. The sweat rate sensor's VCC and GND pins are connected to the ESP8266 microcontroller's 3.3V and GND

pins, allowing the ESP8266 to read sweat rate data. The data flow in the smart headband involves sensors collecting user health and fitness metrics, processing it on-board or sending it to the web interface for further analysis.

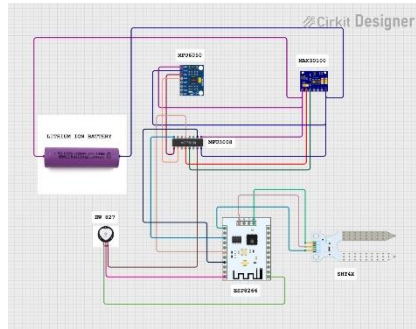


Fig. 2. Circuit diagram

C. Flow chart

The system involves collecting and processing data from various sensors, such as heart rate, blood oxygen saturation, accelerometer, and sweat sensors, to calculate parameters like mobility effort index and cardiovascular fitness index. The ESP8266 microcontroller handles sensor interfacing and data processing, and is integrated with the ThingSpeak cloud platform. The data is transmitted to the cloud at regular intervals, and the system uses visualization tools to create graphs and charts for monitoring and analysis. Custom MATLAB analytics algorithms may be implemented for advanced data processing. A user interface is developed to access and visualize the data stored on ThingSpeak, providing real-time feedback on health metrics and activity levels. Users can set

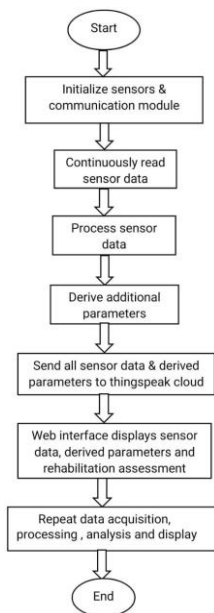


Fig. 3. Flow chart

Goals, track progress, and receive alerts if certain thresholds are crossed. Feedback mechanisms are enabled to provide personalized recommendations for fitness routines, activity

levels, and health improvements. The system continuously updates algorithms and parameters based on user feedback and advancements in health science. This comprehensive system provides actionable insights for maintaining or improving cardiovascular fitness and overall well-being.

IV. RESULT

Connect sensors to an ESP8266 microcontroller, ensure proper power supply, and test each individually. Write code for the ESP8266 using Arduino IDE, read data from each sensor, and implement Wi-Fi connectivity. Create functions to format and send data to ThingSpeak, create an account, and set up a new channel with fields for heart rate, SpO2, sweat level, and accelerometer data. Note the provided API key. Design an HTML web interface to visualize the data

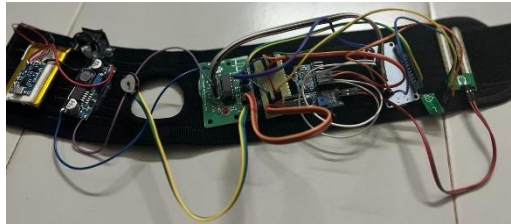


Fig. 4. Smart headband

from the sensors. Use JavaScript to fetch data from ThingSpeak using its API. Display the data in a user-friendly format on the web interface. You can use libraries like Chart.js for graphical representation of data. Integrate the HTML web interface with your ESP8266 code. Make sure the ESP8266 sends data to ThingSpeak periodically. Update the web interface to fetch and display the latest data from ThingSpeak.

Smart Band Data					
BPM	SPO2	SWEAT (ml/hr)	MOVEMENT	MFI	CVI
75	96	0.92 ml/hr	4.20182	2.56	85.50

Fig. 5. Web interface

V. CONCLUSION

The Smart Headband project offers rehabilitation support for stroke patients, empowering them to be self-aware and active participants. It allows them to make informed decisions about safe exercise and improves their quality of life. This technology has the potential to revolutionize rehabilitation services, enhancing overall outcomes.

REFERENCES

- [1] S.Kim, D.Ryoo and C.Bae, "Implementation of Smart Headband for the Wearable Healthcare," 2008 Digest of Technical Papers - International Conference on Consumer Electronics, Las Vegas, NV, USA, 2008, pp.1- 2, doi:10.1109/ICCE.2008.4587995.
- [2] J Clin Med. 2021 Sep; 10(18):4122. Published online 2021 Sep 13. doi:10.3390/jcm1018 PMID: PMC8466602

- [3] Volume2021—ArticleID6626957 <https://doi.org/10.1155/2021/6626957> Dandan Cao,Junyan Wang, and Naihong Liu
- [4] Vakanski A, Jun HP, Paul D, Baker R. A Data Set of Human Body Movements for Physical Rehabilitation Exercises. *Data (Basel)*.2018 Mar;3(1):2.doi:10.3390/ 2018 Jan 11. PMID: 29354641; PMCID: PMC5773117.
- [5] W.Chou,B.-S.Lin,H.C.Hsu,R.-H. Chiu and B.-S.Lin, "Intelligent Head- band System for Evaluating Rehabilitation Effectiveness," in *IEEE Transactions on Neural Systems and Rehabilitation Engineering*, vol. 31, pp. 1180-1187, 2023, doi:10.1109/TNSRE.2023.3241998.
- [6] K.B.Sa,can and G. Erta,s, "Performance assessment of MAX30100 SpO₂/heartratesensor,"2017 Medical Technologies National Congress (TIPTEKNO),Trabzon,Turkey,2017,pp.1-4,doi:10.1109/TIPTEKNO.2017.8238126.
- [7] A.S.M.Steijlen,J.Bastemeijer,K.M.B.Jansen,P.J.French and A.Bossche,"A novel sweat rate and conductivity sensor patch made with low-cost fabrication techniques,"2020 IEEE SENSORS,Rotterdam,Netherlands, 2020,pp.1-4,doi:10.1109/SENSORS47125.2020.9278850.
- [8] C.Pham,"MobiRAR: Real-Time Human Activity Recognition Using Mobile Devices," 2015 Seventh International Conference on Knowledge and Systems Engineering(KSE),Ho Chi Minh City,Vietnam, 2015,pp. 144-149, doi: 10.1109/KSE.2015.43.
- [9] J.Y.Seo,Y.H. Noh and D.U.Jeong, "Implementation of EMG data-basedrehabilitation assistance system,"2018 International Conference on Electronics,Information, and Communication (ICEIC), Honolulu,HI,USA, 2018, pp. 1-2, doi:10.23919/ELINFOCOM.2018.8330632.
- [10] Bartur G, Joubran K, Peleg-Shani S, Vatine JJ, Shahaf G. An EEG Tool for Monitoring Patient Engagement during Stroke Reha- bilitation: A Feasibility Study.*Biomed Res Int*. 2017;2017:9071568. doi:10.1155/2017/9071568. Epub 2017 Sep 24.PMID: 29147661; PM- CID: PMC5632877.
- [11] H.Yang,J.Wan,Y.Jin, X.Yu and Y.Fang, "EEG- and EMG- Driven Poststroke Rehabilitation: A Review,"in *IEEE Sensors Journal*,vol.22, no.24,pp.23649-23660,15 Dec.15, 2022, doi: 10.1109/JSEN.2022.3220930.
- [12] Brueck A,Iftekhhar T,Stannard AB,Yelamarthi K, Kaya T. A Real-Time Wireless Sweat Rate Measurement System for Physical Activity Moni- toring. *Sensors (Basel)*.2018 Feb 10;18(2):533.doi: 10.3390/s18020533. PMID:29439398;PMCID: PMC5855985.
- [13] Maceira-Elvira,P.,Popa,T, Schmid,AC. et al. Wearable technology in stroke rehabilitation: towards improved diagnosis and treatment of upper-limb motor impairment.*J NeuroEngineering Rehabil* 16, 142(2019). <https://doi.org/10.1186/s12984-019-0612-y>
- [14] A.Arivarisi ;D.Thiripurasundari;A.Arockia selva Kumar ; Bhuvan kumaar;Nanotechnol. *Precis. Eng.* 6, 043004 (2023) <https://doi.org/10.1063/10.0020290>

- [15] W.Chou,P.J.Wu,C.C. Fang,Y.S.Yen and B.S.Lin, "Design of Smart Brain Oxygenation Monitoring System for Estimating Cardio-vascular Disease Severity,"in IEEE Access, vol.8,pp.98422-98429, 2020,doi:10.1109/ACCESS.2020.2997865.
- [16] Yang CC,Hsu YL. A review of accelerometry-based wearable motion detectors for physical activity monitoring. *Sensors (Basel)*. doi: 10.3390/s100807772.PMID:22163626;PMCID: PMC3231187.
- [17] G.Yang et al.,"An IoT-Enabled Stroke Rehabilitation System Based on SmartWearable Armband and Machine Learning," in IEEE Journal of Translational Engineering in Health and Medicine, vol.6, pp. 1-10, 2018, Art no. 2100510,doi:10.1109/JTEHM.2018.2822681.
- [18] Rodgers MM, Alon G, Pai VM, Conroy RS. Wearable technologies for active living and rehabilitation: Current research challenges and future opportunities. *J Rehabil Assist Technol Eng*.2019 Apr 26;6:2055668319839607.doi: 10.1177/2055668319839607.PMID:31245033; PMCID:PMC6582279.
- [19] Maceira-Elvira, P.,Popa, T.,Schmid,AC.et al.Wearable technology in stroke rehabilitation: towards improved diagnosis and treatment of upper-limb motor impairment. *J NeuroEngineering Rehabil* 16, 142 (2019).<https://doi.org/10.1186/s12984-019-0612-y38>
- [20] Roffe C, Sills S, Wilde K, Crome P.Effect of hemiparetic stroke on pulse oximetry readings on the affected side. *Stroke*.2001 .doi: 10.1161/01.str.32.8.1808.PMID:11486109.
- [21] S K.Lin, Istiqomah, L.-C. Wang, C.-Y. Lin and H. Chiueh, "An Ultra-Low Power Smart Headband for Real-Time Epileptic Seizure Detection,"in IEEE Journal of Translational Engineering in Health and Medicine, vol. 6, pp. 1-10, 2018, Art no.2700410,doi: 10.1109/JTEHM.2018.2861882.
- [22] M.R.Carneiro, A.T. de Almeida and M. Tavakoli, "Wearable and Comfortable e-Textile Headband for Long-Term Acquisition of Forehead EEG Signals,"in IEEE Sensors Journal, vol.20, no.24,pp. 15107-15116, 15 Dec.15,2020,doi:10.1109/JSEN.2020.3009629.
- [23] De Fazio R, Mastronardi VM, De Vittorio M, Visconti P. Wearable Sensors and Smart Devices to Monitor Rehabilitation Parameters and Sports Performance: An Overview. *Sensors (Basel)*. 2023 Feb 7;23(4):1856.doi: 10.3390/s23041856. PMID:36850453; PMCID: PMC9965388.
- [24] Postolache, Monge, J., Alexandre, R., Geman, O., Jin, Y., Postolache, G.(2021). Virtual Reality and Augmented Reality Technologies for Smart Physical Rehabilitation. In: Kanoun, O., Derbel, N.(eds) *Advanced Systems for Biomedical Applications. Smart Sensors, Measurement and Instrumentation*, vol 39. Springer,Cham.<https://doi.org/10.1007/978-3-030-71221-18>
- [25] Troisi E, Matteis M, Silvestrini M, Paolucci S, Grasso MG, Pasqualetti P, Vernieri F, Caltagirone C. Altered cerebral vasoregulation predicts the outcome of patients with partial anterior circulation stroke. *Eur Neurol*. 2012;67(4):200-5.doi: 10.1159/000334851.

Heart Disease Detection Using ECG Waveforms

Afeefa Askar

Dept. of Biomedical
Engineering KMCT CEW
Kozhikode, India
fafeefaskar246@gmail.com

Ahla CT

Dept. of Biomedical
Engineering KMCT CEW
Kozhikode, India
ctahla43@gmail.com

Amal Abdulsalam KC

Dept. of Biomedical
Engineering KMCT CEW
Kozhikode, India
amalkc2002@gmail.com

Nandana Raj

Dept. of Biomedical
Engineering KMCT CEW
Kozhikode, India
nandanarajlibra@gmail.com

Ms Irfana Izzath OP

Dept. of Biomedical
Engineering KMCT CEW
Kozhikode, India
irfana@kmctcew.ac.in

Abstract — cardiovascular diseases, also known as CVDs, are still the main reason for sickness and death worldwide, with around 17.5 million deaths linked to them in 2012. The electrocardiogram (ECG) signal shows the heart's electrical activity on the body's surface, providing important information about heart function. It is often used to spot any irregularities in heart rhythm and structure. Over the years, many techniques have been created and researched to classify and detect abnormalities in ECG signals, showing potential for use in medical settings. Current research frequently does not provide thorough comparisons of different heart abnormalities. Some studies focus on specific conditions such as atrial fibrillation, while others look at ST changes. This study introduces a new method using deep convolutional neural networks to classify heartbeats and accurately detect five types of arrhythmias. Our technique involves training a Convolutional Neural Network (CNN) on a meticulously selected dataset, thoroughly validating it, and fine-tuning it with specific parameters and epochs. By feeding ECG images into the model, users can quickly determine whether the cardiac condition is normal or abnormal.

Index Terms—Healthcare service system, Cardiovascular diseases, ECG waveform, Convolutional Neural Network (CNN), ADAM optimizer, Dart with Flutter, MySQL Database, Kaggle figure, Electrocardiogram (ECG), Heart's electrical activity, Irregular heart rhythms, Atrial fibrillation (AFib), Ventricular tachycardia (VT), Softmax tensor, Disease probability detection.

I. INTRODUCTION

This paper introduces an advanced framework for Electrocardiogram (ECG) analysis employing machine learning techniques to enhance the detection of cardiac abnormalities. It underscores the critical importance of accurate cardiovascular disease diagnosis and proposes a deep neural network architecture specifically trained for arrhythmia detection. Notably, the

framework demonstrates the transferability of learned representations to myocardial infarction (MI) prediction, facilitating knowledge sharing across different ECG recognition tasks.

The methodology encompasses a comprehensive pipeline, starting with the collection of patient ECG data and rigorous preprocessing steps to enhance data quality. Subsequent training on a Convolutional Neural Network (CNN) algorithm, comprising convolution layers, hidden layers, and a dense layer, is followed by optimization using the ADAM optimizer and model compilation. Post-training, the model undergoes thorough testing using a separate dataset to evaluate its performance accurately, distinguishing between normal and abnormal cardiac conditions based on input ECG images.

Additionally, the paper provides an insightful overview of the ECG waveform and its components, including the P wave (atrial depolarization), QRS complex (ventricular depolarization), and T wave (ventricular repolarization). Understanding these components is pivotal for effectively diagnosing various cardiac irregularities, such as atrial fibrillation (AFib) or ventricular tachycardia (VT), and assessing coronary artery blood flow adequacy.

II. LITERATURE SURVEY

Hu et.al [1] This paper presents an algorithm for accurately locating QRS complex onsets and offsets in ECG signals without requiring an isoelectric segment. By employing straight-line fitting and angle calculations, it identifies candidate R peaks and determines QRS complex boundaries, achieving improved accuracy and robustness compared to traditional methods.

Jain et.al [2] This paper presents an ultra-low-power ASIC design with a novel cardiovascular disease diagnostic algorithm for real-time ECG signal processing. Implemented in 130-nm CMOS technology, the ASIC occupies a compact 1.21 mm² area and consumes only 96 nW at a 1 kHz operating frequency, ideal for energy-efficient wearable ECG monitoring devices.

Al Rahhal et.al [3] This paper introduces a novel deep learning method for active classification of ECG signals. It utilizes stacked denoising autoencoders (SDAEs) for unsupervised feature learning and incorporates a softmax regression layer for classification. By iteratively updating network weights based on expert-labeled beats, it achieves improved accuracy with less interaction and faster retraining.

Liu et.al [4] This paper introduces a convolutional neural network (CNN) algorithm for myocardial infarction detection using multilead electrocardiogram (ECG). The multilead-CNN (ML-CNN) model integrates sub 2-D convolutional layers and lead asymmetric pooling (LAP) layers, achieving high sensitivity (95.40 percent), specificity (97.37 percent), and accuracy (96.00 percent). Real-time analyses on MATLAB and ARM Cortex-A9 platforms demonstrate its potential for mobile healthcare applications.

Li et.al [5] This study proposes a method to enhance CNNs for ECG beat classification by converting signal data into a two-dimensional format. The model, incorporating adaptive learning and dropout techniques, outperforms existing methods in detecting irregular heartbeats. Tested on the MIT-BIH arrhythmia database, it achieves high accuracy, making it promising for portable cardiovascular monitoring.

Verma et.al [6] This research proposes a Deep Learning model combining Convolutional Neural Networks and Long Short-Term Memory, aided by Oversampling, to classify the 2017 PhysioNet/CinC Challenge dataset into four classes: normal sinus rhythm, atrial fibrillation, others, and noisy classes. The model achieves superior accuracy, potentially integrating with CPS-heart for heart abnormality detection.

Mohamad and Bazi et.al [7] This article introduces an eigendomain-based deep representation learning approach for automated myocardial infarction (MI) detection from 12-lead ECG trace images. Utilizing transfer learning and concatenated probability scores, the proposed method achieves 100 accuracy for MI detection and outperforms existing models with 99.03 overall accuracy in classification.

Kachuee et.al [8] This paper introduces a deep convolutional neural network method for accurately classifying five different arrhythmias based on ECG signals, adhering to the AAMI EC57 standard. It also proposes a knowledge transfer method for myocardial infarction classification. Evaluation on PhysionNet's MIT-BIH and PTB Diagnostics datasets shows average accuracies of 93.4 and 95.9 for arrhythmia and MI classification, respectively.

Iqbal et.al [9] Heart disease is a leading cause of death globally, with significant mortality rates in the United States and underdeveloped regions. This study utilizes Ordinary Learning Method for heart disease detection, achieving 98.4615 accuracy on UCI Cleveland Heart Disease dataset. Compared to other techniques, OLM demonstrates superior performance in diagnosis.

Ran et.al [10] Recent research suggests that 1D-CNN is effective for ECG arrhythmia detection. This study introduces an adaptive CNN combining 2D and 1D layers to exploit morphological similarities among ECG leads. Evaluating on 8-lead ECG data, it outperforms traditional 1D-CNN in accuracy without increasing model size, enhancing diagnostic precision. Ding et.al [11] This study proposed a classification method of premature ventricular contraction based on single lead electrocardiograph (ECG), and compared the classification results of AlexNet and convolutional neural network (CNN) model based on AlexNet.

Khan et.al [12] This study proposes a method for detecting cardiac disorders using a generalized approach to process various formats of ECG images. It employs a Single Shot Detection (SSD) MobileNet v2-based Deep Neural Network, achieving 98 accuracy in detecting four major cardiac abnormalities. The dataset comprises 11,148 annotated ECG images collected from healthcare institutes, endorsed by cardiologists for screening cardiac disorders.

Mengze et.al [13] This paper introduces a robust and efficient 12-layer deep one-dimensional convolutional neural network for classifying five micro-classes of heartbeat types using MIT-BIH Arrhythmia database. Utilizing wavelet self-adaptive threshold denoising, it outperforms BP neural network, random forest, and other CNN networks in accuracy, sensitivity, robustness, and anti-noise capability, conserving medical resources and aiding clinical practice.

Yao et.al [14] This paper presents a method for classifying ECG signals using wavelet transform for denoising and data enhancement to address imbalanced datasets. It proposes an integrated CNN-GRU classifier consisting of convolution layers, local feature extraction modules,

GRU, Dense, and Softmax layers to classify beats into five categories, aiding in computer-aided ECG diagnosis.

Cheng et.al [15] This study introduces a novel approach for automatic ECG identification and classification. It employs a dense heart rhythm network combining deep CNN and BiLSTM to extract hierarchical and time-sensitive features from ECG data. The method achieves an accuracy of 89.3 and an F1 score of 0.891 on the PhysioNet/CINC challenge dataset, improving automatic ECG classification accuracy for clinical diagnosis and self-monitoring of atrial fibrillation.

Xiaolin et.al [16] This paper introduces a novel multistage pruning technique for reducing the computational complexity of CNN models used in ECG classification for smart wearable devices. At 60 sparsity, it achieves 97.7 accuracy and a 93.59 F1 score, improving upon traditional pruning methods while decreasing runtime complexity by 60.4.

Suhail et.al [17] This paper presents a framework for automated heart disease detection using ECG analysis and symptom-based detection. It combines multi-field extraction and nonlinear analysis methods. Discrete wavelet transform preprocesses data, while a Neural Network predicts disease presence. Tested on UCI and Physio net data, it achieves 92.0 sensitivity, 89.33 specificity, and 90.67 accuracy, outperforming traditional methods.

Fang et.al [18] This paper proposes an automated method for ECG classification to aid in diagnosing heart disease, aiming to alleviate the burden on medical staff. Utilizing the MIT-BIH ECG database, it employs the Pan-Tompkins algorithm for QRS feature extraction, followed by K-means clustering and RBF neural network analysis. Achieving a 98.9 classification accuracy, the method effectively detects ECG signal abnormalities.

Doku et.al [19] In a retrospective study at Korle-Bu Teaching Hospital, Ghana, 42 patients with life-threatening arrhythmias were analyzed. Tachyarrhythmias were most prevalent (66.7), with 52 having structural heart diseases. Cardioversion (52.4) and pacemaker implantation (23.8) were common interventions. A high survival rate (88.1) was observed, emphasizing the challenge in resource-limited settings.

Ansari et.al [20] This survey explores Deep Learning (DL) architectures for ECG arrhythmia detection (2017–2023), crucial for early cardiovascular disease diagnosis. DL models like CNNs, MLPs, Transformers, and RNNs are compared for performance. It serves as a roadmap for researchers, offering guidelines and highlighting future research areas to enhance ECG anomaly detection.

Bhaskarpandit et.al [21] This article introduces an eigendomain-based deep representation learning approach for automated myocardial infarction (MI) detection from 12-lead ECG trace images. Utilizing transfer learning and concatenated probability scores, the proposed method achieves 100 accuracy for MI detection and outperforms existing models with 99.03 overall accuracy in classification.

III. METHODOLOGY

In this “Disease detection using ECG waveform” a comprehensive solution that seamlessly integrates admin control, doctor support site, and a user. It categorizes the patient as healthy or diseased corresponding to the patient's ECG data, community support via donation requests, and direct access to medical professionals. The project is used for evaluating the algorithms of electrocardiogram rhythm and morphology abnormality detection and access the database model for the detection of cardiovascular diseases. CNN algorithm with ADAM: The prediction is carried out using a Convolutional Neural Network (CNN) algorithm and ADAM optimizer, a popular optimization algorithm. Implementing Dart with Flutter: It creates a data API for Flutter, handling data, security, and deployment separately. Testing and security are critical. MySQL Database: It is an open-source relational database management system that organizes data in tables, suitable for structured data. Over the past few decades, methods for classification and detection of rhythm or morphology abnormalities in ECG signals have been widely studied.

Many methods have demonstrated potential to accurately detect pathologies in clinical applications. Unfortunately, the current works lack comprehensive comparisons performed on as many as heart abnormal types. Existing works focus on single or a few combination, such as atrial fibrillation, while some studied ST changes. The process starts with the collection of patient ECG data. The data are gathered and enter the preprocessing phase. The missing values are filled or removed using the technique elaborated in the data preprocessing section. Several preprocessing techniques were applied to the dataset for its improvement. The training dataset was used for training the model using training data on the CNN algorithm via inputting through the various convolution layers and hidden layers and lastly dense layer. Then the model is optimized using ADAM and compiled, hence training ends. The trained model undergoes testing. The testing data were used for evaluating the performance of the proposed model. After model training and testing, the proposed system outputs the result. The proposed system categorizes the patient as healthy or diseased as shown. ECG is a recording of

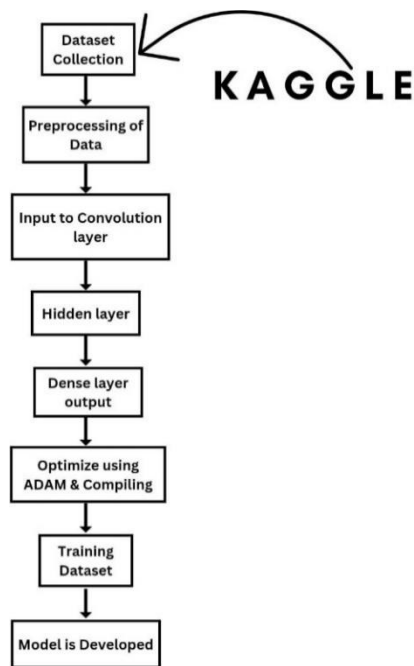


Fig. 1. Block diagram of ECG model development

the heart's electrical activity through repeated cardiac cycles, using electrodes placed on the skin to detect small electrical changes. It is used to detect cardiac abnormalities, such as irregular heart rhythms. A mobile app uses a Convolutional Neural Network (CNN) to detect cardiovascular diseases from 2D ECG waveform images. The model is trained on a curated dataset and validated through rigorous processes. Patients input ECG data, which is processed through a loaded model using a softmax tensor for disease probability detection. This approach redefines emergency response and healthcare support by leveraging advanced technology, community collaboration, and comprehensive medical guidance. OpenCV (Open Source Computer Vision Library) is a popular open-source computer vision and machine learning software library. It provides a wide range of functionalities for image and video processing, including image filtering, feature detection, object recognition, and more. In this context, OpenCV could be used for tasks such as image loading, preprocessing, and augmentation, to prepare the input data for training the CNN model. CNN is a type of deep neural network commonly used for analyzing visual imagery. It is well-suited for tasks such as image classification, object detection, and image segmentation. In this scenario,

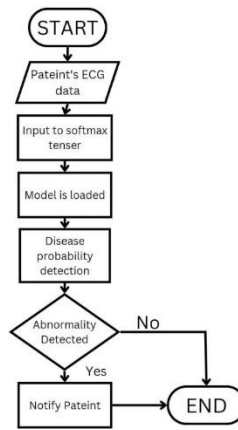


Fig. 2. Flowchart of ECG module implementation.

the modified model is likely based on a CNN architecture, such as Inception-v3, which is pre-trained on a large dataset like

ImageNet. The additional fully connected layer with soft-max activation is added on top of the CNN to adapt it for the specific classification task. scikit-learn is a popular machine learning library in Python, providing simple and efficient tools for data mining and data analysis. While scikit-learn is not explicitly mentioned in the provided paragraph, it could potentially be used for tasks such as data preprocessing, feature extraction, or even as an alternative classification model. For example, scikit-learn's preprocessing modules could complement OpenCV in preparing the input data, and its classification algorithms could be used as an alternative to the CNN for comparison or in scenarios where deep learning is not suitable or feasible.

IV. RESULT

We offer a thorough, methodical, and standardized workflow pipeline that is essential for advancing research endeavors, resolving historical constraints, and standardizing the clinical assessment procedure. Researchers can use this pipeline as a fundamental guide when creating and assessing deep learning (DL) models especially for the categorization of cardiac arrhythmias. It is important to emphasize that when feature extraction and classification are done in separate steps, these recommendations perform best in heartbeat classification circumstances. For detection systems containing arrhythmias like AF or VF, which require segments as input and allow end-to-end learning, different problems can arise, necessitating a modified approach. Observe Fig.3

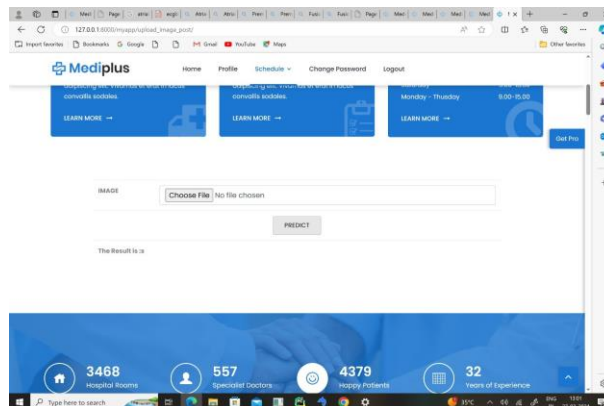


Fig. 3. Result of Atrial fibrillation

The script conducts transfer learning by retraining a pre-trained Inception-v3 model on a new dataset for image classification. It starts with database selection, utilizing the MIT-BIH database for impartial comparisons. Preprocessing involves standard signal filtering techniques, and unfiltered raw signals are used for performance assessment. The script sets up directory structure, downloads the pre-trained model, and defines command-line arguments. Data preparation involves organizing images into sets and applying data augmentation if necessary. Model modification adds a new fully connected layer for the classification task. Training iterates over a fixed number of steps, adjusting model weights using gradient descent. Evaluation assesses performance on training and validation datasets, while testing evaluates the final model on a separate dataset for generalization. The trained model is saved along with its labels for deployment, showcasing the use of TensorFlow for deep learning tasks.

V. CONCLUSION

ECG waveform analysis is a promising avenue in medical diagnostics, detecting cardiac diseases like arrhythmias and heart failure with high accuracy. Advanced signal processing and machine learning differentiate normal from abnormal ECG patterns, enabling early intervention. Integration into clinical practice enhances diagnostic accuracy and personalized treatment, potentially saving lives. Challenges include data standardization and interoperability. Advancements hold promise for revolutionizing cardiac disease management, fostering early detection, and prevention, ultimately improving global healthcare. Integration across platforms and leveraging machine learning algorithms further enhance efficiency, offering valuable insights for proactive intervention and improved patient outcomes.

VI. ACKNOWLEDGEMENT

It goes without saying that without THE ALMIGHTY's mercy towards me over the years, I would not be in this position today. For that reason, I would like to express my gratitude. I want to put on record, my deepest gratitude to everyone that helped us to successfully finish this project. I gratefully recall the invaluable advice and unwavering support of the BM Department Head, Dr. Sameera V. Mohd Sagheer, and the project coordinator, Ms. Minilal M., for their insightful recommendations during the project's duration. I would like to convey my sincere appreciation to the principal, Ms. Dr. D. Jerline Sheeba Anni, for the first-rate facilities and unwavering assistance during the course work and project. I'm grateful.

REFERENCES

- [1] Xiao Hu, Jingjing Liu, Jiaqing Wang, Zhong Xiao, and Jing Yao. Automatic detection of onset and offset of qrs complexes independent of isoelectric segments. *Measurement*, 51:53–62, 05 2014.
- [2] Sanjeev Kumar Jain and Basabi Bhaumik. An ultra low power ecg signal processor design for cardiovascular disease detection. In *2015 37th Annual International Conference of the IEEE Engineering in Medicine and Biology Society (EMBC)*, pages 857–860, 2015.
- [3] Mohamad Al Rahhal, Yakoub Bazi, Haikel Alhichri, Naif Alajlan, Farid Melgani, and Ronald Yager. Deep learning approach for active classification of electrocardiogram signals.

Information Sciences, 345, 02 2016.

- [4] Wenhan Liu, Mengxin Zhang, Yidan Zhang, Yuan Liao, Qijun Huang, Sheng Chang, Hao Wang, and Jin He. Real-time multilead convolutional neural network for myocardial infarction detection. *IEEE Journal of Biomedical and Health Informatics*, 22(5):1434–1444, 2018.
- [5] Jia Li, Yujuan Si, Tao Xu, and Jiang Saibiao. Deep convolutional neural network based ecg classification system using information fusion and one-hot encoding techniques. *Mathematical Problems in Engineering*, 2018:1–10, 12 2018.
- [6] Dhvaj Verma and Sonali Agarwal. Cardiac arrhythmia detection from single-lead ecg using cnn and lstm assisted by oversampling. pages 14–17, 09 2018.
- [7] Mohamad Al Rahhal, Yakoub Bazi, Nassim Ammour, Mansour Zuair, Bilel Benjdira, and Esam Othman. Convolutional neural networks for electrocardiogram classification. *Journal of Medical and Biological Engineering*, 04 2018.
- [8] Mohammad Kachuee, Shayan Fazeli, and Majid Sarrafzadeh. Ecg heartbeat classification: A deep transferable representation. In *2018 IEEE International Conference on Healthcare Informatics (ICHI)*, pages 443–444, 2018.
- [9] Javid Iqbal, Muhammad Munwar Iqbal, Umair Khadam, and Ali Nawaz. Ordinary learning method for heart disease detection using clinical data. In *2020 3rd International Conference on Computing, Mathematics and Engineering Technologies (iCoMET)*, pages 1–6, 2020.
- [10] Jinming Ran. Detection of arrhythmias for multi-lead electrocardiogram using convolutional neural network. In *2020 IEEE 5th International Conference on Signal and Image Processing (ICSIP)*, pages 690–694, 2020.
- [11] Ling-Juan Ding, Xin-Kang Wang, Jie Gao, Tao Yang, Fa-Xiang Wang, and Liang-Hung Wang. Ecg automatic classification model based on convolutional neural network. pages 1–2, 09 2020.
- [12] Ali Khan, Muzammil Hussain, and Muhammad Malik. Cardiac disorder classification by electrocardiogram sensing using deep neural network. *Complexity*, 2021:1–8, 03 2021.
- [13] Mengze Wu, Yongdi Lu, Wenli Yang, and Shen Wong. A study on arrhythmia via ecg signal classification using the convolutional neural network. *Frontiers in Computational Neuroscience*, 14:564015, 01 2021.
- [14] Guoliang Yao, Xiaobo Mao, Nan Li, Huaxing Xu, Xiangyang Xu, Yi Jiao, and Jinhong Ni. Interpretation of electrocardiogram heartbeat by cnn and gru. *Computational and Mathematical Methods in Medicine*, 2021:1–10, 08 2021.
- [15] Jinyong Cheng, Qingxu Zou, and Yunxiang Zhao. Ecg signal classification based on deep cnn and bilstm. *BMC Medical Informatics and Decision Making*, 21, 12 2021.
- [16] Xiaolin Li, Rajesh Panicker, Barry Cardiff, and Deepu John. Multistage pruning of cnn based ecg classifiers for edge devices. volume 2021, pages 1965–1968, 11 2021.
- [17] Muhammed Suhail and T. Razak. Cardiac disease detection from ecg signal using discrete wavelet transform with machine learning method. *Diabetes Research and Clinical Practice*, 187:109852, 03 2022.
- [18] Yan Fang, Jianshe Shi, Yifeng Huang, Taisheng Zeng, Yuguang Ye, Lianta Su, Daxin Zhu, and Jianlong Huang. Electrocardiogram signal classification in the diagnosis of heart disease based on rbf neural network. *Computational and Mathematical Methods in Medicine*, 2022:1–

9, 01 2022.

- [19] Alfred Doku, Bernard Asiamah-Asare, Richard Osei, Chris Owoo, Robert Djagbletey, Joseph Akamah, Aniteye Ernest, and Dzifa Ahadzi. Outcome of life-threatening arrhythmias among patients presenting in an emergency setting at a tertiary hospital in accra-ghana. *BMC Cardiovascular Disorders*, 22:361, 08 2022.
- [20] Yaqoob Ansari, Omar Mourad, Khalid Qaraqe, and Erchin Serpedin. Deep learning for ecg arrhythmia detection and classification: an overview of progress for period 2017–2023. *Frontiers in Physiology*, 14, 09 2023.
- [21] Sathvik Bhaskarandit, Anurag Gade, Shaswati Dash, Dinesh Dash, Rajesh Tripathy, and Ram Pachori. Detection of myocardial infarction from 12-lead ecg trace images using eigendomain deep representation learning. *IEEE Transactions on Instrumentation and Measurement*, pages 1–12, 01 2023.

IoT Based Prototype For Patient Monitoring And Medical Infusion Intravenously

*

IoT Based Prototype For Patient Monitoring And Medical Infusion Intravenously

Aparna Devaraj

Dept. of Biomedical Engineering
KMCT CEW Kozhikode, India
aparnadevaraj03@gmail.com

Ann Sunny

Dept. of Biomedical Engineering
KMCT CEW Kozhikode, India
annsunny329@gmail.com

Rana Abdul Rasheed

Dept. of Biomedical Engineering
KMCT CEW Kozhikode, India
ranarasheed2903@gmail.com

Shifa Thasneem

Dept. of Biomedical Engineering
KMCT CEW Kozhikode, India
shifathasneem3443@gamil.com

Minilal M

Dept. of Biomedical Engineering
Assistant Professor
KMCT CEW Kozhikode, India
minilal.raj@gmail.com

Abstract—an Important advancement in healthcare technology is represented by our groundbreaking “iot based prototype for patient monitoring and medical infusion intravenously” project. When iot technology is combined with iv set and patient monitoring, new capabilities are introduced. One such feature is the ability to manage the drip rate remotely via a mobile app, which guarantees accurate medicine delivery. Our system provides flexibility in the way medication administration in accordance with individual patient demands. Additionally, the integration of vehicle control makes it easier for patients to shift the iv set remotely, which maximises resource allocation and reduces operational disturbances in the healthcare system. In order to improve patient safety, the system uses advanced sensors at the same time. The system makes use of cutting-edge sensors at the same time, such as an accelerometer for posture detection, an infrared (ir) sensor for obstacle iden- tification, and an alarm system for improved patient safety. These sensors support thorough patient monitoring, guarantee precise and reliable infusion rates, and notify medical professionals of any possible problems. Vital patient information, including temperature, heart rate, and infrared data for drip level monitoring, is safely archived for review and analysis at a later time. This integrated solution’s adaptability and scalability improve patient safety, medication administration efficiency, and overall healthcare outcomes—offering healthcare professionals a comprehensive, technologically advanced innovation.

Index Terms—iot, ESP32, L293D

I. INTRODUCTION

In the ever-evolving landscape of contemporary healthcare, the fusion of state-of-the-art technology and medical ingenuity consistently molds the provision of patient care. Our inno- vative endeavor, titled the “IoT Based Prototype For Patient Monitoring And Medical Infusion Intravenously,” signifies a substantial advancement, fueled by the overarching objective of

improving patient care, safety, and operational efficacy. Through the seamless integration of Internet of Things (IoT) technology with conventional IV set and patient monitoring, we seek to redefine the benchmarks for medication administration and patient monitoring within healthcare environments.

The foundation of our system facilitates remote control of drip rates through an intuitive mobile application, ensuring accurate and personalized medication delivery while providing healthcare providers with real-time adjustment capabilities. Furthermore, our initiative introduces vehicle control integration, enabling the efficient and remote transfer of IV set between patients, optimizing resource allocation and minimizing disruptions.

Incorporating infrared (IR) data for monitoring and controlling drip levels, coupled with continuous monitoring of critical patient parameters, our system adopts a holistic approach to patient care. The securely stored data within a compliant database supports real-time healthcare management and serves as a valuable resource for future reference and analysis. The adaptability and scalability of our IoT-based system make it suitable for diverse healthcare settings, spanning from hospitals to home care environments.

Our project introduces an accelerometer for posture detection, thereby adding essential dimensions to its functionality, and an integrated alarm system for enhanced patient safety. In summary, our “IoT Based Prototype For Patient Monitoring And Medical Infusion Intravenously” project is positioned to catalyze a transformative shift in healthcare, embodying our dedication to harnessing technology’s full potential for the well-being of patients, the efficiency of healthcare providers, and the evolution of healthcare practices towards a more patient-centered and data-driven future.

II. LITERATURE SURVEY to pressure changes and the requirement for valves are possible

The document describes steps chemists can take to avoid mistakes while administering IV medications. In order to avoid drawbacks. The paper [9] evaluates the benefits of a central control programming errors, chemists are essential in determining dosage limits utilising “smart” infusion technology ^[1]. Error prevention is positively impacted by smart infusion systems, as the Vanderbilt University Medical Centre has found. Notwithstanding, obstacles can encompass technology aspects and the want for enhanced adherence.

The paper ^[2] assesses the effect of decision-supporting intelligent IV infusion pumps on medication mistakes in cardiac units. Despite identifying errors, the research reveals that poor compliance has no discernible impact on the frequency of serious prescription errors. The promise of smart pumps is highlighted in the conclusion, however the focus is on tackling behavioural and technological aspects for better medication safety.

A spatiotemporal algorithm and cameras are used by a system to identify faults in the operation of a home infusion pump ^[3]. It guarantees correct action sequences, improving patient safety. Real-time error correction, algorithm training, and video capturing are all part of the process. Complexity of the system and possible resistance are issues, especially for older users.

Issues with accurately measuring medication dosages for young children utilising infusion pumps are discussed in [4]. Models for age-specific issues are part of the methodology. The intricacy of the modelling and the requirement for age-specific modifications are possible drawbacks.

The design of an infusion pump calibrator [5], including signal detection, processing/display, and control components, is the main goal of this work. It exhibits minimal mistakes in flow rate and occlusion pressure testing thanks to microcontrollers and sensors. Patient safety is prioritised through routine calibration, addressing issues with quickness, and stressing the critical need of infusion pump dependability. Maintenance issues are one possible drawback.

The goal of a microfluidic electroosmotic infusion pump is to achieve low voltage and high flow rates. It could be difficult to sustain the low voltage needs. Microelectrodes and simulations are used in the process to maximise pumping efficiency.

Non-lead composites are used to protect infusion pumps from problems caused by radiation exposure [7]. Among the possible drawbacks is the requirement for additional development. By integrating bismuth oxide into materials, the approach shows promising X-ray attenuation.

In [8], a unique portable micro-pump intended for medication delivery systems with excellent precision, low cost, and efficiency is presented. The design, production, and testing phases of the process demonstrate the methodology's capacity to produce high performance with an error of less than 1 percent. The micro-pump discussed in [8] finds uses in chemotherapy, insulin delivery, pain management, and antibiotic therapy. It seeks to address shortcomings in current pumps. Sensitivity interface for IV infusion pump management in intensive care units in terms of usability. A task-based usability test that contrasts the central interface with individual pump controls is part of the methodology. The central control interface addresses human factors and usability difficulties and shows better performance, fewer errors, and good user responses. The study adheres to the usability standards of ISO 9241-11.

The focus is on vulnerabilities that raise safety issues with Wireless Infusion Pumps in Hospital Delivery Organisations (HDOs) [10]. The report contains parts covering the pump ecosystem, cyber-physical systems, and security measures and suggests cybersecurity controls during software development. A "smart self-monitored syringe infusion pump" in [11] incorporates a patient monitor for simultaneous data recording in order to mitigate the dangers associated with syringe infusion. The goal is to increase efficiency and safety, however there may be drawbacks, such as constant surveillance and information overload for medical personnel.

The difficulties in IV therapy monitoring are covered in the paper [12], along with a thorough solution that makes use of Arduino, IR sensors, RF transmitters, and Wi-Fi modules. By keeping an eye on IV fluid levels, the automated device avoids problems like blood loss or backflow. The focus lies in mitigating stress among healthcare practitioners and augmenting patient safety, so contributing to the wider movement of utilising technology to improve healthcare. Promising for effective health monitoring during IV therapy is the suggested system.

In order to improve safety, an LD20 flow sensor for syringe infusion pumps is introduced in [13]. It measures infused flow directly. It talks about the shortcomings of the pumps that are in use

today and stresses how crucial precise infusion rates are. As part of the technique, the sensor is integrated to fix issues and enhance safety features.

The study ^[14] addresses issues with manual monitoring during IV therapy by introducing an Internet of Things-based Automated Intravenous Drip Monitoring System. Improving patient safety and lightening the strain on medical personnel are the objectives. Complexity of the technology and its incorporation into current healthcare systems could be obstacles.

Paper ^[15] suggest utilising Arduino and infrared sensors to create an automated saline flow monitoring system for effective healthcare. The emphasis is on cost-effectiveness and minimising human intervention. Remote monitoring is a benefit, but there may be drawbacks such as difficulties with implementation and technology resistance.

An inexpensive portable infusion pump guarantees accurate drug dosage and detects air bubbles ^[16]. The process makes use of fluidic, mechanical, and electrical concepts. Difficulties include the possibility of medication delivery problems, with a focus on mobility and affordability.

The difficulties in modifying target-controlled infusion (TCI) pumps for use with younger patients are discussed in this paper ^[17], with a focus on how growth and organ function affect drug clearance. Using allometric models for size standardisation and maturation, such as the sigmoid Emax or Hill model, is part of the process. The two most used medications for paediatric IV anaesthesia are propofol and remifentanyl. The advantages of computerised TCI systems and their pharmacokinetic/pharmacodynamic variability are recognised, along with the limitations of manual regimens in children. One drawback is that TCI pumps are currently insufficient for newborns.

Using a DC motor, microprocessor, and GSM module for wireless control, a low-cost medical syringe pump is intended for use in remote locations. The objective of ^[18] is to offer a clever, mobile telemedicine solution with IoT connectivity. One or more such drawbacks could be poor connectivity in isolated locations.

An open-source platform for wireless infusion pumps used in security research ^[19] is called secpump. Its objective is to assess and create solutions to medical equipment security vulnerabilities. The platform is open-source, which makes it easier to launch assaults and mount defences while also advancing knowledge of the weaknesses in cyber-physical systems.

It is explained how technology is driving a revolution in healthcare, with a particular emphasis on a wireless system for IV fluid flow monitoring in real time. The study ^[20] highlights how IoT may automate healthcare functions, lowering the demand for ongoing human interaction. Device interoperability and security issues could be difficulties.

To solve issues with human estimating and inaccuracies, an Internet of Things (IoT) based drip monitoring and control device for IV infusion settings is presented ^[21]. Physical and electrical separation are stressed throughout the paper's discussion of infrared-based drop detection. Ambient lighting influences on detection accuracy could be a challenge.

Accurate drug delivery in ^[22] is the goal of passive im- planted infusion pumps incorporating MEMS technology. Po- tential drawbacks include the requirement for additional test- ing. The process incorporates microfluidic chips for accurate control, supporting pain relief and cancer treatment.

An alternative effective IoT-based drip rate monitoring and regulating device is suggested ^[23]. The approach uses observa- tion, surveying, and clinical immersion to find problems with current systems. The gadget is intended to address issues such as blood backflow and air embolism.

The paper ^[24] presents a smart infusion pump that uses Arduino to monitor and regulate IV systems remotely. It makes use of optical sensors and laser diodes to track fluid levels and identify obstructions. Ensuring dependable wireless data transmission for remote monitoring could present difficulties.

The goals of two-provider verification in ^[25] for configuring anaesthesia infusion pumps are effectiveness and safety. One of the challenges is the ongoing requirement for training. The “model for improvement” with main drivers, interventions, and PDSA cycles is used in the methodology.

III. METHODOLOGY

The project “IoT Based Prototype For Patient Monitoring And Medical Infusion Intravenously” approaches healthcare issues methodically. By creating communication protocols, it incorporates Internet of Things technologies into conventional IV set and patient monitoring systems. The intuitive mobile ap- plication facilitates remote drip rate control, and flexibility in the way medications are administered. Vehicle control systems provide the efficient and remote transfer of the infusion pump between patients, hence optimising the allocation of resources. With an accelerometer, IR sensor, and alarm system for safety and accuracy, advanced sensors improve patient monitoring. Patient data that is kept in a compliant database for later analysis is safeguarded by strong data security procedures. The system is adaptable and expandable to fit a range of healthcare environments. The objective is to improve patient care and transform healthcare technology.

A. Block Diagram

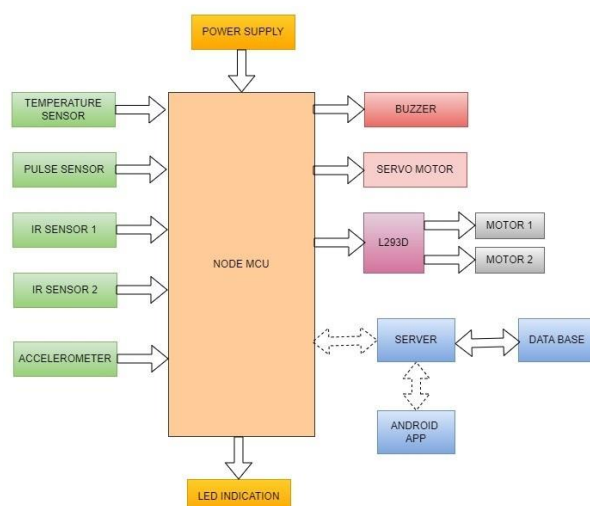


Fig. 1. Block Diagram

Components and Modules

1) Hardware Components:

- **ESP32:** The ESP32 is a low-cost, Bluetooth-enabled, Wi-Fi-equipped device. In addition to integrated features like filters, power management, RF components, and antenna switches, it makes use of many microprocessors, such as Tensilica Xtensa and RISC-V.
- **Temperature Sensor:** It is possible that the temperature sensor is utilised to keep an eye on the body temperature of patient. In hospital settings, where it's critical to maintain the proper temperature for pharmaceuticals, this information may be useful.
- **IR Sensor (Infrared Sensor):** There are a lot of uses for IR sensors. They might be employed in this situation to sense the closeness of things in order to make sure the IV set is positioned properly or to identify any obstructions in its path.
- **Pulse Sensor:** The patient's heart rate is determined via the pulse sensor. In the medical field, it is crucial to keep an eye on vital indications like heart rate, particularly while administering drugs via an infusion pump.
- **Accelerometer:** A sensor that detects acceleration and may identify forces such as gravity or motion-induced forces is called an accelerometer. It provides essential motion-related data and is frequently employed in devices for features like screen rotation and step counting.
- **Buzzer:** A buzzer is a basic electrically powered device that emits a sound, usually a buzzing or beeping sound. Frequently observed in alarm clocks, timers, and electronic gadgets, it functions to deliver auditory notifications or cautions by transforming electrical impulses into sound waves via a vibrating component. Employ as a warning
- **DC Motor:** A DC motor is a mechanical device that generates motion from electrical energy. It works by using the interaction of a magnetic field and a current-carrying coil to produce rotating movement. DC motors are widely utilised in industrial, robotic, and appliance applications. They are renowned for their ease of use and effectiveness in transforming

electrical power into mechanical effort.

- L293D Motor Driver: The stepper motor is driven by the L293D. It's a motor driver integrated circuit (IC) that gives the motor the power and control signals it needs to move the system precisely.
- Servo Motor: A servo motor is an electrical device that precisely moves machine parts. It's a BLDC motor with a feedback sensor for accurate control over angle, location, and velocity. It's a key component in closed-loop motion control systems.

2) *Software Components:*

- Mobile App: You indicated using a mobile app to operate the system. In order to give users (healthcare providers) the opportunity to remotely adjust the drip rate of the system, monitor patient data, and handle other capabilities, it is likely that the app will connect to the server. The application may provide control and data visualisation interfaces that are easy to use.
- Database: The server gathers information from the several sensors (temperature, infrared, pulse, etc.), safely stores it in a database, and links it to patient data. Accurate administration of drugs and patient monitoring depend heavily on these data.
- IoT Connectivity: Since your project is Internet of Things (IoT) based, it connects different devices to a network—likely Wi-Fi or cellular—through the usage of a network. Real-time data transfer between sensors, the server, and the mobile app is made possible by this link.
- Security: Security is crucial since healthcare data is sensitive. Strong security measures must to be in place on your system to safeguard patient information and guarantee that unwanted access is avoided.
- Data Visualisation and Analysis: The programme offers instruments for examining past patient data. In order to help healthcare professionals make well-informed decisions about patient care and medication administration, it can produce reports, trends, and alarms.
- Error Handling and Alerts: The software must to possess the capability to identify problems or irregularities within the system (such as incorrect medicine administration) and promptly notify healthcare providers.

RESULT AND DISCUSSION

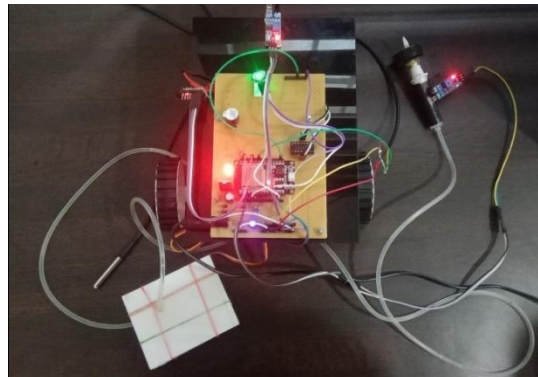


Fig. 2. result

The system is connected to the patient, and the drip rate is controlled and monitored with the patient monitoring system where the parameters including patient posture in the app. The data is collected by the system and sent to the cloud, where it is displayed in the Android app. The patient's data will be continuously monitored and updated in the app. The system's movement can be controlled by the app, allowing it to move forward, backward, left, and right.

Table 1: Initial readings

Temperature	Drip Count	Pulse	Position	Date	Time
0	0	0	Straight	26-03-2024	18:17:03
0	0	0	Straight	26-03-2024	18:17:05
0	0	0	Straight	26-03-2024	18:17:08
0	0	0	Straight	26-03-2024	18:17:10
0	0	0	Straight	26-03-2024	18:17:13
0	0	0	Straight	26-03-2024	18:17:16

Table 1 shows the drip count and pulse rate at initial condition with corresponding time.

Table 2: Final readings

Temperature	Drip Count	Pulse	Position	Date	Time
0	0	0	Straight	26-03-2024	18:18:34
28.45	3	110	Straight	26-03-2024	18:18:38
29.20	7	110	Left	26-03-2024	18:18:41
29.45	9	100	Left	26-03-2024	18:18:45
30.00	13	95	Right	26-03-2024	18:18:49
30.00	15	99	Right	26-03-2024	18:19:00

Table 2 shows the varying values of drip count and pulse rate with respect to time.

IV. CONCLUSION

The project "IoT Based Prototype For Patient Monitoring And Medical Infusion Intravenously" is a trailblazing development in healthcare technology that aims to strategically solve contemporary issues and promote improvements in patient care. By incorporating IoT technology into IV set and patient monitoring system with ease and offering cutting-edge capabilities like remote drip rate control, and effective vehicle control, the methodical approach used guarantees a comprehensive approach. The integration of cutting-edge sensors improves medicine administration accuracy and safety by facilitating thorough patient monitoring. Strong data security protocols ensure that private patient data is kept safe, and the flexible, scalable architecture enables adaptability to a range of health-care environments. The system's effectiveness and safety are confirmed by usability testing and regulatory compliance. The project promises to revolutionise healthcare procedures and improve patient care through digital innovation, and as it approaches

deployment, continual monitoring and optimisation highlight its dedication to continuous development.

REFERENCES

- [1] Preventing medication errors with smart infusion technology, Karen Wilson, Mark Sullivan, 2004.
- [2] A controlled trial of smart infusion pumps to improve medication safety in critically ill patients, Jeffrey M.Rothschild, Carol A.Keohane, 2005.
- [3] Multi-camera monitoring of infusion pump use, Zan Gao, 2010 IEEE.
- [4] Pediatric models for adult target-controlled infusion pumps, Brian J.Anderson, 2010.
- [5] The design and construction of infusion pump callibrator, Nuntachai Thongpance, 2012 IEEE.
- [6] Design simulation and a novel DC electroosmotic micro-infusion pump, Firouz Safaifar, Nima Talebzadeh, Hadi Veladi, 2014 IEEE.
- [7] Application of polymer composite material for radiation protection of infusion pumps, Isabella L.Grassetti, Samantha L.Curran, Anita M.Petrilli, 2015 IEEE.
- [8] Evaluation of novel portable micro-pump and infusion system for drug delivery, Paul Pankhurst, Zahra MC Guinness Abdolahi, 2016 IEEE.
- [9] Improved usability of a multi-infusion set up using a centralised control interface:A task based usability test, Frank Doesberg, Fokie Cnossen, 2017.
- [10] Information security consideration for wireless infusion pump, Pooja Rajendra Prasad, Sergey Butakov, 2018 IEEE.
- [11] Semi automated self monitored syringe infusion pump, Hasnaa Elkheshen, Ibrahim Deni, 2018 IEEE.
- [12] Innovative intravenous fluid control and emergency monitoring system, Dr K Sampath Kumar, 2018.
- [13] An intelligent infusion flow controlled syringe infusion pump, Jeorge Hajj Moussa, 2019 IEEE.
- [14] Intra intravenous drip monitoring system for smart hospital using IOT, Ms Sinaj, Joseph, Mrs Asha Baby, 2019 IEEE.
- [15] Low-cost digitization of infusion pump for real time automated flow rate monitoring and warning, Shohag Hossain, Shraboni Sharmin, 2019 IEEE.
- [16] Designing a low-cost and portable infusion pump, Muhammed Irfan Ali, 2019 IEEE.
- [17] Design and development of a low cost , smart infusion pump to deliver medications for patients using labview interface with Arduino, Sakthivel Sankaran, M Pallikonda Rajesekaran, 2019.
- [18] Design of low cost smart infusion pump, Muhamed Eltahir Mansour, 2020 IEEE.
- [19] Sec pump : A connected open source infusion pump for security research purpose, Cyril Brech, Roman Lysecky, 2020 IEEE.
- [20] IOT based health care monitoring and intravenous flow control, Preethi S, 2020 IEEE.
- [21] Design and development of IOT enabled IV infusion rate monitoring and control device for

precision care and probability, Mohammed Arfan, 2020 IEEE.

- [22] Design and characterization of 3-stack MEMS based passive flow regulators for implantable and ambulatory infusion pumps, Dimitry Dumont-Fillon, 2020 IEEE.
- [23] An IOT based intravenous drip rate controlling and monitoring device, Ananya Madhav, 2021 IEEE.
- [24] A smart infusion pump system for remote management and monitoring of intravenous drips, Muhammad Raimi Rosdi, 2021 IEEE.
- [25] Independent double-check of infusion pump programming: An anesthesia improvement effort to reduce harm, Kavitha C.Raghavan, Jonathan D.Burlison, Edward M.Sanders, Michael G.Rossi, 2022.

Evaluating The Role of Dietary Factors in Predicting Blood Glucose Level for Type-1-Diabetes Using Machine Learning

Mufliha T

Dept. of biomedical engineering
KMCT CEW Kozhikode, India
muflihakmw20bm@kmctcew.ac.in

Naseeba Noori

Dept. of biomedical engineering
KMCT CEW Kozhikode, India
naseebanoorikmw20bm@kmctcew.ac.in

Nida Nishana

Dept. of biomedical
engineering
KMCT CEW Kozhikode,
India
nidanishana0@gmail.com

Tisniya Vironi

Dept. of biomedical engineering
KMCT CEW Kozhikode, India
tisniyavironikmw20bm@kmctcew.ac.in

Shibitha KP

Dept. of biomedical engineering
KMCT CEW Kozhikode, India
shibithakp@kmctcew.ac.in

Abstract—Type 1 Diabetes, or T1D, is a condition where the body's immune system attacks and damages the insulin producing cells in the pancreas. A major challenge for individuals with T1D is effectively controlling their blood sugar levels after eating, by determining the right amount of insulin to inject before meals. This process is known as managing Postprandial Glucose Response (PGR). Here we develop a prediction system for individuals with Type 1 diabetes and helps to manage their blood sugar (glucose) level. Using Machine Learning methods to predict Blood Glucose Levels (BGLs) based on nutritional factors (i.e., carbohydrates, lipids, proteins, fibres and energy intakes) can provide valuable insights into the relationship between diet and health. By collecting comprehensive data on insulin usage and physical activity, this project aim to built accurate predictive model. The user friendly interface will empower individuals to input the dietary information and receive real time prediction. This model will not only forecast blood glucose levels but also provide personalized nutrition recommendation, fostering better day-to-day diabetes management. This suggests that personalized dietary recommendations and interventions could be valuable for managing blood glucose levels in context of diabetes.

Index Terms—Type-1-Diabetes, Postprandial Glucose Response (PGR), Blood Glucose Level (BGL).

I. INTRODUCTION

Type 1 Diabetes (T1D) often referred to as “Type 1 diabetes mellitus” is an autoimmune chronic condition, in which the immune system of the affected individual destroys the pancreas (insulin-making cells which are cells). As a result, the pancreas is unable to produce insulin, which is a hormone necessary for regulating blood sugar (glucose) levels in the body. The main cause of T1D is complex and depends on different factors, including genetic, immunologic and environmental factors. Based on recent epidemiological studies T1D incidence is 15 per 100,000 people and the worldwide prevalence is 9.5 percentage. The incidence and prevalence

of Type-1 diabetes are increasing in the world. In addition to a regular exogenous administration of insulin, patients with T1D have to adhere to a healthy lifestyle and be very careful in monitoring and managing their blood sugar levels to prevent and avoid acute complications, such as severe hypoglycemia, severe hyperglycemia, etc as well as the severe chronic complications involving eye, kidney, and cardiovascular system. In particular, a main issue for T1D patients is managing postprandial glucose response

A. OBJECTIVES

The objective of this machine learning project is to develop a predictive system for individuals with Type 1 diabetes that helps them manage their blood glucose levels more effectively through nutritional insights. By collecting comprehensive data on dietary habits, insulin usage, physical activity, and historical blood glucose measurements, the project aims to build accurate predictive models. These models will not only forecast blood glucose levels but also provide personalized nutrition recommendations, fostering better day-to-day diabetes management. The user-friendly interface will empower individuals to input their dietary information and receive real-time predictions and guidance, while ongoing monitoring and feedback mechanisms will ensure continuous model improvement. Improved diabetes management enables individuals with Type 1 diabetes to make informed dietary choices by considering the impact of different foods on their blood glucose level and reduce the risk of extreme blood glucose fluctuations. By collaborating with healthcare professionals and prioritizing privacy and security, this project aspires to make a meaningful impact on the lives of those with Type 1 diabetes, reducing complications and enhancing their overall quality of life.

B. KEY CHARACTERISTICS

1. **Insulin Dependence:** People with Type 1 diabetes are entirely dependent on external insulin sources because their bodies cannot produce insulin on their own. Insulin therapy, typically administered through injections or an insulin pump, is necessary to manage blood sugar levels.
2. **Onset in Youth:** Type 1 diabetes is often diagnosed in childhood or adolescence, although it can develop at any age. It was previously known as "juvenile diabetes" due to its frequent onset in young individuals.
3. **Rapid Onset of Symptoms:** The symptoms of Type 1 diabetes can develop quickly over a period of days or weeks. Common symptoms include excessive thirst, frequent urination, unexplained weight loss, extreme hunger, fatigue, and blurred vision.
4. **Blood Sugar Management:** Managing blood sugar levels is a critical aspect of living with Type 1 diabetes. This involves regular monitoring of blood glucose levels, calculating insulin doses, and making lifestyle adjustments to keep blood sugar within a target range.
5. **Risk of Hypoglycemia and Hyperglycemia:** People with Type 1 diabetes are at risk of both hypoglycemia (low blood sugar) and hyperglycemia (high blood sugar) episodes. Hypoglycemia can lead to symptoms like shakiness, confusion, and even loss of consciousness, while hyperglycemia can cause fatigue, excessive thirst, and other symptoms.

c. METHOD

In this paper it focuses on a diverse set of features, each of which plays a unique role in the context of T1D prediction: Gender, Age, Urea, Creatinine ratio(Cr), Body Mass Index (BMI), Cholesterol (Chol), Fasting lipid profile, including total LDL, VLDL, Triglycerides(TG) and HDL Cholesterol, HBA1C, Class (the patient's diabetes disease class may be Diabetic, Non-Diabetic, or Predict-Diabetic). A machine learning algorithm with Artificial neural network is used for forecasting future glucose values. Comparative analysis of machine learning algorithms to achieve the goal of accurate T1D prediction. The algorithms under consideration encompass a diverse set of techniques including logistic regression, decision trees, random forest, support vector machines. Each of these algorithms has its strengths and limitations, and the choice of the most suitable one is a critical decision. The selected algorithm should provide the most accurate and reliable T1D predictions based on the considered features, making it an invaluable tool for early diagnosis and management

II. LITERATURE SURVEY

All the below listed surveys were conducted to find the most appropriate algorithm that provide the best leading accuracy for the model.

C. Vetrani et.al [1] 2022 proposed to assess the relationship between meal nutrients and postprandial blood glucose response (PGR) in individuals with type 1 diabetes on a hybrid closed-loop system (HCLS). This shows that nutritional factors other than the amount of carbohydrate significantly influence postprandial blood glucose control.

J Carrillo Morena et.al [3] 2021, R Sendra proposed a prediction of future glucose levels has shown to be fundamental in helping patients to plan and modify their treatment in real-time. This paper, a glucose predictor based on long short-term memory neural networks is designed.

Khodaei, Mohammed Javad et al. [4] 2020 A patient-driven project, the DIY artificial pancreas system (DIYAPS) has the potential to completely transform diabetic control, using open-source algorithms in conjunction with already-existing pumps and CGM to automate insulin delivery. Overall, research on the use of DIYAPS has shown improvements in time in range, HbA1c (glycated hemoglobin), decreased hypoglycemia, and enhanced quality of life.

Istvan Vassanyi et.al [5] 2020 proposed diabetes Mellitus outpatients would benefit from a lifestyle support tool that delivers reliable short term Blood Glucose Level (BGL) predictions. A new training method is proposed for a neural network in which an absorption model is applied that uses the nutrient contents of meals. The numerical characteristics of the computed absorption curve are fed to the neural network as training inputs along with the applied insulin doses and BGL evolution measured by a Continuous Glucose Monitoring System.

K.Li et.al [6] 2020 proposed for people with Type 1 diabetes (T1D), forecasting of blood glucose (BG) can be used to effectively avoid hyperglycemia, hypoglycemia and associated complications. In this introduce GluNet, a framework that leverages on a personalized deep neural network to predict the probabilistic distribution of short-term (30-60 minutes) future CGM

measurements for subjects with T1D based on their historical data including glucose measurements, meal information, insulin doses, and other factors.

E.A Pustozarov et.al [7] 2020 A blood glucose prediction model, which included detailed discussions on feature engineering and particular data pre-processing. This work creates a decision tree gradient boosting algorithm-based data-driven blood glucose model to forecast various postprandial glycemic response features. The program made use of information about meals and each patient's unique eating situation.

Ariya Saunders et.al [8] 2019 Proposed the Automated insulin delivery for people with type 1 diabetes. The MiniMed™ 670G artificial pancreas (AP) system is the first commercially available insulin pump that automates basal insulin delivery, while still requiring user input for insulin boluses.

Levente Kovacs et.al [9] 2019 Proposed automating the delivery of insulin to individuals diagnosed with type 1 diabetes. The first artificial pancreas (AP) system available for purchase is the MiniMed™ 670G. Accessible insulin pump that requires human input for insulin boluses but automates basal insulin delivery.

In 2019 A. Aliberti et al. [10] Continuous glucose monitoring systems (CGMSs) that are now being proposed enable diabetes patients' blood glucose levels to be measured. This study looks into the Prediction models are used to estimate future glucose-level values on a new patient after being trained on the glucose signals of a sizable patient cohort. This study compares two distinct solution types: long short-term memory (LSTM) networks and non-linear autoregressive (NAR) neural networks. Three methods from the literature—feed-forward neural networks (FNNs), autoregressive (AR) models, and recurrent neural networks (RNN)—were empirically compared to these answers. However, the NAR's prediction accuracy was only good for short-term forecasts. For both short- and long-term glucose-level inference, the LSTM demonstrated remarkably good performance.

Ali Idri et al. [11] 2019, Proposed Data-mining offers strong methods to extract knowledge from massive volumes of data, providing important information for decision making. The use of DM prediction approaches to diabetic self-management (DSM) is the topic of this research.

Jauher Ben Ali et.al [12] 2018 proposed Recent technology developments in diabetes management, such Continuous Glucose Monitoring (CGM) systems, offer trustworthy sources for blood glucose information. This paper suggests a novel approach for blood glucose level prediction in Type 1 Diabetes (T1D) that solely uses CGM data as inputs and is based on Artificial Neural Networks (ANN).

I Contreras et.al [13] 2018 proposed when paired with cutting-edge technology like mobile computing, medical devices, and sensor technologies, artificial intelligence techniques could make it possible to develop and provide improved chronic disease management services. Here, artificial intelligence approaches are used to help control diabetes and its related difficulties.

M.D.Van Der Walt et.al [14] 2017 proposed the 30-minute blood glucose level prediction utilizing clinical data from continuous glucose monitoring devices. This study looks at how a deep network may be built efficiently if domain expertise is used to infer the values of the component functions and the compositional structure of the goal function..

K. Tuksoy et.al [15] 2013 proposed early warning signs of hypoglycemia are crucial, and they should provide people ample time to take preventative measures. An improved substitute to capture glucose changes and forecast blood glucose concentrations in the future is the introduction of subject-specific recursive linear time series models. Recursive models' predictions of future glucose concentrations are used to construct the hypoglycemia alarm method. The modeling technique gives good glucose concentration prediction with comparatively modest error and allows models to dynamically adjust to inter- and intra-subject variation and glycemic disturbances..

III. METHODOLOGY

This study used a diabetes dataset. The data were collected from the laboratory of Medical City Hospital. Patients file were taken and data extracted from them and entered into database to construct the diabetes dataset. The data consists of medical information and laboratory analysis. The data was prepared by removing unwanted attributes, missing values and redundant records. The model was trained from training dataset and tested with test data. The prediction is done in the form of three classes. The study aimed to improve better day-to-day diabetes management.

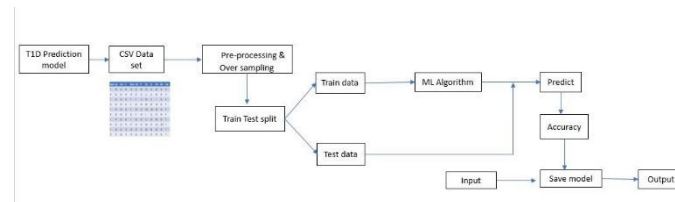


Fig. 1. Block Diagram

A. ALGORITHMS

- 1) *K-Nearest Neighbour*: The k-Nearest Neighbors (kNN) algorithm is a simple and widely used classification and regression technique. It belongs to the family of instance-based, lazy learning algorithms. The kNN algorithm is known for its simplicity and effectiveness, but it may not scale well to large datasets due to the need to calculate distances for each test point against all training points. Additionally, the choice of k and the distance metric can significantly impact the algorithm's performance. Cross-validation and tuning are often used to find suitable values for these parameters.
- 2) *Naive Bayes*: Naive Bayes is a probabilistic machine learning algorithm that is based on Bayes' theorem. It is particularly popular for classification problems, especially in text classification and spam filtering. Naive Bayes is a probabilistic machine learning algorithm that is based on Bayes' theorem. It is particularly popular for classification problems, especially in text classification and spam filtering.
- 3) *Decision Tree*: A decision tree is a flowchart-like tree structure where each internal node

represents a test on an attribute, each branch represents the outcome of the test, and each leaf node represents a class label (in the case of classification) or a numerical value (in the case of regression). Decision trees are interpretable and easy to understand, making them popular for tasks where interpretability is crucial. However, they are prone to overfitting, especially when the tree is deep. This problem can be addressed with the use of ensembles (like Random Forests) and pruning techniques. Using the random forest approach has several advantages, the primary one being that it requires less training time than other algorithms. It operates effectively even with a large dataset and predicts output with high accuracy.

- 4) *Random Forest*: This algorithm is used for the creation of our model since it provides maximum accuracy for the prediction which is of 99 percentage. Random Forest is an ensemble learning algorithm that operates by constructing a

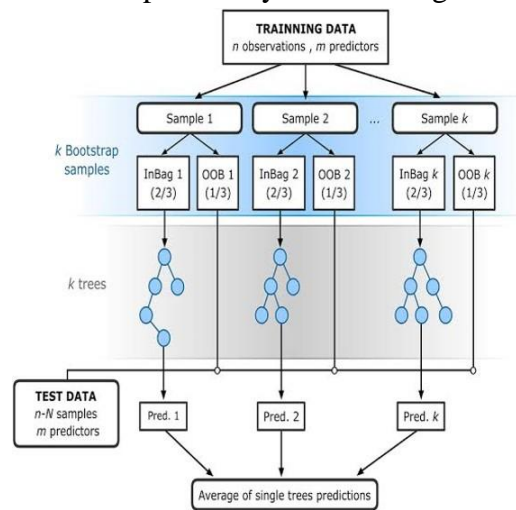


Fig. 2. Random forest

multitude of decision trees during training and outputting the mode of the classes (classification) or the mean prediction (regression) of the individual trees.

IV. RESULT AND DISCUSSION

We develop a prediction system by collecting the comprehensive data on insulin usage and physical activity. The data includes various parameters like Urea, Creatinine ratio, HbA1c, Cholesterol, Triglycerides, High density lipoprotein, Low density lipoprotein, very-low-density-lipoprotein, and Body mass index to predict blood glucose levels for individuals with Type-1 Diabetes and helps to manage their blood glucose levels. Clean the collected data to handle missing values, outliers, and inconsistencies. Normalize the data to ensure uniformity and prepare it for analysis. Here we aim to build accurate predictive model. The user friendly interface will empower individuals to input their dietary information and receive real time predictions. These model will not only forecast blood glucose levels but also provide personalized nutrition recommendation, fostering better day-to-day diabetes management. To determine the best prediction for each model, We train our model with four of the machine learning algorithms which are K- Nearest Neighbour, Naive Bayes, Random Forest and Decision Tree. Finally, we compare accuracy of each model. The algorithm that provide the maximum accuracy is selected for the prediction for blood

glucose level. Here we select Random Forest algorithm which provides the maximum accuracy of 99 percentage. We also have the K-nearest neighbour algorithm with the accuracy of 96 percentage along with Naive Bayes with 91 percentage and at last the Decision tree with 96 percentage. Train the selected machine learning models using the training dataset. Fine-tune hyper parameters to optimize model performance. We develop a user-friendly interface for T1D patients to input meal information and view blood glucose predictions. The interface should be accessible via web or mobile applications. Incorporate features for issuing alerts in case of critical blood glucose levels and providing personalized dietary recommendations. By analysing all the features our model predicts the blood glucose levels. Whether the patient is subjected to be diabetic, then they fall into the 'YES' class. If not they fall into 'NO' class and if the model finds any slight possibility to have type-1-Diabetes then they fall into the 'POSSIBLE' class. According to the result, the patient receives a report that provides them with personalized nutritional recommendation and creates a unique diabetic profile for each individual. In addition, it helps the patients to chart their food intake and dietary choices.

V. CONCLUSION

This research demonstrates that integrating nutritional data into machine learning models can enhance blood glucose predictions in Type 1 Diabetes. The study emphasizes the significance of considering dietary information in diabetes management, potentially leading to more personalized care and improved predictive accuracy. Future advancements in this field may involve integrating advanced machine learning algorithms, deep learning techniques, and big data analytics to further enhance prediction accuracy. Additionally, incorporating real-time data from wearable devices and telemedicine technologies could enable proactive monitoring and intervention. Collaboration between healthcare institutions, research organizations, technology companies, and regulatory bodies will be crucial for the development and implementation of these systems. It's essential to prioritize data security, consent mechanisms, transparency in algorithmic decision-making, and compliance with regulatory standards to ensure the ethical use of these technologies.

VI. ACKNOWLEDGEMENT

We would like to thank THE ALMIGHTY's mercy towards me over the years; it goes without saying that without them, We would not be where we are today. We would like to place on record, sincere thanks to all those who have contributed to the successful completion of this project. We recollect with gratitude the valuable guidance and the whole-hearted support of the project Coordinator Ms. Mini Lal (Asst Prof) and the Head of the department Dr. Sameera V M, BM Department for their valuable suggestions throughout the project work. We wish to express the deep sense of gratitude and the thanks to the Principal Dr. Jerline Sheeba Anni for the excellent facilities and continual support provided during the course study and project work. We thank all the staff members of Biomedical Engineering Department for their valuable suggestions. We also thank all beloved friends for their encouragement, timely help and suggestions.

REFERENCE

1. M. J. Khodaei, N. Candelino, A. Mehrvarz, and N. Jalili, "Physiological closed-loop control (PCLC) systems: Review of a modern frontier in automation," *IEEE Access*, vol. 8, pp. 23965–24005, 2020.
2. A. Saunders, L. H. Messer, and G. P. Forlenza, "Min- iMed 670G hybrid closed loop artificial pancreas system for the treatment of type 1 diabetes mellitus: Overview of its safety and efficacy," *Exp. Rev. Med. Devices*, vol. 16, no. 10, pp. 845–853, Oct. 2019.
3. L. Kovacs, G. Eigner, M. Siket, and L. Barkai, "Control of diabetes mellitus by advanced robust control solution," *IEEE Access*, vol. 7, pp. 125609–125622, 2019.
4. C. Toffanin, M. Messori, F. D. Palma, G. De Nicolao, C. Cobelli, and L. Magni, "Artificial pancreas: Model predictive control design from clinical experience," *J. Diabetes Sci. Technol.*, vol. 7, no. 6, pp. 1470–1483, Nov. 2013.
5. A. Aliberti, I. Pupillo, S. Terna, E. Macii, S. Di Cataldo, E. Patti, and A. Acquaviva, "A multi-patient data- driven approach to blood glucose prediction," *IEEE Access*, vol. 7, pp. 69311–69325, 2019.
6. K. J. Bell, C. E. Smart, G. M. Steil, J. C. Brand- Miller, B. King, and H. A. Wolpert, "Impact of fat, protein, and glycemic index on postprandial glucose control in type 1 diabetes: Implications for intensive diabetes management in the continuous glucose monitoring era," *Diabetes Care*, vol. 38, no. 6, pp. 1008–1015, Jun. 2015.
7. R. A. H. Karim, I. Vassányi, and I. Kósa, "After-meal blood glucose level prediction using an absorption model for neural network training," *Comput. Biol. Med.*, vol. 125, Oct. 2020, Art. no. 103956.
8. A. Apicella, P. Arpaia, E. De Benedetto, N. Donato,
9. L. Duraccio, S. Giugliano, and R. Prevete, "Enhancement of SSVEPs classification in BCI-based wearable instrumentation through machine learning techniques," *IEEE Sensors J.*, vol. 22, no. 9, pp. 9087–9094, May 2022.
10. J. B. Ali, T. Hamdi, N. Fnaiech, V. Di Costanzo, F. Fnaiech, and J.-M. Ginoux, "Continuous blood glucose level prediction of type 1 diabetes based on artificial neural network," *Biocybern. Biomed. Eng.*, vol. 38, no. 4, pp. 828–840, 2018.
11. T. E. Idrissi, A. Idri, and Z. Bakkoury, "Systematic map and review of predictive techniques in diabetes self- management," *Int. J. Inf. Manag.*, vol. 46, pp. 263–277, Jun. 2019.
12. J. Carrillo-Moreno, C. Pérez-Gandía, R. Sendra- Arranz, G. García-Sáez, M. E. Hernando, and Á. Gutiérrez, "Long short-term memory neural network for glucose prediction," *Neural Comput. Appl.*, vol. 33, no. 9, pp. 4191–4203, May 2021.
13. I. Contreras and J. Vehi, "Artificial intelligence for diabetes management and decision support: Literature review," *Med. Internet Res.*, vol. 20, no. 5, May 2018, Art. no. e10775.
14. K. Li, C. Liu, T. Zhu, P. Herrero, and P. Georgiou, "GluNet: A deep learning framework for accurate glucose forecasting," *IEEE J. Biomed. Health Informat.*, vol. 24, no. 2, pp. 414–423, Feb. 2020.

15. C. Vetrani, I. Calabrese, L. Cavagnuolo, D. Pacella, D. Napolano, S. Di Rienzo, G. Riccardi, A. A. Rivellese, G. Annuzzi, and L. Bozzetto, "Dietary determinants of postprandial blood glucose control in adults with type 1 diabetes on a hybrid closed-loop system," *Diabetologia*, vol. 65, no. 1, pp. 79–87, Jan. 2022.
16. E. I. Georga, V. C. Protopappas, D. Ardigo, M. Marina, Zavaroni, D. Polyzos, and D. I. Fotiadis, "Multivariate prediction of subcutaneous glucose concentration in type 1 diabetes patients based on support vector regression," *IEEE J. Biomed. Health Informat.*, vol. 17, no. 1, pp. 71–81, Jan. 2013.
17. H. N. Mhaskar, S. V. Pereverzyev, and M. D. Van Der Walt, "A deep learning approach to diabetic blood glucose prediction," *Frontiers Appl. Math. Statist.*, vol. 3, p. 14, Jul. 2017.
18. M. Verleysen and D. Francois, "The curse of dimensionality in data mining and time series prediction," in *Proc. Int. Work-Confer. Artif. Neural Netw. Cham, Switzerland: Springer*, 2005, pp. 758–770.
19. K. Turksoy, E. S. Bayrak, L. Quinn, E. Littlejohn, Rollins, and A. Cinar, "Hypoglycemia early alarm systems based on multivariable models," *Ind. Eng. Chem. Res.*, vol. 52, no. 35, pp. 12329–12336, Sep. 2013.
20. T. Zhu, L. Kuang, J. Daniels, P. Herrero, K. Li, and P. Georgiou, "IoMT-enabled real-time blood glucose prediction with deep learning and edge computing," *IEEE Internet Things J.*, early access, Jul. 14, 2022, doi:10.1109/JIOT.2022.3143375.
21. A. Apicella, P. Arpaia, M. Frosolone, G. Improta, N. Moccaldi, and A. Pollastro, "EEG-based measurement system for monitoring student engagement in learning 4.0," *Sci. Rep.*, vol. 12, no. 1, pp. 1–13, Apr. 2022.
22. A. Apicella, S. Giugliano, F. Isgro, and R. Prevete, "Exploiting auto encoders and segmentation methods for middle-level explanations of image classification systems," *Knowl.-Based Syst.*, vol. 255, Nov. 2022, Art. no. 109725.
23. A. Apicella, F. Isgro, A. Pollastro, and R. Prevete, "Toward the application of XAI methods in EEG-based systems," 2022, arXiv:2210.06554.
24. M. Parillo, G. Annuzzi, A. A. Rivellese, L. Bozzetto,
25. R. Alessandrini, G. Riccardi, and B. Capaldo, "Effects of meals with different glycaemic index on postprandial blood glucose response in patients with type 1 diabetes treated with continuous subcutaneous insulin infusion," *Diabetic Med.*, vol. 28, no. 2, pp. 227–229, Feb. 2011.
26. E. A. Pustozarov, A. S. Tkachuk, E. A. Vasukova, A. D. Anopova, M. A. Kokina, I. V. Gorelova, T. M. Pervunina, E.
27. N. Grineva, and P. V. Popova, "Machine learning approach for postprandial blood glucose prediction in gestational diabetes mellitus," *IEEE Access*, vol. 8, pp. 219308–219321, 2020.
28. S. E. Berry, A. M. Valdes, D. A. Drew, F. Asnicar, M. Mazidi, J. Wolf, J. Capdevila, G. Hadjigeorgiou, R. Davies, H. Al Khatib, and C. Bonnett, "Human postprandial responses to food and potential for precision nutrition," *Nature Med.*, vol. 26, no. 6, pp. 964–973, Jun. 2020.

COVID-19 INFECTED LUNG IMAGE CLASSIFICATION USING INCEPTION-Res Net

Zahda Raheem

Dept. of Biomedical Engineering
KMCT CEW Kozhikode, India
zahdarhm@gmail.com

Sreeja S

Dept. of Biomedical Engineering
KMCT CEW Kozhikode, India
sreejasudhan2002@gmail.com

Sharika E

Dept. of Biomedical Engineering
KMCT CEW Kozhikode, India
sharika15082001@gmail.com

Maneesha

Dept. of Biomedical Engineering
KMCT CEW Kozhikode, India
maneeshakumar2003@gmail.com

Dr. Sameera V Mohd Sagheer

Dept. of Biomedical Engineering
KMCT CEW Kozhikode, India
hodbm@kmctcew

Abstract—This paper focuses on the use of Inception-ResNet V2 for the automated classification of X-ray images to aid in the early diagnosis of COVID-19. Its aim is to eliminate human error in the diagnosis process by utilizing the Inception-ResNet V2 model, which helps identify the true severity of the condition. The model has been trained using X-ray images obtained from online resources, allowing for timely treatment of the illness and the identification of issues caused by COVID-19. Adoption of this approach has significant potential to improve the efficiency and accuracy of X-ray diagnosis of COVID-19. The accuracy of the network is calculated and then tested. This is done to eliminate errors in diagnostic interpretations.

I. INTRODUCTION

The SARS-CoV-2 virus, which caused COVID-19, caused over 6 million deaths globally and prompted the World Health Organization to declare it a Public Health Emergency of International Importance (PHEIC). [1]. Early diagnosis and effective treatment are critical in reducing the virus's incidence and mortality. Active infection in COVID-19 can be detected using RT-PCR as the gold standard. While CT scans and X-ray examinations are not primary diagnostic tools for COVID-19, they play a vital role in determining lung involvement and treating severe cases. Automated tools for classifying X-ray images can support the efficiency and precision of such assessments, aiding in the monitoring of disease progression and management of the affected patients.

A. Convolution Neural Network

As of right now, Convolutional Neural Networks (CNN) is the most popular machine learning technique and deep artificial neural networks with good capabilities for feature extraction and detection. One of its most important features is weight sharing, which greatly reduces the number of weights and the complexity of the network model. By utilizing pooling layers, nonlinear activation functions, and many convolution filters, Convolutional Neural Networks (CNNs) minimize the loss function. Every part of a convolutional neural network simulates the activity

of biological neurons, and each parthas several inputs, represented by the letters $x_1, x_2, x_3, \dots, x_n$, or the so-called characteristic matrix. Convolutional and pooling layers (also known as pooling layers) are typically found at the conclusion of a CNN network structure, followed by one or more fully-connected layers. After the convolution is finished, a non-linear excitation function (in a neural network this excitation function is usually Rectifier activation function) must be applied to the result to get the final result of the layer.

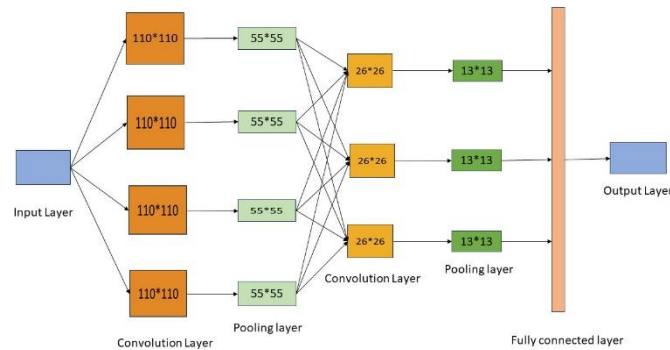


Fig. 1. CNN Model

II. LITERATURE SURVEY

Residual learning framework is used to reformulate layers to learn residual functions, making these networks easier to optimize and improving their accuracy as training deeper neural networks is a more challenging task [2]. A residual learning approach can address the degradation problem, which occurs when deeper networks start converging with higher training error [3]. An identity map for signal propagation in deep residual networks, improving training and generalization. 1001-layer

ResNet and 200-layered Resnet were more effective in CIFAR-10 and ImageNet respectively. [4]. TensorFlow platform was utilized to train and test a CNN model with two convolutional layers using data from the MNIST dataset. This model can be used to extract features and make classification decisions. [5]. The application of transfer learning techniques, integration modeling with deep neural networks, and integrated models with COVID-19 technology is a practical and economical approach to diagnose the disease effectively. [6].

COVID-GATNet, a neural network model, is utilized to diagnose COVID-19 through chest X-rays. The model uses augmented data from three datasets and combines DenseNet and GAT, improving classification performance. The accuracy of the model was 94.1% [7]. ULNet model uses augmented data from three datasets and is based on U-net with added features and achieved an accuracy of 94.1% [8]. Co-ResNet neural network model achieved an accuracy of 94.1% [9]. Image regrouping and ResNet-SVM showed an accuracy of 93% [10]. enhanced Inception-ResNetV2, model for diagnosis of COVID-19 based on chest X-rays. The model uses augmented

data from three datasets and is based on Inception- ResNetV2 with additional features. The accuracy of the model was 94.1% [11].

Lung tissue images are classified using SegNet and U-Net deep learning networks. SegNet with an accuracy of 0.95 in bi-nary classification outperforms U-Net with an accuracy of 0.91 in multiclass classification and U-Net performs better in multi-class classification with an accuracy of 0.91. [12]. ResNet-101 and pretrained U-Net for lung segmentation in large x-ray images generated a heat-map to highlight COVID-19 signals [13]. Using Convolutional Neural Networks can provide a quick and accurate method for diagnosing the disease [14] [15]. Prediction vectors are generated using a guided depth network with simple distance scaling (MAG-SD) and attention from multiscale feature maps for COVID-19 diagnosis and demonstrated high efficiency for COVID-19 classification and segmentation. [16] The DenseNet169 model uses the ANOVA (analysis of variance) feature selection method and can be used for the diagnosis of COVID-19 by CXR [17]. AI has been found to have an efficient application in healthcare and researchers are encouraged to develop an AI algorithm to help identify and isolate people with Coronavirus symptoms [18]. Multiscale residual U-Net, The automatic segmentation algorithm for lung nodules is designed to accurately segment lung nodules with complex geometric structures [19]. Automated lung disease detection system to address COVID-19 will help reduce diagnostic time for radiologists [20].

Improved results can be achieved by utilizing multi-class segmentation, which eliminates any missing tag data [21]. AdaD-FNN is what transfers the learned knowledge from one FNN estimator to the next in a sequential manner, while also adjusting Weighted training set model with decreasing learning rate. The F-U2MNet-C image processing model has been improved, which analyzes image features using fuzzy stacking and removes unwanted elements using U2MNet segmentation [22]. AAF-U-Net, the lung segment classification system, is effective in categorizing and classifying COVID-

19. Moreover, it has good classification capabilities [23]. The image extraction framework and visual inversion approach can provide the most accurate classification of chest X-ray images for cancers using the global quadratic clustering and clustering methods [24]. According to experimental findings, Inception- Resnet performs better in assessment indicators than other image classification techniques, and the technique possesses more resilience, precision, and intuitiveness [25]

III. INCEPTION-RESNET V2

A. Inception-ResNet V2 for Feature Extraction in Medical Images

In recent years, the emergence of deep learning has had a significant impact on medical image analysis, especially for disease diagnosis and classification. The COVID-19 pandemic has demonstrated the need for accurate and effective diagnostic tools and spurred research into advanced technologies such as the Inception-ResNet V2 architecture for lung shape classification. Inception-ResNet V2, a hybrid neural network that combines elements of the Inception and

ResNet architectures, has achieved success in a variety of computer vision tasks due to its ability to capture complex situations at many scales.

This section of the conference document describes how to apply Inception-ResNet V2 to classify images from COVID-19 patients. The network's unique architecture, which incorporates residual connections and parallel feature extraction modules, is used in this way to improve the accuracy and robustness of the classification model. The intricate nature of lung abnormalities associated with COVID-19 necessitates a comprehensive analysis of image features, and Inception-ResNet V2 model's sophisticated design proves instrumental in capturing both local and global patterns crucial for accurate classification.

The experimental results, presented in subsequent sections, showcase the efficacy of Inception-ResNet v2 in distinguishing COVID-19 infected lung images from non-infected counterparts. The introduction of this advanced neural network architecture offers the potential to contribute to ongoing efforts to combat the global pandemic by improving diagnostic accuracy and accelerating the identification of COVID-19 cases through automated image analysis.

IV. METHODOLOGY

A. Dataset

The images used for this purpose are X-rays. The image dataset was obtained from the COVID-19 radiography database, the chest radiography database, and the COVID-19 lung mask database... These images were taken from Kaggle which is a platform for data science and machine learning competitions, as well as a community of data scientists and machine learning practitioners. It provides a platform for users to find and share datasets.

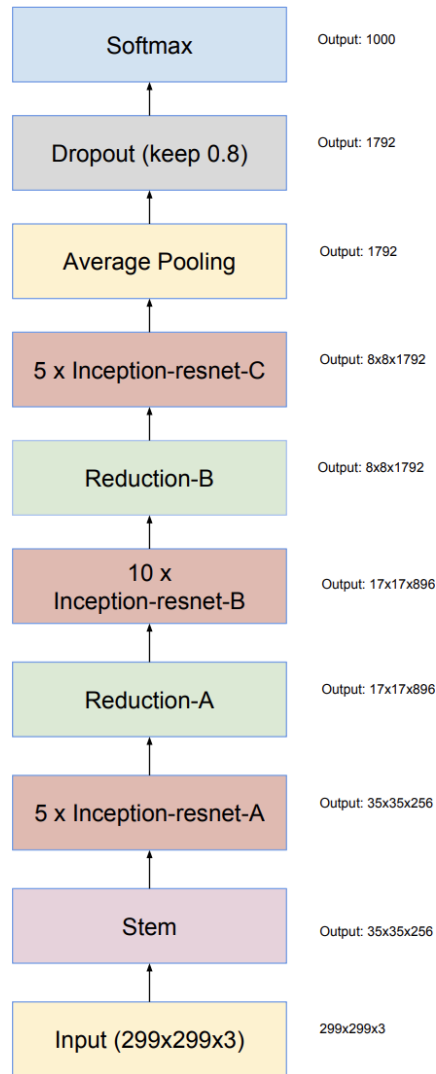


Fig. 2. Structure of Inception-ResNet

B. Feature Extraction

Feature Extraction is performed on lung pictures used to identify COVID-19 to capture relevant information that can aid in distinguishing between normal and COVID-19 affected cases. Inception-ResNet v2 Convolutional Neural Network (CNN) is used as the core network to capture the main and additional features of the pre-processed chest X-ray images. The Inception module, the core component of the Inception-ResNet V2 model, consists of parallel convolutional layers with different sized kernels. This architecture allows the network to capture features from different scales, improving its characteristic separation capabilities. Inception-ResNet V2 incorporates residual connections, which connect input features to corresponding output features. These connections help alleviate the vanishing gradient problem and enable deeper network architectures. The Inception-ResNet V2 networks are a type of convolutional neural network (CNN) that uses residual connections. Residual connections allow the network to learn more complex

features by passing information directly from previous layers to subsequent layers. This makes the system more efficient and less prone to overfitting.

Inception-ResNet V2 networks have been shown to achieve superior performance in several image classification tasks, including the ImageNet Large Scale Visual Recognition Challenge (ILSVRC). Below is a more in-depth explanation of the various elements of Inception-ResNet V2 networks. The stem is the first layer of the web. It consists of a convolution layer and a joining layer. Inception-ResNet blocks are the basic building blocks of Inception-ResNet V2 networks. The convolution layers, converging layers and residual connections are present in every block. In feature maps, the spatial dimensions are reduced using reduction blocks. This is done using a combination of convolutional layers, pooling layers and residual joins.

Spatial sizes are reduced on destination maps with reduction blocks. Convolutional layers, pooling layers and residual joins are employed to achieve this. How does it work. A drop layer is used to prevent the network from being overlaid. Softmax layer is used to calculate the probability distribution between different classes.

C. Architecture and Model Training

The algorithm is built on the Inception-ResNet V2 model. Preprocessing such as rotation, zooming and flipping were applied on the images. Preprocessing helps the model learn from a more diversified dataset, making it robust against different orientations and scales of images. The Inception-ResNet V2, which has been trained in advance using the ImageNet dataset, extracts features necessary for classification into normal or infected lungs. Following the initial base model which is the Inception-ResNet V2, A global averaging layer is included to reduce output space size. After that, fully connected layers are added in order to classify the data. The last level employs the Softmax activation function to generate output probabilities.

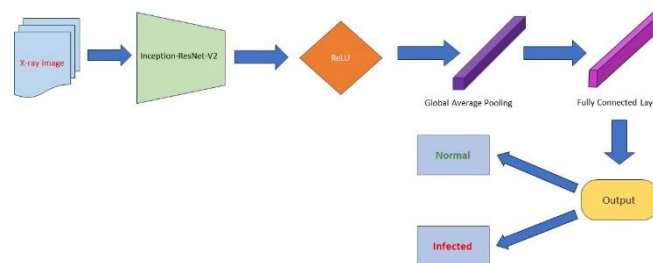


Fig. 3. Architecture

The model is compiled with an optimizer (such as Adam), a loss function (categorical cross-entropy, suitable for multi-class classification), and metrics (like accuracy) to evaluate the model. Images from the training catalog are utilized to train the model. Validation is also performed using a separate set of images to monitor the model's performance on unseen data. This training allows the model to adjust its weights based on the errors it makes, effectively learning from the training data.

V. RESULT & DISCUSSION

The model was trained with the accuracy increasing and the loss value decreasing over time suggesting that the model was effectively learning from the training data. Further, the continuous decrease in loss indicates that the model was effectively learning patterns from the training data. The increase in accuracy indicates improving reliability. The Inception-ResNet V2 model achieved an accuracy of 93.78%. There is an inconsistency in validation accuracy indicating an overfitting issue. Strategies such as introducing dropout layers or regularization techniques could be explored to mitigate overfitting and enhance model performance on validation data.

REFERENCES

- [1] Susanna Felsenstein, Jenny A Herbert, Paul S McNamara, and Christian M Hedrich. Covid-19: Immunology and treatment options. *Clinical immunology*, 215:108448, 2020.
- [2] Kaiming He, Xiangyu Zhang, Shaoqing Ren, and Jian Sun. Identity mappings in deep residual networks. In *Computer Vision—ECCV 2016: 14th European Conference, Amsterdam, The Netherlands, October 11–14, 2016, Proceedings, Part IV 14*, pages 630–645. Springer, 2016.
- [3] Kaiming He, Xiangyu Zhang, Shaoqing Ren, and Jian Sun. Deep residual learning for image recognition. In *Proceedings of the IEEE conference on computer vision and pattern recognition*, pages 770–778, 2016.
- [4] Liang Yu, Binbin Li, and Bin Jiao. Research and implementation of cnn based on tensorflow. In *IOP Conference Series: Materials Science and Engineering*, volume 490, page 042022. IOP Publishing, 2019.
- [5] Ningwei Wang, Hongzhe Liu, and Cheng Xu. Deep learning for the detection of covid-19 using transfer learning and model integration. In *2020 IEEE 10th international conference on electronics information and emergency communication (ICEIEC)*, pages 281–284. IEEE, 2020.
- [6] Feng He, Yu Deng, and Weina Li. Coronavirus disease 2019: What we know? *Journal of medical virology*, 92(7):719–725, 2020.
- [7] Junfeng Li, Dehai Zhang, Qing Liu, Rongjing Bu, and Qi Wei. Covid-gatnet: A deep learning framework for screening of covid-19 from chest x-ray images. In *2020 IEEE 6th International Conference on Computer and Communications (ICCC)*, pages 1897–1902. IEEE, 2020.
- [8] Tianbo Wu, Chen Tang, Min Xu, Nian Hong, and Zhenkun Lei. Ulnet for the detection of coronavirus (covid-19) from chest x-ray images. *Computers in Biology and Medicine*, 137:104834, 2021.
- [9] Subrato Bharati, Prajoy Podder, M Mondal, and VB Prasath. Co-resnet: Optimized resnet model for covid-19 diagnosis from x-ray images. *International Journal of Hybrid Intelligent Systems*, 17(1-2):71–85, 2021.
- [10] Changjian Zhou, Jia Song, Sihan Zhou, Zhiyao Zhang, and Jinge Xing. Covid-19 detection based on image regrouping and resnet-svm using chest x-ray images. *Ieee Access*, 9:81902–81912, 2021.
- [11] Madallah Alruwaili, Abdulaziz Shehab, and Sameh Abd El-Ghany. Covid-19 diagnosis using an enhanced inception-resnetv2 deep learning model in cxr images. *Journal of Healthcare*

Engineering, 2021:1–16, 2021.

- [12] Adnan Saood and Iyad Hatem. Covid-19 lung ct image segmentation using deep learning methods: U-net versus segnet. *BMC Medical Imaging*, 21(1):1–10, 2021.
- [13] Worapan Kusakunniran, Sarattha Karnjanapreechakorn, Thanongchai Siriapisith, Punyanuch Borwarnginn, Krittanat Sutassananon, Trong-tum Tongdee, and Pairash Saiviroonporn. Covid-19 detection and heatmap generation in chest x-ray images. *Journal of Medical Imaging*, 8(S1):014001–014001, 2021.
- [14] Maad M Mijwil and Ehsan Ali Al-Zubaidi. Medical image classification for coronavirus disease (covid-19) using convolutional neural networks. *Iraqi Journal of Science*, 62(8):2740–2747, 2021.
- [15] Yu-Huan Wu, Shang-Hua Gao, Jie Mei, Jun Xu, Deng-Ping Fan, Rong-Guo Zhang, and Ming-Ming Cheng. Jcs: An explainable covid- 19 diagnosis system by joint classification and segmentation. *IEEE Transactions on Image Processing*, 30:3113–3126, 2021.
- [16] Jingxiong Li, Yaqi Wang, Shuai Wang, Jun Wang, Jun Liu, Qun Jin, and Lingling Sun. Multiscale attention guided network for covid-19 diagnosis using chest x-ray images. *IEEE Journal of Biomedical and Health Informatics*, 25(5):1336–1346, 2021.
- [17] Hamid Nasiri, Seyed Ali Alavi, et al. A novel framework based on deep learning and anova feature selection method for diagnosis of covid-19 cases from chest x-ray images. *Computational intelligence and neuroscience*, 2022, 2022.
- [18] Yassir Edrees Almalki, Abdul Qayyum, Muhammad Irfan, Noman Haider, Adam Glowacz, Fahad Mohammed Alshehri, Sharifa K Al-duraibi, Khalaf Alshamrani, Mohammad Abd Alkhalik Basha, Alaa Alduraibi, et al. A novel method for covid-19 diagnosis using artificial intelligence in chest x-ray images. In *Healthcare*, volume 9, page 522. MDPI, 2021.
- [19] Jianshe Shi, Yuguang Ye, Daxin Zhu, Lianta Su, Yifeng Huang, and Jian-long Huang. Comparative analysis of pulmonary nodules segmentation using multiscale residual u-net and fuzzy c-means clustering. *Computer Methods and Programs in Biomedicine*, 209:106332, 2021.
- [20] Wessam M Salama and Moustafa H Aly. Framework for covid-19 segmentation and classification based on deep learning of computed tomography lung images. *Journal of Electronic Science and Technology*, 20(3):100161, 2022.
- [21] O Elharrouss, N Subramanian, and S Al-Maadeed. An encoder-decoder-based method for segmentation of covid-19 lung infection in ct images. *sn comput sci* 3 (1): 13, 2022.
- [22] Xujing Yao, Ziquan Zhu, Cheng Kang, Shui-Hua Wang, Juan Manuel Gorriz, and Yu-Dong Zhang. Adad-fnn for chest ct-based covid-19 diagnosis. *IEEE Transactions on Emerging Topics in Computational Intelligence*, 7(1):5–14, 2022.
- [23] Anupam Das. Adaptive unet-based lung segmentation and ensemble learning with cnn-based deep features for automated covid-19 diagnosis. *Multimedia Tools and Applications*, 81(4):5407–5441, 2022.
- [24] Chiagoziem C Ukwuoma, Zhiguang Qin, Md Belal Bin Heyat, Faijan Akhtar, Abla Smahi, Jehoiada K Jackson, Syed Furqan Qadri, Abdul-lah Y Muaad, Happy N Monday, and Grace

U Nneji. Automated lung-related pneumonia and covid-19 detection based on novel feature extraction framework and vision transformer approaches using chest x- ray images. *Bioengineering*, 9(11):709, 2022.

- [25] Yunfeng Chen, Yalan Lin, Xiaodie Xu, Jinzhen Ding, Chuzhao Li, Yim-ing Zeng, Weili Liu, Weifang Xie, and Jianlong Huang. Classification of lungs infected covid-19 images based on inception-resnet. *Computer methods and programs in biomedicine*, 225:107053, 2022.

Mindmapper: Predicting Alzheimer's with Magnetic Resonance Imaging

Fathima Fidha MT

Dept. of Biomedical Engineering
KMCT CEW Kozhikode, India
fidhamt@gmail.com

Fitha Firose

Dept. of Biomedical Engineering
KMCT CEW Kozhikode, India
fithafirose09@gmail.com

Devika Sreekumar

Dept. of Biomedical Engineering
KMCT CEW Kozhikode, India
devikasreekumar66@gmail.co

Fathimathu Riyada

Dept. of Biomedical Engineering
KMCT CEW Kozhikode, India
riyadafathimathu@gmail.com

Ms Anusha EP

Dept. of Biomedical Engineering
KMCT CEW Kozhikode, India
anushachandran08@gmail.com

Abstract—Alzheimer's, a progressive ailment impacting memory and overall brain function, lacks a definitive diagnostic test. Relying solely on brain scans is insufficient for conclusive identification. Presently, physicians assess Alzheimer's based on reports from the patient's relatives, social behaviour, and past medical records. Integrating Artificial Intelligence (AI) and Machine Learning (ML) algorithms could enhance this diagnostic approach. Big processing, harnessing data from diverse sources amidst evolving scenarios, offers a comprehensive perspective. This proposed solution involves a big processing model from a data mining standpoint. Employing various ML classifiers, the paper focuses on training Alzheimer's detection models, treating attributes as a complex system. Notably, the Support Vector Machine (SVM) with a linear kernel model demonstrated superior accuracy compare.

Index Terms—Machine learning, deep learning, artificial intelligence, moderate demented, non-demented, mild demented and very-mild demented, convolutional neural networks, dementia.

I. INTRODUCTION

Alzheimer's Disease (AD) is a progressive neurological condition affecting around 5.1 million people in the United States, with no definitive treatment. Early detection is crucial for effective management, but the process is challenging and costly. Automated systems, particularly using deep learning methods, have shown superior accuracy in diagnosing AD compared to human assessments. These systems analyze various data sources, including MRI scans, biomarkers, and numerical data, significantly reducing time and costs.

In the early stages of AD, individuals may function independently, but subtle signs like memory issues become apparent. As the disease progresses, symptoms worsen, requiring 24/7 assistance.

Deep learning models, especially convolutional neural networks (CNN), are employed to analyze MRI brain data, offering high-resolution localizations for accurate diagnosis.

Diagnosing AD in its early stages is crucial, as late treatment can lead to irreversible brain damage. Modern imaging technologies, such as MRI and PET scans, play a vital role in early detection, even before symptoms appear. Machine learning techniques, particularly deep learning, have revolutionized the field, providing high-performance models for accurate diagnosis.

Researchers are exploring various machine learning algorithms, including random forest, logistic regression, and support vector machines, for multi-classifier architectures in AD diagnosis. Deep neural networks, such as CNNs, can identify intricate changes in brain structure and analyze disease progression with large datasets.

The proposed end-to-end framework in this paper utilizes CNNs for detailed AD classification based on scanned MRI images. The goal is to enhance prediction accuracy by combining deep learning algorithms and feature engineering. This project aims to develop a prediction model using diverse clinical data to identify patients at high risk of developing Alzheimer's, enabling early intervention and improved management.

II. LITERATURE SURVEY

Jessen et.al [1] 2014 Deep learning excels in Alzheimer's detection, surpassing traditional methods in handling complex neuroimaging data. A review of studies from 2013 to 2018 revealed accuracies up to 98.8% for AD classification, with stacked auto-encoder (SAE) and multimodal approaches yielding promising results. Ongoing advancements in deep learning, incorporating diverse data types, showcase its evolving potential for accurate diagnostic classification in Alzheimer's research.

Yongliang et al [2] 2018 The paper introduces a device-free localization method for sensor networks using artificial neural networks, enabling accurate location predictions when individuals enter the area, eliminating the need for devices. Lee Kuok Leong et al [3] 2019 Alzheimer's disease (AD) is a common incurable neurodegenerative condition associated with memory loss. A study proposes a machine learning approach, using the Random Forest Grid Search Cross Validation model, achieving 94.39% accuracy in early AD detection. Their Graphical User Interface (GUI) tool is evaluated on a dataset, showing promising results aligned with dementia status.

Martinez-Murcia FJ et.al [4] 2019 The study uses deep convolutional autoencoders to analyze Alzheimer's disease data, linking cognitive symptoms to neurodegeneration. It achieves over 80% classification accuracy, estimating the influence of each coordinate over the brain.

Heger K et.al [5] 2020 This study uses a systematic literature review and Delphi consensus to identify modifiable risk factors for dementia, analyzing observational studies and international experts' rankings for dementia prevention.

Al-Shoukry et.al [6] 2020 Accurate early diagnosis of Alzheimer's is crucial for timely treatment, and Deep Learning (DL) emerges as a key tool, enabling researchers to diagnose the

disease before irreversible brain damage occurs. Recent studies highlight DL's potential for enhancing predictive capabilities in identifying Alzheimer's at its early stages.

Sivakani GA et.al [7] 2020 Alzheimer's, a form of dementia, is a global concern affecting individuals as young as middle age. Researchers are shifting focus from drug discovery to early-stage prediction, emphasizing feature extraction in large datasets. This paper employs machine learning for feature extraction, selection, and classification on the oasis longitudinal dataset.

Neelaveni et.al [8] 2020 Alzheimer's, a neurodegenerative disorder, starts with benign symptoms that worsen over time. As there's no cure, early prediction is crucial for slowing progression. This study employs machine learning algorithms, utilizing psychological parameters like age, visits, MMSE, and education to predict Alzheimer's disease, aiming to enhance early diagnosis and intervention.

Bari Antor et.al [9] 2021 Alzheimer's, affecting around 45 million people, is a degenerative brain disease primarily linked to Dementia. To combat this, a machine learning system was developed using the OASIS dataset, analyzing its small yet valuable data with models like SVM, logistic regression, decision tree, and random forest. Results indicate that fine-tuned support vector machine outperforms, offering a simple yet effective means to detect Dementia.

Naif K. Al-Shammari et.al [10] 2021 A cardiac stroke results from a blocked heart blood vessel, often due to plaque buildup. Symptoms include pressure, nausea, and fatigue. Deep Neural Networks aid in predicting strokes by enhancing accuracy in processing medical information.

Tanuja Kothakota et.al [11] 2021 Epilepsy seizures happen due to messed-up electrical activity in brain cells, making them hard to predict. This study proposes a new method to detect seizures using brain scans. The method involves training a special algorithm on normal and seizure brain activity. Tested on real patient data, the algorithm was able to identify seizures with 97.32% accuracy.

Bai et.al [12] 2021 Alzheimer's, a challenging neurodegenerative disease, is extensively researched using data from various sources like MRI and PET scans, genetics, and biomarkers. A multi-task learning algorithm is applied to predict cognitive scores in the next 3 years, aiding in assessing future cognitive trends. The study also employs machine learning for classifying cognitive stages and proposes a scalable technical architecture for managing and sharing Alzheimer's data.

Khan P et.al [13] 2021 This study explores machine learning and deep learning techniques for detecting four brain diseases: Alzheimer's, brain tumor, epilepsy, and Parkinson's, aiming to improve future detection methods and datasets

Prajapati R et.al [14] 2021 This paper presents a deep neural network designed for binary classification in medical research. The model uses three activation functions for hidden layers and undergoes k-folds validation. The model is tested on Alzheimer's Disease and Cognitively Normal groups. The proposed DNN achieved high accuracy scores, outperforming traditional machine learning algorithms, with 85.19%, 76.93%, and 72.73% accuracy respectively.

Sathiyamoorthi et al [15] 2021 Alzheimer's disease involves protein deposits called biomarkers, crucial for diagnosis accuracy. A proposed technique uses brain MRI data, employs neural networking for attribute mapping, and integrates fuzzy logic for reliable decision-making. The method demonstrates high performance, with an 89.27% sensitivity and 93.91% accuracy in Alzheimer's disease evaluation and diagnosis.

Gadekallu et al [16] 2021 This study employs a 50-layer Residual network to identify obesity or malnutrition and estimate body mass index (BMI) based on face picture analysis. It focuses on gender-based BMI prediction and uses Multi-task Cascaded Convolutional Neural Networks for face detection. The system emails the relevant health officer the person's photo and health information so they can do additional evaluation.

Helaly HA et.al [17] 2022 This study develops an end-to-end framework for early detection and medical image classification of Alzheimer's disease using convolutional neural networks. The web application helps doctors and patients remotely check and advise on their AD stage.

Kavitha et al [18] 2022 This approach has the potential to significantly improve healthcare. Early and accurate diagnosis of Alzheimer's disease is crucial for managing the disease and making treatment decisions that can slow its progression. Machine learning techniques like Decision Tree and Support Vector Machine have shown promise in this area, with studies achieving an 83% accuracy rate in predicting Alzheimer's. This could be a valuable tool for early diagnosis and potentially reduce mortality rates.

K Thanuja et al [19] 2023 The paper presents a feature optimization and classification technique for epileptic seizure, a critical medical emergency. The technique uses dynamic feature set extraction, categorization labels, and grey-wolf optimization to identify feature-attribute relationships.

M Sudharsan et al [20] 2023 Alzheimer's disease damages brain cells, affecting memory and behavior. Early diagnosis is key, but challenges exist. This study explores a new method for early detection using machine learning.

III. METHODOLOGY

The study used a longitudinal Alzheimer's disease dataset, utilizing MRI data. The data was analyzed using machine learning techniques to predict Alzheimer's disease at an early stage. They cleaned the data and trained a model on one part, then tested it on unseen data. To make sure the results were reliable, they split the data into multiple sections and repeated the test. This approach aimed to improve the accuracy of predicting Alzheimer's with machine learning.

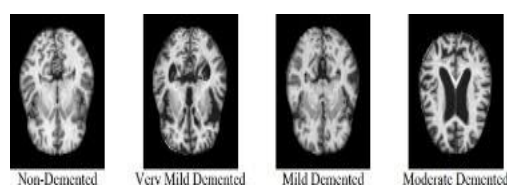


Fig. 1. Classes Of MRI

A. Convolutional Neural Network

A convolutional neural network (CNN) is a subset of machine learning used for image recognition and processing pixel data. It is particularly suitable for computer vision tasks and object recognition applications like self-driving cars and facial recognition. CNNs are a core element of deep learning algorithms, with recurrent neural networks (RNNs) being suitable for natural language processing, speech recognition, and image captioning. CNNs can uncover key information in both time series and image data, making them valuable for image-related tasks like image recognition, object classification, and pattern recognition. They also classify audio and signal data. The results help patients understand their Alzheimer's disease

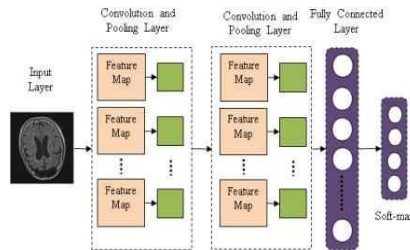
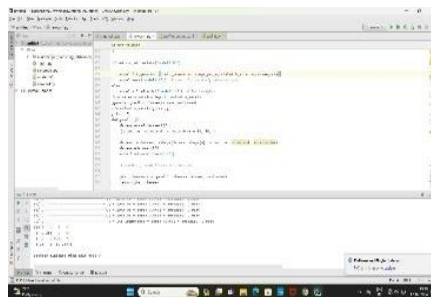


Fig. 2. CNN Model

stage, which is crucial for doctors to better understand the disease's impact. The research uses various environments, tools, and libraries for experiments and analysis.

IV. RESULT

The study conducted evaluations on various machine learning models including Decision Tree, SVM, Random Forests, Naive Bayes, and Voting using 4-fold cross-validation. Performance metrics such as accuracy, precision, recall were employed to determine the best algorithm for model. Overfitting and parameter tuning issues were addressed using multiple techniques post-model development. The evaluation involved binary and multiclass performance assessments utilizing confusion matrices. A machine learning classifier was devised to distinguish individuals with true Alzheimer's disease from a given population. Evaluation measures including precision, recall and accuracy were computed. The report provided to patients indicates their current stage of Alzheimer's disease, crucial for understanding its progression and guiding treatment. Various environments, tools, and libraries were utilized for conducting experiments and analysis in this research.



V. CONCLUSION

This project investigated the potential of MRI images for Alzheimer's disease (AD) detection and severity level prediction. We explored the use of machine learning, particularly deep learning techniques, to analyze these images and identify patterns associated with AD progression.

VI. ACKNOWLEDGEMENT

We express our sincere gratitude to Dr. Jerline Sheeba Anni, Principal, KMCT College of Engineering for Women, for facilitating a congenial academic environment in the college. We also express our gratitude to our Head of Department Dr. Sameera V Mohd Sagheer, project coordinator Mrs. Minilal and project supervisor Mrs. Anusha E P for guiding us right from the inception till the successful completion. We sincerely acknowledge them for the valuable support they had provided to us at all the stages of the project. Finally, We would like to add a few heartfelt words for the people who were part of the project in various ways, especially my teachers and classmates. We also extend our gratitude to our family without whose support, persistence and love we would not be where we today.

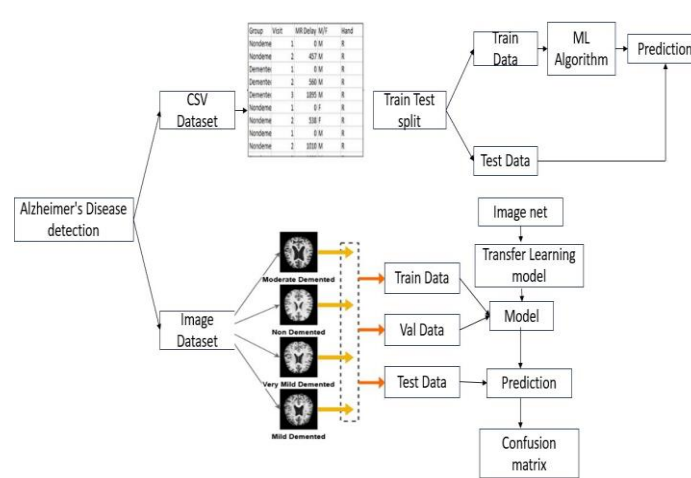


Fig. 3. Block Diagram

REFERENCES

- [1] Frank Jessen, Rebecca E Amariglio, Martin Van Boxtel, Monique Breteler, Mathieu Ceccaldi, Gae'l Che'telat, Bruno Dubois, Carole Du- fouis, Kathryn A Ellis, Wiesje M Van Der Flier, et al. A conceptual framework for research on subjective cognitive decline in preclinical alzheimer's disease. *Alzheimer's & dementia*, 10(6):844–852, 2014.
- [2] Yongliang Sun, Xuzhao Zhang, Xiaocheng Wang, Xinggan Zhang, et al. Device-free wireless localization using artificial neural networks in wireless sensor networks. *Wireless Communications and Mobile Computing*, 2018, 2018.

- [3] Lee Kuok Leong and Azian Azamimi Abdullah. Prediction of alzheimer's disease (ad) using machine learning techniques with boruta algorithm as feature selection method. In *Journal of Physics: Conference Series*, volume 1372, page 012065. IOP Publishing, 2019.
- [4] Francisco J Martinez-Murcia, Andres Ortiz, Juan-Manuel Gorriz, Javier Ramirez, and Diego Castillo-Barnes. Studying the manifold structure of alzheimer's disease: a deep learning approach using convolutional autoencoders. *IEEE journal of biomedical and health informatics*, 24(1):17–26, 2019.
- [5] Irene Heger, Sebastian Koehler, Martin van Boxtel, Marjolein de Vugt, KlaasJan Hajema, Frans Verhey, and Kay Deckers. Raising awareness for dementia risk reduction through a public health campaign: a pre-post study. *BMJ open*, 10(11):e041211, 2020.
- [6] Suhad Al-Shoukry, Taha H Rassem, and Nasrin M Makbol. Alzheimer's diseases detection by using deep learning algorithms: a mini-review. *IEEE Access*, 8:77131–77141, 2020.
- [7] R Sivakani and Gufran Ahmad Ansari. Machine learning framework for implementing alzheimer's disease. In *2020 International conference on communication and signal processing (ICCSP)*, pages 0588–0592. IEEE, 2020.
- [8] J Neelaveni and MS Geetha Devasana. Alzheimer disease prediction using machine learning algorithms. In *2020 6th international conference on advanced computing and communication systems (ICACCS)*, pages 101–104. IEEE, 2020.
- [9] Morshedul Bari Antor, AHM Jamil, Maliha Mamtaz, Mohammad Monirujjaman Khan, Sultan Aljhdali, Manjit Kaur, Parminder Singh, and Mehedi Masud. A comparative analysis of machine learning algorithms to predict alzheimer's disease. *Journal of Healthcare Engineering*, 2021, 2021.
- [10] Naif K Al-Shammari, Ahmed A Alzamil, Mohammd Albadarn, SA Ahmed, MB Syed, Ahmed Saud Alshammari, and Ahmed Maher Gabr. Cardiac stroke prediction framework using hybrid optimization algorithm under dnn. *Engineering, Technology & Applied Science Research*, 11(4):7436–7441, 2021.
- [11] Tanuja Kothakota, Kirankumari Patil, and Karthik Reddy Kanjula. Epilepsy seizure prediction model based on dual mode eeg overlapping technique using neural network. In *Conference of Open Innovations Association, FRUCT*, number 28, pages 582–588. FRUCT Oy, 2021.
- [12] Xiao Bai, Xiang Wang, Xianglong Liu, Qiang Liu, Jingkuan Song, Nicu Sebe, and Been Kim. Explainable deep learning for efficient and robust pattern recognition: A survey of recent developments. *Pattern Recognition*, 120:108102, 2021.
- [13] Protima Khan, Md Fazlul Kader, SM Riazul Islam, Aisha B Rahman, Md Shahriar Kamal, Masbah Uddin Toha, and Kyung-Sup Kwak. Machine learning and deep learning approaches for brain disease diagnosis: principles and recent advances. *IEEE Access*, 9:37622–37655, 2021.
- [14] Rukesh Prajapati, Uttam Khatri, and Goo Rak Kwon. An efficient deep neural network binary classifier for alzheimer's disease classification. In *2021 International Conference on Artificial Intelligence in Information and Communication (ICAIIIC)*, pages 231–234. IEEE, 2021.
- [15] V Sathiyamoorthi, AK Ilavarasi, K Murugeswari, Syed Thouheed Ahmed, B Aruna Devi, and Murali Kalipindi. A deep convolutional neural network based computer aided diagnosis system for the prediction of alzheimer's disease in mri images. *Measurement*, 171:108838, 2021.

- [16] Thippa Reddy Gadekallu, Celestine Iwendi, Chuliang Wei, and Qin Xin. Identification of malnutrition and prediction of bmi from facial images using real-time image processing and machine learning. *IET Image Process*, 16:647–658, 2021.
- [17] Hadeer A Helaly, Mahmoud Badawy, and Amira Y Haikal. Deep learning approach for early detection of alzheimer’s disease. *Cognitive computation*, 14(5):1711–1727, 2022.
- [18] C Kavitha, Vinodhini Mani, SR Srividhya, Osamah Ibrahim Khalaf, and Carlos Andre’s Tavera Romero. Early-stage alzheimer’s disease prediction using machine learning models. *Frontiers in public health*, 10:853294, 2022.
- [19] K Thanuja, M Shoba, and Kirankumari Patil. Epileptic seizure classification and feature optimization technique using grey wolf algorithm on dynamic datasets. *SN Computer Science*, 4(3):311, 2023.
- [20] M Sudharsan and G Thailambal. Alzheimer’s disease prediction using machine learning techniques and principal component analysis (pca). *Materials Today: Proceedings*, 81:182–190, 2023.

Exoarm: Empowering Monoparesis Rehabilitation

Yamuna S

Dept. of biomedical engineering
KMCT CEW Calicut, India
yamunashanmughan@gmail.com

Asiya N

Dept. of biomedical engineering
KMCT CEW Calicut, India
asiyanizar21@gmail.com

Aleena K S

Dept. of biomedical engineering
KMCT CEW Calicut, India
aleena4790@gmail.com

Rukkya P N

Dept of biomedical engineering
KMCT CEW Calicut, India
rukkyapn@gmail.com

Sivanath P I

Dept. of biomedical engineering
KMCT CEW Calicut, India
sivanathpi@gmail.com

I. ABSTRACT

The Arduino Uno and NodeMCU microcontrollers are used in the smart exoskeleton system to control the movements of the elbow, wrist, and fingers using servo and stepper motors. Flex sensors and an Android app are the two techniques used here. These two are attached to the Arduino board as input. The efficiency of the exoskeleton in improving upper limb mobility and fine motor activities is assessed; prospective uses include industrial duties, assistive technology, and rehabilitation therapy.

Index Terms—Exoskeleton, Arduino Uno, Node MCU, Android

App, Flex sensors, servo stepper motor

II. INTRODUCTION

ExoArm: Empowering Monoparesis Rehabilitation” is a ground-breaking program that combines state-of-the-art robotics with intricate control systems to effectively address the multifaceted obstacles faced by people with monoparesis. This creative project’s main goal is to develop a wearable robotic system that will not only try to restore the crippled limb’s capabilities but also improve them, giving users the ability to regain their independence and improve their quality of life in general. A network of servo motors, a precisely calibrated stepper motor, and a cluster of carefully positioned flex sensors are all seamlessly integrated into the meticulously designed ExoArm, which is envisioned as a versatile and adaptive solution. A specialized and user-friendly Android application can be used to effortlessly operate and control the ExoArm’s connected components, which include the precisely calibrated servo motors for precise and nuanced finger movements, the responsive and fluid-stepper motor that facilitates natural and seamless arm movements, and the strategically positioned array of five flex sensors for dynamic and intuitive control and manipulation. All of these components work together to create a seamless and user-friendly system. The core of the ExoArm is the highly flexible and efficient Arduino Uno microcontroller, which maintains an optimal and continuous operating framework by facilitating the smooth and responsive interaction between the stepper motor, servo motors, and flex sensors.

Additionally, the NodeMCU module's seamless integration acts as a wireless communication channel between the Android application and the ExoArm, enabling real-time adjustments and a highly customizable control interface that can be precisely tailored to meet the various and ever-evolving needs and preferences of each individual user. Concurrently, the finely tuned and extremely responsive stepper motor functions as a crucial element that efficiently permits smooth and natural arm motions, greatly augmenting the user's ability and potential to competently perform a variety of tasks with increased ease, efficiency, and fluidity. Additionally, the very cleverly placed and highly adaptive flex sensors are seamlessly integrated into the ExoArm to further improve its overall responsiveness and adaptability. This allows users to control and modulate the robotic system's movements with subtle, natural gestures, thereby strengthening the already existing symbiotic relationship between the user and the ExoArm. In addition to offering users an intuitive, approachable, and highly interactive interface that efficiently streamlines the entire operational framework and ensures an immersive and captivating user experience, the user-friendly Android application acts as a centralized and seamlessly integrated control hub. The main goal of this ground-breaking initiative is to offer a complete platform that not only makes it easier to restore lost motor abilities but also acts as a catalyst to speed up and simplify the user's rehabilitation process. The ExoArm project seeks to promote and create a more inclusive and supportive workplace by combining technology innovation with a deeply rooted human-centric approach, highlighting the critical relevance of independence and empowerment throughout the continuous healing process. . Through the development of a cooperative and mutually beneficial interaction between the user and the technology components, the ExoArm is ideally positioned to provide a customized and personalized rehabilitation experience that is painstakingly adapted to meet the particular needs and skills of every user.

III. LITERATURE SURVEY

[1] Khokhar, Z.O. et al., 2010. This paper presents the utilization of design acknowledgment to appraise the torque connected by a human wrist and its real-time usage to control a novel two degree of opportunity wrist exoskeleton model (WEP). [2] Troncossi M., et al. 2012. The hand exoskeleton has 2 degrees of flexibility (DOFs) for the flexion/extension of the thumb and for the flexion/extension of the gaster composed by the other four fingers. Current impediments of existing devices depend within the truant or decreased capability to foresee the aiming activity of the patient. [3]. Vaca Benitez L.M., et al., 2013. The control is based on limit capacities which are related to most extreme amplitudes measured in both muscles. In this way the bolster is continually diminished until the point the persistent does not need any external help for moving his arm. [4] Soltani Zarrin R, et al. 2017. It features eight degrees of freedom (DoF), six dynamic and two detached, empowering comprehensive scope of bear support, glenohumeral (GH) joint, elbow, and wrist movements. [5] Lambelet, C., et al. 2017. They created the eWrist, a wearable one degree-of-freedom fueled exoskeleton which underpins wrist extension training. [6] Noor, S., et al., 2017. The most component of the framework is an accelerometer which depends on the motions of the hands. This system moreover capacities utilizing Arduino where the computer motion of the robot is controlled by human hand movements. [7] Cheng, L., et al. 2018. To lighten the weight connected on the patient's hand and arm, here the complete control framework is set within the patient's

rucksack and the cabledriven approach is utilized to attain the long-distance control transmission. This paper proposes a wearable hand restoration robot for helping patients to do restoration preparing such as the flexion and expansion of fingers. [8] Ambrosini E, et al. 2019. Here, The displayed half breed mechanical framework is exceedingly customizable, permits to screen the day by day execution, requires moocapability to perform ADLs and appear little but supervision of the advisor and might have the potential to noteworthy changes in engine control and muscle quality upgrade arm recuperation after stroke. [9] Rudd, G., et al. 2019 proposed a low-cost, delicate mechanical hand exoskeleton made of delicate silicone elastic actuators, it helps with getting a handle on and hand developments, controlled through a basic interface and microcontroller. [10] Abdul-Amir D.Q, et al. 2019 propose a shrewd exoskeleton robotic arm for elbow recovery, highlighting a 2-DOF plan with arrangement flexible actuators (Oceans) and a cable-driven differential instrument. This plan gives exact torque control and free development control. [11] Nizamis K, et al. 2019. Bionic arms, controlled by electrical signals from muscles or nerves, reestablish upper appendage work with different developments. Sensor innovation and control frameworks from bionic arms can upgrade stroke recovery and exoskeleton functionality. [12] Imtiaz M.S.B, et al. 2021. The exoskeleton was created concurring to the measurements of a persistent employing a 3D scanner, and after that created with a 3D printer; the mechanism for the development of the hand could be a ligament flexion component with servo engine actuators controlled by an ATmega2560 microcontroller. [13] Henderson J, et al. 2021. The hand exoskeleton has 2 degrees of flexibility (DOFs) for the flexion/extension of the thumb and for the flexion/extension of the gather composed by the other four fingers. Within this system the creators planned and made the distal portion of the by and large exoskeleton, i.e. the hand-and-wrist framework. [14] Secciani N, et al. 2021. a hand exoskeleton plan including a 5-DOF cable-driven instrument with a secluded structure, made of lightweight materials like aluminum and carbon fiber and fueled by little servo motors. [15] He, C., Xiong, C.H. et al., 2021. A recently created exoskeleton (Armule) outlined particularly for post-stroke upper appendage recovery [16] Xie, Q, et al. 2021, propose a comprehensive human-exoskeleton coupling energetic show for upper appendage recovery preparing, considering the structure of the exoskeleton, human arm biomechanics, and in-teraction powers. Custom fitted to both detached understanding preparing (PPT) and patient active preparing (PAT) modes. [17] V´elez-Guerrero, M.A., et al., 2021. These exoskeletons give assistive and resistive powers amid preparing, possibly revolutionizing recovery by upgrading adequacy, proficiency, and persistent engagement. [18] De Oliveira, A.C., et al., 2021. This investigates the accuracy of upper-extremity joint point estimation utilizing the Agreement exoskeleton. Comes about appear great to excellent agreement with optical movement capture markers, proposing the exoskeleton's potential as a tool for assessing arm and shoulder joint kinematics. [19] Islam, M.R. et al., 2021. This investigate work pointed to create an imaginative sensorized upper arm cuff to measure the wearer's interaction forces in the upper arm [20] Blanco-Ortega, A. et al. 2022. a strong GPI controller for direction following in upper appendage restoration exoskeletons, utilizing as it were yield estimations for computational effectiveness and real-time implementation. [21] In 2022, Palazzi, et al. Individuals who endure from upper-limb incapacities may discover their quality of life much improved by the low-cost

upper-limb exoskeleton that the creators have effectively made. They are able to utilize smaller, less expensive engines since of their design's capacity to significantly minimize the crest torques required for working. [22] Peng, X. et al., 2022, optimizing fuelled lower leg exoskeleton control. Members in a think about strolled on a treadmill wearing such exoskeletons, deciding their just noticeable distinction (JND) in activation timing. [23] Dunkelberger, N. et al. 2023. The MPC taken a toll work is outlined to disperse activation on a single degree of opportunity to favor FES control exertion, decreasing exoskeleton control utilization, whereas guaranteeing smooth developments along diverse trajectories. This control technique diminished exoskeleton torque for the crossover framework with similar following precision compared to using the exoskeleton alone. [24] Greco, C, et al. 2023. The creators propose utilizing delicate and flexible carbon fiber-based turned and coiled fake muscles (TCAMs) to control a lightweight, ungrounded, delicate exoskeleton for wrist rehabilitation. Exercises for wrist rehabilitation that can be done passively or actively with the device. [25] Barrutia, W.S., et al. 2023. This phantom, featuring 3D-printed bones surrounded by ballistic gel and a motorized hexapod system, replicates physiological knee motion during gait. Testing with a torsional spring exoskeleton demonstrates the importance of including soft tissue deformation, indicating its crucial role in energy absorption and transmission.

Based on the findings of our survey we developed a 3D-printed Exoskeleton that is controlled by flex sensors in addition to an android app. This model serves as a rehabilitation to assist individuals with monoparesis condition.

IV. METHODOLOGY

7) **Server**

PyCharm is used to code a Python server, facilitating connection between the Android app and NodeMCU.

8) **LED indication**

LEDs offer visual feedback, displaying various colors, blink patterns, or steady states to convey information.

B. Circuit Diagram

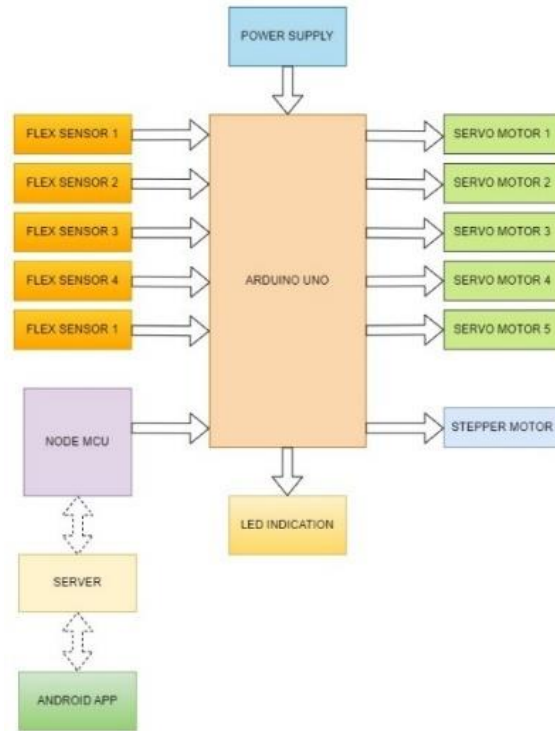


Fig. 1. Block Diagram

A. Block Diagram

1) Power supply

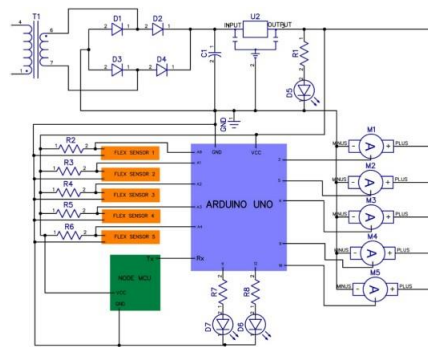


Fig. 2. Circuit Diagram

The circuit starts with a step-down transformer converting 230V AC to 12V AC. The 12V AC is rectified to DC using a bridge rectifier and filtered with a capacitor. An LM7805 regulator converts the 12V DC to stable 5V DC. An LED indicates the presence of the 5V supply. The Arduino Uno, flex sensors, and NodeMCU transmitter are connected, with the Arduino providing power to servo motors and LEDs.

C. Flow Chart

A power supply converts 230V AC to 5V DC for electronic projects.

2) **Arduino Uno**

Arduino Uno is a microcontroller board with 14 digital I/O pins, 6 analog inputs, and uses embedded C for programming via the Arduino IDE.

3) **NodeMCU**

NodeMCU ESP8266 is a popular IoT development board with built-in Wi-Fi, compatible with Arduino IDE and programmed in embedded C.

4) **Servo Motor**

MG90S servo motors are self-contained devices used for precise rotation in machines. They're controlled by a standard servo signal with pulse widths determining their position. They act as fingers in this project.

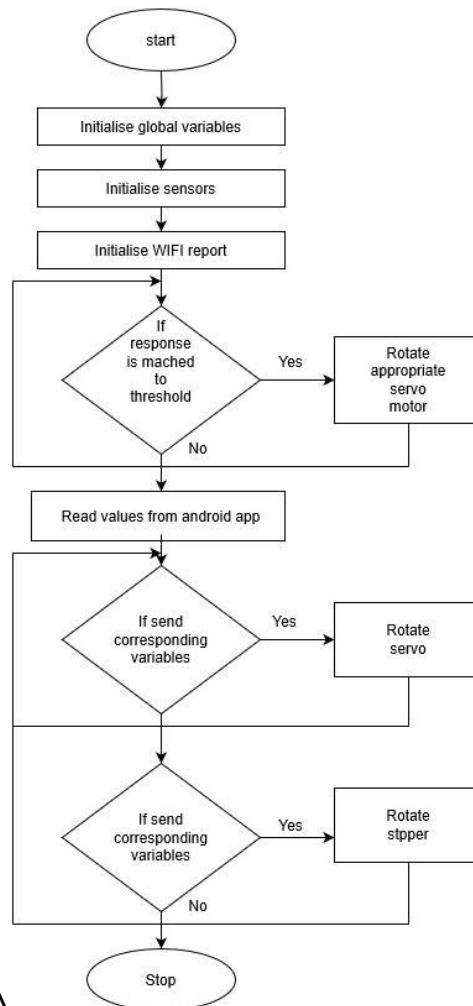
5) **Stepper motor**

The stepper motor used here aids in elbow extension, converting electrical pulses into precise mechanical motion through discrete steps.

6) **Android App**

The Android app, created in Android Studio using Java, controls the exoarm via buttons to rotate the servo motor.

- 1) Initialization: System connects to Android app and sets up servo motor control and flex sensor pins.
- 2) Receiving Commands from the Android App: System checks for commands from Android app rotate servo motor to angle or read flex sensor value
- 3) Processing Command: Upon receiving a servo rotation command, the system identifies the target servo motor and adjusts it to the specified angle. For flex sensor reading commands, the system retrieves the current value of the specified flex sensor, indicating the degree of sensor bending.
- 4) Checking Flex Sensor Threshold: System checks flex sensor value against preset threshold to detect significant bends
- 5) Triggering Servo Rotation based on Flex Sensor: If flex sensor value surpasses threshold, system rotates corresponding servo to preset angle.
- 6) System Stop: Once all commands and sensor readings have been processed, the system enters a stop state. This revised version uses standard language and avoids technical jargon to improve clarity and accessibility for a broader audience



A

Fig. 3. Flow Chart

D. Abbreviations and Acronyms

DOF - degrees of freedom GH - glenohumeral PPT - passivepatient training TCAM - twisted and coiled artificial muscles LED - light emitting diode AC - Alternating current DC - Direct current ADL -Activities of daily living

v. RESULT

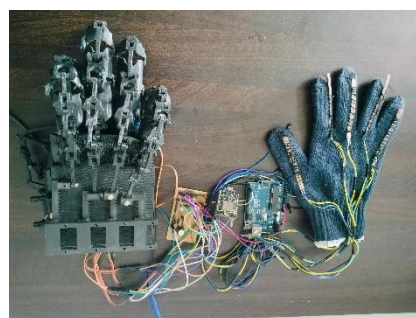


Fig. 4. Exo arm

The intricately interwoven components of the ExoArm, including the meticulously calibrated servo motors and step- per motor is facilitated using flex sensors and user-friendly Android application.

A. *Flex sensor*

The servo motors and flex sensors are connected to the node mcu and arduino uno respectively. The node mcu and arduino uno are connected to each other. The code to rotate servo motor is uploaded to the node mcu. Calibration has to be done for each and every finger, upload the code with threshold on arduino uno According to the calibrated values, the servomotors will rotate

B. *Android app*

The android app is designed using android studio IDE and the programming language used is JAVA. The control buttons are provided on the android app The code for server is done using python and the IDE is pycharm The exoarm function based on the command given by the user via android app

REFERENCES

- [1] Zeeshan O, Khokhar, Zhen G Xiao, Cario Menon, 2010. Surface EMG pattern recognition for real-time control of a wrist exoskeleton. *BioMedical Engineering OnLine* 2010, 9:41 <http://www.biomedical-engineering-online.com/content/9/1/41>
- [2] Troncossi, M., Mozaffari Fomashi, M., Mazzotti, C., Zannoli, D. and Parenti Castelli, V., 2012. Design and manufacturing of a hand-and- wrist exoskeleton prototype for the rehabilitation of post-stroke patients. *Quaderni del DIEM-GMA. Atti della Sesta Giornata di Studio Ettore Funaioli*, pp.111-120.
- [3] Vaca Benitez, L.M., Tabie, M., Will, N., Schmidt, S., Jordan, M. and Kirchner, E.A., 2013. Exoskeleton technology in rehabilitation: Towards an EMG-based orthosis system for upper limb neuromotor rehabilitation. *Journal of Robotics*, 2013. doi:10.1155/2013/610589
- [4] Soltani-Zarrin, R., Zeiaee, A., Eib, A., Langari, R. and Tafreshi, R., 2017. CLEVERarm: A Novel Exoskeleton for Rehabilitation of Upper Limb Impairments. *arXiv preprint arXiv:1712.02322*. doi:10.48550/arXiv.1712.02322
- [5] Lambelet, C., Lyu, M., Woolley, D., Gassert, R. and Wenderoth, N., 2017, July. The eWrist—A wearable wrist exoskeleton with sEMG-based force control for stroke rehabilitation. In *2017 International Conference on Rehabilitation Robotics (ICORR)* (pp. 726-733). IEEE. doi:10.1109/ICORR.2017.8009334
- [6] Noor, S., Shohan, J.A., Wares, M.S., Ahmed, A., Khan, A.I., Fattah, S.A. and Shahnaz, C., 2017, December. Real time hand movement controlled robotic arm for risk prevention. In *2017 IEEE Region*

10 Humanitarian Technology Conference (R10-HTC) (pp. 465-469).

IEEE.doi:10.1109/R10-HTC.2017.8289000

- [7] Cheng, L., Chen, M. and Li, Z., 2018. Design and control of a wearable hand rehabilitation robot. IEEE access, 6, pp.74039-74050. doi:10.1109/ACCESS.2018.2884451
- [8] Ambrosini, E., Zajc, J., Ferrante, S., Ferrigno, G., Dalla Gaspe- rina, S., Bulgheroni, M., Baccinelli, W., Schauer, T., Wiesener, C., Russold, M. and Gfoehler, M., 2019. A hybrid robotic sys-tem for arm training of stroke survivors: Concept and first evalua- tion. IEEE Transactions on Biomedical Engineering, 66(12), pp.3290-3300.doi:10.1109/TBME.2019.2900525
- [9] Rudd, G., Daly, L., Jovanovic, V. and Cuckov, F., 2019. A Low-cost soft robotic hand exoskeleton for use in therapy of limited hand–motor function. Applied Sciences, 9(18), p.3751.doi:10.3390/app9183751
- [10] Abdul-Amir, D.Q., Hashim, A. and Ameer, A., Design a Smart Ex- oskeleton Robotic Arm for Elbow Rehabilitation.doi:10.9790/1684- 1602024347
- [11] Nizamis, K., Stienen, A.H., Kamper, D.G., Keller, T., Pletten- burg, D.H., Rouse, E.J., Farina, D., Koopman, B.F. and Sartori, M., 2019. Transferrable expertise from bionic arms to robotic ex- oskeletons: perspectives for stroke and duchenne muscular dystrophy. IEEE Transactions on Medical Robotics and Bionics, 1(2), pp.88-96.doi:10.1109/TMRB.2019.2912453
- [12] Imtiaz, M.S.B., Babar Ali, C., Kausar, Z., Shah, S.Y., Shah, S.A., Ahmad, J., Imran, M.A. and Abbasi, Q.H., 2021. Design of portable exoskeleton forearm for rehabilitation of monoparesis patients using ten- don flexion sensing mechanism for health care applications. Electronics, 10(11), p.1279.doi:10.3390/electronics10111279
- [13] Henderson, J., Condell, J., Connolly, J., Kelly, D. and Curran, K., 2021. Review of wearable sensor-based health monitoring glove devices for rheumatoid arthritis. Sensors, 21(5), p.1576.doi:10.3390/s21051576
- [14] Secciani, N., Brogi, C., Pagliai, M., Buonamici, F., Gerli, F., Van- netti, F., Bianchini, M., Volpe, Y. and Ridolfi, A., 2021. Wearable robots: An original mechatronic design of a hand exoskeleton for assistive and rehabilitative purposes. Frontiers in Neurorobotics, 15, p.750385.doi:10.3389/fnbot.2021.750385
- [15] Chang He, Cai- Hua Xiong, Member, IEEE, Ze- Jian Chen, Wei Fan, Xiao-Lin Huang, and Chenglong Fu, Member, IEEE, 2021.IEEE Trans Neural Syst Rehabil Eng. 2021;29:1795-1805. doi: 10.1109/TNSRE.2021.3107376. Epub 2021 Sep 10. PMID: 34428146.
- [16] Xie, Q., Meng, Q., Zeng, Q., Fan, Y., Dai, Y. and Yu, H., 2021. Human exoskeleton coupling dynamics of a multi-mode therapeutic exoskeleton for upper limb rehabilitation training. IEEE Access, 9, pp.61998-62007. doi:10.1109/ACCESS.2021.3072781
- [17] V´elez-Guerrero, M.A., Callejas-Cuervo, M. and Maz- zoleni, S., 2021. Artificial Intelligence- Based Wearable Robotic Exoskeletons for Upper Limb Rehabilitation. DOI: 10.3390/s21062146

- [18] De Oliveira, A.C., Sulzer, J.S. and Deshpande, A.D., 2021. Assessment of upper-extremity joint angles using harmony exoskeleton. *IEEE Transactions on Neural Systems and Rehabilitation Engineering*, 29, pp.916- 925.doi:10.1109/TNSRE.2021.3074101
- [19] Md Rasedul Islam, Md Assad-Uz- Zaman, Brahim Brahmi, Yassine Bouteraa, Inga Wang and Mohammad Habibur Rahman, 2021. Design and Development of an Upper Limb Rehabilitative Robot with Dual Functionality. doi: 10.3390/mi12080870
- [20] Blanco-Ortega, A., Va'zquez-Sa'nchez, L., Adam-Medina, M., Col'in- Ocampo, J., Abu'ndez-Pliego, A., Cort'es-Garc'ia, C. and Garc'ia- Beltr'an, C.D., 2022. A Robust controller for upper limb rehabilitation exoskeleton. *Applied Sciences*, 12(3), p.1178. doi:10.3390/app12031178
- [21] Palazzi, E., Luzi, L., Dimo, E., Meneghetti, M., Vicario, R., Luzia,R.F., Vertechy, R. and Calanca, A., 2022. An affordable upper-limb exoskeleton concept for rehabilitation applications. *Technologies*, 10(1), p.22. doi:10.3390/technologies10010022
- [22] Peng, X., Acosta-Sojo, Y., Wu, M.I. and Stirling, L., 2022. Actua-tion timing perception of a powered ankle exoskeleton and its as- sociated ankle angle changes during walking. *IEEE Transactions on Neural Systems and Rehabilitation Engineering*, 30, pp.869-877.doi: 10.1109/TNSRE.2022.3162213
- [23] Dunkelberger, N., Berning, J., Schearer, E.M. and O'Malley, M.K., 2023. Hybrid FES-exoskeleton control: Using MPC to distribute actuation for elbow and wrist movements. *Frontiers in Neurorobotics*, 17, p.1127783. doi:10.3389/fnbot.2023.1127783
- [24] Greco, C., Weerakkody, T.H., Cichella, V., Pagnotta, L. and Lamuta, C., 2023. Lightweight Bioinspired Exoskeleton for Wrist Rehabilitation Powered by Twisted and Coiled Artificial Muscles. *Robotics*, 12(1), p.27.doi:10.3390/robotics12010027
- [25] Barrtia, T.L., Ramirez, A.A., Emerson, M.A., Lathrop, R.A., Mahoney, A.W., Gilbert, H.B., Liu, C.L., Russell, P.T., Labadie, R.F., Weaver, K.D. and Webster III, R.J., 2023. A modular, multi-arm concentric tube robot system with application to transnasal surgery for orbital tumors. *The International Journal of Robotics Research*, 40(2-3), pp.521- 533.doi:10.1177/02783649211000074

Head Gesture Controlled and Obstacles Detected Automatic Wheelchair for Quadriplegic Patients

Akshaya T V
Dept. of Biomedical Engineering
KMCT CEW Kozhikode, India
akshayaard100@gmail.com

Aziya Ashraf
Dept. of Biomedical Engineering
KMCT CEW Kozhikode, India
asharafcompanil777@gmail.com

Nashwa T
Dept. of Biomedical Engineering
KMCT CEW Kozhikode, India
nashwat333@gmail.com

Navya Babu
Dept. of Biomedical Engineering
KMCT CEW Kozhikode, India
navyababu.pc@gmail.com

Anusha E P
Dept. of Biomedical Engineering
Assistant Professor
KMCT CEW Kozhikode, India
anushachandran08@gmail.com

Abstract—The research focuses on developing a head gesture- controlled wheelchair with obstacle detection capabilities for quadriplegic patients. For precise control, seamless navigation, and enhanced safety, the system incorporates an MPU 6050 sensor, Arduino UNO controller, and ultrasonic sensors. The system captures intricate head movement data, allowing quadriplegic patients to regain mobility and independence. Ultrasonic sensors detect obstacles and elevation changes in real-time, preventing collisions and navigating complex terrains. The wheelchair is designed cost-effectively, ensuring user safety and flexibility.

I. INTRODUCTION

The study introduces an innovative approach to enhance the quality of life for quadriplegic individuals through the creation of a head gesture-controlled wheelchair equipped with advanced obstacle detection features. The innovative wheelchair combines cutting-edge technology and human-centered design, providing independence, mobility, and safety. The project integrates an MPU 6050 sensor, an Arduino UNO controller, and ultrasonic sensors for precise control and obstacle avoidance. The project is designed with cost-effectiveness in mind, ensuring user safety and flexibility without exorbitant costs. This innovative head gesture-controlled wheelchair represents a significant leap forward in improving the quality of life for individuals with limited mobility, breaking down barriers and redefining the boundaries of mobility and independence.

II. LITERATURE SURVEY

Aleksandar Pajkanovic et. al A novel head motion recognition technique based on accelerometer data processing and a mechanical actuator is utilized in this paper to present a microcontroller system that allows for the control of standard electric wheelchairs through head motion. The system has been tested and verified through an experiment and can be implemented with different types of standard electric wheelchairs.

Mr. Gangadhara, Karthik B K Smart hand-glove-controlled wheelchairs are crucial for disabled individuals who rely on others for mobility. These wheelchairs use accelerometer

sensors and wireless communication to control movement and direction. Users wear instrumented gloves, which communicate with a controller sandwiched between their seat and wheels. The goal is to make wheelchairs more cost-effective and accessible to people with disabilities, enabling them to use more hi-tech wheelchairs more widely.

Dulari Sahu This paper presents an eye-controlled electronic wheelchair designed for disabled individuals, eliminating the need for assistance. The system uses a camera to capture eye movements and tracks pupil position, with an ultrasonic sensor for safety and a central switch for emergency purposes. The wheelchair is controlled using a Raspberry Pi board, making it an independent and cost-effective solution.

Ali Abed The aim of this paper is to introduce a technologically advanced wheelchair that is specifically designed for individuals with physical disabilities. This wheelchair is equipped with a smart, motorized system that can be controlled using voice commands. To achieve this, an Arduino microcontroller and a voice recognition processor that is dependent on the user's voice are utilized. The wheelchair is capable of recognizing Arabic words through an isolated word recognition system (IWRS). It is powered by two 14A/24V/200Watt DC motors and has been successfully tested using a speech password and seven Arabic commands. The wheelchair demonstrates excellent performance in both quiet and noisy environments, ensuring safe and reliable movement for the user.

Losit et. al The aging population and increasing disability rates necessitate constant monitoring and assistance from specialists. Assistive and intelligent robotics research can help provide a solution for these individuals, allowing them to live independently and with increased personal autonomy. However, these technologies are still far from replacing human providers. An intelligent robotic wheelchair is proposed to assist users in daily activities, aiming for real-time response and active participation, ultimately improving quality of life for certain categories of people in need.

Mubdi-UI Alam Sajid et. al The paper suggests a clever wheelchair design that incorporates a hand movement device and a smartphone to assist individuals with disabilities. The wheelchair uses gyro sensors, accelerometers, and Bluetooth for automatic movement. Users wear a gesture system, controlling the wheelchair with Arduino Mega and Arduino Nano. The wheelchair has fewer minimum threshold angles and linearity compared to microcontroller-based wheelchairs.

Konduru sujana et. al This paper presents a Raspberry Pi-based hand gestured wheelchair system, utilizing Python OpenCV software and Arm11 controller. The system captures hand movement and controls the wheelchair based on the number of fingers. Image processing techniques like RGB conversion, threshold, contour detection, and convexity defects enhance the system's efficiency, making it useful for physically handicapped individuals.

Saish S. Shinde et. al This paper aims to develop a wheelchair control system that uses hand movement or gesture recognition using Acceleration technology. The system includes navigation, dark room sensors, automatic messaging, and obstacle detection. The project aims to make users' lives more comfortable, independent, cost-effective, and requires low maintenance.

The system includes touch plate sensors for movement control, Bluetooth obstacle detection, panic switches, LED illumination, and navigation through Google maps.

Sharmila Ashok presents a Solar Powered Multi-Controller Smart Wheelchair, which uses eye blink sensors, Joystick and Keypad modules, and additional sensors like heartbeat and temperature sensors to monitor health. A urine level indicator and fall detection system help prevent inconvenience. The system prioritizes patient safety and the wheelchair's use of solar power, allowing for immediate action in case of a fall.

Yoon Ket Lee et. al The objective of this project is to create a navigation and obstacle avoidance system for an autonomous wheelchair by utilizing camera sensors and image processing methods such as Canny Edge Detection and Erosion to recognize and detect obstacles. Compass sensors will be employed for navigation, calibration, reading, and comparison. Additionally, the project seeks to improve autonomous wheelchairs by incorporating internet connectivity, allowing for the implementation of Internet of Things (IoT) applications for individuals with disabilities who require independence.

Prashant Lahane This paper proposes a cost-effective application of Brain Computer Interface (BCI) technology to improve mobility for physically disabled people. The system uses EEG signals to control a mechanical wheelchair, triggering an action based on an eye blink pattern. This technology can overcome the limitations of conventional wheelchairs and improve overall development for those with disabilities.

Theja Ram Pingali et. al A system known as Social Following has been created to ensure that a powered wheelchair and its accompanying person maintain a conversational distance. By utilizing ultrasonic range sensors and transducers, the system is able to detect the person's location and direction. This allows the wheelchair to navigate according to the person's path, enabling hands-free control during social engagements. Jigme Wangchuk Machangpa et. al The health service sector is focusing on improving mobility assistance services for quadriplegic patients. A robotic wheelchair, called the Robotic WheelChair, has been developed, using sensors and artificial intelligence to navigate, detect obstacles, and move automatically. The wheelchair is equipped with an accelerometer, gyroscope, ultrasonic sensor, relay, battery, DC stepper motor, and Raspberry Pi. Head movement is detected by the MPU 6050 sensor, and obstacles are avoided with the help of ultrasonic sensors. The wheelchair is designed to be cost-effective while prioritizing the safety, flexibility, and mobility of its users.

Mohammed Abdul Kader et. al The wheelchair is equipped with an accelerometer, gyroscope, ultrasonic sensor, relay, battery, DC stepper motor, and Raspberry Pi. Head movement is detected by the MPU 6050 sensor, and obstacles are avoided with the help of ultrasonic sensors. The wheelchair is designed to be cost-effective while prioritizing the safety, flexibility, and mobility of its users.

Huda Farooq Jameel et. al The EMOTIV Insight is a wearable tool that allows disabled individuals to control their wheelchairs through a human-computer interface. The system utilizes a gyroscope for detecting head tilt, a DC motor driver for managing speed and directions, a

wheelchair, a micro-controller, and a laptop. It has undergone testing on different surfaces, demonstrating remarkable accuracy, sensitivity, and specificity levels of 99.1percentage, 99.16percentage, and 98.83 percentage, correspondingly.

Shadman Mahmood Khan Pathan et. al A robotic wheelchair uses sensors and intelligence for navigation and obstacle detection. A cap-controlled wheelchair was developed for testing gesture operation. A real-time wheelchair with joystick and head gesture control modes was developed. The wheelchair is equipped with an MPU6050 sensor, joystick module, RF module, battery, dc motor, toggle switch, and Arduino. It possesses the capability to maneuver in different directions and achieves a speed of 4.8 km/h. msaba anwer et al The novel system described in this document utilizes optical signals to enhance the maneuvering of wheelchairs for individuals with physical disabilities. It comprises two main components: detecting eye movements and processing optical signals, as well as controlling the wheelchair via motor driving circuitry. Real-time images are captured by a web camera, while a Raspberry-Pi processor running a Linux operating system is employed. The system's performance is assessed through a basic wheelchair skill test, demonstrating an average response time of 3 seconds for eye control and 3.4 seconds for voice control.

Mohammed kutbi et. al The egocentric computer vision-based co-robot wheelchair, proposed by the authors, aims to enhance mobility for elderly and disabled individuals who have limited hand functionality. By modifying the wheelchair to utilize an egocentric camera mounted on the user's head for controlling head motion, this system provides a more intuitive interface between humans and robots, enabling seamless control over speed and direction. The authors conducted three usability studies involving 37 subjects, which emphasized the potential for future research involving disabled individuals.

Aayushi B Thakur et. al The Solar-powered wheelchair described in this document features a 3-axis accelerometer and Bluetooth module for recognizing gestures, with the configuration being done using an Arduino board and mathematical algorithms. The wheelchair recognizes physical movements and uses voice recognition through an Android application. This method enables computer understanding of human body language and bridges the computer with the human world.

Rajdeep Sarkar et. al The "Smart Wheelchair" project aims to enhance independence for wheelchair users by providing an inbuilt health monitoring facility, enabling them to overcome emergency conditions. The project envisions the future of Smart Wheelchair research and its best service for individuals with disabilities.

Farah Binte Haque et. al The project aims to design a head-movement controlled wheelchair for physically disabled individuals, addressing their daily challenges. This intelligent wheelchair uses head movements to navigate, recognize obstacles, and move automatically. The prototype uses a microcontroller, accelerometer, and ultrasound detector to perform head motions. The wheelchair has been created with a cost-effective price point, ensuring it is within reach for

individuals in less developed or developing nations. The system memorizes headgestures and uses DC motors during control mode.

Hadish Habte The research paper examines an eye-tracking electric wheelchair (EWC) designed for the elderly and dis-abled individuals. By utilizing edge detection to locate the eye pupil position, a PID controller to manage the DC motor, and object detection, the system attains a 90percentage accuracy rate and reduces response time in comparison to current approaches..

R. Priyatharshini et. al Paralyzed individuals can now ben-efit from a newly developed Raspberry Pi device that enablesthem to operate wheelchairs using their eyes and voice. This innovative device tracks the movement of the user's eyeballs, adjusts the direction of the wheelchair based on the location ofthe pupils, and allows users to receive feedback through their cell phones. Moreover, in case of emergencies, users have theoption to send voice commands to their designated guardian.Md Abdullah Al Rakib Wheel chairs are mechanical devices that enable independent movement, reducing personal effortand force. Smart wheelchairs, with voice commands and but- ton controls, are increasingly popular for mobility assistance, especially in nursing homes and for those with mobility loss. New generations of smart wheelchairs incorporate artificial intelligence, leaving users vulnerable. The project aims todevelop a similar wheel chair with intelligence.

Muhammad Sheikh Sadi et. al The proposal put forwardin this document is for a smart wheelchair system that iscontrolled by gestures and includes a fall detection feature en- abled by IoT technology. The goal is to address the expensive nature, technical constraints, and safety concerns associated with contemporary wheelchairs. By utilizing ConvolutionalNeural Network and computer vision algorithms, the system ensures user safety while remaining cost-effective, secure, andbeneficial for individuals with physical disabilities.

III. METHODOLOGY

A. *Proposed System*

During navigation, the ultrasonic sensors are utilized todetect obstacles, and the computed data is used to implement safety measures. The patient's wheelchair allows for an in- clination angle of approximately 20°. The system description can be categorized as follows:

- Head Orientation: This component determines the orien-tation of the head.
- Motion Detection: This component detects and calculatesthe signal data obtained from head orientation.
- Wheelchair Locomotion: This component converts thedata from motion detection into actual locomotion.

B. *Block Diagram*

The automated wheelchair uses a microcontroller, gyro-scopic sensor, ultrasonic sensor, and power supply to capture head movement data, detect obstacles, and change elevations. The microcontroller processes these data to facilitate naviga- tion, and the output is sent to the motor driver IC (L293D), which distributes a 6V voltage to each motor.

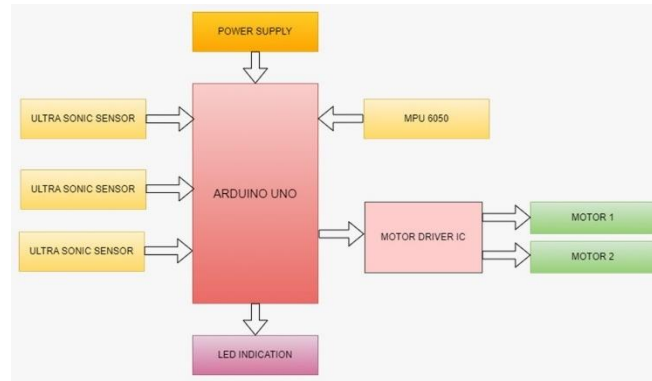


Fig. 1. block diagram.

c. *Arduino UNO*

The Arduino Uno, which is part of the megaAVR family, is a microcontroller board that utilizes the ATmega328 single-chip microcontroller. It is equipped with digital I/O pins, a power jack, 6 analog inputs, a ceramic resonator with a frequency of 16 MHz, a USB connection, an RST button, and an ICSP header. This board can be powered by an AC to DC adapter, a USB cable, or a battery. Other variations of the Arduino Uno include the Arduino Pro Mini, Arduino Nano, Arduino Due, Arduino Mega, and Arduino Leonardo. The features of the Arduino Uno ATmega328 encompass the following.

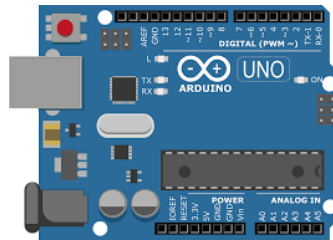


Fig. 2. Arduino UNO.

- voltage for operation is 5V
- The suggested input voltage falling between 7V to 12V.
- 14 digital input/output pins.
- 6 analog input pins.
- 32 KB of Flash Memory
- 2 KB of SRAM.
- 1 KB of EEPROM.
- clock speed of 16 MHz.

d. *MPU6050 Sensor*

The MPU6050 sensor module is a small motion tracking device that has an I2C bus interface for communication with microcontrollers and an auxiliary I2C bus for connecting a 3-axis magnetometer. The specifications of the MPU6050 Sensor Gyroscope include:

- It can sense motion in 3 axes with a full-scale range of

± 250 , ± 500 , ± 1000 , or ± 2000 degrees per second (dps).

- The sensitivity is measured in LSBs (Least Significant Bits) per dps, with values of 131, 65.5, 32.8, or 16.4.
- The output data rate (ODR) can range from 8kHz to 1.25Hz.



Fig. 3. MPU6050 sensor

Accelerometer include:

- The sensor offers 3-axis sensing capabilities.
- maximum range of $\pm 2g$, $\pm 4g$, $\pm 8g$, or $\pm 16g$.
- sensitivities of 16384, 8192, 4096, or 2048 LSBs per g.
- output data rate range from 8kHz to 1.25Hz.

E. Ultrasonic sensor

The distance is measured by an ultrasonic sensor through the emission of ultrasonic sound waves and their conversion into electrical signals. They are used in proximity, robotic obstacle detection, manufacturing, and level monitoring. Ultra-sonic technology has applications in medical imaging, tumor identification, and fetal health. The circuit consists of an ultrasonic receiver and transmitter, with the output amplified by a 741 op-amp. Features:



Fig. 4. Ultrasonic sensor

- 5V DC power supply
- 15mA working current
- 15° effectual angle
- 0.3 cm ranging distance
- 30 degree measuring angle

- 10uS TTL pulse width.

F. L293D motor driver IC

The L293D motor driver IC functions based on the Half H-Bridge principle, enabling the operation of motors in both clockwise and anti-clockwise directions. It is essential to ground the ground pins, and two power pins are required: $V_{ss}(V_{cc1})$ for voltage (+5V) and $V_s(V_{cc2})$ for motor voltage (4.5V-36V), which should be connected to +12V. Notable features includes:

- The ability to run two DC motors using the same IC.
- The possibility of speed and direction control.
- The maximum peak motor current is 1.2A.
- The maximum continuous motor current is 600mA.
- This IC is available in 16-pin DIP, TSSOP, and SOIC packages.

IV. RESULT

After our project was finished, we conducted tests on the Head motion controlled wheelchair designed for disabled individuals in various situations, and it performed impeccably. By making simple movements with our head, we were able to effortlessly maneuver the wheelchair in any direction, including forward, backward, left, or right, as well as stop and detect obstacles.

V. CONCLUSION

This automated wheelchair is beneficial for individuals who are unable to move independently. The robotic wheelchair assists quadriplegic individuals in living without additional aid. The integration of accelerometer and gyroscope data guarantees smooth wheelchair movement for quadriplegic patients. Additionally, the cost-effective assembly parts have made this wheelchair more accessible. It was employed to measure the distance of obstacles that obstruct the prototype's path. Utilizing obstacle detection is a valuable application in vehicles, reducing the risk of accidents and saving lives.

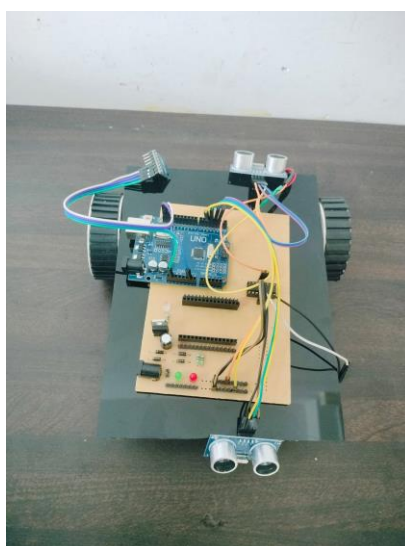


Fig. 5. Head gesture controlled Automatic wheelchair

ACKNOWLEDGEMENT

We express our sincere gratitude to Dr. Jerline Sheeba Anni, Principal, KMCT College of Engineering for Women, for facilitating a congenial academic environment in the college. We extend our thanks to Dr. Sameera V Mohd Sagheer, Mrs. Minilal, and Mrs. Anusha E P for their guidance throughout the project. We appreciate the support they provided at every stage. Additionally, we would like to express our gratitude to everyone involved in the project, including teachers, class-mates, and our families, for their support, dedication, and love.

REFERENCES

- [1] Aleksandar Pajkanovic, Branko Dokic "Wheelchair control by head motion" Vol. 10, No. 1, February 2013, 135-151.
- [2] Mr. Gangadhara, Karthik B K "Gesture Controlled Advanced Wheelchair for Physically Challenged" Reference No.:45SBE1659 June 2014.
- [3] Dulari Sahu "Automatic Camera Based Eye Controlled Wheelchair System Using Raspberry Pi" 2015 International Conference on Innovations in Information, Embedded and Communication Systems (ICIIECS), Coimbatore, India, 2015, pp. 1-6, doi: 10.1109/ICIIECS.2015.7192876.
- [4] Ali Abed "Design of Voice Controlled Smart Wheelchair" International Journal of Computer Applications (0975 – 8887) Volume 131 – No.1, December 2015.
- [5] Losit, Papadakis, Ktistakis "An autonomous intelligent robotic wheelchair to assist people in need" A case study. 1-7. 10.1109/IISA.2015.7388066.
- [6] Mubdi-Ul Alam Sajid; Md Firoz Mahmud "Design of An Intelligent Wheelchair for Handicap People Conducting by Body Movement" Conducting by Body Movement. 10.1109/ICC-CNT49239.2020.9225663 July 2016.
- [7] Konduru Sujana, N. Gunasekhar Reddy "Hand Gesture Controlled Wheelchair using Raspberry Pi and Open CV" SSN 2319-8885 Vol.05, Issue.29 September-2016.
- [8] Saish S. Shinde, Sayli R. Kadam "Hand gesture controlled wheelchair with obstacle detection wireless and GPS technology" IJRET: International Journal of Research in Engineering and Technology eISSN: 2319-1163 — pISSN: 2321-7308.
- [9] Sharmila Ashok Ankur Saini Shubham Choudhary "Solar Powered Multi-Controlled Smart Wheelchair for Disabled: Development and Features" Development and Features. Journal of Computational and Theoretical Nanoscience. 16. 4889-4900. 10.1166/jctn.2019.8401.
- [10] Yoon Ket Lee; Jay Ming Lim "Real time image processing based obstacle avoidance and navigation system for autonomous wheelchair application" 2017 Asia-Pacific Signal and Information Processing Association Annual Summit and Conference (APSIPA ASC), Kuala Lumpur, Malaysia, 2017, pp. 380-385, doi: 10.1109/APSIPA.2017.8282062.
- [11] Prashant Lahane; Swarada Pushkar Adavardkar "Innovative Approach to Control Wheelchair for Disabled People Using BCI," 2018 3rd International Conference for Convergence in Technology (I2CT), Pune, India, 2018, pp. 1-5, doi: 10.1109/I2CT.2018.8529473.

- [12] Pingali TR, Lemaire ED, Baddour N. Ultrasonic Tethering to Enable Side-by-Side Following for Powered Wheelchairs. *Sensors (Basel)*. 2018 Dec 30;19(1):109. doi: 10.3390/s19010109. PMID: 30598029; PMCID: PMC6338950.
- [13] Jigme Wangchuk Machangpa "Head Gesture Controlled Wheelchair for Quadriplegic Patients" *Procedia Computer Science* 132 (2018) 342–351.
- [14] Mohammed Abdul Kader; Md. Eftekhar Alam "Design and implementation of a head motion-controlled semi-autonomous wheelchair for quadriplegic patients based on 3-axis accelerometer". 1-6. 10.1109/IC- CIT48885.2019.903851.
- [15] Huda Farooq Jameel, Salim Latif Mohammed "Wheelchair Control System based on Gyroscope of Wearable Tool for the Disabled" *IOP Conference Series: Materials Science and Engineering*. 745. 012091. 10.1088/1757-899X/745/1/012091.
- [16] Shadman Mahmood Khan Pathan, Wasif Ahmed "Wireless Head Gesture Controlled Robotic Wheel Chair for Physically Disable" Vol.10 No.4, December 2020.
- [17] Saba Anwer ,Asim Waris"Eye and Voice-Controlled Human Machine Interface System for Wheelchairs Using Image Gradient Approach" *Sensors* 2020, 20(19), 5510; <https://doi.org/10.3390/s20195510>.
- [18] Mohammed kutbi , xiaoxue, "Usability Studies of an Egocentric Vision-Based Robotic Wheelchair" *ACM Transactions on Human-Robot Interaction*, Vol. 10, No. 1, Article 4. Publication date: July 2020.
- [19] Aayushi B Thakur, Dr. Shubhangi D C "Design and development of smart solar based wheelchair using voice recognition and head gesture control system" 2020 *IJCRT — Volume 8, Issue 6 June 2020 — ISSN: 2320-2882*.
- [20] Rajdeep Sarkar , Gunjan Ganguly "smart wheelchair with in built health monitoring system" © 2020 *IJCRT — Volume 8, Issue 9 September 2020 — ISSN: 2320-2882* .
- [21] Farah Binte Haque; Tawhid Hossain Shuvo "Head Motion Controlled Wheelchair for Physically Disabled People" 2021 *Second International Conference on Smart Technologies in Computing, Electrical and Electronics (ICSTCEE)*, Bengaluru, India, 2021, pp. 1-6, doi: 10.1109/IC- STCEE54422.2021.9708577.
- [22] Hadish Habte "Stimulation of Eye Tracking Control based Electric Wheelchair Construction by Image Segmentation Algorithm" Article in *Journal of Innovative Image Processing*, published April 2021 Authors Hadish Habte Tesfamikael, Adam Fray, Israel Mengsteab, Adonay Semere, Zebib Amanuel DOI 10.36548/jiip.2021.1.003.
- [23] R. Priyatharshini; S Muthu Selvam "A Voice Controlled and Vision based Smart Wheel Chair for Paralyzed People" 2021 *2nd Global Conference for Advancement in Technology (GCAT)*, Bangalore, India, 2021, pp. 1-6, doi: 10.1109/GCAT52182.2021.9587726.
- [24] Md Abdullah Al Rakib Salah Uddin [22]"Smart Wheelchair with Voice Control for Physically Challenged People" Vol. 6 no 7(2021) ISSN: 2736-576X (Online).
- [25] Muhammad Sheikh Sadi ,ORCID,Mohammed Alotaibi" Finger-Gesture Controlled

Wheelchair with Enabling IoT” Sensors (Basel). 2022 Nov 11;22

(22):8716. doi: 10.3390/s22228716. PMID: 36433326; PMCID: PMC9693444.

Telecom Customer Churn Prediction Using Machine Learning

Akshay Remesh P	Akshay Dath MV	Sanusha AK	Vinaya BR	Asst.prof anjusha MS
Dept of CSE MDIT	Dept of CSE MDIT	Dept of CSE MDIT	Dept of CSE	Dept. of CSE
Kozhikode	Kozhikode	Kozhikode	MDIT Kozhikode	MDIT Kozhikode
Kozhikode, India	Kozhikode, India	Kozhikode, India	Kozhikode, India	Ulliyeri, India
akshayremeshp47@g mail.com	akshaydath4593@g mail.com	Sanushaak2002@g mail.com	vinayabr2002@gm ail.com	mmanjusha@gm ail.com

Abstract—In telcom Sector, Captivating the Customer acquisition channels are becoming more competitive since here Retaining existing customers requires fewer resources. Churn management becomes pivotal in telcom industry. The framework comprises six elements, encompassing data preprocessing, exploratory data analysis (EDA), churn prediction, factor analysis, customer segmentation, and customer behavior analytics. By merging churn prediction and customer segmentation processes, this framework delivers a comprehensive churn analysis to aid telco operators in effectively managing customer churn. The experimentation involves three datasets and employs six machine learning classifiers. Initially, Lot of Machine learning Algorithms are utilized to predict the churn status of customers. To address imbalanced datasets, the Synthetic Minority Oversampling Technique (SMOTE) is employed on the training set. Model assessment is conducted using 10-fold cross-validation, with accuracy and F1-score serving as the metrics for evaluation. After carrying out churn prediction, Bayesian Logistic Regression is used here for performing factor analysis and to determine some important features for segmentation of customer. Here in System, Customer segmentation is done by utilizing K-means clustering

Customers are partitioned to multiple segments, which grants the marketers and decision-making team to execute retention strategies with most precised output.

Index Terms—Data pre-processing, Churn management, Churn prediction, Customer segmentation, Customer behavior analytics.

I. INTRODUCTION

The emergence of 5th Generation technology and the Relocating customer Predeterminations have brought forth a wealth of opportunities for telecommunication (telcom) companies. Massive commerce opportunities have also led to the predatory Contestation in the telcom sector, which linked with a pronounced customer churn rate. It is implemented for telcom operators to develop productive marketing campaigns based on extensive customer analytics to prevent the customer turnover and sustained company revenue. Customer evaluation in the telcom sector which includes two major parts, namely churn prediction and customer segmentation. As telcom sector may tends for being saturated, extreme level enlightenment of captivating new

customers is obsolete to the telecom industry. The outlay for attracting latest clients through investment of abundant resources is confirmed to be substantially higher than that of the continuation costs for current customers

Here, churn management becomes instrumental in telecom industry. Customers who are prone to churn and providing pertinent suggestions based on their aspects. There are two types of methods to reduce customer attrition which are reactive and proactive. Customer churn prediction grants the operators to have a period of time to adopt and execute a series of retention strategical measures before existing customers relocate to other operators. Alternatively, customer segmentation is a crucial determinant in performing customer analytics, which goals customers into many different groups according to the different schemes. The principal segmentation method in the telecom industry is segmentation based on customer value and behaviour. Through effective customer segmentation, telecom operators can provide distinguished products and personalised services and also carry out personalized marketing based on the customer needs and consumption traits in different customer segments.

To support telecom marketers to take enhanced decisions, churn prediction is anticipated to be combined with customer segmentation. Additionally, telecom operators often need more than that of the just predictions about whether the customers will churn or not. They must also need a thorough examination of factors that could contribute to both churn and the overall likelihood of customer churn. Among all customers who are on the verge of churning, during practice, telecom operators are not expected to implement identical strategies for each individual customer. To be more specific, not all customers are of high-value, so that telecom operators should spend more retention resources on those high-valued customers. And for some customers who are not much helpful to company's revenue, telecom operators do not necessarily need to allocate excessive focus to them.

Integrated Customer Churn prediction proposes an integrated Consumer Insights Framework for the supervision of churn in telecom industry, here aspiring this to accomplish the agile resource allocation and increase client retention. The cost of attracting new clients by investing adequate provisions is confirmed that leave far behind the cost of ensuring customer satisfaction [1]. Specifically, Telecom churn prediction imparts enlightenment on customer churn prediction and customer segmentation while combining Bayesian Analysis to merge seamlessly. After Customer Churn Prediction, Bayesian Analysis put into use for selecting important factors and save them into customer segmentation, enhancing the effectiveness of the segmentation process. And the characteristics of each cluster will be examined to deliver preferred recommendations to the operator and lay the groundwork for further counter measures in future. [5] [6] compared the performance of more than 100 classifiers in the churn prediction problem in the telecom industry. To make comparisons and get the best predictive model, [3] performed three experiments on different feature sets with 5 prediction methods, which are Precision, Recall, F1Score, Accuracy and Support. [7] suggests that this model can figure out more of the churn customers, which is very much important in the context of churn management.

II. PROPOSED SYSTEM

The proposed system represents a comprehensive and integrated customer analytics framework designed to tackle the critical issue of churn management in the highly competitive telecommunications (telco) industry. Its primary objective is to enhance customer retention while optimizing the allocation of company resources. At its core, this framework combines two fundamental aspects: churn prediction and customer segmentation. Churn prediction is a predictive modeling component that employs advanced data analysis and machine learning techniques to identify customers who are at risk of leaving the telco service. This predictive capability is invaluable as it allows the telco to take proactive measures, retaining customers before they churn, which is often a more cost-effective strategy compared to acquiring new customers. Concurrently, customer segmentation plays a pivotal role in breaking down the diverse customer base into distinct groups based on shared characteristics, behaviors, or preferences. The most common segmentation method in the telco industry is segmentation based on customer value and behaviour [2]. These segments empower the telco to tailor their retention strategies for each customer group, ensuring that the efforts are specifically tailored and, therefore, more effective. SVM, Random Forest [5], Decision tree, and ANN were used by [1] [4] to predict customer turnover. In the research of [4], Decision Tree were used to predict customer discontinuation. Here they utilized the Synthetic Minority Over-sampling Technique (SMOTE) to rebalance the instances in their dataset.

In addition to churn prediction and customer segmentation, Bayesian Analysis is introduced as an intermediate process within the framework. Bayesian analysis offers a probabilistic approach to modeling relationships between variables, providing a nuanced understanding of the key factors contributing to customer churn. This probabilistic approach is particularly useful in identifying the often multifaceted and interrelated drivers of churn, allowing for a more in-depth analysis of the root causes. With these insights, the telco can develop more precisely targeted retention strategies that directly address the underlying issues that lead customers to churn.

To ensure the effectiveness of the system, various preparatory steps are also integrated. Data pre-processing is vital for cleaning and structuring the data, involving tasks such as handling missing data, removing outliers, and normalizing or scaling features. Clean and well-prepared data is a prerequisite for accurate modeling and analysis. Exploratory Data Analysis (EDA) is another crucial step in the process, where data is visually and statistically explored to uncover trends, patterns, and potential relationships that may not be immediately evident. The insights gained from EDA can guide the subsequent analysis and strategy development.

Factor analysis is yet another essential component, helping to identify latent variables that underlie patterns in the data. It is instrumental in unearthing hidden drivers of churn and customer behavior, which can be crucial in developing retention strategies that target these underlying factors.

The system also includes a customer behavior analytics component, which delves into the analysis of customer interactions with the telco's services. Understanding how customers engage with the telco's offerings and identifying behavioral patterns that may signal potential churn is a pivotal piece of the puzzle. This information can significantly inform the development of tailored

retention strategies that address the specific behaviors and preferences of different customer segments.

A. System Architecture

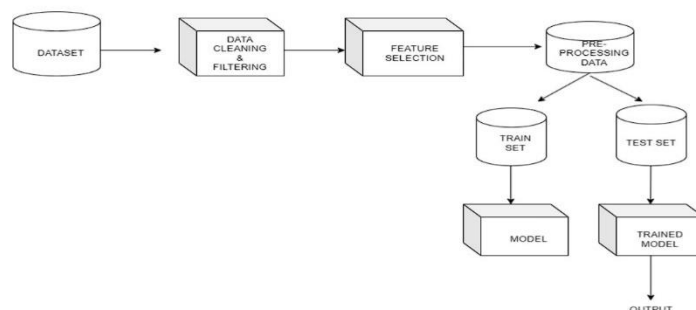


Fig. 1. System Architecture

The Figure 1 explains the entire Strategic architecture of Telecom Customer churn prediction. It begins with a dataset of historical customer data, which is then cleaned and filtered to ensure quality. Key features that could influence customer churn, such as contract details and usage patterns, are selected. This data is pre-processed to fit the requirements of a machine learning model, which is then trained using a portion of the data, known as the training set. The model's performance is evaluated with a test set. Once the model is adequately trained, it can predict potential churn, allowing the telecom company to implement retention strategies. This system [8] is crucial for identifying at-risk customers and reducing churn rates.

III. IMPLEMENTATION

A. Modules

- Admin - The Admin module provides administrative functionalities to manage user accounts within the system. Admins have the capability to add, edit, and delete user accounts as necessary. This module ensures the proper management and control of user access and permissions, maintaining the integrity and security of the system.
- Data entry - The Data Entry module is responsible for capturing and managing customer data within the system. Data entry personnel utilize this module to add new customer information into the database and make necessary edits or deletions when required. This module plays a crucial role in ensuring the accuracy and completeness of customer records, facilitating effective data management processes.
- Tele Callers - The Tele Callers module caters to the needs of telecommunication personnel who engage with customers via phone calls. It provides functionalities such as viewing churn percentage to assess customer retention rates and marking call statuses to track interactions with customers. This module aids tele callers in efficiently managing and monitoring customer communications, contributing to enhanced customer relationship management efforts.

B. Working

The proposed framework aims to address the gaps in current system by combining churn prediction and customer segmentation. The framework includes data cleaning, transformation, and normalization as pre-processing steps. Exploratory data analysis (EDA) is then conducted to better understand the data. Four machine learning classifiers, including Decision Tree, Random Forest, Support Vector Machine and Artificial Neural Network are used for churn prediction. To improve the accuracy and correctness of the prediction Sampling technique is used in this project. Sampling is a technique used to handle the imbalanced dataset. Here two sampling technique are used: SMOTE used in over-sampling and ENN for under-sampling. Then split the sampled dataset into two: train set and test set. Set up specific classifiers at first. Use the feature train and target train to train those classifiers. Utilize a feature test and train model to predict. Utilizing the ground truth target test and the projected target test, calculate accuracy. Preserve the trained model. In SVM and ANN we have to add a extra feature scaling technique standardization to improve the quality and trustworthiness of insights derived from that data. The framework also utilizes factor analysis to identify the key factors contributing to customer churn. By segmenting the churn customers into different groups, the framework enables the development of effective churn management programs and precision marketing strategies. The experimental results show the performance of the framework on three datasets, demonstrating its accuracy and effectiveness in predicting customer churn and providing valuable insights for retention strategies.

IV. FIGURES AND TABLES

A. Class Diagram

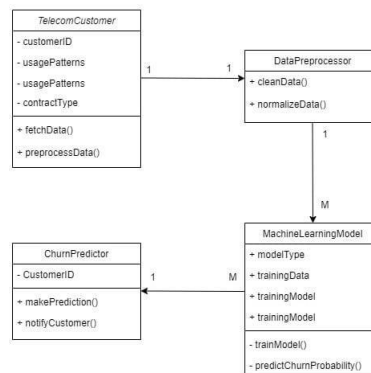


Fig. 2. Class diagram

The figure 2 consists of four classes: Telecom Customer, DataPreprocessor, ChurnPredictor, and MachineLearningModel.

The Telecom Customer class has attributes like customerId, usagePatterns, and contractType, and methods to fetchData() and preprocessData(). This class is associated with the DataPreprocessor class, which is responsible for cleaning and normalizing the data through its cleanData() and normalizeData() methods.

The cleaned data is then fed into the MachineLearning- Model class. This class contains attributes like modelType and trainingData, and methods for trainModel() and predictChurn-Probability(). The model is trained using the cleaned and normalized data.

Finally, the ChurnPredictor class takes the customerId as an attribute and has methods to makePrediction() based on the machine learning model's output and notifyCustomer() about their churn probability. This class interacts with the MachineLearningModel class to make predictions and notify customers.

In summary, this system fetches and preprocesses telecom customer data, uses a machine learning model to predict customer churn, and notifies customers about their churn probability. It's a clear representation of how data flows through a customer churn prediction system in the telecom industry.

Algorithms	Advantages	Disadvantages	Techniques Used
Random Forest	<ul style="list-style-type: none"> Reduces overfitting. Handle missing values. No feature selection. 	<ul style="list-style-type: none"> Complexity. Longer training period. 	Bagging
Decision Tree	<ul style="list-style-type: none"> Easy to understand. Robust to outliers. Automatic feature selection. 	<ul style="list-style-type: none"> Greedy nature. Lack of smoothness. Limited expressiveness. 	Classification and Regression
Support Vector Machine	<ul style="list-style-type: none"> Generalization. Robustness to noise. Handling small datasets. 	<ul style="list-style-type: none"> Choice of kernel. Memory intensive. Computationally expensive. 	Kernel trick
Artificial Neural Network	<ul style="list-style-type: none"> Learningability. Fault tolerance. Parallel processing. 	<ul style="list-style-type: none"> Overfitting. Data requirements. Sensitivity to noise. 	Gradient based methods

Fig. 4. Performance analysis of Algorithms

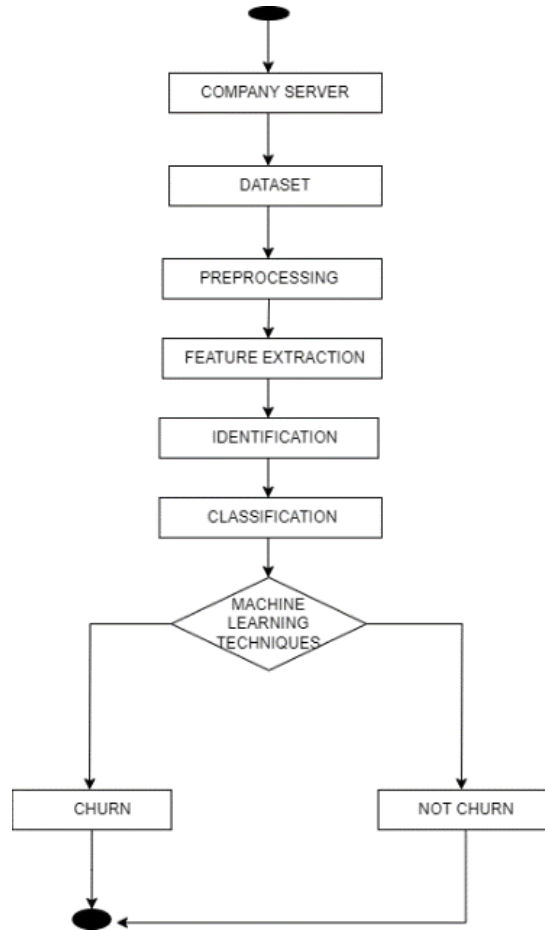


Fig. 3. Activity Diagram

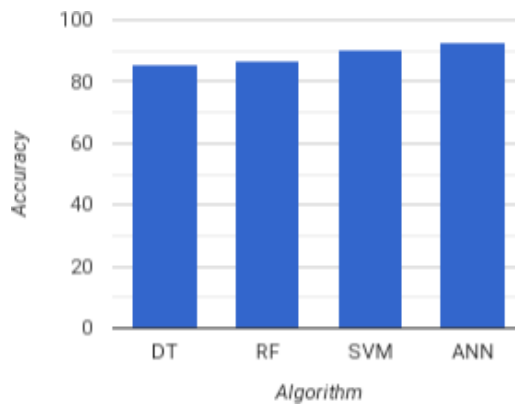


Fig. 5. Performance analysis graph

The figure 3 is the activity diagram for telecom customer churn prediction which describes a systematic process that begins with data collection from the company server. This data is then subjected to preprocessing to ensure it is clean and well-organized. Following this, feature extraction takes place, where significant variables that could influence customer churn are

identified. The identification phase involves analyzing these features to detect patterns or trends that may indicate a likelihood of churn.

Once the relevant features are identified, classification is applied using various machine learning techniques. These techniques are employed to categorize customers into two groups: those likely to churn (labeled as “CHURN”) and those who are not (labeled as “NOT CHURN”). The process is iterative, with feedback from the classification results used to refine the model and improve prediction accuracy. This continuous loop of feedback ensures that the prediction model remains up-to-date and effective in identifying potential churn among telecom customers.

PERFORMANCE ANALYSIS

As in the table mentioned in figure 5 , Precision, recall, f1 score, support, accuracy, and other metrics will be used by the proposed system to compare several machine learning methods, including Decision Tree , Random Forest ,Support Vector Machine and Artificial Neural Network . Comparing artificial neural networks to existing machine learning techniques, they are more accurate.

CONCLUSION

The Unified churn prediction and customer segmentation framework for the telcom business aims to improve customer retention and resource allocation. The framework integrates churn prediction and customer segmentation by utilizing Bayesian Analysis to select important factors for segmentation. It provides insights on customer turnover prediction and analyzes characteristics of each customer cluster to provide recommendations for the telcom operator. The framework achieves high F1-scores and AUC values for different datasets using machine learning classifiers like Decision Tree, Random Forest, SVM and ANN . The overall probability of churning is calculated for each cluster, helping the telco operator identify customers at a higher risk of churn. The framework emphasizes the significance of using sampling for handling imbalanced datasets .It discusses superior evaluation metrics for models. Overall, the framework offers a comprehensive approach to churn management in the telco industry.

ACKNOWLEDGEMENT

We owe our heartfelt gratitude to Almighty for all the blessings showered on us during this project work. We take this opportunity to express our sincere gratitude to all the people who have been instrumental in bringing out this work to the correct form. First off all we express our gratitude to Principal Dr. P M Maheesan and Director Mr. H. Ahinus for the excellent facilities and cordial support provided during the project work. We express our sincere thanks to Head of Department Ms. Nithya V P, Assistant Professor for their exemplary guidance and constant encouragement. We would like to express our immense pleasure and great sense of gratitude towards our project guide Ms Manjusha MS, Assistant Professor and project coordinators Ms. Krishnapriya C and Ms. Nithya VP, Assistant Professors, Department of Computer Science and Engineering for sharing their valuable knowledge and idea for doing our work. We express our thanks to all staff members and friends for all the help and co-

ordination extended in bringing out this project successfully in time. And Finally, We thank our families and friends and all those who helped us directly and indirectly in the completion of our project.

a 10-Days internship at REVERTECH IT Solutions. She was excellent in front-end development.

REFERENCES

- [1] G. Esteves and J. Mendes-Moreira, 'Churn prediction in the telecom business,' in Proc. 11th Int. Conf. Digit. Inf. Manage. (ICDIM), Sep. 2016, pp. 254–259.
- [2] J. Bayer, 'Customer segmentation in the telecommunications industry,' *J. Database Marketing Customer Strategy Manage.*, vol. 17, nos. 3–4, pp. 247–256, Sep. 2010.
- [3] B. Huang, M. T. Kechadi, and B. Buckley, 'Customer churn prediction in telecommunications,' *Expert Syst. Appl.*, vol. 39, no. 1, pp. 1414–1425, Jan. 2012.
- [4] K. Dahiya and S. Bhatia, 'Customer churn analysis in telecom industry,' in Proc. 4th Int. Conf. Rel., Infocom Technol. Optim. (ICRITO), Sep. 2015, pp. 1–6.
- [5] D. D. Adhikary and D. Gupta, 'Applying over 100 classifiers for churn prediction in telecom companies,' *Multimedia Tools Appl.*, vol. 248, pp. 1–22, Aug. 2020.
- [6] A. A. Q. Ahmed and D. Maheswari, "Churn prediction on huge telecom data using hybrid firefly based classification," *Egyptian Informat. J.*, vol. 18, no. 3, pp. 215–220, Nov. 2017.
- [7] U. Ahmed, A. Khan, S. H. Khan, A. Basit, I. U. Haq, and Y. S. Lee, 'Transfer learning and meta classification based deep churn prediction system for telecom industry,' 2019, arXiv:1901.06091 .
- [8] A. Amin, F. Al-Obeidat, B. Shah, A. Adnan, J. Loo, and S. Anwar, "Customer churn prediction in telecommunication industry using data certainty," *J. Bus. Res.*, vol. 94, pp. 290–301, Jan. 2019.

Akshaydath MV is pursuing BTECH in Computer Science and Engineering under APJ Abdul Kalam Technological University (APJKTU) from MDIT, Kozhikode. He has completed a 10-Days internship at REVERTECH IT Solutions.

Akshay Remesh P is currently pursuing his BTECH in Computer Science and Engineering from APJ Abdul Kalam Technological University, MDIT Kozhikode. He has completed a 10-Days internship at REVERTECH IT Solutions and is presently serving as a UI/UX Designer Intern at Topdrove Foundation. Additionally, he has held the position of Technical Coordinator in IEEE at MDIT for 1 year. Akshay also contributed an Office automation website demonstration as a new idea to MDIT.

Sanusha A K is currently enrolled in the BTECH program for Computer Science and Engineering at MDIT, Kozhikode, under the APJ Abdul Kalam Technological University (APJKTU). During her academic journey, she embarked on a 10-Days internship at REVERTECH IT Solutions, where she gained valuable practical experience in the field. Sanusha is passionate about exploring

the intersection of technology and innovation, and she looks forward to leveraging her skills and knowledge to make meaningful contributions in the tech industry.

Vinaya BR is pursuing BTECH in Computer Science and Engineering under APJ Abdul Kalam Technological University (APJKTU) from MDIT, Kozhikode. She has completed

Asst.Professor Manjusha M S with many year of dedicated teaching experience, specializes the field of Computer Science and Engineering with in Data Mining as the Area of interest. As the Project Guide, Asst.prof Manjusha plays a pivotal role in overseeing and supporting the entire project lifecycle. Her unwavering dedication and meticulous attention to detail ensure smooth coordination and efficient progress of research initiatives. Manjusha's commitment to excellence significantly contributes to the success and advancement of projects under her supervision.

Foss folio: A Seamless Event

Operations Platform

Nandagopan P
Dept of CSE
MDIT College of
Engineering
Kozhikode, India
nandagopanp2003@g
mail.com

Sreehari Jayaraj
Dept of CSE
MDIT Kozhikode
Kozhikode, India
sreeharijayaraj03@g
mail.com

Surya N
Dept of CSE
MDIT Kozhikode
Kozhikode, India
suryaparvathi2001@g
mail.com

Swathi P P
Dept of CSE
MDIT Kozhikode
Kozhikode, India
swathivinod70@gm
ail.com

Asst.prof Nithya VP
Dept. of CSE
MDIT Kozhikode
Ulliyeri, India
nithyavp@mdit.ac.in

Abstract—Efficient event coordination is of paramount importance in today's fast-paced world, as it can significantly impact the success of any gathering, from educational events to entertainment functions. In response to this need, the proposed system offers a modern and user-friendly solution that empowers organizations to effortlessly register and create multiple events through dedicated dashboards. With a strong focus on catering to students and a diverse user base, this system is designed to serve as a catalyst for improved collaboration, engagement, and overall event planning practices. It places a particular emphasis on student-centric event discovery, ensuring that events are tailored to the specific interests and needs of the student community. The system also facilitates seamless financial transactions for paid events and incorporates QR-enhanced ticketing to enhance the attendee experience, ensuring easy ticket generation and verification via a dedicated mobile app. Moreover, the system provides secure collaboration through Role-Based Access Control and leverages AI-driven event materials to enhance engagement and visibility. Built as a cloud-based platform with universal accessibility and a user-friendly interface, it is poised to transform event coordination into a more efficient and engaging process.

Index Terms—Event Coordination, Collaboration, Role-Based Access Control, AI-Driven, Cloud-Based, Universal Accessibility

I. INTRODUCTION

In today's fast-paced world, marked by the ever-growing importance of connectivity and collaboration, the demand for streamlined event management has reached unprecedented heights. From pivotal meetings to international conferences, exhilarating hackathons, spirited

competitions, and enriching educational initiatives like technical fests, the need for a comprehensive event management application has become more evident than ever. The current landscape underscores the vital role of seamless coordination, whether it occurs in the physical or virtual realm, in ensuring the success of these diverse events. This is where the proposed system comes into play, offering a web application that not only provides versatile solutions for students, emphasizing student-centric event discovery, but also extends its utility to a broader user base.

In an environment where college campuses and the broader community host an abundance of events, including hackathons and student-focused activities, the centralized platform serves as a vital hub for event information. It empowers students to discover, engage, and actively participate in these events, acting as a bridge between their aspirations and opportunities. Simultaneously, it caters to the needs of event organizers from various backgrounds, providing efficiency, seamless collaboration, and enhanced user experiences. In a world where effective event management is crucial, the proposed system emerges as a cornerstone for effortless coordination, enriching the experiences of students and a diverse spectrum of event organizers alike.

II. PROPOSED SYSTEM

A. Introduction

The proposed system is an innovative event management application strategically crafted to meet the distinctive needs of students while retaining flexibility for hosting diverse events. At its core, the application facilitates organizational administrators in effortlessly creating and managing organizations, inviting team members for collaborative event planning. Admins have the capability to update, delete, and oversee organizations, while team members, working in tandem with administrators, can collectively create and manage events, presenting a comprehensive solution for streamlined event management. Central to the system is a comprehensive dashboard tailored for administrators and team members. This dashboard offers insights into participant details, team information, aids in event description development using AI tools, and provides a real-time overview of revenue details. Functioning as a centralized hub, this dashboard enhances organizational efficiency and serves as a pivotal tool for effective event management. Concurrently, the system addresses the student-centric event discovery process, ensuring participants can easily search and discover events aligned with their interests. To fortify secure collaboration, the system incorporates Role-Based Access Control [3], granting administrators and team members distinct levels of access for heightened control and security. Moreover, the system integrates a robust payment gateway through Stripe, ensuring secure payment processing and real-time revenue tracking. This feature enhances financial management for event organizers, providing a seamless and secure transaction experience. Additionally, the proposed system includes a dedicated mobile app, further elevating attendee experiences. This app facilitates swift ticket generation, QR code verification, and offers convenient access to event details. As a cloud-based platform with a user-friendly interface, the system ensures universal accessibility, making it a comprehensive solution that aligns administrative tools with participant-centric features.

B. Process Design

The chosen design pattern for the project is the Model-View-Controller (MVC) pattern, a widely adopted pattern in modern web development [6]. In this context, the web and mobile applications serve as the View, displaying information from the model (PostgreSQL database). The backend acts as the Controller, managing user interactions and modifying data accordingly, while the PostgreSQL [7] database serves as the Model, handling data management and logic independently of the user interface. This structure aligns with the liquid architecture manifesto, accommodating multiple implementations such as web and mobile versions. The synchronization of application data is facilitated through a unified repository, specifically the PostgreSQL database. This approach allows users to seamlessly switch between devices while maintaining consistent data representation. The project components interaction is represented in figure 4.1. Another approach that was used to support liquid architecture is responsive web design (RWD). RWD need to render well all web page data on a different devices regardless of the screen size and type of device. The main idea for the responsive web design was in creating several views for one web page. These web page views depended on the current screen size of the device from which the page display request was came [1]. And the modern stylistics of the web page - tailwind css [8] allows to achieve RWD using a minimum of effort for this.

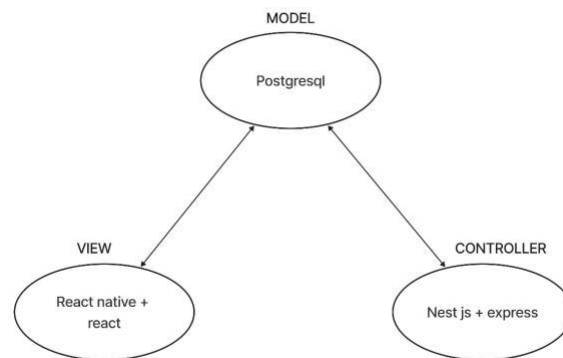


Fig. 1. System Architecture

III. IMPLEMENTATION

A. Module Description

There are 3 modules: Participant, Admin, Team Member 1) Participant:

- Login with required credentials.
- Create and Update profile .
- Search and view events.
- Student-centric event discovery.
- Event registration.

- Payment processing for paid events.

2) Admin:

- Login with required credentials.
- Organization management, including creation, update, and deletion.
- Role-based access control to invite team members and manage their permissions.
- Access to event dashboard .
- Event dashboard must include registration and revenue details, event statistics, and an AI tool for generating event descriptions.
- Event management, including creation, update, and deletion.
- Remove participants or team members.
- Delete organisation.

3) Team Member:

- Login with required credentials.
- Event management, including creation, update, and deletion.
- Access to event dashboard . B. Working

1) Authentication and Authorization: Authentication within the system relies on Google OAuth2 [9], providing a secure and standardized process to verify user identities. This authentication mechanism ensures a robust and trustworthy user validation, instilling confidence in user interactions. For authorization, the system utilizes cookies and sessions. These components work in tandem, enabling the system to grant users specific roles, such as Admin, Team members, or Participants, based on their permissions. Cookies store authentication tokens, and sessions maintain user states, allowing for persistent and secure authorization across different system functionalities. This role-based approach ensures that users only access features aligned with their assigned roles, enhancing overall security and control within the application. The combination of Google OAuth2 for authentication and cookies/sessions for authorization creates a comprehensive and reliable user verification and access control system [10].

2) Role-Based Access Control (RBAC): The application implements Role-Based Access Control (RBAC) [3] to ensure that users only have access to features and functionalities aligned with their assigned roles. This approach significantly enhances overall security and control within the application. Specific roles such as Admin, Editor, Viewer, and No Access are defined, each with corresponding permissions tailored to their responsibilities. An object is created to map roles to permissions using boolean flags, allowing for clear and granular control over user capabilities. Additionally, a custom hook called useRoles is developed to determine user permissions based on their assigned role. This hook seamlessly integrates into various components of the application, enforcing access control consistently throughout the user experience. Fallback mechanisms are implemented in cases where roles are undefined or unrecognized, ensuring that access restrictions are enforced appropriately.

This comprehensive implementation of RBAC strengthens the application's security posture and ensures that users interact with functionalities pertinent to their roles, enhancing both usability

and data protection. Once roles such as Editor or Viewer are assigned to team members by the organization's admin, an automated email invitation is sent to them using an integrated email service provider's API. This email contains a unique link that, upon clicking, directs recipients to a login page within the application. From this login page, team members can seamlessly join the organization using their Google or GitHub accounts, leveraging familiar authentication methods for convenience and security. This streamlined process ensures that team members receive their role assignments promptly and facilitates easy access to the organization's platform, enhancing overall collaboration and productivity.

3) Event Publication, Ticket Generation, and Management: The event publication, ticket generation, and management system have been seamlessly integrated into the platform to enhance the overall experience for both administrators and participants. Administrators have access to a user-friendly form that allows them to create and publish events effortlessly. Simultaneously, unique tickets are generated automatically for each event, and their details, including ticket IDs, are securely stored in a database.

For ticket generation, JavaScript libraries specifically designed for QR code generation have been implemented. Each ticket is assigned a unique QR code that encapsulates all necessary information about the event, such as event name, date, time, and venue. This QR code serves as a digital representation of the ticket and can be easily scanned for validation purposes during the event.

Participants can access their tickets conveniently through the "My Tickets" page on the platform. Here, they can view and manage all their tickets, including details such as event name, ticket ID, and the QR code itself. The inclusion of QR codes not only simplifies the check-in process during events but also adds an extra layer of security by making each ticket uniquely identifiable.

4) Mobile App Integration for Entry Regulation : A

A mobile app was also developed specifically for entry regulation into events, providing a convenient solution for organizers to authenticate attendees by scanning the QR codes of their tickets. To implement this functionality, React Native [11] was utilized within the development environment and a new project was initialized using Expo for streamlined development and deployment processes. Additionally, a QR code scanning library such as react-native-qrcode-scanner [12] was integrated into the app to enable efficient scanning of QR codes.

A dedicated component was created within the app to handle the QR code scanning process seamlessly. This component interacts with the installed library to access the device's camera and scan QR codes effectively. Furthermore, the app was designed to request permission from users to access the camera, ensuring compliance with privacy and security standards.

On the web app side, QR codes containing ticket information were generated and displayed for attendees. These QR codes serve as digital tickets and are scanned by organizers using the

mobile app during entry regulation processes. This integration of a mobile app for QR code scanning adds an extra layer of security and convenience, allowing organizers to authenticate attendees swiftly and accurately during events.

5) Form Builder for Custom Forms : A comprehensive Form Builder module was developed to facilitate the creation of custom forms with ease and efficiency in the web application. The core design involved the development of a robust data structure that represents the form schema. This schema was implemented using a stack-based approach, allowing for efficient organization and management of form fields. Each form field was represented within the schema with pertinent properties such as type (e.g., text input, dropdown, checkbox) and validation rules (e.g., required, minimum length, format constraints). This ensured that the Form Builder could accommodate a wide range of form field types and enforce necessary validation criteria for data integrity. One of the key features of the Form Builder was its real-time synchronization capability. As users modified form fields or made changes to the schema, the stack structure underlying the Form Builder was dynamically updated to reflect these modifications. This ensured that changes were immediately propagated throughout the form-building process, providing users with a seamless and responsive experience.

The Form Builder leveraged React components for dynamic rendering, iterating through the stack structure to display form fields accordingly. This dynamic rendering approach enabled immediate UI updates as users added, removed, or adjusted form fields. For instance, adding a new field to the schema would result in the Form Builder instantly displaying the corresponding input element on the form UI. Overall, the Form Builder module significantly enhanced the web application's capabilities by empowering users to create custom forms effortlessly. Its intuitive design, real-time synchronization, and dynamic rendering features contributed to a seamless form-building experience, making it a valuable addition to the project.

AI Supported Event Description Generation: For AI-supported event description generation, the Mistral AI [13] model was integrated into the web application to provide advanced natural language processing capabilities. To begin, the system registered on Mistral AI and obtained an API key for authentication, enabling secure access to the model's functionalities. Next, the Mistral AI model was seamlessly incorporated directly into the frontend of the website using JavaScript. This integration allowed leveraging Mistral AI's powerful language generation capabilities within the application.

With the Mistral AI model integrated, requests were made to its endpoint using the API key obtained during registration. These requests were made to generate event descriptions based on specified parameters and inputs. The generated event descriptions were then displayed on the frontend of the website, providing users with dynamically generated and contextually relevant content for event descriptions. This approach not only enhances the efficiency of creating event descriptions but also ensures consistency and quality in the generated content, ultimately improving the overall user experience.

7) Storage Solution with Amazon S3: A robust storage solution using Amazon S3 (Simple Storage Service) [14] was implemented to efficiently manage and store various types of files, including event descriptions and form submissions. The integration process began with the incorporation of the Amazon S3 SDK into the web application. This SDK provided the necessary tools and functionalities to interact with S3 buckets seamlessly. Once the SDK was integrated, files could be uploaded directly to the designated S3 buckets from within the application. For example, when generating event descriptions using Mistral AI or processing form submissions from users, the resulting files were automatically stored in the respective S3 bucket. This ensured that all relevant data, such as event details or user inputs, were securely stored in a centralized location.

One of the key benefits of using Amazon S3 for storage is its scalability and reliability. S3 buckets can accommodate a large volume of files and are designed to provide high availability and durability. This means that the application can handle varying levels of data storage requirements without compromising performance or data integrity. Additionally, the integration with Amazon S3 enabled efficient data retrieval when needed. Files stored in S3 buckets can be easily accessed and retrieved by authorized users or processes within the application, streamlining the data management workflow.

8) Payment Gateway Integration: Integrating Stripe [15] into the web application for payment processing involved a structured approach to ensure secure and efficient transactions. Initially, a Stripe account was created to gain access to the Stripe Dashboard, where API keys crucial for communication with Stripe's API were obtained. These keys, including a publishable key for client-side interactions and a secret key for server-side operations, were securely managed to maintain the integrity of the payment system. On the client-side of the web application, Stripe Elements were integrated, which are pre-built UI components provided by Stripe. These elements, such as payment forms and card input fields, were seamlessly integrated into the frontend to enhance the user experience and ensure PCI compliance. By leveraging Stripe's client-side JavaScript library, encrypted communication of payment information was facilitated, generating a payment token to be sent securely to Stripe for processing.

Concurrently, on the server-side of the application, logic was developed to handle payment processing using Stripe's API. This included utilizing the secret API key for authentication and interacting with Stripe's servers to charge users' cards and process payments. Error handling mechanisms were implemented to manage responses from Stripe's API, providing users with clear feedback regarding payment success or any encountered issues. Thorough testing was conducted throughout the integration process to validate the functionality of the payment system. It was ensured that payments were processed accurately, and sensitive data handling adhered to industry standards and best practices. Stripe's robust security measures, such as PCI compliance and tokenization, were leveraged to safeguard user payment information and maintain a high level of security throughout the payment process.

IV. FIGURES AND TABLES

A. Class Diagram

A class diagram is an essential component of object-oriented modeling, providing a comprehensive overview of a software system's structure. It visualizes the system's classes, their attributes, operations (or methods), and the relationships among objects. Classes serve as blueprints for creating objects, encapsulating both data (attributes) and behavior (methods) related to specific entities or concepts within the software. Attributes define the characteristics or state of objects, while operations represent the actions objects can perform, such as manipulating attributes or interacting with other classes. Class diagrams are a fundamental part of the Unified Modeling Language (UML), a standardized notation for software design. They are used not only during the initial design phase but also throughout the software development lifecycle for documentation, communication, and maintenance purposes.

In addition to depicting class internals, class diagrams illustrate various relationships that contribute to system functionality. These relationships include inheritance, association, aggregation, and composition. Inheritance signifies a hierarchical "is-a" relationship, where one class inherits attributes and methods from another, establishing a specialization-generalization hierarchy. Associations denote bi-directional connections between classes, indicating that objects from one class are related to objects from another. Aggregation and composition represent whole-part relationships, with aggregation indicating that a class contains or is composed of other classes, and composition signifying stronger ownership semantics. Our system comprises 8 classes, which are account, admin, team member, participant, organization, event, dashboard, and payment.

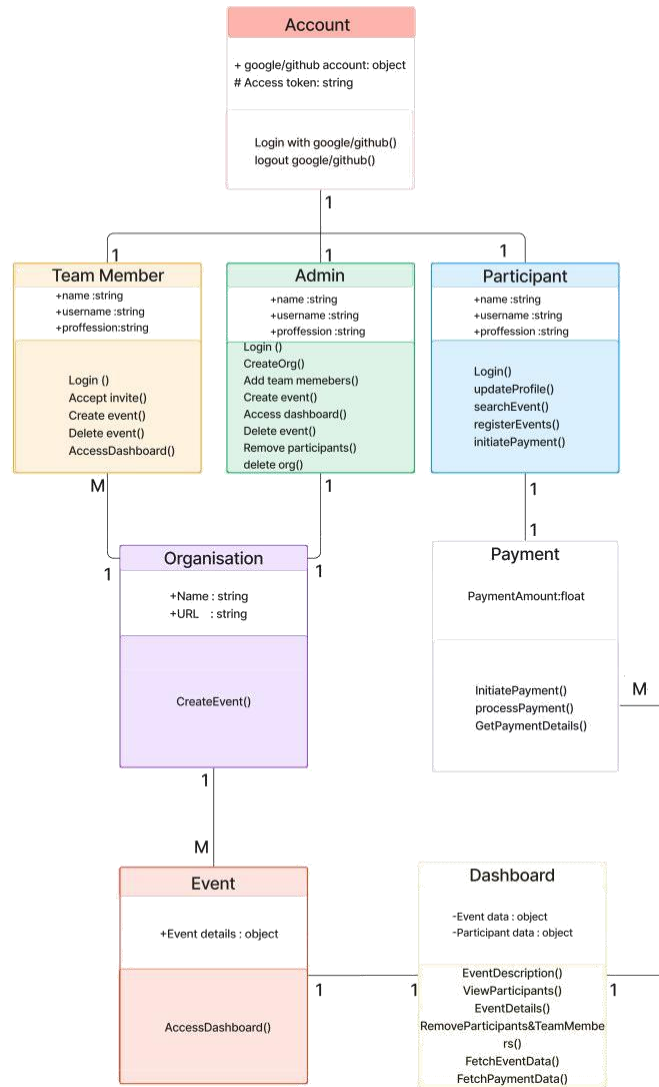


Fig. 2. Class diagram

B. Activity Diagram

The activity diagram in our system serves as a visual roadmap illustrating the dynamic behavior and interactions among the three main modules: Admin, Team Member, and Participants. Each module is depicted as a distinct swimlane in the diagram, showcasing the activities they perform and how they interact with each other during the system’s operation.

By mapping out the activities and their flow, the activity dia-gram provides a comprehensive view of how users and system components interact, ensuring clarity in system functionality and facilitating effective communication among stakeholders and developers.

The diagram’s use of symbols such as action states, deci-sion points, and transitions helps in capturing the logic and sequence of activities, making it an essential tool for system design, analysis, and refinement throughout the software de-velopment lifecycle.

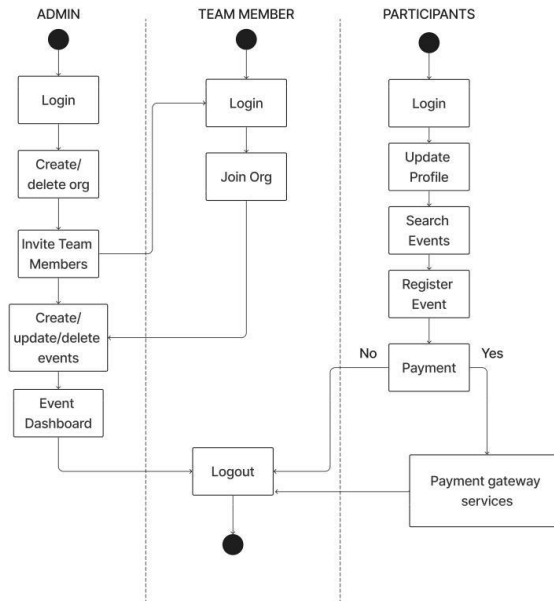


Fig. 3. Activity Diagram

V. PERFORMANCE ANALYSIS

Website performance encapsulates the speed at which a website loads and operates within a web browser, along with critical dimensions such as usability, interactivity, and reliability, which collectively define the user experience. The image given below is a screenshot of our website performance analysis tool called PageSpeed Insights [16]. The tool is by Google and it analyzes the performance of a website on both mobile and desktop devices. The analysis shows that the website is performing well. It has a score of 100 for performance on the device. Here is a breakdown of the score

Desktop :

- Performance: 100
- Accessibility: 92
- Best Practices: 96
- SEO: 100

Overall, the website is performing well according to Google's PageSpeed Insights tool. Here are some additional things to keep in mind about website performance: Website performance can affect SEO (search engine optimization). A website that performs well is more likely to rank higher in search results. Website performance can also affect user experience. A web-site that loads slowly is likely to frustrate users and cause them to leave the site.

CONCLUSION

In the dynamic realm of event management, simplicity and efficiency are paramount. Recognizing the need for seamless event creation and hosting, we've developed a comprehensive solution that empowers users to orchestrate events effortlessly. Our platform not only streamlines the event planning process but also ensures a smooth experience for both organizers and participants. With a special focus on hosting college events such as tech-fests and hackathons, we cater to the specific needs of student organizers, providing tailored features to enhance their planning experience. Furthermore, with the integration of a secure payment gateway and the development of a user-friendly mobile app, we've elevated the functionality and accessibility of our system. Now, organizers can manage their events with ease, while participants can engage and register with convenience. By combining these features into a single, cohesive platform, we're revolutionizing the event management landscape, setting a new standard for efficiency and user satisfaction.

ACKNOWLEDGEMENT

First of all we express our gratitude to Principal Dr. P M Maheesan and Director Mr. H. Ahinus for the excellent facilities and cordial support provided during the project work.

We express our sincere thanks to Head of Department Ms. Nithya V P, Assistant Professor for their exemplary guidance and constant encouragement.

We would like to express our immense pleasure and great sense of gratitude towards our project guide Ms. Nithya V P, Assistant Professor and project coordinators Ms. Kr-ishnapriya C and Ms. Nithya V P, Assistant Professors, Department of Computer Science and Engineering for sharing their valuable knowledge and idea for doing our work

We express our thanks to all staff members and friends for all the help and co-ordination extended in bringing out this project successfully in time.

And finally, We thank our families and friends and all those who helped us directly and indirectly in the completion of our project.

REFERENCES

- [1] R. Khatipov, A. Negimatshanov, I. Zamaleev, A. Zakirov, M. Mazzara and V. Rivera, "Hikester - The Event Management Application," 2018 32nd International Conference on Advanced Information Networking and Applications Workshops (WAINA), Krakow, Poland, 2018, pp. 462-468, doi: 10.1109/WAINA.2018.00129.
- [2] S. Islam, R. Majumder, S. Sultana, S. Nasrin and R. Islam, "Toward a Generic Event Management System for Academia," 2019 5th International Conference on Advances in Electrical Engineering (ICAEE), Dhaka, Bangladesh, 2019, pp. 706-711, doi: 10.1109/ICAEE48663.2019.8975626.
- [3] R. S. Sandhu, E. J. Coyne, H. L. Feinstein and C. E. Youman, "Role-based access control models," in *Computer*, vol. 29, no. 2, pp. 38-47, Feb. 1996, doi: 10.1109/2.485845

- [4] A. Gal and J. Mylopoulos, "Toward Web-based application management systems," in IEEE Transactions on Knowledge and Data Engineering, vol. 13, no. 4, pp. 683-702, July-Aug. 2001, doi: 10.1109/69.940740.
- [5] Arsheen Khan, Aarti Pundlik, Tanvi Shinde, Sneha Gupta, S.T. Patil, "Event Management System", International Research Journal of Engineering and Technology (IRJET), Volume: 06 Issue: 01 — Jan 2019.
- [6] Rober Morales-Chaparro, Marino Linaje, Juan Preciado, and Fernando S´anchez-Figueroa. Mvc web design patterns and rich internet applications. 01 2007.
- [7] <https://aws.amazon.com/rds/postgresql/what-is-postgresql/>
- [8] <https://tailwindcss.com/docs/responsive-design>
- [9] <https://developers.google.com/identity/protocols/oauth2>
- [10] <https://kubernetes.io/docs/reference/access-authn-authz/rbac/>
- [11] <https://reactnative.dev/docs/getting-started>
- [12] <https://www.npmjs.com/package/react-native-qrcode-scanner>
- [13] <https://docs.mistral.ai/>
- [14] <https://docs.aws.amazon.com/AmazonS3/latest/userguide/Welcome.html>
- [15] <https://docs.stripe.com/>
- [16] <https://developers.google.com/speed/docs/insights/v5/about>

AR Menu Fusion: Seamless Dining With Augmented Reality

Adarsh K E	Gautham Unni T K	Vishnu P	Yaser Arafath
Dept of CSE	Dept of CSE	Dept of CSE	Dept of CSE
MDIT Kozhikode	MDIT Kozhikode	MDIT Kozhikode	MDIT Kozhikode
Kozhikode, India	Kozhikode, India	Kozhikode, India	Kozhikode, India
adarshke50@gmail.com	gauthamunnitk@gmail.com	vishnup.2107@gmail.com	yaserarafath987@gmail.com

Sona NM
Asst. Prof
Dept. of CSE
MDIT Kozhikode
Ulliyeri, India
sona@mdit.ac.in

Abstract—In the realm of modern dining experiences, “AR Menu Fusion” emerges as a transformative project, introducing augmented reality (AR) to redefine how patrons engage with restaurant menus. The innovative approach involves a simple yet powerful concept: customers can scan a QR code at their table using their mobile devices, unlocking a captivating AR-enhanced menu. This immersive experience allows diners to explore each dish in augmented reality, providing a visual and interactive preview before making their culinary selections.

The methodology of [2] AR Menu Fusion leverages cutting-edge AR frameworks, ensuring a seamless integration between the physical dining space and digital content. By strategically incorporating AR elements into menu design, users gain access to a wealth of information about each dish, from detailed visualizations to ingredient insights. This approach not only enhances customer interaction but also empowers patrons to make informed and delightful choices, contributing to an overall elevated dining experience.

The advantages of AR Menu Fusion are clear. It fosters heightened customer engagement by offering an interactive and visually appealing menu interface. The ability to virtually explore dishes before ordering enhances the decision-making process, providing a unique and informative dimension to the dining encounter. Despite potential challenges related to technical infrastructure and user adoption, AR Menu Fusion stands as a trailblazing project, pushing the boundaries of dining innovation. In essence, AR Menu Fusion envisions a future where augmented reality seamlessly integrates with culinary exploration, creating a delightful and memorable dining adventure for all.

Index Terms—Augmented Reality, Digital Food Menu, Restaurant Management System, 3D Visualization, Food Service Innovation.

I. INTRODUCTION

In the dynamic landscape of contemporary dining, the project "AR Menu Fusion" [2] introduces a groundbreaking paradigm shift by seamlessly integrating [4] augmented reality (AR) technology into the restaurant menu experience. This innovative endeavor redefines how patrons interact with menus, offering an immersive and interactive journey through the culinary offerings of a restaurant. With a simple QR code scan at the table, customers unlock a new dimension of dining, where the physical and digital worlds converge to elevate the overall gastronomic adventure.

The project's methodology is rooted in the strategic incorporation of cutting-edge AR frameworks, ensuring a harmonious blend of the physical dining environment and digital enhancements. Through a thoughtfully designed menu infused with AR elements, users gain access to captivating visualizations and comprehensive information about each dish. This approach transcends traditional menu formats, fostering informed decision-making and transforming the act of choosing a dish into an engaging and delightful experience.

AR Menu Fusion brings forth a multitude of advantages, fostering heightened customer engagement, informed decision-making, and an overall enhanced dining experience. While potential challenges in technical infrastructure and user adoption may arise, the project stands as a testament to the limitless possibilities when technology intersects with culinary exploration. AR Menu Fusion envisions a future where augmented reality seamlessly integrates with the dining experience, leaving an indelible mark on the way we perceive and engage with restaurant menus.

II. PROPOSED SYSTEM

The proposed system for AR Menu Fusion revolutionizes the dining experience through the integration of augmented reality technology. At its core, the system consists of an [7] [8] Augmented Reality (AR) application designed to enhance user interaction with virtual [2] [3] 3D models of food items. This application leverages the camera of a smartphone or tablet to overlay digital content onto the physical environment, allowing users to visualize menu items in a realistic and immersive manner.

Complementing the AR application is a comprehensive digital food menu accessible to users within the AR interface. This menu offers detailed descriptions, images, and pricing information for a wide range of food items available at the restaurant. By integrating the digital menu with augmented reality, AR Menu Fusion provides users with a dynamic and engaging platform for exploring menu offerings.

Central to the system's functionality are image targets strategically placed throughout the restaurant. These image targets serve as markers for the AR application, enabling it to recognize specific locations within the physical space. When users point their device's camera at these image

targets, the AR application detects them and superimposes virtual food items onto the real-world environment, creating an interactive and visually compelling experience.

AR Menu Fusion also features an interactive ordering system that allows users to place orders directly from the AR application. With just a few taps on the screen, customers can browse the digital menu, select items of interest, and add them to their order. The system seamlessly integrates with a backend database to ensure accuracy and efficiency in order processing, providing users with a convenient and streamlined ordering experience. Additionally, the system includes a chatbot feature that offers assistance and recommendations to users, enhancing overall customer satisfaction and engagement. Through the innovative integration of augmented reality, digital menus, and interactive ordering capabilities, AR Menu Fusion redefines the traditional restaurant experience, offering users a novel and immersive dining experience.

A. System Architecture

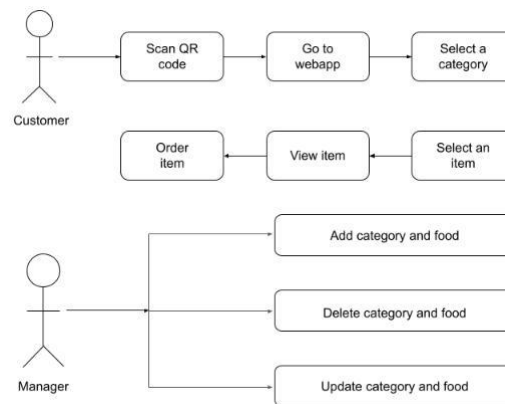


Fig. 1. System Architecture

The Figure 1 delineated through two principal diagrams. the Customer diagram and the Manager diagram. The Customer diagram illustrates the seamless journey a customer undergoes while engaging with the AR Menu Fusion application. It commences with the customer scanning a QR code, which seamlessly directs them to the web application. From there, customers can effortlessly navigate through food categories, select specific items of interest, view comprehensive details about each item, and subsequently proceed to order their desired food items. Conversely, the Manager diagram encapsulates the functionalities available to the management side of AR Menu Fusion. Managers wield the capability to seamlessly add, delete, and update both food categories and individual food items, thereby ensuring the menu remains current and reflective of the restaurant's offerings.

III. IMPLEMENTATION

A. Modules

- Customer - The Customer module of AR Menu Fusion is designed to facilitate a seamless and engaging dining experience for patrons. Customers begin by scanning a QR code conveniently

placed on their table, which instantly directs them to the AR Menu Fusion web application. Within the application, customers are pre-sented with intuitive navigation options to explore various food categories and select individual items of interest. Detailed descriptions and visual representations of each menu item enhance the browsing experience, allowing customers to make informed decisions. Once a selection is made, customers can effortlessly place their orders directly through the application, streamlining the entire ordering process. Overall, the Customer module aims to enhance customer satisfaction and streamline the food ordering experience through intuitive design and user-friendly features.

- **Manager** - The Manager module of AR Menu Fusion em-powers restaurant management to efficiently oversee and manage menu offerings, ensuring a seamless operational workflow. Managers have access to a comprehensive set of tools and functionalities to manage food categories and individual menu items. They can easily add new categories or items, update existing ones, and remove outdated offerings as needed. Additionally, the Manager module provides insights into customer preferences and ordering trends, enabling managers to make data-driven decisions to optimize menu offerings and enhance cus-tomer satisfaction. Through the Manager module, restau-rant management can maintain a dynamic and up-to-date menu, catering to evolving customer preferences and maximizing operational efficiency.

B. Working

The AR Menu Fusion system operates seamlessly to enhance the dining experience for customers while streamlin-ing operations for restaurant management.

For customers, the process begins with scanning a QR code placed on their table using their smartphone. This action di-rects them to the AR Menu Fusion web application, where they can explore various food categories and select individual items of interest. The augmented reality feature allows customers to view realistic 3D models of menu items, enhancing their visual experience and aiding in decision-making. Once a selection is made, customers can conveniently place their orders directly through the application, eliminating the need for traditional paper menus and manual order-taking processes.

On the management side, the AR Menu Fusion system provides restaurant managers with a comprehensive set of tools to efficiently manage menu offerings and operations. Managers bean easily add, update, or remove food categories and items as needed, ensuring that the menu remains dynamic and up-to-date. Additionally, the system provides valuable insights into customer preferences and ordering trends, enabling managers to make data-driven decisions to optimize menu offerings and enhance overall customer satisfaction.

IV. FIGURES AND TABLES

A. Class Diagram

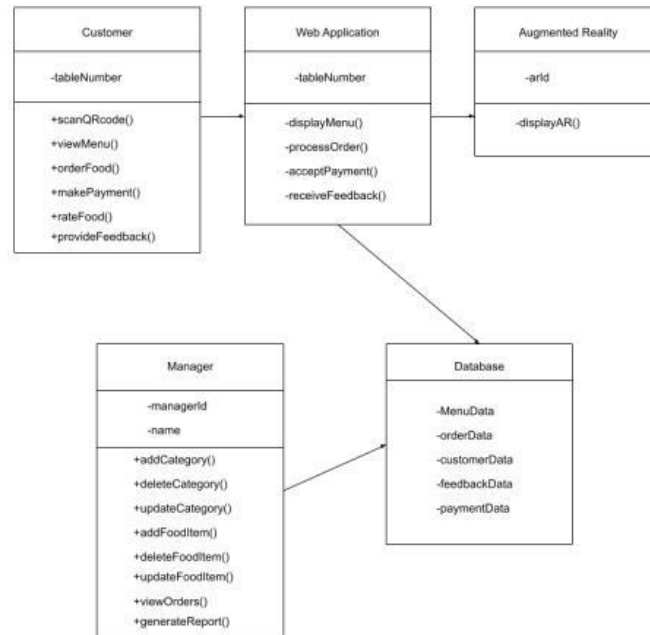


Fig. 2. Class diagram

The figure 2 illustrates the fundamental components of the AR Menu Fusion system, comprising five essential classes: Customer, Web Application, Augmented Reality, Manager, and Database. Each class contributes distinct functionalities crucial to the seamless operation of the system. The Customer class encompasses features tailored to enhance the customer experience, such as scanning QR codes, exploring menus, and placing orders. Concurrently, interactions with the Web Application class facilitate essential processes like payment acceptance and feedback reception, ensuring a smooth trans-action flow for users. Augmented Reality further enriches the user journey by providing immersive visualizations of food items, enhancing the overall dining experience.

On the management front, the Manager class empowers restaurant personnel to efficiently oversee food categories and items, while the Database class serves as the central repository for critical data storage and retrieval. Together, these classes form a cohesive framework that enables seamless interac-tions between customers, restaurant staff, and the underlying database infrastructure. Through effective collaboration and interaction, the AR Menu Fusion [1] [2] system delivers a sophisticated yet user-friendly platform that revolutionizes the dining experience for customers and streamlines operations for restaurant management.

B. Activity Diagram

The figure 3 is the activity diagram for the AR Menu Fusion system, illustrating the sequential flow of actions involved in the user journey within the application. It begins with the

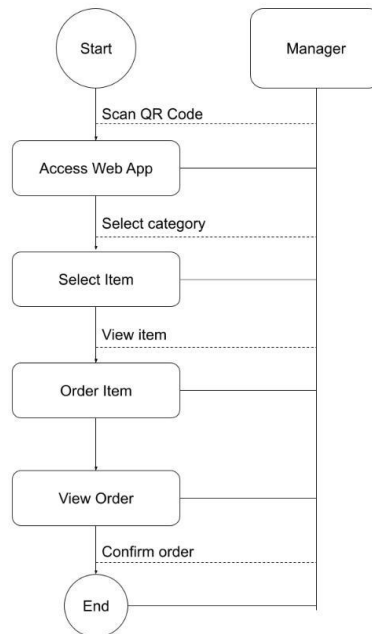


Fig. 3. Activity Diagram

“Start” node, where the user initiates the process by scanning the QR code to access the web application. From there, the user proceeds to select a food category, followed by choosing a specific item from the menu. Subsequently, the user views the selected item before placing an order. Once the order is confirmed, the user can view the order details before reaching the “End” node, indicating the completion of the process.

This activity diagram provides a clear visualization of the steps involved in the user interaction with the AR Menu Fusion system, guiding users through the process of browsing the menu, selecting items, and [5] [6] placing orders seamlessly. It highlights the logical flow of actions, ensuring a user-friendly experience and efficient navigation within the application.

PERFORMANCE ANALYSIS

As in the first graph mentioned in figure 4 we analyze the error rates in order processing between the AR Menu Fusion system and traditional restaurant systems as the number of customers escalates. In traditional systems, the likelihood of order errors notably amplifies with an increasing number of customers, reflecting the challenges associated with manual order-taking processes. However, in the AR Menu Fusion system, the impact of customer volume on order accuracy is minimal, indicating the system’s capacity to maintain order precision even during peak

periods. This underscores the efficiency and reliability of the AR Menu Fusion system in mitigating order errors, thereby enhancing overall customer satisfaction and dining experience.

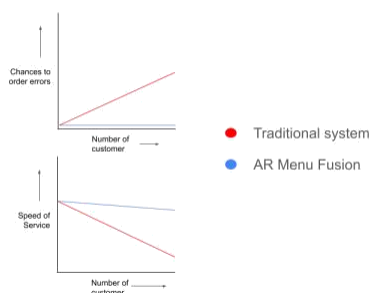


Fig. 4. Performance analysis

In the second graph, also presented in Figure 4, we delve into the speed of service concerning the number of customers served by both the AR Menu Fusion system and traditional restaurant systems. In traditional systems, the speed of service markedly declines as the number of customers rises, often resulting in prolonged wait times and delayed order processing. Conversely, the AR Menu Fusion system exhibits only a marginal decrease in service speed with increasing customer numbers, showcasing its adeptness in handling higher volumes of orders efficiently. This underscores the scalability and responsiveness of the AR Menu Fusion system, [1]enabling restaurants to uphold timely service even during peak hours and accommodate fluctuating customer demand effectively.

CONCLUSION

AR menu Fusion emerges as a revolutionary solution that seamlessly integrates augmented reality into the dining experience, transcending traditional menu interactions. The project introduces a novel approach to menu exploration, allowing customers to visualize dishes in a realistic 3D space through their smartphones. This immersive encounter not only captivates users but also facilitates informed decision-making. The inclusion of online ordering and secure payment mechanisms aligns with contemporary expectations for convenience and contactless transactions, enhancing the overall efficiency of restaurant operations.

AR menu Fusion addresses the evolving needs of both customers and restaurant managers by offering a sophisticated and user-friendly platform. The amalgamation of augmented reality and digital functionalities propels the dining experience into the future, providing a unique and engaging interface for users. The real-time feedback feature contributes to customer satisfaction and enables continuous improvement in restaurant offerings. As a forward-thinking project, AR menu Fusion signifies the potential of technology to redefine the landscape of the food service industry.

This project not only showcases the capabilities of augmented reality in a practical setting but also underscores the importance of embracing innovation to stay competitive in the modern market. AR menu Fusion exemplifies how technology can elevate traditional practices, offering a

glimpse into the future of dining. As the project concludes, it leaves a lasting impression as a trailblazer in the realm of augmented reality-enhanced dining experiences.

ACKNOWLEDGEMENT

We owe our heartfelt gratitude to Almighty for all the blessings showered on us during this project work. We take this opportunity to express our sincere gratitude to all the people who have been instrumented in bringing out this work to the correct form. First of all we express our gratitude to Principal Dr. P M Maheesan and Director Mr. H. Ahinus for the excellent facilities and cordial support provided during the project work. We express our sincere thanks to Head of Department Ms. Nithya V P, Assistant Professor for their exemplary guidance and constant encouragement. We would like to express our immense pleasure and great sense of gratitude towards our project guide Ms. Sona N M, Assistant Professor and project coordinators Ms. Krishnapriya C and Ms. Nithya V P, Assistant Professors, Department of Computer Science and Engineering for sharing their valuable knowledge and idea for doing our work We express our thanks to all staff members and friends for all the help and co-ordination extended in bringing out this project successfully in time. And finally, We thank our families and friends and all those who helped us directly and indirectly in the completion of our project.

REFERENCES

[1] AZAHARI, M. H.,HAMID ALI, F. A. (2022).

The Development of an Online Food Ordering System for

JomMakan Restaurant. Applied Information Technology

And Computer Science, 3(1), 369–376. Retrieved from

<https://publisher.uthm.edu.my/periodicals/index.php/aitcs/article/view/2545>

[2] <https://www.irjet.net/archives/V9/i10/IRJET-V9I1010.pdf>

[3] Minghui Sun., Mingming Cao., Limin Wang., Qian Qian ,PhoneCursor: Improving 3D Selection Performance With Mobile Device in AR, IEEE, April 2020.

[4] Haitian Sun., Mengbo You., Chao Zhang., Takuya Akashi., A Visual Marker based Image Annotation Tool with Projective Transformation, IEEE, October 2018.

[5] <https://www.swiggy.com/>

[6] <https://www.zomato.com/>

[7] <https://www.flipkart.com/>

[8] <https://www.amazon.in/>

Conversion of Conventional Energy Meter to Smart Energy Meter

O Asokan
Professor
Dept.of EEE
M Dasan Institute of
Technology
Kozhikode, India
asokan@mdit.ac.in

Nithya V G
Assistant Professor,
Dept.of EEE
M Dasan Institute of
Technology
Kozhikode, India
nithyavg@mdit.ac.in

Alfin Mohammed P K
UG Student,
Dept.of EEE
M Dasan Institute of
Technology
Kozhikode, India
alfinmohammedpk@gmail.com

Adarsh Kumar E
UG Student,
Dept.of EEE
M Dasan Institute of
Technology
Kozhikode, India
adarsh2255017@gmail.com

Swetha Santhosh
UG Student,
Dept.of EEE
M Dasan Institute of
Technology
Kozhikode, India
swethajithuz@gmail.com

Abstract— In the modern age it is impossible to imagine a life without electricity. With growing population and the increasing power requirements in industrial, commercial and domestic purposes, the power consumption also rises and therefore the need for power measurement is very vital. As the amount of electricity consumption rises day by day, the amount of energy wastage is also rises. The consumption of energy can be measured with energy meters. This paper proposes a system that reduces human interaction in meter readings and bill generation that typically result in energy related corruption. The conventional meter can be slightly modified and converted to the proposed smart metering system by integrating a dual core processor and a relay. The suggested method senses the LED blinks and sends the information to the micro controller. The micro controller processes the data and send to a server over Wi-Fi. The system has the capability to give the user an SMS with the final bill generation and an update on energy use, as well as the freedom to reconfigure the load. Relays are used to accomplish the on-demand control of the power supply. The results of the hardware implementation indicate that the suggested system's accuracy is comparable to that of existing meters. With the same capability, the system is expected to cost less than the current smart meters that are on the market. By utilizing cutting-edge technology that works with both outdated metering units and newer models, the proposed system can generate user friendly billing system with minimal human error. Users may effortlessly track and manage their energy use with the help of this device.

Keywords—*Smart Energy Meter, Micro Controller, SMS, Billing.*

Introduction

Electricity has emerged as a crucial commodity in contemporary society, essential for the functioning of homes, offices, companies, and industries, supporting various aspects of daily life and operations. For any electricity utility, measuring energy use accurately is vital. This not only informs consumers about their energy usage patterns but also promotes wise energy utilization [7]. Research indicates that approximately 40% of electricity consumption in illuminated buildings is attributed to energy wastage, estimated at 10-15%. This wastage often results from human oversight regarding energy conservation [5]. To address these energy challenges, modernizing energy monitoring systems is imperative, with Internet of Things (IoT) technology offering effective solutions for energy measurement and billing [1]. The Internet of Things (IoT) represents the interconnection of numerous objects, including smart devices, sensors, and actuators, with a server or cloud via an IP gateway. The primary objective of IoT is to bridge the gap between the physical or real domain and the digital or virtual domain. An IoT framework serves as a complex system where a multitude of devices and gadgets are interconnected through communication and data infrastructure to deliver valuable services aligned with smart planning and applications. Implementing such technology is anticipated to enhance power and energy management efficiency. Accurate metering, theft detection, and the implementation of proper tariff and billing systems are crucial for managing electrical energy consumption [6].

Traditionally, electricity consumption data is collected by utility personnel through periodic visits to consumer sites to record the meter readings. However, this method is fraught with drawbacks, including time consumption, reliance on human resources, potential for human error, and susceptibility to corruption. Moreover, adverse weather conditions or consumer unavailability can disrupt the billing process, leading to delays. The current energy billing system is prone to errors, labor-intensive, and time-consuming, with inaccuracies introduced at various stages, such as electro-mechanical meter errors and human errors during meter reading. Transitioning to smart energy meters can mitigate these challenges [2-4].

The primary objective of this project is to develop a smart energy meter from conventional counterparts. A microcontroller retrieves pulses from the energy meter, calculates energy units, and transmits data to users via mobile phones or laptops. This bi-directional communication facilitates ease of reading and load disconnection/ reconnection, making our proposed metering system a superior alternative to existing methods. Moreover, the manufacturing cost of our proposed meter is projected to be lower than that of comparable conventional meters.

In alignment with the nation's digital progression, our proposed metering system addresses existing meter shortcomings. This paper provides detailed specifications of the proposed system, including software and hardware implementations, along with experimental results and conclusions.

Proposed system

The proposed system shown in figure 1 involves conversion of conventional meter to smart energy meter by integrating an external circuit which consist of microcontroller and relay. The

systems sense the quantity of LED blinks emitted by the conventional energy meter which was then fed to the micro controller as the input signal. The microcontroller was programmed with code designed to compile and compute the user's energy consumption. Micro controller used here is ESP 32 which has inbuilt Wi-Fi and Bluetooth facility. The processed data from micro controller are updated over the web server which can easily accessed by the user through a mobile phone or laptop. In this setup, users have the control to toggle the power supply of household appliances using a smartphone app on their Android device. The Wi-Fi module facilitates the transmission and reception of data with the cloud, which is then forwarded to the microcontroller. The controller, in turn, manages the relay to activate or deactivate the home circuit as required.

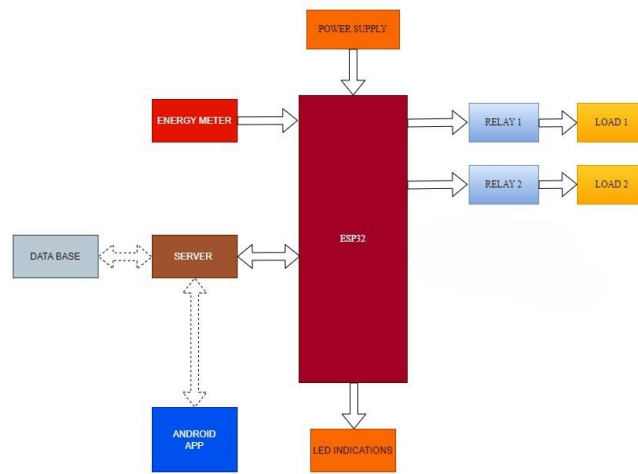


Fig. 1. Block Diagram of Proposed System

HARDWARE IMPLEMENTATION

The hardware implementation of the proposed smart energy meter system involves the integration of key components to conventional energy meter to enable seamless communication and control functionalities. Central system of this implementation is the ESP32 module, acting as the core interface between the conventional digital LED blinking energy meter and the user's control device, typically a smartphone running the Android application.

1. Conventional Energy Meter

The standard metering system shown in figure 2 synchronizes the number of LED blinks with energy use. The proposed approach uses LED blinks sensing to calculate units effectively.



Fig. 2. Conventional Energy Meter

J. ESP 32 Microcontroller

The ESP32 module as shown in figure 3 serves as the central processing unit for the proposed smart energy meter system. The LED blinking signal from the conventional energy meter is connected to one of the general purpose input output(GPIO) pins of the ESP32 module, allowing it to detect and interpret energy consumption data. The inbuilt Wi-Fi module of the ESP32 enables wireless communication, facilitating remote control and monitoring functionalities.



Fig. 3. ESP 32 Microcontroller

K. Relays

To enable remote load control capabilities, two 12V sugar cube relays have been integrated into the system. These relays are connected to additional GPIO pins of the ESP32 module, allowing it to toggle the power supply to connected appliances based on user commands received via the Android application. Each relay is capable of controlling a separate electrical load, providing users with flexibility and convenience in managing their energy usage.

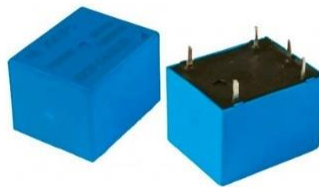


Fig. 4. 12V Sugar Cube Relay

By carefully integrating these hardware components and ensuring seamless communication between them, the smart energy meter system offers a robust and reliable solution for monitoring and controlling energy usage in real-time.

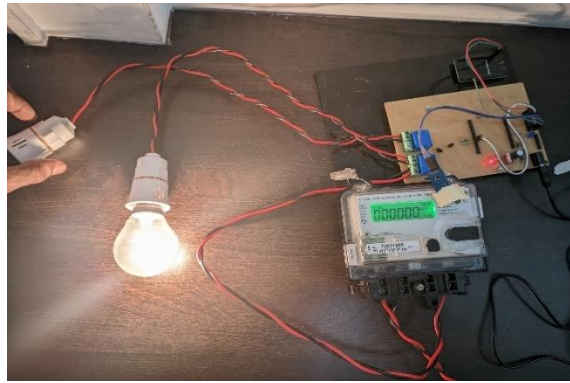


Fig. 5. Hardware set up of the proposed system

SOFTWARE IMPLEMENTATION

The software implementation of the proposed system is essential for enabling seamless communication between the hardware components and providing users with intuitive control and monitoring functionalities.

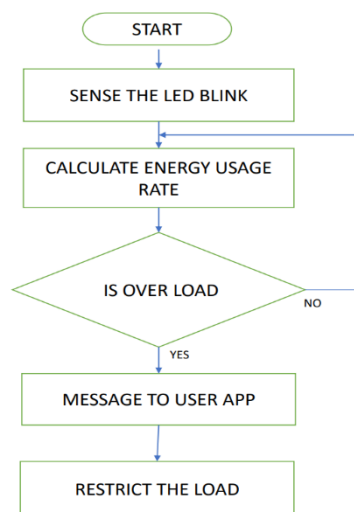


Fig. 6. Flow chart of the program code

The ESP32 module is programmed using the Arduino Software (IDE), leveraging its user-friendly interface and extensive library support. Arduino sketches are developed to handle tasks such as detecting the LED blinking signal from the energy meter, controlling the sugar cube relays for load management, and establishing Wi-Fi connectivity for communication with the server. Figure 6 depicts a flowchart that outlines the logical process for creating program code for the proposed system. An Android application as shown in figure 7 is developed to provide users with a convenient interface for controlling and monitoring their energy usage. Figure 8 shows the image of local server created to store the data.

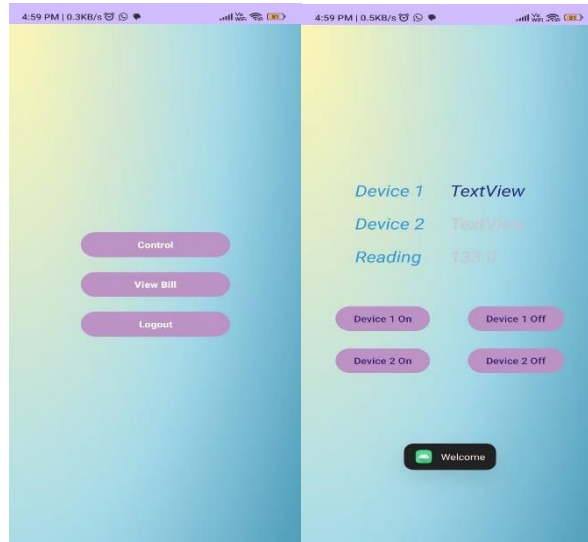


Fig. 7. Android Application View

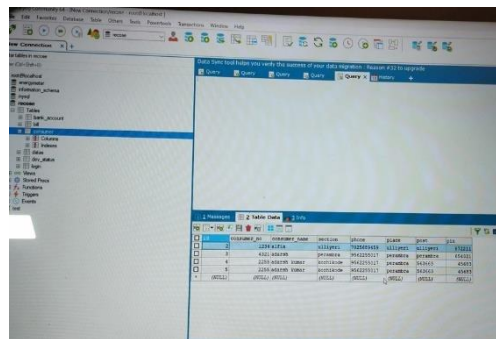


Fig. 8. Image of Server made to collect data

EXPERIMENTAL RESULTS

The The accuracy of the proposed meter was evaluated across different load scenarios, and the obtained results were juxtaposed with readings obtained from a standard meter subjected to identical loading and duration conditions. Table 1 presents a subset of the results, comparing readings between the traditional meter and the proposed smart energy meter.

TABLE V. METER READING COMPARISON

<i>Conventional meter reading (kwh)</i>	<i>Proposed smart meter reading (kwh)</i>
0.5	0.499
1	0.998

The results described earlier indicate that the suggested smart energy meter yields result comparable to traditional meters. In the tabulated data, the largest deviation from the reading of the conventional energy meter is 0.002 units, while the smallest deviation is 0.001 units over the measured values of

1 and 0.5 units, respectively. Therefore, the tabulated results validate the efficiency of the proposed meter, affirming its equivalence to conventional meters.

TABLE VI. FUNCTIONAL COMPARISON

	<i>Conventional meter</i>	<i>Proposed smart meter</i>
Information on usage of energy	yes	yes
Remote reading and billing	no	yes
Remote load reconfiguration	no	yes

Table II demonstrates the superiority of the proposed meter in terms of both economy and accuracy compared to current smart meters.

CONCLUSION

A user-friendly billing system utilizing modern technology has been developed and validated for compatibility with conventional metering units. By integrating a dual-core processor, ESP32 and a relay into conventional meters and utilizing LED blink sensing technology, this system facilitates accurate billing, real time energy usage updates allowing users to conveniently monitor and track their energy usage. Notably, users receive consumption updates via messages and can easily disconnect loads from the supply when not required. The ability to control loads on-demand enhances user flexibility and control over their electricity usage. Also, the proposed smart metering system offers a solution to reduce human interaction in meter readings and bill generation, thus mitigating potential energy-related corruption. This integration of modern technology with existing electrical architecture fosters an energy-efficient and economically viable environment. Consequently, the entire system ensures user-friendliness without compromising its simplicity in implementation.

Currently tailored for domestic use, further research is needed to assess the economic feasibility of implementing this metering system on a commercial scale for industries. Industrial applications may involve power factor metering and the control of power correction systems under various loading conditions. Such advancements would not only benefit industries by preventing penalties for low power factor implementation but also contribute to energy and economic efficiency.

ACKNOWLEDGMENT

We express our sincere gratitude to the experts for their invaluable recommendations aimed at enhancing the quality of this paper.

REFERENCES

- [62] Shubham Hadap , Deepti Ighe , Dhanashri Kadam , Rahul Niakm “IoT Based Smart Energy Meter” [Electrical Engineering MET Institute of Engineering, Nashik, Maharashtra, India.IJARSCT 2022] [Electrical Engineering MET Institute of Engineering, Nashik, Maharashtra, India.IJARSCT 2022]

- [63] Rutuja Kajrolkar, Aastha Deshmukh, Poonam Nakti , Deepashree Datar, Mahalaxmi Palinje “A survey on smart energy meter with billing and theft detection”[Electronics and Telecommunication, Atharva College of Engineering, Mumbai, India .2021 IRJET]
- [64] Aman Shah, Pramod Kumar Shah, Nabin Kumar Singh, Shailendra Kumar Jha “Smart energy meter”[Electrical and Electronics Engineering, Kathmandu University, Dhulikhel, Nepal . 2021 IRJET]
- [65] Naziya Sulthana,Rashmi N, Prakyathi N Y, Bhavana S K , B Shiva Kumar “Smart Energy Meter and Monitoring System using IoT” [Sri Siddhartha Institute of Technology Tumakuru, India, IJERT 2020]
- [66] Dr. Ravi Mishra-1, Anjali Pandey-2, Jhalak Savariya “Application of Internet of Things: Last meter smart grid and smart energy efficient system” [1-Electronics and Telecommunication GHRIET 2020]
- [67] K. Ragul , M. Mukul, P. Vijay, P. Rajkuma “Design and implimentation of smart energy meter using IoT” [Department of ECE KGISL Institute of Technology, Coimbatore, Tamil Nadu. IRJET 2020]
- [68] Himanshu K. Patel, Tanish Mody, Anshul Goyal “Arduino Based Smart Energy Meter using GSM” [Institute of Technology, Nirma University IEEE 2019]

Eco trim auto-mower

Jitha Bhaskar M
Assistant Professor
Dept of ECE
M-DIT Kozhikode, India
jitha@mdit.ac.in

Kailas Krishna
Dept of ECE
M-DIT Kozhikode, India
kailaskannan00@gmail.com

Muhammed Amod MP
Dept of ECE
M-DIT Kozhikode, India
amoodmp@gmail.com

Muhammed Swalih V
Dept of ECE
M-DIT Kozhikode, India
vswalih7@gmail.com

Aswanth UK
Dept of ECE
M-DIT Kozhikode, India
aswanthbabuuk@gmail.com

Athul CP
Dept of ECE
M-DIT Kozhikode, India
athulcp898@gmail.com

Abstract— Automation, fueled by technological progress, has transformed various sectors, including traditional grass-cutting methods. Historically, manual labor and non-renewable energy sources characterized conventional grass cutters, leading to energy waste and environmental harm. However, amid rising energy demands and environmental concerns, there's a pressing need for sustainable alternatives. Enter solar-powered grass cutters, powered by Arduino UNO microcontrollers, offering a compelling solution[1]. Utilizing solar energy as a clean and renewable source eliminates reliance on non-renewable fuels, cutting operational costs and pollution. Outfitted with ultrasonic sensors for obstacle detection and DC motors for propulsion, these autonomous systems operate efficiently sans human intervention. By prioritizing cost-effectiveness and eco-friendliness, this initiative seeks to optimize energy usage and curb environmental impact, marking a significant stride towards sustainable grass-cutting practices. With such innovations, the blend of automation and renewable energy heralds a greener future for lawn maintenance, balancing efficiency with environmental responsibility.

Keywords- *Arduino UNO*, renewable energy sources, autonomous systems, automower, BLDC

INTRODUCTION

Solar energy is a renewable resource categorized into passive and active solar sources depending on how it is captured distributed and converted into solar power. The utilization of solar energy is cost-effective as it is freely available. The solar grass cutter is presented as an alternative to traditional options in the market such as gasoline-based and electrical grass cutters[2]. Traditional grass cutters whether powered by electricity or gasoline come with certain drawbacks. Electrical grass cutters depend on a constant supply of electricity while gasoline-based ones

contribute to air and noise pollution. Additionally the conventional cutter machines require large cable wires for extensive grass-cutting areas and the motors are often heavy. In contrast the automated solar-based grass cutter offers a sustainable and environmentally friendly solution[3]. It operates using freely available solar energy eliminating the need for traditional power sources like electricity or fuel. This transition aligns with advancements in technology emphasizing the importance of adopting cleaner and more efficient alternatives to traditional grass cutting methods. The development of an automated solar-based grass cutter marks a significant leap in eco-friendly and efficient lawn maintenance technology. This innovative device addresses various challenges associated with traditional grass cutters offering a sustainable[4] and pollution-free solution. The heart of the system lies in its power configuration. A 12V battery serves as the primary power source complemented by a solar panel designed to capture and store solar energy efficiently. This combination ensures a continuous and renewable power supply eliminating the need for external wires or fuel. The reliance on solar energy not only makes the device cost-effective but also contributes to environmental conservation by reducing carbon footprints. The grass cutter is equipped with a total of five DC motors each playing a specific role in its operation. Four motors are dedicated to the movement of the device facilitating its mobility across various terrains[5]. The fifth motor(BLDC) is responsible for the cutting of grass providing a robust and efficient cutting mechanism. The coordination of these motors is orchestrated by an Arduino UNO microcontroller adding a layer of intelligence to the device. To enhance the grass cutter's autonomy and prevent collisions during operation an ultrasonic sensor is integrated for obstacle detection. This sensor employs sound waves to identify obstacles in the device's path allowing it to navigate around them intelligently. This feature contributes to the efficiency and safety of the grass-cutting process. In the grass cutter operates autonomously following a predetermined path while efficiently trimming the grass. The absence of wires and fuel in the device aligns with the goal of creating a pollution-free and eco-friendly solution for grass cutting[6]. The solar-powered operation not only minimizes environmental impact but also addresses the growing concern of energy sustainability.

The ultimate goal of our project is to engineer a cost-effective solution that not only replicates but surpasses the functionality of traditional grass cutters[7], particularly in terms of efficiency. Through the integration of solar power, smart sensors, and wireless control, we aim to revolutionize the landscape of lawn maintenance, offering an eco-friendly alternative that minimizes operational costs and maximizes technological innovation. Traditional grass cutters have long relied on manual labor and non-renewable energy sources, contributing to both environmental degradation and economic inefficiency. However, by embracing advancements in solar power technology, we can drastically reduce reliance on conventional energy sources while simultaneously minimizing carbon emissions. Solar power presents an inexhaustible and clean energy source, offering a sustainable solution to the energy demands of grass-cutting operations. Incorporating smart sensors into our design further enhances efficiency and precision. These sensors enable the Eco Trim Automower to autonomously navigate its environment, detecting obstacles and adjusting its trajectory accordingly. By minimizing human intervention, we not only streamline the grass-cutting process but also reduce the potential for errors and accidents. This autonomous functionality not only saves time and labor but also ensures uniform grass cutting, resulting in a pristine lawn appearance. Wireless control adds another layer of convenience and

accessibility to our solution[8]. Through the use of remote control or smartphone applications, users can easily monitor and adjust the Eco Trim Automower's operation from anywhere, at any time. This remote functionality not only enhances user experience but also enables real-time monitoring of energy consumption and grass-cutting performance, facilitating data-driven decision-making and optimization. Moreover, the integration of wireless connectivity opens up possibilities for future enhancements and updates. Firmware updates and additional features can be easily implemented over-the-air, ensuring that the Eco Trim Automower remains at the forefront of innovation and functionality. This adaptability ensures that our solution remains relevant and competitive in a rapidly evolving technological landscape. By combining solar power, smart sensors, and wireless control, we have created a grass-cutting solution that not only meets but exceeds the functionality of traditional grass cutters. Our Eco Trim Automower offers unparalleled efficiency, precision, and convenience, while also reducing environmental impact and operating costs. Through continuous innovation and improvement, we aim to redefine the standards of lawn maintenance, making eco-friendly and technologically advanced solutions accessible to all. In addition to its practical benefits, the Eco Trim Automower also serves as a symbol of our commitment to environmental sustainability. By harnessing renewable energy sources and minimizing carbon emissions, we are contributing to a cleaner, greener future for generations to come. Our project demonstrates that sustainability and efficiency are not mutually exclusive, but rather complementary goals that can be achieved through ingenuity, innovation, and dedication. In conclusion, the integration of solar power, smart sensors, and wireless control in our Eco Trim Automower represents a significant advancement in the field of lawn maintenance. By surpassing the functionality of traditional grass cutters while reducing environmental impact and operating costs, our solution sets a new standard for efficiency, affordability, and sustainability. Through ongoing research, development, and collaboration, we are confident that our project will continue to push the boundaries of innovation and excellence in the realm of grass-cutting solutions.

PROPOSED SYSTEM

Solar grass-cutting robot introduces an innovative and sustainable system to address the challenges associated with traditional grass-cutting methods. The core of the system comprises a solar-powered robotic platform equipped with cutting edge technologies for efficient grass maintenance[9]. A solar panel integrated into the robot harnesses solar energy to power the onboard components, eliminating the need for conventional energy sources. The robot is designed with autonomous navigation capabilities utilizing sensors and algorithms to detect and navigate around obstacles in its path. A high-speed motor drives a cutting assembly which can include durable blades or a cutting mechanism suitable for diverse grass types. The system incorporates a user-friendly control interface allowing operators to manage the robot's functions set cutting parameters, and monitor its performance remotely[10]. The integration of a solar-powered solution not only reduces environmental impact but also enhances the robot's operational autonomy making it suitable for prolonged use in various settings. This proposed system aims to revolutionize grass-cutting practices by offering an efficient eco-friendly and autonomous alternative that meets the growing demand for sustainable and automated solutions in agriculture landscaping and residential lawn care[11].

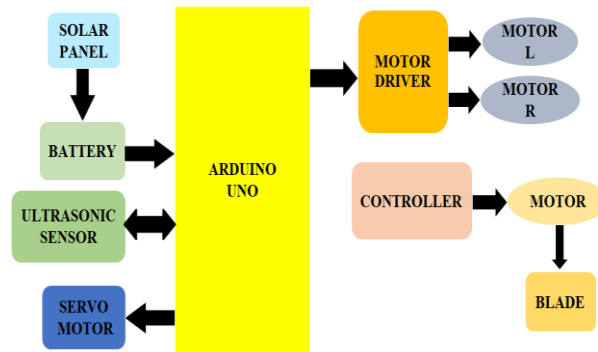


Fig. 1 shows the block diagram of Eco Trim Auto-Mower. The main part of the circuit is the Arduino UNO. All the other devices are connected to the Arduino UNO. It consists of an ultrasonic sensor, servo motor, motor driver, ESC module, Servo meter and BLDC motors. Power supply is given by 12v battery. The solar panel is directly connected to the battery.

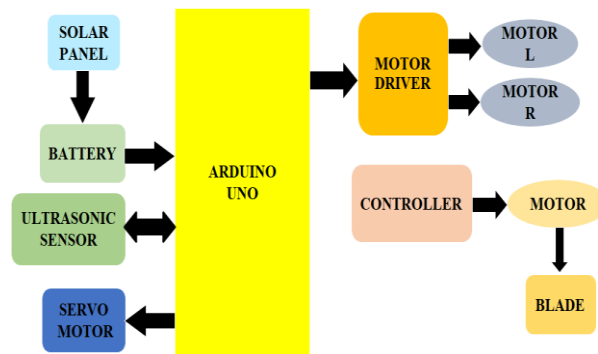


Fig. 1. Block diagram

CIRCUIT DIAGRAM

Fig. 2 shows circuit diagram which describes the architecture of the proposed eco-trim automower. This system consist of Arduino UNO, L293D motor driver shield, ultrasonic sensor HC-SR04, DC gear motors, BLDC motor 2200 KV, servo motor SG-90, ESC module, servo motor tester and 12v battery. Arduino UNO acts as the brain of the system. Connect the L293D motor driver input pins to the designated output pins on the Arduino for motor control. The four DC gear motors are connected to the motor driver shield which is controlled via digital pins D1, D2, D3, and D4 of the Arduino UNO board. The high conductance ultrasonic sensor HC-SR04 has echo trigger VCC and ground pins the echo and trigger pins which are connected to the A0 and A1 pin of the Arduino. It measures the distance to an object using ultrasonic ultrasonic sound waves. The servo motor is connected to the PWM pin D10 of the arduino. The ultrasonic sensor will be attached to the servo motor. It will provide an 180° rotation for the ultrasonic sensor. For cutting mechanism, a 2200KV very high speed BLDC motor is used. A cutting blade is attached to the motor which is used to cut the grass. It is directly connected to the 12V battery through a switch. Used a ESC module and servo tester to control the BLDC motor. The on/off mechanism and speed of the BLDC motor can be controlled by using the servo motor tester. In the intricate circuitry of the eco-trim auto-mower, the 12V solar panel emerges as a linchpin, strategically positioned within the system's power supply framework. Amongst the array of crucial components such as the

Arduino UNO, motor driver shield, ultrasonic sensor, and DC motors, the solar panel stands out as a vital source of renewable energy, profoundly influencing the automower's sustainability and efficiency. Visually, the solar panel is delineated as a distinct module within the circuit diagram, often situated atop the automower's chassis or strategically placed to optimize sunlight exposure. Its connectivity to the rest of the system is represented through clear lines and symbols, illustrating the seamless flow of electrical energy from the solar panel to the onboard battery and subsequently to the various components requiring power for seamless operation. Functionally, the 12V solar panel functions as an autonomous power generation unit, harnessing sunlight and converting it into electrical energy through photovoltaic cells. This harvested energy is then directed towards charging the onboard battery, depicted as a discrete component within the circuit diagram. The battery acts as a reservoir, efficiently storing surplus energy generated by the solar panel, thereby ensuring a consistent power supply for the automower's operation, even during periods of limited sunlight or at night.

The integration of the solar panel into the circuit diagram underscores the automower's unwavering commitment to sustainability and environmental responsibility. By harnessing the power of renewable energy sources like solar power, the automower significantly diminishes its reliance on non-renewable resources and markedly reduces its carbon footprint. This conscious effort towards sustainability fosters a greener and more eco-friendly approach to lawn maintenance, aligning with contemporary environmental values and initiatives. In essence, the inclusion of the 12V solar panel in the circuit diagram serves as a tangible representation of the automower's innovative power supply architecture. It eloquently communicates the automower's reliance on clean and sustainable energy sources for both efficient and environmentally conscious operation. This holistic approach not only ensures the automower's functionality but also resonates deeply with consumers who prioritize eco-friendly solutions in their quest for responsible lawn maintenance practices.

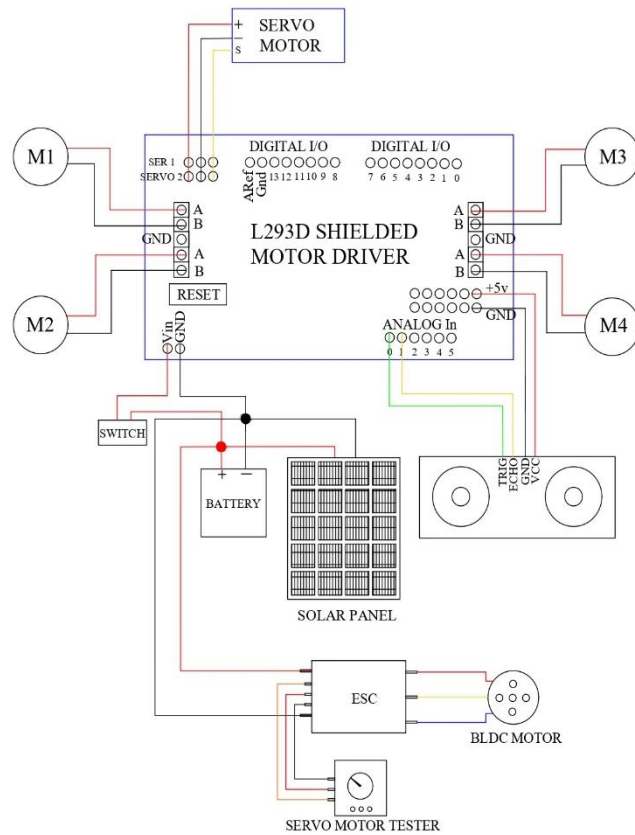


Fig. 2. Circuit diagram

RESULT AND DISCUSSION

Our designed product is an Eco trim automower based on the Arduino microcontroller system. We have presented a functional prototype of the designed product. We have also highlighted some important topics through the report. Our product is not only automated but also pre-programmed to do certain tasks and operations. The motor driver enables the move in various direction and control the speed of cutting motor. The Arduino UNO helps to give direction and command to the ultrasonic sensor which sense obstacles and navigate throughout its operation. Fig. 3 and Fig. 4 represents the front view and top view respectively.



Fig. 3. Front view

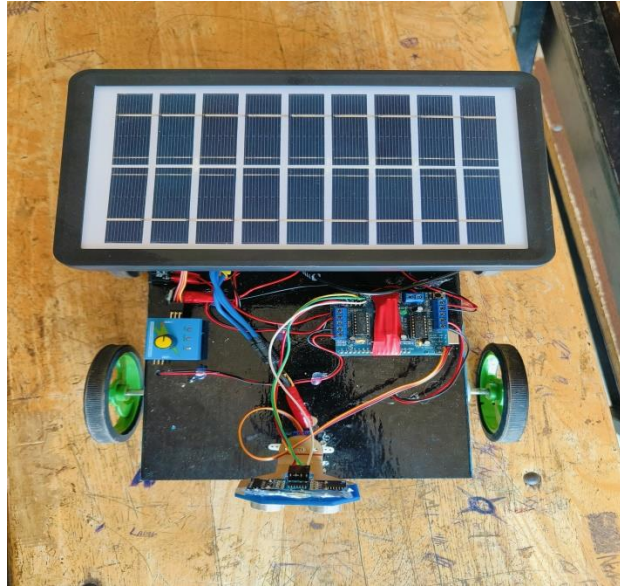


Fig. 4. Top view

CONCLUSIONS

In the design phase of our project, we delved into the intricacies of component selection and circuit design for the Eco Trim Automower, ensuring that every element contributes to its optimal performance. Our meticulously crafted Eco Trim Automower guarantees precise grass cutting, representing a remarkable leap forward in sustainable and efficient lawn maintenance practices. By harnessing the abundant power of solar energy, this innovative robot stands as a beacon of environmental consciousness. It significantly diminishes reliance on conventional energy sources, thereby mitigating the carbon footprint associated with traditional lawn mowers. This transition to solar power not only reduces operating costs but also fosters a cleaner, greener environment for generations to come. Equipped with an autonomous navigation system, the Eco Trim Automower epitomizes efficiency and precision. Its intelligent design enables seamless maneuverability across diverse terrains, ensuring uniform grass cutting without the need for human intervention. This not only saves time and labor but also minimizes the potential for human error, resulting in consistently impeccable lawn maintenance. Moreover, the Eco Trim Automower's eco-friendly operation extends beyond its energy source. Its electric propulsion system produces minimal noise pollution, contributing to a tranquil outdoor environment. Additionally, by eliminating the use of fossil fuels and reducing emissions, it helps combat air and noise pollution, fostering healthier communities. In essence, the Eco Trim Automower embodies a holistic approach to sustainable lawn care, seamlessly blending cutting-edge technology with environmental responsibility. Its adoption heralds a paradigm shift towards a future where efficient lawn maintenance harmonizes with ecological preservation, paving the way for greener, cleaner, and more livable spaces.

REFERENCES

- Sahu, M. M., Manoj Kumar Nayak, and Sabyasachi Sahu. "Design and Fabrication of Battery Operated Grass Cutter." *International Journal of Computational Engineering Research (IJCER)* 8.07 (2018).
- Herrera, N. G., and R. G. Luciano. "Design and development of android controlled grass cutting robot using RPA method." *Int. J. Sci. Technol. Res* 9.3 (2020): 223-234.
- Shanmugaselvam, P., et al. "Design and implementation of android based robot for grass cutting." *AIP Conference Proceedings*. Vol. 2519. No. 1. AIP Publishing, 2022.
- Ramnani, Shyam M., et al. "Unmanned automated lawn mower." *International Research Journal of Engineering and Technology (IRJET)* 7.6 (2020): 2473- 2484.
- Nishimura, Yuki, and Tomoyuki Yamaguchi. "Grass Cutting Robot for Inclined Surfaces in Hilly and Mountainous Areas." *Sensors* 23.1 (2023): 528.
- Hicks II, Rob Warren, and Ernest L. Hall. "Survey of robot lawn mowers." *Intelligent Robots and Computer Vision XIX: Algorithms, Techniques, and Active Vision*. Vol. 4197. SPIE, 2000.
- Egiyi, Modesta Amaka, and Victoria Nnenna Chukwuani. "Robotic Process Automation (RPA): Its Application and the Place for Accountants in the 21st Century." *International Journal of Advanced Finance and Accounting* 2.1 (2021): 30-40.
- Ghorpade, M. S., et al. "Intelligent solar powered grass cutting robot with obstacle avoidance." *International Journal of Modern Electronics and Communication Engineering (IJMECE)* 6.3 (2018): 1-4.
- Das, N. K., Rajib Ghose, and Md Monowarul Islam. "DESIGN AND IMPLEMENTATION OF A ROBOTIC LAWN MOWER." (2015).
- Arunesh, RV Sanjana, Shreyas Arunesh, and N. Nivetha. "Design and Implementation of Automatic Lawn Cutter." *IJSTE–International Journal of Science Technology Engineering* 2.11 (2016).
- Shanmugaselvam, P., et al. "Design and implementation of android based robot for grass cutting." *AIP Conference Proceedings*. Vol. 2519. No. 1. AIP Publishing, 2022.

Multi-Class Skin Disease Classification Using Convolutional Neural Network

Namitha Krishnan

Dept. of Biomedical Engineering
KMCT CEW Kozhikode, India
namithakrishnan15@gmail.com

Surya Gayathri U

Dept. of Biomedical Engineering
KMCT CEW Kozhikode, India
suryagayathri64@gmail.com

Ardra PV

Dept. of Biomedical Engineering
KMCT CEW Kozhikode, India
ardravijaya055@gmail.com

Aparna AK

Dept. of Biomedical Engineering
KMCT CEW Kozhikode, India
aparnaak01@gmail.com

Shibitha KP

Dept. of Biomedical Engineering
KMCT CEW Kozhikode, India
shibitha88@gmail.com

Abstract—Our skin protects our body’s key organs from potential harm by acting as an outer layer. This vital body part is prone to a number of illnesses caused by dust, allergies, bacteria, viruses, and fungi. Millions of people suffer from skin illnesses, which can result in discrimination and societal shame. Effective therapy for skin disorders requires a prompt and accurate diagnosis. Although advanced technologies like lasers and photonics have been used to diagnose skin diseases, they are frequently expensive and unaffordable for areas with low resources. As a result, image-based techniques present a quick and affordable substitute. Prior research has explored image-based diagnostic approaches for skin diseases. This study utilizes convolutional neural networks (CNN) to classify various skin diseases, including Acne and rosacea, Lupus, Psoriasis, Tinea and Ringworm, Bullous disease, Cellulitis and impetigo, Atopic dermatitis, vasculitis, Herpes, and Candidiasis. The image data underwent standardization in terms of size, conversion to grayscale, and intensity balancing. Augmentation techniques were also applied. Comparative analysis was conducted with established CNN architectures like MobileNetV2 and ResNet 50. This project proposes a CNN architecture called Sequential Model which is more accurate and reliable.

Index Terms—CNN, Sequential model, Lupus, Psoriasis, Lichen planus, Bullous disease, Cellulitis impetigo, Exanthems, Herpes, and Seborrheic keratosis.

I. INTRODUCTION

The human skin, our constant companion, is unfortunately prone to an astounding variety of illnesses. The battleground of skin disorders is vast and intimidating, ranging from inflammatory soldiers like eczema and psoriasis to contagious opponents like shingles and scabies to the silent killers of skin cancer. In this case, an accurate diagnosis is essential, not optional. It can help select life-saving therapies, avoid problems like scarring, and distinguish between a passing itch and a ticking time bomb. Patients may suffer for an extended period of time, have fatal symptoms, or even die as a result of a delay in diagnosis or treatment. Finding more precise tools is therefore

crucial to navigating this challenging environment. Herein lies the greatest promise of state-of-the-art technology like as deep learning and convolutional neural networks. Convolutional Neural Networks (CNNs) are specialised deep learning models that are particularly good at image-based tasks, such as the categorization of skin diseases. Salient features of CNN include • *Automatic Feature Extraction:*

In contrast to conventional models that depend on characteristics that are manually created, CNNs automatically extract important patterns from the data. They sort through pixels to find hints that are hidden, such as textures, forms, and edges.

• ***Convolutional Filters:***

Certain features, such as lines, circles, or bumps, are detected by each filter. CNNs extract a map of the presence and location of these characteristics by swiping these filters over the image.

• ***Multiple Layers:***

In order to disclose the true identity of the skin condition in the image, layers with simpler filters are used to recognise basic elements, which are then combined into more complicated patterns by succeeding layers. Convolutional Neural Networks (CNNs) are often constructed using a sequential model, especially when image classification tasks are involved. It entails piling up layers in a straight line, with each layer's output serving as the subsequent layer's input. In the end, this enables the network to produce the required classification output by gradually extracting and transforming information from the input image

Diseases that the proposed model can detect are:

1. *Acne and Rosacea*

The prevalent skin ailment known as acne is typified by the appearance of whiteheads, blackheads, and occasionally deeper cysts or nodules. It frequently happens when dead skin cells and grease block hair follicles. Although it can also affect the chest, back, and other regions with a high density of oil glands, acne mostly affects the face. Rosacea is a long-term skin disorder marked by flushing, redness, visible blood vessels, and occasionally tiny red pimples filled with pus. Rosacea often affects the cheeks, nose, forehead, and chin in the center of the face. Although redness on the face can be caused by both rosacea and acne, both conditions have different underlying causes and call for different management and treatment strategies.

2. *Atopic dermatitis*

Atopic dermatitis, often known as eczema, is a chronic, inflammatory skin disorder marked by itchy, red, and swollen skin. Atopic dermatitis symptoms might vary, but they typically include extreme itching, redness, dryness, and the appearance of tiny, raised bumps. In extreme situations, the skin might fracture and weep. Atopic dermatitis often affects specific parts of the body, including the face, hands, elbows, and knees. In babies, it frequently develops on their cheeks and scalp.

3. *Bullous disease*

A class of skin conditions known as bullous illnesses is defined by the development of fluid-filled blisters, or bullae, on the skin. These blisters can be isolated or widespread, and their sizes might vary. Numerous reasons, such as autoimmune responses, genetics, infections, and exposure to certain drugs or poisons, can result in bullous disorders.

4. Cellulitis and Impetigo

A bacterial skin infection known as cellulitis damages the underlying tissue as well as the skin's deeper layers. Redness, swelling, warmth, and discomfort in the afflicted region are typical symptoms. In addition, the skin might seem shiny and feel tight. Impetigo is a highly transmissible bacterial skin illness that appears as red sores or blisters that have the potential to burst and turn into crusts that are yellowish-brown in color. Impetigo is frequently characterized by itchy sores, fluid-filled blisters, and the recognizable honey-colored crusts.

5. Herpes

Herpes simplex viruses are the source of herpes; the two most prevalent forms are HSV-1, which is frequently linked to oral herpes, and HSV-2, which is frequently linked to genital herpes. In the earliest stages of outbreaks, it can induce flu-like symptoms accompanied with painful sores or blisters in the oral or vaginal region. Direct skin-to-skin contact with an infected individual is the main way that herpes is spread, particularly during sexual activity. Different symptoms may appear during a recurring infection episode than during the first episode, which is commonly referred to as the "outbreak." In the region where the sores may eventually form, burning, stinging, or tingling are often the first signs to appear. Common symptoms of oral herpes include blisters (cold sores) or open sores (ulcers) in or around the lips.

6. Lupus

Systemic lupus erythematosus (SLE), sometimes known as lupus, is a chronic autoimmune illness that can impact several bodily components, such as the kidneys, heart, lungs, brain, skin, joints, blood cells, and more. Inflammation results from the immune system wrongly attacking healthy tissues in lupus. The symptoms of lupus can vary greatly and include joint discomfort, photosensitivity, fever, rashes on the skin (facial rashes resembling butterflies are prevalent), exhaustion, and involvement of various organs leading to problems in severe instances.

7. vasculitis

A collection of uncommon illnesses known as "vasculitis" are typified by blood vessel inflammation and can impact different bodily areas. Damage to blood artery walls due to inflammation can result in impaired blood flow, harm to organs, and other issues. Vasculitis can present with a wide range of symptoms and severity. Vasculitis symptoms can vary in severity and include fever, exhaustion, weight loss, joint and muscular discomfort, skin rashes, and symptoms unique to a particular organ according to which blood artery is impacted.

8. Psoriasis

A chronic skin ailment called psoriasis is typified by a fast accumulation of skin cells that results in the creation of large, red areas that are coated in silvery scales. This autoimmune condition causes an increased rate of skin cell turnover when the immune system unintentionally targets healthy skin cells. Red, raised skin patches coated in silvery scales are one of the warning signs of psoriasis. It frequently affects the lower back, knees, elbows, scalp, and nails. It could also have an influence on other bodily parts.

9. *Tinea and Ringworm*

A class of fungal illnesses that may impact the appearance of the skin, human hair, or fingernails is known as tinea. Red, itchy rashes that may take the form of rings are a common characteristic. A frequent term for several forms of tinea infections is ringworm. Usually, ringworm manifests as a red, round rash with elevated margins and a distinct core. It can impact the outer layer of skin, scalp, and nails, among other body parts.

10. *Candidiasis*

A yeast infection called candidiasis is typically brought on by *Candida albicans*. It can impact the layers of skin in the tongue, throat, and genital region, among other sections of the body. Satellite lesions and red, itchy rashes are possible side effects. Since the above-mentioned causes are very common, even healthy persons can get candidiasis; however, immunocompromised individuals are definitely more susceptible. The delicate microbial balance in our systems can occasionally be disrupted, which might allow *Candida* to become a problem.

II. LITERATURE SURVEY

In 2017 Jihong Hu, et al proposed a mobile network called Mobilenet-RseSK for classifying skin diseases. It enhances the original network by introducing a new attention mechanism called seSK module, which improves feature extraction and network performance compared to the original attention module. Additionally, the network utilizes RBN normalization, which maintains the benefits of BN while enhancing the representation of specific features, leading to the identification of skin diseases. Testing on the HAM10000 dataset shows that Mobilenet-RseSK outperforms MobilenetV3, Ghost, and other advanced networks, achieving an 85% accuracy rate on the test set.

A MobileNet model was suggested by Jessica Velasco et al. in 2019 and used, using transfer learning, to create a skin disease categorization system for an application for Android. To improve MobileNet's accuracy, they experimented with various sampling strategies and preprocessing approaches. The Android app was updated to include this model. While utilizing the unbalanced database with default preprocessing produced accuracy of 93.6%, under sampling with standard preprocessing produced accuracy of 84.28%. An investigation into oversampling methods produced a 91.8% model accuracy. [3] In order to assist skin experts in identifying and diagnosing serious skin conditions including eczema, psoriasis, and lichen planus, as well as benign growths, infections caused by fungi, and viral infections, Moolchand Sharma, et al. set out to develop a system in 2019. Python programming is used to build the expert system. A 50-layer by layer residual neural network (RN) is used to train the system using a dataset that was acquired via DERMNET. The neural network gains the ability to recognize patterns and characteristics in skin photos that are suggestive of different skin conditions through intensive training.

A research that looks at how effectively a convolutional neural network (CNN) can categorize various forms of psoriasis skin condition was proposed by Rosniza Roslan et al. in 2020. They utilized 187 photos through Psoriasis Image Library, International Psoriasis Council, and DermNet NZ, among other sources. Out of them, 105 pictures showed guttate psoriasis and 82 showed plaque psoriasis. The kind of psoriasis was determined by analyzing the photos using CNN. The findings demonstrated that the CNN had an 82.9% accuracy rate in classifying plaque psoriasis and a 72.4%

accuracy rate in classifying guttate psoriasis. This implies that using skin image analysis, CNNs may prove helpful in the diagnosis of psoriasis.

2020 saw the proposal of a study by Tanzina Afroz Rimi, et al. using deep neural networks (DNN) to identify a number of skin disorders, including ulcers, lichen simplex, dermatitis hand, eczema subcute, and statis dermatitis. The investigation focuses on the combination of image processing and machine learning methods. In order to provide data for a Convolutional Neural Network (CNN), which classifies the skin conditions into predetermined groups, photographs must be processed. 500 photos taken from the dermnet database were utilized as the training dataset, yielding an accuracy rate of 73%.

In 2020, Yunendah Nur Fu'adah et al. suggested a methodology that uses convolutional neural networks (CNN) to automatically identify lesions from benign tumors and skin cancer. Three hidden layers make up the model, and each layer has channel sizes of 16, 32, and 64. As a result, skin lesions from the ISIC dataset may be categorized into four groups: melanoma, nevus pigmentosus, carcinoma of the squamous cells, and dermatofibroma. These findings are superior than those of the current approaches for classifying skin cancer.

A novel mobile deep neural network intended to assess skin affected by Systemic Sclerosis (SSc) was presented by Metin Akay et al. in 2021. To improve picture segmentation and classification accuracy, their network architecture integrates extra classifier layers with UNet, a convolutional neural network (CNN) with dense connection. They made use of "MobileNetV2," a training model created especially for embedded and mobile applications. They used a regular laptop equipped with a 2.5 GHz Intel Core i7 to construct the network.

Vinay Gautam et al. set out in 2021 to develop a project that deals with precisely classifying and detecting different skin illnesses, with a focus on early identification. For this reason, it suggests using an efficient Convolutional Neural Network (CNN). The methodology consists of three steps: first, employing processing techniques to preprocess photos of skin diseases; second, extracting significant characteristics from the images; and third, using a DCNN, or Deep Convolutional Neural Network, to analyze the preprocessed images at various stages.

Taehan Koo, et al. presented a study in 2021 that leverages microscope photos from actual medical practices to swiftly, conveniently, and reliably detect hyphae using deep learning. Using pictures from microscopy, they built a convolutional neural network named YOLO v4 for object detection. The investigation was carried out at the Veterans Health Service Medical Center's dermatology department in Seoul, Korea. They used the curve of receiver operating characteristic analysis for image classification, precision-recall curve assessment for hyphal localization, and average precision to assess the accuracy.

Tahir Alyas et al. set out to create a system in 2022 that uses deep machine learning methods to classify and diagnose fungus infections. A Convolutional Neural Network (CNN) was created in order to do this. Early fungal spore identification and classification by CNNs allowed for the estimation of possible fungal-related dangers. The suggested approach is referred to as Innovative Fungal Disease Diagnosis, or IFDD.[11] A method that uses convolutional neural networks (CNNs) to scan color photographs of skin lesions and categorize them into six groups—

acne, vitiligo, athlete's foot, chick-enpox, eczema, and skin cancer—was suggested by Ramzi Saifan and Fahed Jubair in 2022. For training, a collection of 3000 colored pictures was assembled from the Internet and public databases. The model's accuracy in experiments was 81.75%. By applying the holdout approach, which uses 90% of the pictures for training and 10% for out-of-sample accuracy testing, this accuracy was ascertained.

Koteswara Rao Kodepogu, et al. present a novel Deep Convolutional Neural Network (DCNN) in 2022 for the purpose of diagnosing skin conditions. Skin images are treated to improve quality and eliminate noise. The images are classified using the softmax classifier method, which uses DCNN to extract features and produce a diagnosis report.

Preeti Gupta and Sachin Meshram planned to introduce a hybrid CNN model for classifying skin lesions in 2022. To build this hybrid architecture, they mix a pre-trained ResNet-50 CNN model with an optimized VGG-16 model. They used dermoscopic pictures from the ISIC 2016–17 dataset to assess our hybrid CNN model's performance.

In 2023, Abdul Rafay and Waqar Hussain presented a report that combined two preexisting datasets to create a new dataset with 31 skin disorders. On this dataset, they used three different CNN types—EfficientNet, ResNet, and VGG—for transfer learning. EfficientNet demonstrated the best testing accuracy among them, necessitating more tweaking. The model's first testing accuracy was 71% with a 70% training split. The accuracy increased to 72% after adding more samples to the training split. This makes prompt treatment and early identification of skin conditions possible.

Tsedenya Debebe Nigat et al. present a study in 2023 that uses a convolutional neural network (CNN) to detect four common fungal skin diseases: tinea pedis, tinea capitis, tinea corporis, and tinea unguium. The preparation steps include modifying the image's intensity, converting Color to grayscale, and normalizing the image's size. The developed model showed a 93.3% accuracy in identifying the four fungal skin illnesses, outperforming MobileNetV2 and ResNet 50 architectures.

A proposal for deep learning for skin condition diagnosis with end-to-end confidentiality of data was made in 2023 by Shriya Pingulkar, Diti Divekar, and others. The suggested approach facilitates the safe exchange of diagnostic data amongst medical practitioners by employing deep learning algorithms to precisely diagnose skin conditions. It guarantees speedy and accurate diagnosis by guaranteeing information safety, confidentiality, and regulatory compliance.

A previously trained convolutional neural network (CNN) based autonomous facial skin disease approach was proposed by Rola EL SALEH et al. in 2019. The pictures are initially pre-processed in order to make the database larger. Following that, these images are used for training and validation. The model can accurately identify eight facial skin disorders, normal skin class, and no-face class with an accuracy rate of 88%.

Deep learning-based skin disease detection was suggested by Syed Inthiyaz et al. in 2023. This paper provides an automated image-based method for the identification and categorization of skin diseases using machine learning classification. In order to consider the many qualities of the photographs under processing, computer approaches will be employed for the analysis, processing,

and relegation of picture data. Compared to the conventional method, this program will be a more trustworthy and efficient method of identifying dermatological disorders, with higher accuracy and faster results delivery.

Deep Convolutional Neural Network Learning is the basis of a method that P Nagaraj et al. suggested in 2022, and employing it can yield remarkably precise results. The patient gives the prototype input by taking a picture of the affected skin region. This picture displays the result of the Deep Learning method, which is the identified skin condition.

2018 saw the proposal of Automatic Skin Disease Identification using Deep Learning Algorithm by Sourav Kumar Patnaik et al. This study offers a deep learning-based approach based on visual recognition for the autonomous diagnosis of various skin conditions. Based on the maximum vote from the three networks—three publicly accessible image recognition designs: Inception V3, Inception Resnet V2, and Mobile Net with modifications for skin disease application—the system accurately predicts the skin ailment. The system uses deep learning technology to educate itself using various skin pictures. The main objective of this system is to achieve the best degree of precision in forecasting for skin disorders. The Skin Cancer Classification using ResNet method was developed by Niharika Gouda et al. in 2020. A total of 8238 photographs were evaluated, consisting of 25,331 clinical skin sickness images, training images from various conditions of eight categories, and no skin issues at different anatomic sites. Robust techniques, such as the Deep Learning Neural Network type Residual Neural Network (ResNet), are employed to identify pictures and precisely generate an assessment report by means of a confidence score. Abdurrahim Yilmaz and colleagues (2022) presented a study that involved the acquisition of 297 microscopic full field photos of fragmented keratin from normal nail samples and 160 microscopic full field shots of the fungal element from onychomycosis patients. Smaller patches containing keratin ($n = 5238$) and fungus ($n = 1835$) were recovered from these whole field pictures. The VGG16 and InceptionV3 models were developed to identify fungus and keratin using these patches. The models' diagnostic ability was evaluated with 16 dermatologists using 200 test patches. The application of AI and computer-based technologies has greatly improved in the detection of facial skin illnesses. In 2023, Raghav Agarwal and Deepthi Godavarthi suggested CNN Algorithms to handle the rising number of dermatological disorders. This study's application of deep neural network models for photo categorization has produced encouraging findings.

A system for categorizing skin conditions was presented by Fahed Jubair and Ramzi Saifan in 2022. This research describes a system that classifies color photos of skin lesions into six skin diseases: vitiligo, acne, athlete's foot, the chickenpox a form of and skin cancer. The system uses convolutional neural networks to do this classification. Promising testing results showed that the model outperformed state-of-the-art research with an accuracy of 81.75%. This accuracy was calculated using the holdout approach, which employs 90% of the pictures to provide training plus 10% for assessing out-of-sample accuracy.

2020 saw the proposal by Honey Janoria et al. to use transfer learning to classify skin diseases based on skin image analysis. This study introduced a number of deep learning-based techniques that employ machine learning classifiers to extract characteristics from different skin cancer

photographs in order to determine the kind of skin illness. Our study leads to the creation of a transfer learning model. Support vector machines, decision trees, linear discriminate analysis, K-Nearest Neighbor, and the best linear classification algorithms are used for feature extraction (the VGG-16 layer CNN design can extract 1000 features from the input picture). The research was carried out utilizing well-known ISIC open datasets. The experimental results were produced by combining the VGG16 CNN model with the K-Nearest Neighbour method.

III. METHODOLOGY

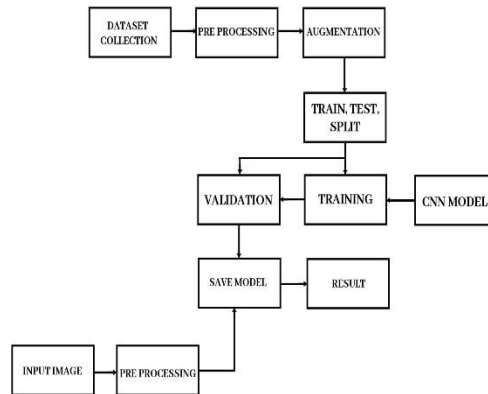


Fig. 1. Block diagram.

A. Dataset Collection

The training of our suggested neural networks for automated diagnosis depends heavily on the dataset. We have gathered a wide range of more than 10,000 dermatoscopic photos from people all around the world. Ten different skin disorders are included in the dataset; they range from typical issues like eczema and acne to less frequent presentations like vasculitis and bullous illness. The study's dataset was gathered via Kaggle. Acknowledging a natural disparity in the quantity of photos corresponding to each type of lesion, we deliberately applied data augmentation methods. This approach effectively addressed the disparity, ensuring each skin condition possessed a comparable volume of training data. The 10 different conditions of skin disorders that have been included in our dataset are as follows:

- 1) Acne & rosacea
- 2) Atopic dermatitis
- 3) Bullous disease
- 4) Cellulitis impetigo
- 5) Herpes HPV
- 6) Lupus
- 7) Vasculitis
- 8) Psoriasis.
- 9) Tinea ringworm candidiasis
- 10) Candidiasis



Fig. 2. Different condition of skin disorders.

B. Pre processing

Image preprocessing is a method to apply several approaches to enhance the quality of images. Preprocessing is necessary since the majority of original medical photos contain unnecessary elements. In order to eliminate such unnecessary portions of the images before classification, image preprocessing techniques are applied. The three most crucial techniques in this process were normalization, color conversion, and image scaling. The original photos were scaled to 48×48 pixels to ensure consistency in pixel intensity values between images. This was done first since normalization helped to decrease variances in brightness and contrast that may otherwise confound analysis. To make the data format simpler while keeping important elements for classification, an RGB to grayscale image colour conversion was then carried out. Every acquired image had a consistent size and colour conversion from RGB to grayscale.

C. Augmentation

A method called "data augmentation" is applied to artificially expand a dataset. This is a way to keep deep learning models from overfitting. Large dataset collection may be expensive and time-consuming. In order to artificially enlarge the dataset, data augmentation is a crucial deep learning technique. Many methods of data augmentation exist, including scaling, translation, cropping, rotations, and contrast modification.

D. Train, Test, Split

The dataset is usually split into training and test sets in image processing, especially for tasks like object detection, image classification, or segmentation. By splitting the data, this makes sure that the model is trained on a single subset. Typically, the training set makes up roughly 80% of the entire dataset. The model modifies its parameters as it gains the ability to identify patterns and characteristics in the images during training. wherein the dataset is split into two parts: the testing dataset, which makes up 20%, and the training dataset, which makes up 80%. Testing is the

process of assessing a trained model's performance and capacity for generalisation using a different set of unseen images. This procedure plays a crucial role in evaluating the model's performance on new, untested data and offers valuable insights into its practicality.

E. Convolutional Neural Network

convolutional neural network is a deep learning algorithm which work with images. It is specially designed for image processing. in this project we utilize sequential model for dermatological image processing. sequential model refers to specific type CNN architecture where layers are stacked sequentially. sequential model can provide a simple and intuitive way to built a neural network. sequential model also have high compatibility with keras and high efficiency in training. sequential model in CNN can maintain both simplicity and effectiveness

F. Validation

The performance of a trained CNN model is estimated by a process called validation. In CNN image classification validation processes and training process occur simultaneously. During training phase on each epoch the model is fed group (batches) of training data (images). This process is continued until a stopping criterion is reached. A validation set, which is a sperate portion of data is used to evaluate the CNN model. The validation phase may occur after each epoch or periodically during training.

G. Input

An input image is fed to the CNN pretrained model to obtain an output indicating the disease. We utilize dermatological image as input image. Dermatological images capture, skin rashes, lesions and other conditions like eczema, psoriasis. Input image is preprocessed before feeding to the CNN model.

IV. RESULT

Skin diseases pose a significant global health challenge affecting millions of people. The project highlights the diverse range of skin conditions, including fungal infections, autoimmune disorders like lupus, inflammatory conditions such as eczema and psoriasis, as well as viral and bacterial infections like herpes and impetigo. The psychological impact of these diseases is also emphasized, underscoring the importance of early detection and appropriate treatment not only for physical well-being but also for mental health. The development of a multiclass skin disease classification system using Convolutional Neural Networks (CNN) is a significant advancement in medical image analysis. This system was specifically designed to classify ten classes of skin diseases: Acne and Rosacea, Psoriasis, Bullous Disease, Cellulitis and Impetigo, Atopic Dermatitis, Herpes, Lupus, Vasculitis, Tinea and Ringworm, and Candidiasis. The achievement of a 97% accuracy rate demonstrates the effectiveness of the model in accurately classifying skin diseases. To ensure robustness and generalization, the dataset was carefully prepared with equal numbers of images for each class. Furthermore, the dataset was split into testing and training sets, with 20% of the photos going toward testing and the remaining 80% going toward training. The photos underwent a thorough preprocessing procedure before the model was trained. This involved converting the photographs to grayscale to reduce the input data, shrinking them to a standard size, normalizing them to guarantee constant intensity values, and augmenting them to broaden the

training dataset's variety. By employing these preprocessing techniques and training on a well-structured dataset, the CNN model was able to effectively learn discriminative features from the images, enabling accurate classification of diverse skin diseases. This achievement holds promise for improving diagnostic accuracy in clinical settings, ultimately leading to better patient outcomes and more efficient healthcare delivery. In the process of disease identification using the developed Convolutional Neural Network (CNN) model, an image undergoes several preprocessing steps before being fed into the network for analysis. Initially, the input image is resized to meet the model's input specifications, ensuring uniformity in processing. Subsequently, grayscale conversion is applied to simplify the image data, reducing computational complexity and enhancing feature extraction. Normalization techniques are then employed to standardize pixel values, promoting stable and efficient model training. Following preprocessing, the input image is compared against the trained CNN model, which has been previously trained on relevant datasets, facilitating the identification of potential diseases or abnormalities.

V. CONCLUSION

In this project we explore the use of Convolutional Neural Networks (CNNs), a type of artificial intelligence technology, to classify common skin diseases based on image data. The goal is to develop an automated tool for accurate diagnosis, addressing the challenges posed by expensive diagnostic methods and improving accessibility to effective healthcare, particularly in resource-limited areas. Addressing the diverse array of skin diseases is crucial due to their widespread prevalence and significant impact on global health. Skin, being the body's first line of defense, demands attention for the overall well-being of individuals. With over 3000 known skin diseases affecting approximately 900 million people worldwide, the implications extend beyond physical health, influencing psychological aspects and various facets of daily life. Prominent skin conditions such as melanoma, vitiligo, mycosis, papillomas, impetigo, scabies, herpes, dermatitis, warts, psoriasis, acne, and others pose substantial health risks, and their contagious nature requires prompt identification and treatment. The disabilities resulting from these conditions can have profound psychological impacts, affecting education, relationships, self-esteem, and overall quality of life. Fungal skin diseases, including superficial infections, are prevalent, impacting various parts of the skin, hair, nails, and mucous membranes. Specific skin conditions like acne rosacea, lupus, eczema, psoriasis, lichen planus, bullous disease, cellulitis, impetigo, exanthems, herpes, and seborrheic keratosis add to the complexity of dermatological challenges. Recognizing the challenges in accurate diagnosis and treatment, the potential of image-based methods for detecting and diagnosing skin diseases is highlighted. Timely identification is essential for administering appropriate treatment and preventing further spread. Traditional diagnostic approaches, while effective, are time-intensive and subject to subjective errors. In the ongoing pursuit of dermatological health, continued research, technological advancements, and a holistic approach to both physical and psychological aspects are imperative. This project emphasizes the importance of a comprehensive understanding of skin diseases and the need for accessible, accurate, and timely diagnostic methods to improve outcomes and enhance the overall well-being of individuals globally. Leveraging convolutional neural networks (CNNs) and image processing techniques presents a promising avenue for advancing the detection and diagnosis of various skin diseases. By incorporating image-based methods into the diagnostic process, we

can enhance the efficiency of identifying skin diseases, especially considering the challenges posed by the similarity in symptoms among different conditions. CNNs, with their ability to learn hierarchical features from images, offer a powerful tool for automated recognition of skin disorders. The integration of image processing technologies allows for the extraction of meaningful features from dermatological images, aiding in the differentiation of various skin conditions. This not only streamlines the diagnostic process but also reduces the subjectivity associated with traditional methods such as visual examination. Timely identification facilitated by these advanced technologies is crucial for administering appropriate treatment and preventing further spread of skin diseases. Furthermore, the implementation of CNNs and image processing can potentially address the limitations of conventional diagnostic approaches, which are time-intensive and susceptible to subjective errors. In the realm of dermatological health, the convergence of artificial intelligence, particularly CNNs, and image processing holds great promise for revolutionizing diagnostic practices. Continued research and development in this direction can significantly contribute to improving health-care outcomes, empowering clinicians with efficient tools for accurate and early detection of skin diseases.

ACKNOWLEDGMENT

We express our sincere gratitude to Dr. Jerline Sheeba Anni, Principal, KMCT College of Engineering for Women, for facilitating a congenial academic environment in the college. We also express our gratitude to our Head of the Department

Dr. Sameera VMohd Sagheer, project coordinator Ms. Mini Lal and project supervisor Ms. Shibitha KP for guiding us right from the inception till the successful completion. We sincerely acknowledge them for the valuable support they had provided to us at all the stages of the project. Finally, we would like to add a few heartfelt words for the people who were part of the project in various ways, especially my teachers and classmates. We also extend our gratitude to our family without whose support, persistence and love we would not be where we today.

REFERENCES

- [1] Hu, J., Qi, Y., & Wang, J. (2022, December). Skin Disease Classification Using MobileNet-RseSK Network. In *Journal of Physics: Conference Series* (Vol. 2405, No. 1, p. 012017). IOP Publishing. doi:10.1088/1742-6596/2405/1/012017
- [2] Jessica Velasco et al., International Journal of Advanced Trends in Computer Science and Engineering, 8(5), September - October 2019, 2632- 2637 A Smartphone-Based Skin Disease Classification Using MobileNet CNN <https://doi.org/10.30534/ijatcse/2019/116852019>
- [3] Moolchand Sharma, Bhanu Jain and many other aimed to create a system which utilizes residual neural networks DETECTION AND DIAGNOSIS OF SKIN DISEASES USING RESIDUAL NEURAL NETWORKS (RESNET): International Journal of Image and Graphics, Vol. 21, No. 05, 2140002 (2021), No Access, <https://doi.org/10.1142/S0219467821400027>
- [4] Abdul Rafay, Waqar Hussain, EfficientSkinDis: An EfficientNet-based classification model for a large manually curated dataset of 31 skin diseases, Biomedical Signal

Processing and Control, <https://doi.org/10.1016/j.bspc.2023.104869>.

- [5] T. A. Rimi, N. Sultana and M. F. Ahmed Foysal, "Derm-NN: Skin Diseases Detection Using Convolutional Neural Network," *2020 4th International Conference on Intelligent Computing and Control Systems (ICICCS)*, Madurai, India, 2020, pp. 1205-1209, doi: 10.1109/ICI-CCS48265.2020.9120925.
- [6] Fu'adah, Y. N., Pratiwi, N. C., Pramudito, M. A., & Ibrahim, N. (2020, December). Convolutional neural network (cnn) for automatic skin cancer classification system. In *IOP conference series: materials science and engineering* (Vol. 982, No. 1, p. 012005). IOP Publishing. doi:10.1088/1757-899X/982/1/012005
- [7] M. Akay *et al.*, "Deep Learning Classification of Systemic Sclerosis Skin Using the MobileNetV2 Model," in *IEEE Open Journal of Engineering in Medicine and Biology*, vol. 2, pp. 104-110, 2021, doi: 10.1109/OJEMB.2021.3066097.
- [8] Gautam, V., Trivedi, N. K., Anand, A., Tiwari, R., Zaguia, A., Koundal, D., & Jain, S. (2023). Early Skin Disease Identification Using Deep Neural Network. *Computer Systems Science & Engineering*, 44(3). doi10.32604/csse.2023.026358
- [9] Koo T, Kim MH, Jue M-S (2021) Automated detection of superficial fungal infections from microscopic images through a regional convolutional neural network. *PLoS ONE* 16(8): e0256290. <https://doi.org/10.1371/journal.pone.0256290>
- [10] alyas2022innovative, title:Innovative Fungal Disease Diagnosis System Using Convolutional Neural Network, author:Alyas, Tahir and Alissa, Khalid and Mohammad, Abdul Salam and Asif, Shazia and Faiz, Tauqeer and Ahmed, Gulzar, journal:Computers, Materials , Continua, volume:73, number:3, year:2022,
- [11] *Ramzi Saifan, Fahed Jubair* :Six skin diseases classification using deep convolutional neural network This journal is published by the <https://iaes.or.id> Institute of Advanced Engineering and Science (IAES) in collaboration with <https://ipmuonline.com> Intelektual Pustaka Media Utama (IPMU). <http://doi.org/10.11591/ijece.v12i3.pp3072-3082>
- [12] Kodepogu, K.R., Annam, J.R., Vipparla, A., Krishna, B.V.N.V.S., Kumar, N., Viswanathan, R., Gaddala, L.K., Chandanapalli, S.K. (2022). A novel deep convolutional neural network for diagnosis of skin disease. *Traitement du Signal*, Vol. 39, No. 5, pp. 1873-1877. <https://doi.org/10.18280/ts.390548>
- [13] International Journal of Creative Research Thoughts (IJCRT) ,Volume 10, Issue 6 June 2022 ,Skin Lesion Detection using VGG-16 and ResNet50 based Hybrid CNN Model, <https://ijcrt.org/papers/IJCRT22A6730.pdf>
- [14] Abdul Rafay, Waqar Hussain, EfficientSkinDis: An EfficientNet-based classification model for a large manually curated dataset of 31 skin diseases, *Biomedical Signal Processing and Control*. Volume 85, 2023, 104869, ISSN 1746-8094, <https://doi.org/10.1016/j.bspc.2023.104869>.
- [15] Tsendenya Debebe Nigat, Tilahun Melak Sitote, Berihun Molla Gedefaw, "Fungal Skin Disease Classification Using the Convolutional Neural Network", *Journal of Healthcare Engineering*, vol. 2023, Article ID 6370416, 9 pages, 2023. <https://doi.org/10.1155/2023/6370416>
- [16] Shriya Pingulkar, Diti Divekar, Aryaman Tiwary (2023) Deep Learning for Skin Disease Diagnosis with End-to-End Data Security <https://doi.org/10.1109/ICI60088.2023.10421188>

- [17] Rola EL SALEH, Sambit BAKHSHI,•Amine NAIT-ALI (2019) Deep convolutional neural network for face skin diseases identification. <https://doi.org/10.1109/ICABME47164.2019.8940336>
- [18] Syed Inthiyaz, Baraa Riyadh Altahan, Sk Hasane Ahammad, V Ra-jesh, Ruth Ramya Kalangi, Lassaad K. Smirani, Md. Amzad Hossain, Ahmed Nabih Zaki Rashed, Skin disease detection using deep learning, *Advances in Engineering Software*, Volume 175, 2023, 103361, ISSN 0965-9978, <https://doi.org/10.1016/j.advengsoft.2022.103361>.
- [19] P Nagaraj, V Muneeswaran, B Karthik Goud, k Arjun, G Vigneshwar Reddy, P Girish Kumar Reddy, "Identifying Multiple Diseases in the Human Body using Machine Learning", 2023 4th International Conference on Electronics and Sustainable Communication Systems (ICESC), pp.872-877, 2023 <https://doi.org/10.1109/ICESC54411.2022.9885330>
- [20] Patnaik S. K, Sidhu M. S, Gehlot Y, Sharma B, Muthu P. Automated Skin Disease Identification using Deep Learning Algorithm. *Biomed Pharmacol J* 2018;11(3). Available from: <http://biomedpharmajournal.org/?p=22169>
- [21] Niharika Gouda, J Amudha (2020) Skin Cancer Classification using ResNet <https://doi.org/10.1109/ICCCA49541.2020.9250855>
- [22] Abdurrahim Yilmaz, Fatih Göktay, Rahmetullah Varol, Gulsum Gencoglan, Huseyin Uvet (2022) Deep convolutional neural networks for onychomycosis detection using microscopic images with KOH examination <https://doi.org/10.1111/myc.13498>
- [23] Agarwal R, Godavarthi D. Skin Disease Classification Using CNN Algorithms. *EAI Endorsed Transactions on Pervasive Health and Technology*. 2023 Oct 2;9(1). <http://dx.doi.org/10.4108/eetpht.9.4039>
- [24] Ramzi Saifan, Fahed Jubair. Six skin diseases classification using deep convolutional neural network. <http://dx.doi.org/10.11591/ijece.v12i3.pp3072-3082>
- [25] Honey Janoria, Jasmine Minj, Pooja Patre. Classification of Skin Disease from Skin images using Transfer Learning Technique. <https://doi.org/10.1109/ICECA49313.2020.9297567>

Brain Abnormality Classification by Combination of Machine Learning And Deep Learning

Shamna Backer N
Dept. Of Biomedical Engineering
KMCT CEW Kozhikode, India
shamnabackern8@gmail.com

Raihana TK
Dept. of Biomedical Engineering
KMCT CEW Kozhikode, India
raihana81380@gmail.com

Sweety PJ
Dept. of Biomedical Engineering
KMCT CEW Kozhikode, India
sweetypj2002@gmail.com

Farhana Sherin
Dept. of Biomedical Engineering
KMCT CEW Kozhikode, India
febifazal123@gmail.com

Irfana Izzath OP
Dept. of Biomedical Engineering
KMCT CEW Kozhikode, India
irfana@kmctcew.ac.in

Abstract—Brain abnormalities, such as tumors and strokes, and normal MRI data and their early detection is paramount for timely intervention and effective treatment. This research describes a novel method for identifying a variety of brain abnormalities, such as tumours and strokes, in medical imaging data obtained from magnetic resonance imaging (MRI) scans by combining the strengths of deep learning (DL) and machine learning (ML). The proposed methodology integrates DL and ML to provide a comprehensive and accurate diagnostic tool. Convolutional Neural Networks (CNNs) are employed for feature extraction, enabling the model to automatically identify intricate patterns and abnormalities within the brain images. The extracted features are subsequently fed into a carefully designed algorithm of ML classifiers, k-Nearest Neighbors (KNN). This ensemble approach capitalizes on the strengths of ML to make precise diagnostic decisions based on the rich feature representations derived from the DL component.

Index Terms—Machine Learning, Deep Learning, Convolutional Neural Network, K-Nearest Neighbours, Magnetic Resonance Imaging, Tumor, Meningioma, Glioma, Pituitary, Stroke, Grayscale, Normalisation.

I. INTRODUCTION

Image processing has a pivotal role in modern medical healthcare diagnosis. Through the utilization of advanced algorithms and computational techniques, it enables the extraction of valuable information from medical images, like as X-rays, MRIs, CT scans, and ultrasounds. This technology has revolutionized the field by enhancing the accuracy and efficiency of diagnoses, ultimately improving patient care. This leads to faster diagnosis and treatment decisions, ultimately benefiting patients. Moreover, by minimizing the need for manual image analysis, healthcare facilities can optimize resource allocation, reduce the risk of human error, and enhance the overall quality of care. The need for image processing in healthcare arises from its ability to improve diagnostic accuracy, facilitate quicker decision-making, and streamline healthcare operations, ultimately advancing patient outcomes and healthcare efficiency.

The realm of modern healthcare, timely and accurate detection of brain abnormalities, such as strokes and brain tumours, is of paramount importance. Magnetic Resonance Imaging (MRI), has emerged as an indispensable tool for clinicians and diagnosticians in visualizing the intricate structures of the human brain. However, the manual interpretation of MRI images is not only labour intensive but also subject to human error. This project embarks on a quest to develop a comprehensive system that harnesses the power of CNN and KNN to detect and classify brain abnormalities in MRI images.

A. **BRAIN TUMOR**

An aberrant mass of brain cells is called a brain tumour. These growths may originate from different types of brain cells and may be benign or malignant. Although the precise causes are frequently unknown, radiation exposure and heredity may play a role in their development. Depending on the size and location of the tumour, symptoms may include headaches, seizures, altered eyesight, and neurological problems. A biopsy and or imaging studies are part of the diagnosis process. Treatment options encompass surgery, radiation, chemotherapy, or targeted therapies, depending on the tumor type. Prognosis varies based on tumor characteristics and the patient's health. Managing brain tumors involves a team of medical specialists, including neurosurgeons and oncologists, to provide the best care and support.

By taking precise cross-sectional pictures of the brain, MRI (Magnetic Resonance Imaging) can identify brain tumours. Strong magnetic fields and radio waves cause the body's tissues to create signals during an MRI scan. Tumors appear as abnormal areas with distinct characteristics, such as varying tissue density and irregular blood flow. Radiologists can analyze these images to identify the tumor's size, location, and characteristics, which help in distinguishing it from normal brain tissue. Additionally, contrast agents may be administered to enhance the visibility of certain tumors.

Overall, MRI is a non-invasive and highly effective method for detecting brain tumors and providing essential information for diagnosis and treatment planning.

There are various types of brain tumors, including

1. **Meningioma:** Meningiomas are usually non-cancerous tumors which do develop in the meninges, it is the layer which protects the tissue that cover the central nervous system. They are often slow-growing and can press on nearby brain tissue.
2. **Glioma:** Gliomas are a particular kind of tumour that starts in the glial cells, which in the brain support and shield nerve cells. They are the most prevalent kind of brain tumour and can be benign or malignant.
3. **Pituitary Tumor:** Pituitary tumors are seen in pituitary glands, small in size and situated in base of brain. These tumors can affect hormone production and cause various health problems, but most are non-cancerous.

B. **STROKE**

A cerebrovascular accident (CVA), often known as a stroke, is a medical emergency that happens when there is an abrupt stoppage of blood flow to the brain. Because of this disruption,

brain tissue may become damaged due to a shortage of nutrients and oxygen. If treatment for a stroke is delayed, serious effects might result, such as paralysis, trouble speaking, and even death. Diagnosing a stroke is crucial for timely medical intervention. Healthcare professionals typically rely on a combination of clinical evaluation and diagnostic tests to confirm the presence of a stroke. These tests may include imaging techniques like computed tomography (CT) scans or magnetic resonance imaging (MRI), as well as clinical assessments of symptoms, such as weakness, slurred speech, and visual disturbances. Initiating proper therapy and minimising the long-term effects of a stroke depend on a timely and precise diagnosis. A test called magnetic resonance imaging (MRI) utilises radio waves and magnets to produce precise images of the arteries and brain. An MRI can identify alterations in brain tissue and stroke-related cell damage to the brain.

C. MACHINE LEARNING

Machine learning plays a pivotal role in image processing, as it enables computers to automatically learn and extract meaningful information from images. Machine learning models are capable of completing tasks like picture segmentation, object detection, facial recognition, and image classification after they have been trained on labelled image data. A straightforward but powerful method used in image processing for tasks like similarity matching and picture classification is the k-Nearest Neighbours (k-NN) algorithm. A picture is classified using k-NN based on the majority class of its k nearest neighbours in a feature space. Features can be more complicated image descriptors, colour histograms, or pixel values.

D. DEEP LEARNING

Because deep learning makes it possible to create extremely complex and precise models for a variety of applications, image processing has undergone a revolution. In image processing, convolutional neural networks, or CNNs, are the foundation of deep learning. These networks are especially well-suited for tasks like image classification, object identification, picture segmentation, and more because of their ability to automatically learn and extract characteristics from images. A type of deep learning models called Convolutional Neural Networks (CNNs) is intended for image processing applications. They perform exceptionally well in tasks like object detection, segmentation, and image classification because they are adept at autonomously learning and extracting hierarchical features from images. CNNs are made up of a number of layers, such as pooling layers for downsampling, fully linked layers for classification.

II. LITERATURE SURVEY

We have conducted a survey for analysing the best suitable and simpler algorithm and the imaging modality which possess more accuracy for the project. The surveys are listed below.

In 2015, R. Banik et.al [1] a suggested study that describes an automated technique for detecting brain tumours using MRI data. It maximises the intensity of tumour patches while reducing noise by using Frequency Emphasis in Homomorphic Filtering. After extracting the tumour patches, the technique superimposes them on an edge-detected brain image to precisely pinpoint the tumor's location. In 2017, A Minz et.al [2] presented a technique for classifying brain tumour types from MRI images using Adaboost. Preprocessing, feature

extraction, and classification are the three main components of the system that automate labor-intensive manual inspection of medical imaging data that is difficult for humans to recognise. In 2018, T. A. Jemima et al [3] presented the DAPP characteristics for brain tumour segmentation and classification based on the Watershed Algorithm. The WDAPP-CNN detects tumours and non-tumor regions in brain imaging by precisely defining tumour locations and extracting textured characteristics using a watershed algorithm. It was not as precise. Kurnar et al (2018) [4] proposed a K-means clustering algorithm-based approach for the detection of brain tumours in MRI data. Preprocessing, grouping, morphological processes, and tumour area calculation are all part of the process. It demonstrates that KNN is an improved approach for tumour classification as well. T. Kalaiselvi et al [5] 2019 study presents a technique for identifying tumour locations based on particular colours in multimodal MRI brain scans in order to detect brain tumours. Using MRI brain images, the paper proposes a tumour detection method that removes skull impact and improves foreground regions for lesion identification through saliency modelling. Denoising, segmentation, and morphological procedures are used to develop the approach, and experimental evaluations show how effective it is. Chirodip Lodh Choudhury et al [6] suggested a technique that uses a deep neural network and convolutional neural network to detect and classify brain tumours. With a f-score of 97.3, the approach obtains an average accuracy of 96.08 percentage.

Sol, Nik, et al [7] conducted the study explores tumor-educated platelets (TEPs) as promising cancer diagnostic biomarkers for glioblastoma detection and monitoring. TEP-derived RNA panels, identified through swarm intelligence, show accuracy and potential for distinguishing false positives from true progression. Yuan Liu et al [8] created a deep C-LSTM neural network with 98.80 accuracy in identifying seizures and tumours for the purpose of detecting epileptic seizures and employing high-dimensional EEG inputs. Ahmed H. Abdel Gawad et al [9] in 2020 presented an improved edge detection technique for MR image-based brain tumour detection. To determine the best filter coefficients and thresholding techniques, the approach applies a genetic algorithm. The approach demonstrates higher performance across MR scan pictures, outperforming threshold-optimized fractional-order filters, fractional-order filters, and classical edge detection approaches. R. Leon et al [10] A study from 2021 suggests evaluating human normal brain and tumour tissue using hyperspectral VNIR and NIR sensors. Utilising a pair of cameras, the investigators examined brain tissue in vivo and identified discrete absorbance peaks linked to both haemoglobin and water. Significant differences between normal, tumour, and hypervascularized tissue were revealed by statistical analysis H Hu et al [11] 2021 study of the utilisation of MRI scans with deep learning technologies for brain tumour diagnosis is investigated. They employed a YOLO model to determine the position of the tumour and tested a number of models, including VGG16/19, AlexNet, GoogleNet, and Resnet. Findings indicate that deep learning models increase speed and accuracy, possibly treating more complicated illnesses. Md Khairul Islam et al [12] proposed an improved brain tumor detection method in 2021, using template-based K-means, superpixels, and principal component analysis. This method efficiently identifies human brain tumors within a shorter execution time, achieving superior accuracy and reduced execution time compared to existing schemes. Demyana Saleeb et al [13] proposed an early brain cancer

detection technique using a reconfigurable antenna array. The four-element array, designed for 2.4 GHz, detected tumors as small as 5 millimeters. The defects in antenna circuitry can occur. In 2021, K.Ejaz et.al

[14] proposed a hybrid segmentation method for tumor identification, combining confidence region detection with level set algorithm to handle intensity variations in MRI images. The method uses deterministic feature clustering, SOM Pixel Labeling, Reduced Cluster Membership, and Deterministic Feature Clustering to segment complex tumor intensities effectively.

Emre Dandil et.al [15] 2021 research demonstrates the effectiveness of stacked LSTM neural networks in detecting pseudo brain tumors using MR spectroscopy signals. The study uses MRS signals from normal brain tissue, brain tumors, and pseudo-brain tumors in the INTERPRET database. The LSTM-based stacked method achieved classification accuracies of 93.44, 85.56, 88.33, and 99.23 for various types of pseudo brain tumors. Amran Hossain

[16] proposed a YOLOv3 deep neural network model for detecting brain tumors in a portable electromagnetic imaging system. The model uses scattering parameters from a nine-antenna array setup and reconstructs images using a modified algorithm. The model successfully identifies tumors and their locations in testing images, demonstrating its efficacy in a portable electromagnetic head imaging system. In 2022, Disha Sushant Wankhede et.al [17] proposed a dynamic architecture-based deep learning approach for glioblastoma brain tumor survival prediction. They used MRI images to predict glioblastoma, segmenting tumors into compartments using Fuzzy C Means Clustering. A novel dimensionality reduction algorithm was proposed, identifying features to distinguish high-grade and low-grade glioblastoma. The study improved classification performance with a 95 percent accuracy rate and a 2.3 percentage error rate.

Andres Isaza et.al [18] 2022 study on "Data Augmentation and Transfer Learning for Brain Tumor Detection in Magnetic Resonance Imaging" uses data augmentation techniques to train networks with limited datasets, particularly in fields like medicine. The study achieved an F1 score of 92.34 percentage with ResNet50, demonstrating its efficacy and distinctiveness from conventional methods. In 2022, Agrawal et.al [19] proposed a method for brain tumor segmentation and classification using 3D-UNet deep neural networks. The study validated the models' effectiveness and compared them to existing techniques, it outperforms state-of-the-art methods. In 2022, Mohammed Ashraf Ottom [20] The Znet approach, which uses skip-connections, encoder-decoder architectures, and data amalgamation, extends expert tumor knowledge to a larger synthetic dataset. It shows high dice similarity coefficients and is effective in automatically localizing and segmenting brain tumors in MR images. This approach has potential for extension to 3D brain volumes, diverse pathologies, and imaging modalities. It exemplifies the practical application of AI in medical imaging.

From the conducted survey we have concluded that CNN and KNN is the best model for the brain abnormality clas- sification and MRI is the best imaging modality for the classification. We decided to combine both these models to posses higher accuracy.

III. METHODOLOGY

Our paper aims to classify brain abnormalities using tumors (including glioma, meningioma, pituitary), stroke, and normal MRI data, combining machine learning and deep learning for more accurate results.

A. BLOCK DIAGRAM

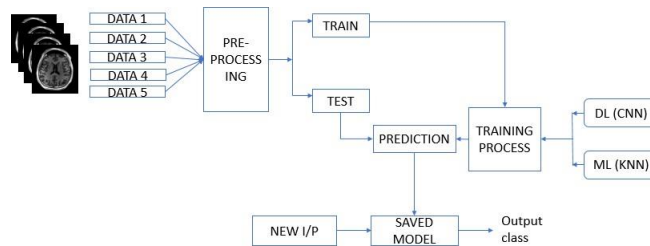


Fig. 1. Block Diagram

Fig.1. depicts the block diagram of the paper. We utilise different types of dataset which include MRI images of tumors (glioma, meningioma, pituitary), stroke and normal data. We collected all the dataset from Kaggle. After collection, the dataset is sent for the preprocessing stage. Preprocessing include image enhancing techniques like resizing, normalization, and gray scaling. Following the completion of preprocessing, the dataset is splitted for training and testing as 80% and 20%. A deep learning model (CNN architecture) is constructed, and this CNN architecture will aid in the feature extraction procedure. Three convolution layers, a pooling layer, and a fully linked layer make up the architecture's various layers. The neural network receives its training from the training set. It will acquire the capacity to identify key characteristics from the brain images throughout training. The model's convolutional and pooling layers are responsible for dimension reduction and feature extraction, respectively.

Following feature extraction a KNN classifier, a straight-forward but efficient technique for feature similarity based classification is modeled. It uses the closest neighbors to the specified value of K to classify. It will facilitate more precise detection of any anomalies. At the conclusion of the process, the data are validated and tested after having been trained and tested using CNN and KNN. Finally after receiving an effective accuracy the model is being given for classification.

B. FLOWCHART

Fig.2. depicts the flowchart of the paper.

1) *ALGORITHM*: The algorithm for the overall process is as shown below :

Step 1 : Start

Step 2 : Data collection

Step 3 : Preprocessing of input data Step 5 : CNN model creation

Step 6 : Train model

Step 7 : Convolution layer extracts features Step 8 : Pooling layer

Step 9 : Fully connected layer Step 10 : KNN Model creation

Step 11 : Loading Input data (CNN output data) Step 12 : Input K value

Step 13 : Train model

Step 14 : Find K Nearest Neighbors Step 15 : Determine majority class Step

16 : Test Model

Step 17 : If gained accuracy above 96 Step 18 : Save Model

Step 19 : Else goto CNN Step 20 : Stop

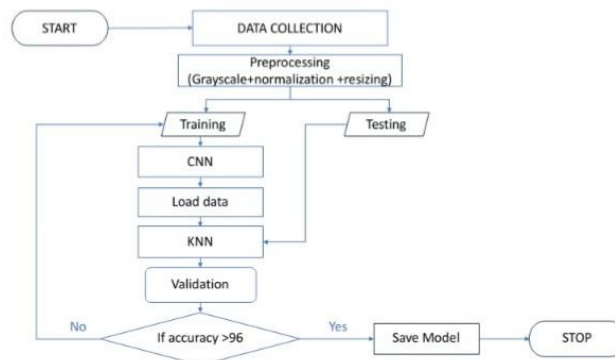


Fig. 2. Flowchart

C. SOFTWARE USED

We have used python for the implementation of the paper. Python is a highly versatile and has extensive library support including TensorFlow, PyTorch, Numpy, Keras, Scikit-learn, Joblib and more which are essential for the implementation of CNN and KNN. Python was very user friendly and very supportive for the implementation.

IV. RESULT AND DISCUSSION

By combining the CNN and KNN models, the glioma, meningioma, pituitary, and stroke conditions were classified very successfully. Our final output after 50 epochs of the model's final evaluation yielded a lower loss rate and a training accuracy of 100%. We have obtained a higher accuracy when combining both CNN and KNN than when using these models separately. Figure 3 displays the accuracy that the model achieved after 50 epochs of training.

After training we have tested the model with new mri images other than one from dataset. Successfully the model has correctly classified all the five classes when tested with new image.

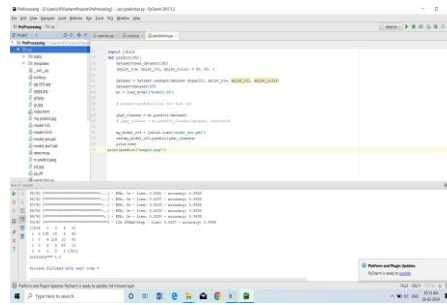


Fig. 3. Training Accuracy

A. DISCUSSION

The model is evaluated using confusion matrix which is as shown in Figure 4. From the confusion matrix we can see that the true positives are very high. From this we can make sure that the proposed model is very accurate, effective and efficient. Hence the combination of deep learning and machine learning has produced a higher accuracy of 100%, which shows the model is highly meticulous.

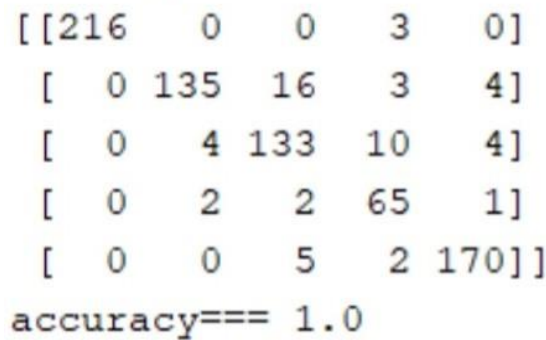


Fig. 4. Confusion Matrix

1) *RATIONALE BEHIND KNN and CNN*: The cooperation between The precise pattern recognition of deep learning and the methodical approach of machine learning improve the efficiency and accuracy of brain abnormality detection. CNN is a better deep learning neural network which has a high advantage in feature extraction. This advantage of feature extraction was taken to account. KNN is machine learning neural network which is weaker in feature extraction. Hence the CNN has taken a supportive role for KNN by providing its feature extracted output as input for the KNN. Also KNN is way more better in classification purpose and the classification of the model is happening using KNN. From these as both there bonding together brought up an better result.

V. CONCLUSION

In our project, a variety of datasets with brain abnormalities and normal conditions were combined to provide a comprehensive approach for tumour and stroke detection. Effective classification has benefited from the later use of neural networks. Through feature extraction, the Convolution Neural Network (CNN) model successfully learned to differentiate between a

variety of brain conditions, such as tumours, strokes, and normal states. Additionally, the addition of a K-Nearest Neighbours (KNN) classifier improved the precision of detections by improving the accuracy of identifying abnormalities based on feature similarity. This hybrid approach shows its promising results of 100% accuracy.

A. ADVANTAGES

The integration of deep learning and machine learning methodologies in brain abnormality detection presents notable benefits for medical diagnostics. Deep learning is particularly good at automatically extracting hierarchical features from complicated data, like medical images, so it can identify minute patterns that point to anomalies. Combining machine learning and deep learning improves detection performance while addressing the need for a trustworthy and understandable medical imaging diagnosis. This helps in early diagnosis and reduce the errors from manual diagnosis. Also very helpful to medical experts in the diagnosis process. Less time consuming than the manual diagnosis hence can provide the timely treatment.

B. DISADVANTAGES

Training data quality and quantity have a major impact on the success of deep learning and machine learning models. The model can have trouble extrapolating to real-world situations if the dataset it was trained on is neither diverse or representative. Another drawback of the model is its computational complexity. In medical applications, it could be detrimental to lack of interpretability because it is important to comprehend the logic behind a diagnosis.

C. FUTURE SCOPE

CNN excel at image recognition and feature extraction from medical scans. By using them for automatic feature learning from brain scans, we can potentially achieve higher accuracy in abnormality classification. Future research could focus on integrating interpretability features from KNN into CNN models. We can integrate the model in the software of imaging modalities and improve it by adding on a self analysis and diagnosis feature.

REFERENCES

- [1] Rana Banik, Md Rabiul Hasan, and Md Saif Iftekhar. Automatic detection, extraction and mapping of brain tumor from mri scanned images using frequency emphasis homomorphic and cascaded hybrid filtering techniques. In *2015 International Conference on Electrical Engineering and Information Communication Technology (ICEEICT)*, pages 1–6. IEEE, 2015.
- [2] Astina Minz and Chandrakant Mahobiya. Mr image classification using adaboost for brain tumor type. In *2017 IEEE 7th International Advance Computing Conference (IACC)*, pages 701–705. IEEE, 2017.
- [3] TA Jemimma and Y Jacob Vetharaj. Watershed algorithm based dapp features for brain tumor segmentation and classification. In *2018 International Conference on Smart Systems and Inventive Technology (ICSSIT)*, pages 155–158. IEEE, 2018.
- [4] Mahesh Kurnar, Aman Sinha, and Nutan V Bansode. Detection of brain tumor in mri images by applying segmentation and area calculation method using scilab. In *2018 Fourth*

International Conference on Computing Communication Control and Automation (ICCUBEA), pages 1–5. IEEE, 2018.

- [5] T Kalaiselvi, P Kumarashankar, P Sriramakrishnan, and S Karthigaiselvi. Brain tumor detection from multimodal mri brain images using pseudo coloring processes. *Procedia Computer Science*, 165:173–181, 2019.
- [6] Chirodip Lodh Choudhury, Chandrakanta Mahanty, Raghvendra Kumar, and Brojo Kishore Mishra. Brain tumor detection and classification using convolutional neural network and deep neural network. In *2020 international conference on computer science, engineering and applications (ICCSEA)*, pages 1–4. IEEE, 2020.
- [7] Nik Sol, Sjors GJG, Adrienne Vancura, Maud Tjerkstra, Cyra Leurs, Francois Rustenburg, Pepijn Schellen, Heleen Verschueren, Edward Post, Kenn Zwaan, et al. Tumor-educated platelet rna for the detection and (pseudo) progression monitoring of glioblastoma. *Cell Reports Medicine*, 1(7), 2020.
- [8] Yuan Liu, Yu-Xuan Huang, Xuexi Zhang, Wen Qi, Jing Guo, Yingbai Hu, Longbin Zhang, and Hang Su. Deep c-lstm neural network for epileptic seizure and tumor detection using high-dimension eeg signals. *IEEE Access*, 8:37495–37504, 2020.
- [9] Ahmed H Abdel-Gawad, Lobna A Said, and Ahmed G Radwan. Optimized edge detection technique for brain tumor detection in mr images. *IEEE Access*, 8:136243–136259, 2020.
- [10] Raquel Leon, Himar Fabelo, Samuel Ortega, and Gustavo M Callico. Hyperspectral vnir and nir sensors for the analysis of human normal brain and tumor tissue. In *2021 XXXVI Conference on Design of Circuits and Integrated Systems (DCIS)*, pages 1–6. IEEE, 2021.
- [11] Hanming Hu, Xin Li, Wenyi Yao, and Zhuocheng Yao. Brain tumor diagnose applying cnn through mri. In *2021 2nd International Conference on Artificial Intelligence and Computer Engineering (ICAICE)*, pages 430–434. IEEE, 2021.
- [12] Md Khairul Islam, Md Shahin Ali, Md Sipon Miah, Md Mahbubur Rahman, Md Shahariar Alam, and Mohammad Amzad Hossain. Brain tumor detection in mr image using superpixels, principal component analysis and template based k-means clustering algorithm. *Machine Learning with Applications*, 5:100044, 2021.
- [13] Demyana A Saleeb, Rehab M Helmy, Nihal FF Areed, Mohamed Marey, Wazie M Abdulkawi, and Ahmed S Elkorany. A technique for the early detection of brain cancer using circularly polarized reconfigurable antenna array. *IEEE Access*, 9:133786–133794, 2021.
- [14] Khurram Ejaz, Mohd Shafry Mohd Rahim, Usama Ijaz Bajwa, Huma Chaudhry, Amjad Rehman, and Farhan Ejaz. Hybrid segmentation method with confidence region detection for tumor identification. *IEEE Access*, 9:35256–35278, 2020.
- [15] Emre Dandıl and Semih Karaca. Detection of pseudo brain tumors via stacked lstm neural networks using mr spectroscopy signals. *Biocybernetics and Biomedical Engineering*, 41(1):173–195, 2021.
- [16] Amran Hossain, Mohammad Tariqul Islam, Mohammad Shahidul Islam, Muhammad EH Chowdhury, Ali F Almutairi, Qutaiba A Razouqi, and Norbahiah Misran. A yolov3 deep neural network model to detect brain tumor in portable electromagnetic imaging system. *IEEE Access*, 9:82647–82660, 2021.
- [17] Disha Sushant Wankhede and R Selvarani. Dynamic architecture based deep learning

approach for glioblastoma brain tumor survival prediction. *Neuroscience Informatics*, 2(4):100062, 2022.

- [18] Andre´s Anaya-Isaza and Leonel Mera-Jime´nez. Data augmentation and transfer learning for brain tumor detection in magnetic resonance imaging. *IEEE Access*, 10:23217–23233, 2022.
- [19] Pranjal Agrawal, Nitish Katal, and Nishtha Hooda. Segmentation and classification of brain tumor using 3d-unet deep neural networks. *International Journal of Cognitive Computing in Engineering*, 3:199– 210, 2022.
- [20] Mohammad Ashraf Ottom, Hanif Abdul Rahman, and Ivo D Dinov. Znet: deep learning approach for 2d mri brain tumor segmentation. *IEEE Journal of Translational Engineering in Health and Medicine*, 10:1–8, 2022.

COMMITTEES

Chief Patrons

Dr. K. Moidu

Chairman, KMCT Group of Institutions

Dr. K. M. Mehboob

Managing Trustee, KMCT

Patron

Dr. D. Jerline Sheebha Anni

Principal, KMCT College of Engineering for Women

General Chair

Dr. Sameera V Mohd Sagheer

HoD, Department of Biomedical Engineering
KMCT College of Engineering for Women

Honorary Chair

Ms. Nutan Hegde

Dean Academics, KMCT College of Engineering for Women

Honorary Vice-Chair

Ms. Anu K. S.

HoD, Department of Computer Science & Engineering
KMCT College of Engineering for Women

Executive Chair

Ms. Aparna S.

HoD, Department of Civil Engineering
KMCT College of Engineering for Women

Executive Vice Chair

Ms. Jayasree A

HoD, Department of Applied Science & Humanities
KMCT College of Engineering for Women

INTERNATIONAL ADVISORY COMMITTEE

- 1 Dr. Arun Kumar Sangaiah, National Yunlin University of Science and Technology, Taiwan
- 2 Dr. Muhammad Mokhzaini, Faculty of Engineering & Built Environment, Universiti Sains Islam Malaysia, Nilai, Malaysia
- 3 Dr. Khairunnisa Hasikin, Department of Biomedical Engineering, Faculty of Engineering, Universiti Malaya, Kuala Lumpur, Malaysia
- 4 Dr. Veena Raj, Faculty of Integrated Technologies, Universiti Brunei Darussalam, Brunei
- 5 Dr. M.Thanihaichelvan, University of Jaffna, Sri Lanka

NATIONAL ADVISORY COMMITTEE

- 1 Dr. P. Parthibhan, Department of Mechanical Engineering, National Institute of Technology Tiruchirapalli
- 2 Dr. J Nafeesa Beegum, Department of Computer Science & Engineering, Government College of Engineering Bargaue
- 3 Dr. Mohammed Shahid Abdulla, Information Systems Area, IIM Kozhikode
- 4 Mr. K S Lalmohan, Advance Computing and Services, National Institute of Electronics and Information Technology (NIELIT)
- 5 Dr. Sameer S. M. , Department of Electronics & Communication Engineering, National Institute of Technolgy Calicut
- 6 Dr. K.Jayanthi, Department of Electronics and Communication Engineering, Puducherry Technological University

TECHNICAL PROGRAM COMMITTEE

- 1 Dr. P. Chinnamuthu, National Institute of Technology Nagaland
- 2 Dr. Geetha V, Department of Information Technology, National
Institute of Technology Suratkal
- 3 Dr. Janakiraman S. , Department of Banking Technology, Pondicherry
University
- 4 Dr. S. Rathi, Department pf Computer Science & Engineering,
Government College of Technology Coimbatore
- 5 Dr. Anoop B K, AIML, Srinivas Institute of Technology Mangalore
- 6 Dr. Adarsh T K, Department of CSE, T. John Institute of Technology,
Bangalore
- 7 Dr. M. Thenmozhi, Department of Networking and Communications,
SRM Institute of Science and Technology
- 8 Dr. Ameer P. M., Department of Electronics & Communication
Engineering, National Institute of Technolgy Calicut
- 9 Dr. M. Prabhu, Department of Computer Science & Engineering,
National Institute of Technolgy Calicut
- 10 Dr Jeena R S, Department of Electronics & Communication
Engineering, Government Engineering College Idukki
- 11 Dr Minimol B, Department of Biomedical Engineering, Model
Engineering College
- 12 Mr. Anish Babu K K, Department of Electronics & Communication
Engineering, Government Engineering College Wayanad
- 13 Dr. Thafseela Koya P., Computer Science Engineering, AWH
Engineering College
- 14 Dr. Abdu Rahiman V, Applied Electronics and Instrumentation
Engineering, Government Engineering College Kozhikode
- 15 Dr. Jessy John, Biomedical Engineering, Model Engineering College
Thrikkakara
- 16 Dr. Arun Kumar T., Department of Database Systems, Vellore Institute
of Technology
- 17 Dr Lalatendu Behera, Department of Computer Science & Engineering,
National Institute of Technology Jalandhar
- 18 D Jinil Persis, Quantitative Methods and Operations Management Area,
Indian Institute of Management Kozhikode

- 19 Mr. Anand Kumar M, National Institute of Technology Surathkal
- 20 Dr Venkatesan M, Department of Computer Science Engineering,
National Institute of Technology Puducherry
- 21 Dr. A. Muthumari, Department of Computer Sceince & Engineering,
University College of Engineering Ramanathapuram
- 22 Dr. Nithya S, Smart Computing, School of Information Technology &
Engineering
- 23 Dr. M. Karthikeyan, Computing Technologies, SRM Institute of
Science and Technology
- 24 Ms. Meethu Miriam Varkey, Axiom Consulting
- 25 Mr. Bhavya Balakrishnan, Department of Computer Science
Engineering, VTU
- 26 Mr. Deepaklal, Performance Engineering, I-Exceed Technology
Solutions
- 27 Dr. Seetha R, School of Information Technology & Engineering,
Information Technology

OPERATIONS COMMITTEE

Organizing Committee

1. Ms. Krishnaja., Assistant Professor/ BME, KMCTCEW
2. Ms.Sindhu V., Assistant Professor/ CE, KMCTCEW
3. Ms. Reena Abraham, Assistant Professor/ CE, KMCTCEW
4. Ms. Mubeena Banu, Assistant Professor/ CE, KMCTCEW
5. Ms. Shamila T. , Assistant Professor/ CE, KMCTCEW
6. Ms. Divya Das, Lab Instructor/ CE, KMCTCEW
7. Ms. Hamna Jasmin, Assistant Professor/ ASH, KMCTCEW
8. Ms. Anusha E. P., Assistant Professor/ BME, KMCTCEW
9. Ms. Jisha, Librarian, KMCTCEW
10. Ms. Jiji, Librarian, KMCTCEW

Finance Committee

1. Ms. Sithara Parveen, Assistant Professor/ ASH, KMCTCEW
2. Ms. Ramla T. P., Assistant Professor/ ASH, KMCTCEW

Marketing Committee

1. Ms. Fahmida Minna, Assistant Professor/ CSE, KMCTCEW
2. Ms. Shamna Jasmi, Lab Instructor/ CSE, KMCTCEW
3. Mr. Anoop M. K., Lab Instructor/ CE, KMCTCEW
4. Mr. Abdul Ravoof P., Lab Instructor/ CE, KMCTCEW
5. Mr. Jameem, Lab Instructor/ BME, KMCTCEW

Food & Hospitality Committee

1. Ms. Shibitha K. P, Assistant Professor/ BME, KMCTCEW

2. Ms. Sindhu Mohan, Lab Instructor/ BME, KMCTCEW

3. Ms. Laya P., Lab Instructor/ BME, KMCTCEW

Programme Committee

1. Mr. Sivanath P. I., Assistant Professor/ BME, KMCTCEW

2. Ms. Swabna E, Assistant Professor/ CSE, KMCTCEW

3. Ms. Aswathi K. V., Assistant Professor/ CE, KMCTCEW

2. Ms. Agamyia Pramod, Assistant Professor/ CSE, KMCTCEW

5. Mr. Adarsh, Lab Instructor/ BME, KMCTCEW

6. Ms. Megha M., Assistant Professor/ CSE, KMCTCEW

7. Ms. Shamna P. A., Assistant Professor/ CSE, KMCTCEW

Publications Committee

1. Ms. Drishya S. G., Assistant Professor/ CSE, KMCTCEW

2. Ms. Binisha P., Assistant Professor/ CE, KMCTCEW

3. Ms. Minilal, Assistant Professor/ BME, KMCTCEW

4. Ms. Aleesha , Assistant Professor/ CE, KMCTCEW

5. Ms. Binusha K., Lab Instructor/ CSE, KMCTCEW

Registration Committee

1. Ms. Chithra U. T., Assistant Professor/ CE, KMCTCEW

Ms. Jouhara C.P., Assistant Professor/ ASH, KMCTCEW

3. Ms. Sowmya, Lab Instructor/ ASH, KMCTCEW

Results Committee

1. Ms. Irafana Izzath O. P., Assistant Professor/ BME, KMCTCEW

2. Ms. Athulya V., Assistant Professor/ CE, KMCTCEW

3. Ms. Najila E., Assistant Professor/ ASH, KMCTCEW